UNIVERSIDAD AUTÓNOMA DE NUEVO LEÓN

FACULTAD DE CIENCIAS BIOLÓGICAS

CONTRIBUCIÓN DE LA MORFOLOGÍA DE LA MICROGLÍA Y EL VOLUMEN DEL FÓRNIX EN LA MEMORIA ESPACIAL Y DE RECONOCIMIENTO EN *Mus musculus* DURANTE EL ENVEJECIMIENTO

POR

M.C. MARCELA CÁRDENAS TUEME

COMO REQUISITO PARCIAL PARA OBTENER EL GRADO DE

DOCTORADO EN CIENCIAS CON ORIENTACIÓN

EN INMUNOBIOLOGÍA

2022

CONTRIBUCIÓN DE LA MORFOLOGÍA DE LA MICROGLÍA Y EL VOLUMEN DEL FÓRNIX EN LA MEMORIA ESPACIAL Y DE RECONOCIMIENTO EN *Mus musculus* DURANTE EL ENVEJECIMIENTO

Dr. Diana Reséndez Pérez
Director

Dr. Cristina Rodriguez Padilla
Secretario

Dr. Diana Elia Caballero Hernández
Vocal 1

Dr. Moisés Armides Franco Molina
Vocal 2

Dr. Pablo Zapata Benavides
Vocal 3

Dra. Katiushka Arévalo Niño
Subdirección de Posgrado

SUBDIRECCIÓN DE POSGRADO

CONTRIBUCIÓN DE LA MORFOLOGÍA DE LA MICROGLÍA Y EL VOLUMEN DEL FÓRNIX EN LA MEMORIA ESPACIAL Y DE RECONOCIMIENTO EN *Mus musculus* DURANTE EL ENVEJECIMIENTO

Dirección de Tesis

El presente trabajo se realizó en el Laboratorio de Inmunología y Virología y fue dirigido por la Dra. Diana Reséndez Pérez

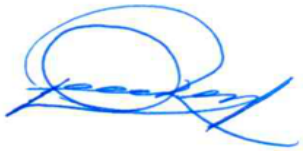

Dr. Diana Reséndez Pérez

AVISO DE DERECHOS DE AUTOR

FINANCIAMIENTO

Este trabajo fue financiado por el Programa de Apoyo a la Investigación Científica y Tecnológica, PAICYT UANL, CN1184-20; IBRO-LARC y Programa de Apoyo a Proyectos de Investigación e Innovación Tecnológico (PAPIIT-IA202120).

AGRADECIMIENTOS

Primeramente, quisiera agradecer a la Dra. Diana Reséndez Pérez por todo su apoyo en la realización de este proyecto. Por la confianza depositada en mi.

Al CONACYT por la beca que me fue otorgada para realizar mis estudios.

Al Laboratorio de Inmunología y Virología (LIV) por ser mi casa todo este tiempo, por todas las prestaciones, los equipos y materiales que se usaron para desarrollar este proyecto.

A mi Comité de Tesis por enriquecer y apoyarme con la realización del proyecto. Gracias Dra. Cristina Rodríguez-Padilla, Dra. Diana Caballero-Hernández, Dr. Moisés Franco-Molina y Dr. Pablo Zapata-Benavides por sus comentarios, por el seguimiento durante cada seminario y por apoyarme en cada paso del proyecto.

A la Facultad de Ciencias Biológicas de la UANL por permitirme realizar el proyecto y nunca negarme sus instalaciones.

Al Dr. José Ignacio Gonzáles Rojas por creer en mi.

Al Laboratorio Nacional de Imagenología por Resonancia Magnética (LANIREM) del Instituto de Neurobiología de la UNAM y de la Universidad Autónoma de Querétaro, principalmente al Dr. Luis Concha y al Dr. Eduardo Garza.

Al grupo de investigación del Dr. Camacho-Morales perteneciente a la Facultad de Medicina, UANL por toda la retroalimentación recibida en seminarios. Principalmente, al M.C. Luis Ángel Trujillo Villarreal por todo el apoyo en el análisis de las resonancias magnéticas y cálculos estadísticos.

DEDICATORIA

Al amor de mi vida, Alberto, estás presente en cada parte de mi vida. Te amo muchísimo.

A mi padre, Carlos Cárdenas Barrera (1953-2021), a quien la vida no le alcanzó para verme lograr esto. Todo esto es por ti papá, te extraño en cada respiro que doy.

A mi mamá, gracias por darme toda la fuerza que me ha faltado en estos años.

A mi hermano, por ser ese amigo entrañable y confidente.

A todo el resto de mi familia, por ser y estar, por apoyarme y aplaudirme en cada decisión.

A mis compañeros de laboratorio, Rubén, Claudia, Gustavo, Alely, Citlalli, Paco, Azeneth, por tantas risas y anécdotas juntos.

A Sofía, por enseñarme a enseñar, te llevo siempre conmigo.

A todos mis maestros, cada uno de ustedes ha dejado una huella en mi vida, gracias por inspirarme.

A mis amigas de toda la vida, Karen, Montse, Aniela, María José y Cynthia por siempre estar presentes. La vida no sería lo mismo sin ustedes, las llevo en mi corazón.

A mi gato Thor, por ser el mejor compañero de pandemia. Por apapacharme el corazón con sus ronrroneos.

ÍNDICE DE TABLAS

ÍNDICE DE FIGURAS

ÍNDICE DE ABREVIATURAS

ASC: Proteína Asociada a Apoptosis

ATP: Adenosín Trifosfato

DAM: Microglía Asociada a Enfermedad

DBM: Morfología Basada en Deformación

EA: Enfermedad de Alzheimer

FDR: Tasa de Descubrimiento Falso

GDNF: Factor Neurotrófico Derivado de la Glía

GM: Materia Gris

LTM: Memoria a Largo Plazo

MEntC: Corteza Medial Entorrinal Izquierda

MRI: Resonancia Magnética Nuclear

NORT: Prueba de Reconocimiento de Objetos

OLT: Prueba de Ubicación de Objetos

PCA: Análisis de Componentes Principales

PFA: Paraformaldehído

ROS: Especias Reactivas de Oxígeno

SI: Sistema Inmune

SNC: Sistema Nervioso Central

STM: Memoria a Corto Plazo

TREM2: Receptor Activador Expresado en Células Mieloides 2

1. RESUMEN

El envejecimiento muestra un perfil proinflamatorio de bajo grado en la sangre y el cerebro. La acumulación de citocinas proinflamatorias, la activación de la microglía y los cambios volumétricos en el cerebro se correlacionan con el deterioro cognitivo en los modelos de envejecimiento. Sin embargo, la interacción entre ellos no se entiende totalmente. El objetivo de esta tesis fue identificar globalmente un perfil proinflamatorio dependiente de la edad y una plasticidad morfológica de la microglía que favorece cambios de volumen importantes en el cerebro asociados con el deterioro cognitivo en un modelo murino. Para ello, se utilizaron ratones macho C57BL/6 en grupos de 2, 12 y 20 meses de edad para determinar su capacidad de memoria y aprendizaje, posteriormente, fueron divididos en dos cohortes para los análisis de resonancia magnética estructural y el análisis morfológico de la microglia, así como para los perfiles citocinas en sangre y en la región fórnix y corteza entorrinal medial. Finalmente, se realizaron análisis estadísticos para determinar correlaciones entre las pruebas de memoria y aprendizaje, los cambios de volumen y los perfiles de citocinas. El análisis de la bateria de las pruebas de memoria y aprendizaje obtenidos de ratones de 2, 12 y 20 meses de edad reveló un deterioro cognitivo dependiente de la edad después de las pruebas del laberinto en Y, el laberinto de Barnes, el reconocimiento de objetos (NORT) y la ubicación de objetos (OLT). El análisis de resonancia magnética (MRI) global mediante morfometría basada en deformación (DBM) en el cerebro identificó un aumento de volumen en el fórnix y una disminución en la corteza entorrinal medial izquierda (MEntC) durante el envejecimiento. En particular, el fórnix muestra un aumento en la acumulación de citoquinas proinflamatorias, mientras que la MEntC izquierda muestra una disminución. La evaluación morfológica de la microglía también confirma un fenotipo activo y distrófico en el fórnix y un fenotipo de vigilancia en la MEntC izquierda. Finalmente, el modelado biológico reveló que el aumento de volumen relacionado con la edad en el fórnix se asoció con microglía distrófica y deterioro cognitivo, como lo demuestra el mal desempeño en las tareas cognitivas que examinan la memoria de la ubicación del objeto y el objeto novedoso. Nuestros resultados proponen que la plasticidad morfológica de la microglía podría contribuir a los cambios volumétricos en las regiones del cerebro asociadas con el deterioro cognitivo durante el envejecimiento fisiológico.

2. ABSTRACT

Ageing displays a low-grade pro-inflammatory profile in blood and the brain. Accumulation of pro-inflammatory cytokines, microglia activation and volumetric changes in the brain correlate with cognitive decline in ageing models. However, the interplay between them is not totally understood. Here, we aimed to globally identify an age-dependent pro-inflammatory profile and microglia morphological plasticity that favors major volume changes in the brain associated with cognitive decline. Cluster analysis of behavioral data obtained from 2-,12- and 20-month-old male C57BL/6 mice revealed age-dependent cognitive decline after the Y-maze, Barnes maze, object recognition (NORT) and object location tests (OLT). Global magnetic resonance imageing (MRI) analysis by deformation-based morphometry (DBM) in the brain identified a volume increase in the fornix and a decrease in the left medial entorhinal cortex (MEntC) during ageing. Notably, the fornix shows an increase in the accumulation of pro-inflammatory cytokines, whereas the left MEntC displays a decrease. Morphological assessment of microglia also confirms an active and dystrophic phenotype in the fornix and a surveillance phenotype in the left MEntC. Finally, biological modeling revealed that age-related volume increase in the fornix was associated with dystrophic microglia and cognitive impairment, as evidenced by failure on tasks examining memory of object location and novelty. Our results propose that the morphological plasticity of microglia might contribute to volumetric changes in brain regions associated with cognitive decline during physiological ageing.

3. INTRODUCCIÓN

El mundo continúa experimentando un cambio sostenido y sin precedentes en la estructura de edad de la población mundial, impulsado por niveles crecientes de esperanza de vida. Según un informe de las Naciones Unidas de 2020 sobre el envejecimiento de la población mundial, durante las próximas tres décadas, se prevé que el número de personas mayores en todo el mundo supere los 1500 millones en 2050 (Naciones Unidas, 2020).

El envejecimiento de la población debería verse como un éxito en la historia de la humanidad; sin embargo, también trae problemas a nivel de salud pública ya que nuestro organismo comienza a fallar y trae consigo varias consecuencias físicas y cognitivas. A pesar de estas mejoras en la esperanza de vida, podría decirse que las enfermedades neurodegenerativas se han convertido en las enfermedades más temidas de las personas mayores.

El envejecimiento se caracteriza por una pérdida progresiva de la integridad fisiológica y, por tanto, es el principal factor de riesgo de las principales patologías humanas, como el cáncer, la diabetes, los trastornos cardiovasculares, el deterioro cognitivo y las enfermedades neurodegenerativas (Currais, 2015; López-Otín et al., 2013).

Previamente se ha informado un perfil proinflamatorio de bajo grado en la sangre y el cerebro durante el envejecimiento (Wyss-Coray, 2016). La infiltración de células inmunes periféricas en el cerebro explica la homeostasis del tejido en etapas más jóvenes, pero esta infiltración promueve la liberación de citocinas proinflamatorias que conducen a la neuroinflamación durante el envejecimiento (Batterman et al., 2021; Dubenko et al., 2021; Fulop et al., 2018; Jeon et al., 2012). De hecho, los ratones de edad avanzada muestran un aumento en las citoquinas inflamatorias circulantes que se correlaciona con una infiltración de neutrófilos y macrófagos relacionada con la edad, lo que permite la activación microglial en el cerebro (Wolfe et al., 2018). La microglía se vuelve disruptiva durante el envejecimiento, exhibiendo plasticidad morfológica al mostrar hipertrofia del citoplasma perinuclear y procesos retraídos, que recuerdan a la microglía activada (Miller and Streit, 2007; Sheng et al., 1998). La microglía activada en el envejecimiento integra las firmas moleculares que se encuentran en estados de lesión

o enfermedad, como una mayor expresión del complejo mayor de histocompatibilidad II (MHCII) y CD11b (p. ej., Iba1, OX6) (Frank et al., 2006). En particular, la neuroinflamación y la activación de la microglia promueven el deterioro cognitivo y aumentan la susceptibilidad a la neurodegeneración en modelos preclínicos y clínicos (Bachstetter et al., 2017; Wolfe et al., 2018; Wyss-Coray, 2016). De manera congruente, el bloqueo farmacológico de la neuroinflamación mejora el rendimiento de la memoria espacial en ratones de edad avanzada (Fung et al., 2020; Zhou et al., 2019). Sin embargo, la interacción entre la plasticidad microglial y la neuroinflamación durante el envejecimiento, y su papel en el deterioro cognitivo, no se han entendido totalmente.

Durante el envejecimiento se han identificado cambios volumétricos en áreas selectivas del cerebro relacionadas con el rendimiento cognitivo. Diversos autores reportan una disminución media en el volumen total de -0,45 % por año entre los 18 y los 97 años (Fotenos et al., 2005), y una reducción lineal persistente en la corteza y un aumento del volumen ventricular a partir de los 20 años (Fillmore et al., 2015). Varios estudios de imágenes por resonancia magnética (MRI) también han informado reducciones volumétricas de la materia gris (GM) en las cortezas de asociación prefrontal, parietal y temporal, y en la ínsula, el cerebelo, los ganglios basales y el tálamo de humanos de edad avanzada (Alexander et al., 2006; Good et al., 2001; Grieve et al., 2005; Jernigan et al., 2001; Kalpouzos et al., 2009; Resnick et al., 2003; Sowell et al., 2004; Taki et al., 2004; Tisserand et al., 2002). Sin embargo, los rasgos celulares y moleculares que contribuyen a los cambios volumétricos del cerebro durante el envejecimiento no se han caracterizado y, en algunos casos, todavía se malinterpretan.

En esta tesis, analizamos la contribución del perfil proinflamatorio central y la plasticidad morfológica microglial durante el envejecimiento y descubrimos que son congruentes con los cambios volumétricos en regiones selectivas asociadas con el deterioro cognitivo. De acuerdo con nuestros resultados, proponemos que los cambios morfológicos en la microglía, contribuyen a los cambios volumétricos en las regiones del cerebro que ayudan al deterioro cognitivo durante el envejecimiento fisiológico.

4. ANTECEDENTES

4.1 Envejecimiento

El envejecimiento es un proceso natural que se asocia con el deterioro fisiológico, tanto físico como cognitivo (Bettio et al., 2017). Biológicamente, el envejecimiento se asocia con una disminución progresiva de la homeostasis fisiológica, lo que resulta en una función deteriorada y una mayor susceptibilidad a la muerte (López-Otín et al., 2013). Históricamente, el declive fisiológico asociado con la edad y su papel como factor de riesgo de enfermedades crónicas se ha considerado inmutable (Sierra, 2016). Sin embargo, en los últimos años, los avances en la biología del envejecimiento han demostrado que la tasa de envejecimiento está, al menos en parte, controlada por genes y vías bioquímicas conservadas en la evolución (López-Otín et al., 2013), lo cual nos hace replantear la idea de que se pueden desarrollar intervenciones efectivas que podrían retrasar o disminuir las múltiples patologías encontradas en los adultos de la tercera edad y por consecuencia, extender su vida saludable, es decir, la duración de la salud y no solamente de la vida.

Con el aumento de la esperanza de vida en la población, así como de la falta de un tratamiento eficaz o bien una estrategia para evitarlas, la prevalencia de las enfermedades neurodegenerativas está aumentando e imponiendo una carga importante a la población, pues las personas mayores pasan la mayor parte de su vida extendida con problemas de salud y múltiples comorbilidades, que incluyen deterioro cognitivo, enfermedades crónicas y discapacidad.

Durante el envejecimiento normal, el deterioro cognitivo puede presentarse como déficits en ciertos dominios que incluyen el aprendizaje espacial, la memoria de trabajo, la memoria episódica, y la atención (Ober, 1996). Sin embargo, la manifestación de este declive exhibe diferencias sustanciales entre los pacientes debido a la variabilidad en la resiliencia y la reserva cognitiva. Algunos de los factores involucrados en la variabilidad de este fenotipo son: la educación, la inteligencia y la estimulación mental, que permiten que el cerebro se adapte al daño patológico y mantenga la función cognitiva. Desafortunadamente, el envejecimiento también está asociado con varias condiciones neurodegenerativas debilitantes, la más común es la enfermedad de Alzheimer (EA). Y

aunque las enfermedades sistémicas cobran el mayor número de víctimas en la salud y el bienestar humanos, cada vez más, un cerebro defectuoso es el árbitro de una muerte precedida por una pérdida gradual de la esencia del ser (Wyss-Coray, 2016).

4.2 Deterioro cognitivo asociado a la edad

El deterioro cognitivo (DC) es un síndrome caracterizado por un cuadro clínico intermedio entre el envejecimiento saludable y el envejecimiento patológico. Las personas con DC no cumplen con el diagnóstico de ningún tipo de demencia, pero tienen un funcionamiento cognitivo alterado, el cual a pesar de que no compromete la capacidad de funcionamiento, y no entra en la clasificación de envejecimiento fisiológico y normal, es un estado intermedio entre la aparición de una patología o bien, envejecer saludablemente. El síntoma de inicio más común es el deterioro de la memoria, como en la EA, seguido de otros déficits cognitivos que no necesariamente involucran a la memoria, tales como, la función ejecutiva, el uso del lenguaje y las habilidades visuoespaciales (Lo et al., 2011; Petersen, 2016).

El DC puede ser clasificado en dos subtipos: amnésico y no amnésico (Petersen, 2016). Las características de cada uno de éstos están implícitamente escritas en su propio nombre. El deterioro cognitivo leve amnésico implica la pérdida o la afectación de la memoria, sin embargo, no cumple los criterios de demencia y a pesar de que éste puede empeorar con el paso del tiempo, otras capacidades cognitivas, como la función ejecutiva, el uso del lenguaje y las habilidades visuoespaciales, se mantienen relativamente conservadas y las actividades funcionales están intactas, excepto quizás por algunas ineficiencias leves. En cambio, el deterioro cognitivo leve no amnésico es caracterizado por una disminución sutil de funciones no relacionadas con la memoria, que afectan la atención, el uso del lenguaje o las habilidades visuoespaciales. También, es el tipo menos común y puede ser el precursor de demencias que no están relacionadas con la enfermedad de Alzheimer, como la degeneración del lóbulo frontotemporal o la demencia con cuerpos de Lewy (Lo et al., 2011) .

Las causas subyacentes del deterioro cognitivo son aún ampliamente desconocidas, sin embargo, con el tiempo y el avance de la ciencia, se han propuesto la inflamación

asociada a la edad *"inflammageing"* y los cambios estructurales en estructuras cerebrales relacionadas a los procesos de aprendizaje y memoria.

Primeramente, abordaremos el fenómeno conocido como *inflammageing* y más adelante se describirán los cambios estructurales que aparecen durante el envejecimiento.

4.3 Inflamación asociada a la edad

El proceso inflamatorio, es una respuesta del sistema inmune innato y humoral ante patógenos, heridas, isquemia, etc. para restablecer la homeostasia fisiológica del cuerpo, éste es regulado por la activación de los inflamasomas. Los complejos macromoleculares denominados inflamasomas están constituidos por un receptor NOD (NLR), un receptor de AIM2 (ausente en melanoma 2) el ALR, la proteína tipo punto asociada a apoptosis (ASC) y la procaspasa-1, los cuales pueden ser activados por variación en la concentración iónica y de ATP intracelular y extracelular, por desestabilización del fagolisosoma, por internalización de cristales insolubles o por mecanismos de oxidoreducción, lo cual permite la activación de la plataforma molecular y el consiguiente procesamiento de las pro-interleucinas inflamatorias a sus formas activas (Suárez and Buelvas, 2015).

A pesar de que la inflamación es utilizada como una herramienta de defensa, un proceso inflamatorio crónico puede dañar tejidos y permitir la aparición o bien, la prevalencia de alguna patología (von Bernhardi et al., 2015).

Una de las características que exhiben las patologías presentes durante el envejecimiento, es que comparten un trasfondo inflamatorio en común, el cual ha sido adjudicado al envejecimiento y ha sido denominado como "*inflammageing*". La palabra "*inflamm-ageing*" está compuesta por dos palabras que vienen del inglés de *inflammation* y *aging,* que significan inflamación y envejecimiento, respectivamente. Este término inflammaging fue detallado por primera vez por Franceschi et al., en el año 2000*,* para describir un fenotipo inflamatorio crónico causado por una reducción en la capacidad de hacer frente a una variedad de factores de estrés (antigénicos, químicos, físicos, etc.) que favorecen la aparición de este fenotipo.

El inflammageing puede resultar por diferentes causas, tales como, la acumulación de daño en los tejidos a lo largo de la vida, la disfunción o bien, la senescencia del sistema

inmune y su inefectividad en la eliminación de patógenos o células disfuncionales, la propensión de las células senescentes a secretar citocinas proinflamatorias, la activación perpetua del factor de transcripción NF-kB, o bien, la aparición de una respuesta de autofagia defectuosa (Salminen et al., 2012). Este fenómeno se presenta en el sistema inmunológico periférico, así como también en el sistema nervioso central (SNC) y ha sido propuesto como un candidato causal del deterioro cognitivo asociado a la edad.

Durante muchos años se creyó que el cerebro era un órgano inmunoprivilegiado, sin embargo, últimamente se ha demostrado que el SNC posee su propio sistema inmune (SI) y que éste además se encuentra intrínsecamente comunicado con el SI periférico (Buckman et al., 2014; Maldonado-Ruiz et al., 2017; Santoro et al., 2018).

El SI del cerebro está principalmente constituido por la microglía. Las células de la microglía son los macrófagos residentes del SNC y están encargadas de supervisar la vigilancia de la integridad del SNC, responder a patógenos, lesiones y también a alteraciones muy sutiles en su microambiente (Soulet and Rivest, 2014).

En cerebros sanos, la microglía se encuentra en un estado altamente ramificado y estable (Davalos et al., 2005). Pero, en cerebros con alguna patología o en caso de alguna lesión, la morfología de la microglía cambia, sus procesos se acortan y toma forma ameboidea, se activa su estado fagocítico y ejecuta funciones similares a las de otros macrófagos residentes de tejido, tales como la secreción de citocinas proinflamatorias, presentación de antígenos, producción de ROS y fagocitosis; entre otros, todas éstas conducen a la neuroinflamación (Davies et al., 2017). La microglía activa también integra regulación negativa de varios genes homeostáticos (Keren-Shaul et al., 2017).

De acuerdo con lo mencionado anteriormente, se puede atribuir que la microglía podría ser la responsable de producir un fenómeno proinflamatorio en el cerebro, conocido como neuroinflamación. Bajo un escenario controlado, la neuroinflamación es beneficiosa y promueve la eliminación de los desechos o las neuronas disfuncionales que pueden tener un impacto negativo en la función del SNC. Sin embargo, bajo un estado patológico, la activación de microglía está regulada positivamente y puede ser dañina para las neuronas debido a la liberación excesiva de ROS y citocinas proinflamatorias que conducen a neuroinflamación (von Bernhardi et al., 2015) y, podría contribuir al daño tisular y patología de la enfermedad o la aparición de alguna.

Se pensaría que una solución sería inactivar la microglía, sin embargo, esta célula también proporciona factores tróficos esenciales para la supervivencia de las neuronas y demás células en el SNC, como el factor neurotrófico derivado del cerebro (BDNF) y el factor neurotrófico derivado de la glía (GDNF) (Salter and Stevens, 2017).

Es de importancia comentar que, en algunas enfermedades neurodegenerativas, el SI del SNC tiene un papel muy importante, por ejemplo, se ha encontrado un fenotipo en especial de la microglía el que ha sido denominado DAM, lo que significa microglía asociada a la enfermedad (por sus siglas en inglés: Disease Associated Microglia). Este fenotipo muestra cambios significativos en la expresión génica en comparación con la microglía no asociada a enfermedades, como la reducción en los niveles de expresión de varios genes homeostáticos de microglía, incluidos los receptores purinérgicos P2ry12 / P2ry13, Cx3cr1 y Tmem119. Lo que se ha propuesto es que DAM no está asociada con la causa primaria específica de patología de la enfermedad o etiología de la enfermedad, sino más bien con una reacción que el organismo está montando para depurar las proteínas mal plegadas y/o agregados proteicos resistentes a proteosoma que, comúnmente, se acumulan en enfermedades neurodegenerativas o en el daño general causado por el envejecimiento natural (Keren-Shaul et al., 2017). Otro ejemplo que le brinda importancia al sistema inmune en las enfermedades neurodegenerativas es el que describen Lee et al., 2018 que la sobreexpresión de TREM2 en la microglía durante el Alzheimer reprograma la capacidad fagocítica de la microglía y favorece la eliminación de las placas amiloideas, mejorando por consecuencia la neuropatología y la capacidad de memoria-aprendizaje en un modelo murino de Alzheimer.

Con todos estos reportes, se puede determinar, que la microglía puede jugar un papel fundamental en las afectaciones del cerebro, ya sean patológicas o fisiológicas, siendo el caso del envejecimiento. Es por ello que la hemos propuesto como un candidato crucial en la aparición del deterioro cognitivo asociado a la edad. Sin embargo, no sólo esta célula podría ser parte de la explicación, sino también lo que sucede en las regiones cerebrales donde reside.

4.4 Cambios estructurales en el cerebro durante el envejecimiento

La estructura del cerebro cambia constantemente, desde el momento que nacemos hasta que envejecemos; estos cambios son considerados normales, siempre y cuando no se presente demencia o alguna alteración cognitiva.

Durante el envejecimiento, no sólo el cuerpo se deteriora, si no que ha sido ampliamente descrito que el cerebro sufre cambios morfológicos y volumétricos durante la edad adulta (Galluzzi et al., 2008). El cambio de volumen parcial más consistentemente reportado es una reducción en el volumen de GM. Ge et al., 2002 describieron un porcentaje de disminución de GM en sujetos de 20 años con una reducción constante durante todo el periodo comprendido entre la edad adulta temprana y la tardía; sin embargo, no sólo este grupo de investigación ha sido responsable de reportar esta reducción de GM durante la edad, sino que tambien otros autores han reportado las relaciones lineales negativas similares entre el volumen de GM cortical y la edad (Good et al., 2001; Lemaître et al., 2005; Sato et al., 2003; Smith et al., 2007; Sullivan et al., 2004; Taki et al., 2004).

Existen estudios previos, donde se ha reportado que existen diferencias en el volumen cerebral total a partir de los 30 años y se ha notificado un descenso medio en el volumen total de -0.45% por año después de los 65 años (Fotenos et al., 2005). Además, durante el envejecimiento se han identificado cambios volumétricos en áreas selectivas del cerebro relacionadas con el rendimiento cognitivo. Diversos autores reportan una disminución media en el volumen total de -0,45 % por año entre los 18 y los 97 años (Fotenos et al., 2005), y una reducción lineal persistente en la corteza y un aumento del volumen ventricular a partir de los 20 años (Fillmore et al., 2015). Varios estudios de imágenes por MRI también han informado reducciones volumétricas de la GM en las cortezas de asociación prefrontal, parietal y temporal, y en la ínsula, el cerebelo, los ganglios basales y el tálamo de humanos de edad avanzada (Alexander et al., 2006; Good et al., 2001; Grieve et al., 2005; Jernigan et al., 2001; Kalpouzos et al., 2009; Resnick et al., 2003; Sowell et al., 2004; Taki et al., 2004; Tisserand et al., 2002). No está de demás agregar que también se han reportado disminuciones volumétricas en la GM occipital, el hipocampo, la circunvolución occipital media, el polo occipital y el tálamo (Armstrong et al., 2020).

5. JUSTIFICACIÓN

Según un informe de las Naciones Unidas de 2020 sobre el envejecimiento de la población mundial, durante las próximas tres décadas se proyecta que el número de personas mayores en todo el mundo supere los 1500 millones en 2050. Con este aumento de la esperanza de vida, la humanidad se enfrenta ahora a patologías que no representaban un problema de salud pública antes, sin embargo, las patologías neurodegenerativas como el deterioro cognitivo se han convertido en las condiciones más temidas de las personas mayores. Varias capacidades cognitivas disminuyen con la edad, incluso en ausencia de Alzheimer, demencia u otras patologías. Un candidato bien descrito para esta pérdida de capacidades cognitivas es el volumen cerebral. Sin embargo, los eventos celulares y moleculares que promueven los cambios volumétricos del cerebro durante el envejecimiento no han sido caracterizados y, en algunos casos, aún son mal entendidos.

Es por esto que, en esta tesis, se analizó la contribución del perfil proinflamatorio central y la plasticidad morfológica de la microglía durante el envejecimiento para describir lo que sucede a nivel celular en los cambios volumétricos en regiones selectivas del cerebro asociadas con el deterioro cognitivo.

6. HIPÓTESIS

La neuroinflamación durante el envejecimiento provoca alteraciones estructurales en el sistema nervioso central que se manifiestan en déficits cognitivos y alteraciones conductuales.

7. OBJETIVOS

7.1 Objetivo General

Identificar el papel de la neuroinflamación en el deterioro cognitivo durante el envejecimiento usando *Mus musculus* como modelo.

7.2 Objetivos específicos

1. Evaluar el aprendizaje y la memoria de ratones macho C57BL/6 durante el envejecimiento en grupos de 2, 12 y 20 meses de edad.
2. Determinar los perfiles inflamatorios central y periférico en el proceso de envejecimiento murino en grupos de 2, 12 y 20 meses de edad.
3. Identificar cambios estructurales en regiones cerebrales de los ratones de 2, 12 y 20 meses relacionadas con el proceso de aprendizaje-memoria MRI.

8. MATERIALES Y MÉTODOS

En la Figura 1 se encuentra descrita la estrategia general.

La estrategia general del proyecto consistió en: todos los ratones de los grupos de 2, 12 y 20 meses de edad realizaron las diferentes pruebas de memoria (Laberinto en Y, NORT, Laberinto de Barnes y OLT) para determinar su capacidad de memoria y aprendizaje. Posteriormente, los grupos fueron divididos en dos cohortes: el cohorte 1 al que se le realizaron los análisis de resonancia magnética estructural y el análisis morfológico de la microglia; y el cohorte 2, que fueron los ratones a los que se le analizaron los perfiles citocinas en sangre y en la región fórnix y corteza entorrinal medial (Fig. 1). Finalmente, se realizaron análisis estadísticos para determinar correlaciones entre las pruebas de memoria y aprendizaje, los cambios de volumen y los perfiles de citocinas.

8.1 Área de estudio

Este proyecto pertenece al área de estudio de las neurociencias y neuroinmunología.

8.2 Materiales

Tabla 1. Materiales utilizados en el modelo de envejecimiento del modelo murino

Reactivo	No. Cat.	Aplicación	Concentración	Proveedor
Pentobarbital	Q-7833-215	Eutanasia	150 mg/kg	PiSA Agropecuaria, Jalisco, México
kit MILLIPLEX MAP Kit Mouse Cytokine / Chemokine Magnetic Bead Panel	MCYTOMAG-70K	Cuantificación de citocinas	N/A	Milli-pore corporation, Massachusetts, USA
Triton X-100	93443	Inmunofluorescencia	0.01%	Sigma-Aldrich, MO,

				USA
Paraformaldehido	158127	Fijación *ex-vivo*	4%	Sigma-Aldrich, MO, USA
Prohance	N/A	MRI	4 mM	Bracco Diagnostics, NJ, USA
Fomblin	N/A	MRI	N/A	Sigma-Aldrich, MO, USA
Anti-Iba1 (rabbit)	ab178846	Inmunofluorescencia	1:200	abcam, Cambridge, MA, USA
Anti-synaptophysin (rabbit)	N/A	Inmunohistoquímica	1:200	GenScript, NJ, USA
Vectashield con DAPI	H-1200-10	Inmunofluorescencia	N/A	Vector Laboratories, CA, USA
Mouse and Rabbit Specific HRP/DAB	ab64264	Inmunohistoquímica	1:200	abcam, Cambridge, MA, USA
Alexa-Fluor 488 goat anti-rabbit	# A32731	Inmunofluorescencia	1:1000	Thermofisher, MA, USA

8.3 Animales de laboratorio

Todos los experimentos con animales fueron aprobados por el Comité Institucional de Cuidado y Uso de Animales de la Universidad Autónoma de Nuevo León (CEIBA-2018-006) y se llevaron a cabo de acuerdo con las regulaciones de la Asociación para la Evaluación y Acreditación de Cuidado de Animales de Laboratorio Internacional, el Departamento de Agricultura de EE. UU. Ley de Bienestar Animal y la Guía para el Cuidado y Uso de Animales de Laboratorio de los NIH. Se hicieron todos los esfuerzos para minimizar el número de animales utilizados y su sufrimiento.

A su llegada, los ratones C57BL/6 macho de 2, 12 y 20 meses de edad (n = 30/grupo de edad) se alojaron en jaulas estilo plexiglás durante al menos 10 días para aclimatarse con acceso ad libitum a Chow estándar, dieta y agua, temperatura de 23-25º C, y 12:12 h control de luz. Los ratones de 2, 12 y 20 meses de edad se dividieron en dos cohortes de 15 ratones cada una para caracterizar los cambios de macro y microplasticidad utilizando resonancia magnética, inmunofluorescencia e inmunohistoquímica y análisis morfológico cerebral (cohorte 1) y análisis Bioplex para central y marcadores proinflamatorios periféricos (cohorte 2) (Fig. 1). El fenotipado conductual se realizó en ambas cohortes como se describe a continuación.

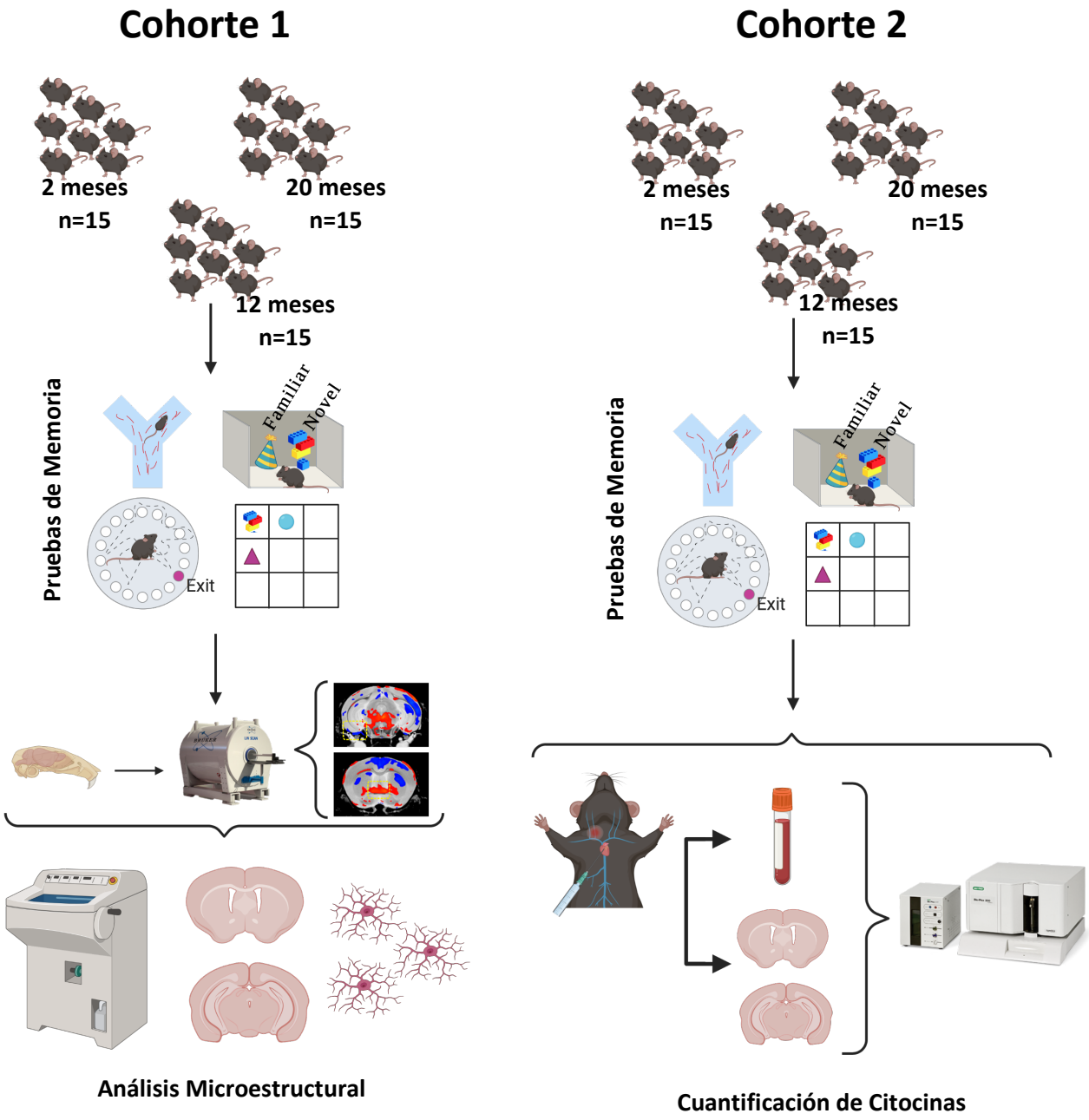

Figura 1. Estrategia general del diseño experimental del modelo de envejecimiento murino. A) Los ratones de la cohorte 1 (n = 15) fueron sometidos a la batería de pruebas de comportamiento seguido de un sacrificio ético, aislamiento de plasma y cuantificación de citocinas utilizando la plataforma BioPlex. B) De la misma manera, los ratones de la cohorte 2 (n = 15) fueron sometidos a todas las pruebas de comportamiento y luego se evaluaron los cambios macroestructurales con MRI y la evaluación microestructural consistió en evaluar la microglía en el fórnix y MEntC izquierda creado con BioRender.com

8.4 Evaluación del deterioro cognitivo a través de pruebas de memoria y aprendizaje

La batería de pruebas de memoria y aprendizaje se realizó en las dos cohortes de ratones exponiéndolos a cuatro pruebas de memoria en el siguiente orden: alternancia forzada del laberinto en Y, Reconocimiento de objetos nuevos (NORT), laberinto de Barnes y Reconocimiento de Ubicación de Objetos (OLT) (Fig. 2 A). Se siguió un orden específico para realizar las pruebas de modo que los ratones tuvieran varios días de descanso entre las tareas y evitar posibles efectos de las pruebas anteriores (Fig. 2 A). Se colocaron señales visuales en las paredes del área de prueba para todas las pruebas excepto la NORT. Todos los ratones se habituaron a la sala de pruebas durante 1 hora antes de cada día de prueba. Todas las pruebas de comportamiento fueron realizadas por el mismo experimentador para evitar un estrés adicional en los animales.

8.4.1 Laberinto en Y

Las pruebas de alternancia forzada se realizaron utilizando un laberinto en Y simétrico, cada brazo tenía 35 cm de largo, 5 cm de ancho y 10 cm de alto, y la pared al final de cada brazo estaba marcada con una señal visual diferente (Fig. 2 B). Seguimos el protocolo informado por Andrea Wolf y colaboradores (Wolf et al., 2016) con ligeras modificaciones. En resumen, la prueba consistió en una prueba de muestra de 15 min (T1) seguida de una prueba de recuperación de 15 min (T2). En T1, el ratón se colocó en el extremo del brazo de inicio, mirando hacia la pared y lejos del centro. Luego se permitió al ratón explorar dos brazos del laberinto en Y, mientras que la entrada al tercer brazo estaba bloqueada por una barrera. Después de la T1, el ratón se devolvió a su jaula de origen durante un intervalo entre pruebas de 30 minutos. En T2, se eliminó la barrera en el brazo 3, se colocó nuevamente al ratón en el brazo de inicio y luego se le permitió acceder a los tres brazos del laberinto. Después de cada animal y entre T1 y T2, el laberinto se limpió con etanol al 70 % para evitar pistas olfativas. El tiempo en el brazo nuevo (segundos) se contó en función de cuántos segundos pasó el ratón explorando el brazo nuevo. La alternancia forzada (%) se definió como el porcentaje de ratones que entraban primero en el brazo novedoso durante T2. Se excluyeron del análisis los ratones con menos de tres entradas de brazos en el primer minuto de T2.

8.4.2 Reconocimiento de Objetos Novedosos

La NORT se estandarizó en el laboratorio de acuerdo a los descrito previamente por (Bevins and Besheer, 2006) (Fig. 2 E). La prueba se llevó a cabo en arenas cuadradas idénticas (40 × 40 cm) rodeadas de paredes (35 cm de alto). En resumen, la prueba se llevó a cabo como un programa de tres pasos que consistió en una fase de habituación de 15 minutos donde el ratón exploró libremente la caja vacía, un paso de familiarización que consistió en colocar los dos objetos idénticos en campo abierto y finalmente la prueba de reconocimiento, donde se colocaron los dos objetos familiares, uno con la copia por triplicado (para asegurarse de que no haya señales olfativas residuales en el objeto utilizado anteriormente) y el otro por un objeto novedoso. Después de cada prueba, los objetos y las cajas se limpiaron con etanol al 70 % para eliminar las pistas olfativas. El tiempo de exploración del nuevo objeto se midió en segundos, los ratones con menos de 7 s de interacción total con el objeto en cualquiera de los ensayos se excluyeron del análisis como se informó previamente (Kalueff et al., 2006). La interacción de objeto [%] para el objeto familiar se calculó como (interacción de objeto familiar x 100) / (interacción de objeto familiar + interacción de objeto nuevo) y la interacción de objeto [%] para el objeto nuevo se calculó como (interacción de objeto nuevo x 100) / (interacción con objetos familiares + interacción con objetos novedosos).

8.4.3 Laberinto de Barnes

Esta prueba se estandarizó en el laboratorio de acuerdo a los descrito previamente por (Sunyer et al., 2007) (Fig. 2 G). Brevemente, la prueba consistió en una fase de adaptación, adquisición espacial y dos pruebas de pruebas de memoria (memoria a corto y largo plazo) como se describirá a continuación: En el período de adaptación, los ratones fueron guiados suavemente hacia la caja de escape y permanecieron allí durante 2 min. Luego, durante la adquisición espacial, los ratones realizaron 4 pruebas por día con un intervalo entre pruebas de 15 minutos durante 4 días. Brevemente, los ratones se colocaron en el medio del laberinto dentro de una cámara de inicio cilíndrica negra. Después de transcurridos 10 s, se levantó la cámara y se permitió al ratón explorar el laberinto libremente durante 3 minutos. Durante estos 3 minutos, el experimentador

midió el número de errores totales y la latencia primaria. Finalmente, la prueba de memoria de referencia corta se realizó el día 5, 24 h después del último día de entrenamiento, y la prueba de memoria de referencia larga se realizó 7 días después del último entrenamiento, que sería el día 12. Durante estos ensayos, los ratones recibieron 30 segundos para Al final de la prueba, el experimentador midió el número total de errores y la latencia para escapar.

8.4.5 Prueba de ubicación de objetos

Esta prueba se estandarizó en el laboratorio de acuerdo a los descrito previamente por (Bello-Medina et al., 2013). El aparato utilizado fue una caja acrílica abierta de 45 cm × 45 cm con paredes de 45 cm de altura. La caja se limpió con etanol al 70 % después de cada ratón. Brevemente, la prueba constaba de cuatro fases: habituación, entrenamiento, intervalo de retención y prueba de memoria. Durante la fase de habituación, se permitió a los ratones explorar libremente la caja abierta sin objetos. Cada animal se colocó individualmente en él durante 3 min durante el primer día. Posteriormente, durante la fase de entrenamiento, cada ratón se colocó en la caja abierta, que contenía los 3 objetos de muestra, durante una prueba de 5 minutos por día. Consecutivamente, durante el intervalo de retención, todos los ratones permanecieron en sus jaulas durante 24 h o 7 días después de la última prueba de entrenamiento. Finalmente, ya sea 24 h o 7 días después del último entrenamiento, se llevó a cabo la prueba, que consistió en utilizar los mismos objetos utilizados durante el entrenamiento (a, b, c) pero la ubicación de un objeto familiar cambió a una ubicación desconocido previamente por cualquiera de los objetos (Fig. 1 J). El tiempo de exploración de los objetos se midió de la siguiente manera: la interacción con el objeto [%] para el objeto familiar se calculó como (interacción con el objeto familiar x 100) / (interacción con el objeto familiar + interacción con el objeto nuevo) y se calculó la interacción con el objeto [%] para el objeto nuevo como (interacción de objeto novedoso x 100) / (interacción de objeto familiar + interacción de objeto novedoso).

8.5 Fijación *ex vivo* y análisis de resonancia magnética por morfometría basada en deformación (DBM)

Se asignaron ratones macho de la cohorte 1 (n = 15 de 2 meses, n = 15 de 12 meses y n = 15 de 20 meses) para realizar un análisis de resonancia magnética (MRI). Después del preprocesamiento y el control de calidad se excluyeron las imágenes de MRI que presentaban artefactos en la adquisición. Finalmente, se analizó un grupo de n = 12 para los ratones de 2 meses, 12 meses y 20 meses.

Se realizó una disección dérmica desde la región abdominal hasta la parte superior de la caja torácica, exponiendo el corazón. Luego, se punzó el ventrículo izquierdo del corazón siguiendo su vértice y se hizo un corte en la aurícula derecha para abrir el sistema circulatorio. Los ratones se perfundieron transcardialmente con PBS 0,1 M + heparina (10 U/ml) + solución de lavado Prohance (4 mM) utilizando una bomba de infusión (Fisher Scientific GP1000) a una velocidad de flujo de 1 ml/min. Posteriormente, la solución de lavado se cambió a la solución fijadora que incluía paraformaldehído (PFA) al 4% en PBS 0,1 M + Prohance 4 mM durante 25 min, siguiendo el mismo flujo, como se reportó anteriormente (Trujillo-Villarreal et al., 2021). Se recolectó el cerebro protegido por el cráneo y las muestras se almacenaron a 4 °C en PFA al 4 % + Prohance 4 mM durante 24 horas y luego se cambió la solución a PBS 0,1 M + azida de sodio al 0,02 % hasta su posterior análisis por MRI.

Para la adquisición de MRI, los cráneos se sumergieron y se fijaron dentro de tubos de plástico llenos de Fomblin (un fluorocarbono de perfluoropoliéter químicamente inerte; Solvay Solexis, Inc.). La obtención de imágenes se realizó en un escáner Bruker 7 T de 16 cm de diámetro interior (Pharmascan 70/16) utilizando un sistema Paravision 6.0.1 y una bobina de volumen Tx/Rx para ratones con un diámetro interior de 72 mm. Después se adquirió un nombre de secuencia T1w Bruker FLASH: 3D_FLASH_Mn_Garza, TR/TE = 32,88/8,64 ms, ángulo de giro = 20 grados, promedios = 1, matriz = 256 × 256 x 256, espaciado = 0,050 mm, ancho de banda de píxeles = 108,507 Hz, FOV = 12,8 x 12,8 x 12,8 mm, n. de cortes = 255. La resolución de las imágenes de resonancia magnética finales fue isotrópica de 0,05 mm. El análisis morfológico se realizó convirtiendo DICOM a formato MINC y luego se preprocesó utilizando una tubería interna basada en MINC-Tools y la tubería pydpiper (https://github.com/Mouse-

Imageing-Centre/pydpiper). Todos los análisis se realizaron con los paquetes pydpiper versión 1.8 (Friedel et al., 2014), R studio versión 3.6.3 (Rstudio, 2020) y RMINC versión 1.5.2.2 (Lerch, JP., 2017) y tidyverse versión 1.3.1 (Wickham, H., 2017).

Todas las imágenes se convirtieron de formato DICOM a MINC y, luego, se preprocesaron utilizando una tubería interna basada en MINC-Tools y ANT, donde se realizaron los siguientes pasos: imagen central, máscara completa y corrección de campo de polarización N4. Después se utilizó un enfoque basado en el registro de imágenes para evaluar las diferencias anatómicas entre los grupos. El registro de imágenes encuentra una transformación espacial suave que alinea una imagen con otra, de modo que se superponen las características anatómicas correspondientes. Se realizó un enfoque de registro grupal basado en la intensidad automatizado (Lerch, JP., 2011) para alinear todos los cerebros del estudio en un sistema de coordenadas común, lo que produjo una imagen promedio de los 45 escaneos T1w. La deformación que alinea las imágenes se convirtió en un resumen de cómo se diferencian. Para evaluar las diferencias de volumen entre los grupos, se realizamó DBM, pues proporciona una definición continua vóxel por vóxel de los cambios de volumen (expansión/contracción) relacionados con la edad del sujeto. Luego, las deformaciones se mapearon desde los escaneos individuales hasta la imagen promedio. Los campos de deformación finales se calcularon con un registro difeomorfo simétrico codicioso (el algoritmo SyN en ANTS) (Avants, B. et al., 2008; Bird, S. et al., 2009), se invirtieron y desdibujaron con un FWHM Gaussiano de 0,1 mm con un núcleo suavizante. Se extrajeron los determinantes jacobianos de estas deformaciones, dando una medida de la expansión/contracción del volumen local en cada vóxel del cerebro. Se utilizaron determinantes relativos jacobianos transformados logarítmicamente (0,2 mm *blurry*) para evaluar las diferencias entre los grupos porque estiman mejor una distribución normal.

8.6 Análisis histológico

Los cerebros del análisis de la cohorte 1 MRI (n = 4) se recolectaron aleatoriamente, se sacaron de los huesos del cráneo y se incubaron en sacarosa al 10 %, 20 % y 30 % + PBS 0,1 M y en un criostato se obtuvieron secciones coronales de 30 μm para dos regiones, fórnix (Fornix, Bregma 4,28 mm a – 0,14 mm) y Corteza Entorrinal medial

izquierda (MentC izquierdo, Bregma 4,04 mm a – 0,22 mm). Los límites anatómicos de cada región del cerebro se identificaron utilizando el atlas de cerebro de ratones (Paxinos y Franklin, 2001).

8.7 Inmunohistoquímica para sinaptofisina

La inmunohistoquímica de los cerebros de la cohorte 1 se realizó como se reportó previamente en (Trujillo-Villarreal et al., 2021).

Los cortes de cerebro de ratón de 2, 12 y 20 meses de edad (n = 4/grupo de edad) se lavaron 2 veces con PBS 0,1 M + TritonX-100 al 0,1 %, se incubaron con el bloqueador de peroxidasa durante 10 minutos (Abcam, Cat. AB64264), después se lavaron con PBS 0,1 M + TritonX-100 al 0,1 % y se incubaron con el bloqueador de proteínas durante 10 minutos (Abcam, Cat. AB64264). Posteriormente, las secciones se incubaron con PBS 0,1 M + TritonX-100 al 0,1 %, seguido del anticuerpo anti-sinaptofisina primario (4 µg/mL, Genscript Cat. A01307) a 4° C durante la noche.

Finalmente, las secciones se expusieron al anticuerpo secundario IgG anti-conejo de cabra biotinilado durante 10 minutos, seguido de estreptavidina (10 min) y solución de cromógeno de diaminobencidina (30 µl en 1,5 ml de sustrato) durante 10 minutos.

El montaje de los cortes se realizó con solución de montaje sobre cubreobjetos. Se prepararon controles por omisión de anticuerpos primarios y se consideraron negativos cuando no se identificó señal de densitometría.

8.8 Inmunofluorescencia para Iba-1

La inmunofluorescencia de los cerebros de la cohorte 1 se realizó como se reportó anteriormente (Maldonado-Ruiz et al., 2019). Sin embargo, se trabajaron en cortes de forma flotante; estas secciones flotantes de 30 µm de ratones de 2, 12 y 20 meses de edad (n = 4/grupo de edad) se lavaron tres veces durante 5 min con 1X PBS + 0,1% TritonX-100 (PBST) y se bloquearon con PBST + suero de cabra al 10% + suero de caballo al 10% a temperatura ambiente durante una hora. Posteriormente, las secciones se incubaron con el anticuerpo primario anti-Iba1 1:200 (ab178847, abcam, Cambridge, MA, EE. UU.) a 4 °C durante 48 h. Dos días después, las secciones se lavaron en PBST tres veces y se incubaron durante dos horas con el anticuerpo secundario Alexa fluor

anti-rabbit 1:1000 (A-11034, Invitrogen) diluido en PBST + suero de cabra al 1% + suero de caballo al 1%. Posteriormente, las secciones de cerebro se lavaron tres veces con PBST y se secaron a temperatura ambiente. Finalmente, las secciones de cerebro se montaron usando Vectashield con DAPI (Vector Laboratories, Burlingame, CA, EE. UU.) en cubreobjetos y se visualizaron en el microscopio confocal.

8.9 Análisis morfológico de la microglía

La morfología de la microglía se analizó en cerebros de la cohorte 1 como se describió previamente por Young and Morrison, 2018 utilizando el software gratuito Fiji: una plataforma de código abierto para el análisis de imágenes biológicas. Brevemente, se describe el procedimiento a continuación: se obtuvieron células Iba1+ positivas en el tejido cerebral y las imágenes se convirtieron en 8 bits y después en escala de grises. Las imágenes se ajustaron a los controles mínimo o máximo según fuera necesario, hasta los bordes del histograma, seguidas por un filtro de máscara de enfoque. Luego, realizamos una eliminación de *background* para eliminar todo el ruido de *salt and pepper*, se convertió a binario y se usó la función de eliminación de valores atípicos. Posteriormente, las imágenes se guardaron por separado y, mediante el uso del complemento *Skeleton*, medimos la longitud de los procesos de la microglía y el número de terminaciones de ésta. Finalmente, los resultados fueron graficados y analizados de acuerdo al protocolo publicado.

8.10 Cuantificación de citocinas en sangre periférica, fórnix y MEntC izquierdo

Se sacrificaron los ratones de la cohorte 2 con una sobredosis de 500 µL i.p. de pentobarbital (PiSA Agropecuaria) y se recolectó la sangre periférica a través de punción cardíaca; ésta se mantuvo en tubos de heparina de plasma de heparina BD Vacutainer™ de grado farmacéutico (BD 368480), y los cerebros se diseccionaron, recolectaron y congelaron (-80 °C) para su uso posterior.

Los tubos de sangre se centrifugaron a 2500 rpm durante 20 minutos y se recogió el plasma. De acuerdo con el análisis de MRI, se seleccionó el fórnix y MEntC izquierda porque mostraron los cambios de volumen más dramáticos con la edad. Para aislar selectivamente el fórnix y el MEntC izquierdo, se obtuvieron en el criostato secciones

coronales de 40 μm del fórnix (Bregma 4,28 mm a –0,14 mm) y MEntC izquierdo (Bregma 4,04 mm a –0,22 mm). Luego, utilizando el atlas de cerebro de ratón (Paxinos y Franklin, 2001) y bajo el estereoscopio de disección (Leica, ez4) con un bisturí, las regiones selectivas se cortaron y recolectaron en tubos de 0.1 mL.

El perfil de citocinas en plasma, fórnix y el MEntC izquierdo se identificó utilizando el panel de microesferas magnéticas de citocinas/quimiocinas de ratón del kit MILLIPLEX MAP (Millipore Corporation, MCY-TOMAG-70K), siguiendo las instrucciones del fabricante. En resumen, para el análisis de citoquinas en el cerebro, Fornix o MEntC izquierda se incubaron en 70 μL de solución de tampón de lisis (Millipore corporation, 43-040), se homogeneizó por sonicación (amplitud 20% 3 pulsos/segundo 10 veces), seguido por centrifugación a 10,000 RPM a 4°C y luego se aisló el sobrenadante.

Las lecturas de las muestras de sobrenadante del plasma, el fórnix y MEntC izquierdo se realizaron empleando el instrumento Luminex® 200™ (Luminex Corporation, LX200-XPON3.1). Medimos las citocinas proinflamatorias IL-1β, IL-6, IL-12, TNF-α y MCP-1.

8.11 Análisis de componentes principales (PCA)

El análisis de PCA implica la composición de una matriz 2D de datos como una herramienta efectiva de reducción de dimensiones que retiene la información de los datos originales tanto como sea posible (Wu et al., 2019). En este estudio, integramos 38 variables (comportamiento, niveles de citoquinas cerebrales y periféricas y volúmenes de regiones cerebrales) para el análisis PCA. El PCA se realizó para proporcionar una indicación de la capacidad de las variables para agrupar a los individuos de acuerdo con su rendimiento en la prueba de memoria y aprendizaje, los niveles de citocinas y el volumen cerebral. Las contribuciones de las variables al análisis PCA se pueden encontrar en la Información complementaria.

8.12 Análisis estadístico

Los resultados se presentan como media ± SEM para todos los datos. Todos los análisis estadísticos, incluída la prueba de la normalidad de la distribución de datos, se realizaron con GraphPad Prism 7.01 y el software estadístico IBM SPSS versión 22 y se consideró significativo un valor de p corregido <0,05. Se probó la normalidad de todos los

resultados usando la prueba de Shapiro-Wilk. Para las diferencias entre los 3 grupos en las pruebas de comportamiento, se utilizó ANOVA de una vía seguido de la prueba de comparación múltiple de Tukey y se calculó el tamaño del efecto en lenguaje R. Las diferencias significativas en el rendimiento cognitivo durante las pruebas de conducta se muestran como la media ± SEM y las diferencias significativas en $p < 0,05$. El análisis estadístico para DBM se realizó utilizando los determinantes jacobianos transformados logarítmicamente como variable dependiente, "grupo de edad" como variable independiente (entre sujetos) y "peso" como covariable (peso del ratón al momento de la eutanasia). Se compararon los tres grupos usando un modelo lineal general y los análisis se corrigieron para comparaciones múltiples usando la tasa de descubrimiento falso (FDR) al 5%. Además, se extrajeron los valores jacobianos de picos significativos en V1: corteza visual primaria, FX: fórnix, S2: corteza somatosensorial secundaria, OB: bulbo olfativo, VIIB: lóbulo paramediano (lóbulo 7), MEntC: corteza entorrinal medial, A1: primaria corteza auditiva, Amg: Amígdala. Los jacobianos de las regiones de interés se correlacionaron con el comportamiento, las citocinas y los datos histológicos para explorar su patrón de asociación mediante la correlación de *Pearson* y se corrigieron mediante el FDR al 5 %. Estos análisis se realizaron en R studio versión 3.6.3.

9. RESULTADOS

9.1 El envejecimiento altera el rendimiento cognitivo y de la memoria en ratones macho

El fenotipado conductual individual se realizó en dos cohortes de sujetos para determinar el efecto del envejecimiento sobre el deterioro cognitivo.

Seleccionamos pruebas de comportamiento para evaluar la memoria de trabajo (alternancia forzada), la memoria espacial (Laberinto de Barnes y OLT), la discriminación de objetos (NORT), y la memoria a corto y largo plazo (Laberinto de Barnes y OLT) (Figura 2 A). Diseñamos la batería de pruebas para su uso en estudios a largo plazo que evalúan el aprendizaje y la memoria y, por lo tanto, consideramos las deficiencias que podrían ocurrir potencialmente en los ratones durante el envejecimiento (p. ej., disminución de la fuerza muscular, la coordinación motora, el equilibrio y la velocidad). Además, para evitar cualquier estrés metabólico en los ratones, omitimos las pruebas que involucraban la restricción de alimentos (Wolf et al., 2016).

9.1.1 Alternancia Forzada

Se encontró un efecto dependiente de la edad sobre la memoria de trabajo en ratones C57BL/6. El envejecimiento disminuyó el porcentaje de alternancia forzada entre los ratones de 12 y 20 meses (ANOVA, F(2,42)= 12 meses: $^{**}p = 0.0049$ y 20 meses: $^{**}p = 0.0018$, respectivamente) en comparación con ratones de 2 meses (Fig. 2 B, C y D). Aproximadamente, el 60 % de los ratones de 12 meses y cerca del 20 % de los ratones de 20 meses que realizaron la prueba de alternancia forzada reconocieron el brazo bloqueado como novedoso y lo eligieron como su primera opción en comparación con el de 2 meses. En cambio, los ratones viejos mostraron una preferencia del 80% por el brazo conocido (Fig. 2 C). Cabe destacar que, los ratones de 12 y 20 meses asignaron menos tiempo al grupo nuevo en comparación con los ratones de 2 meses (ANOVA, F(2,42)= 12 meses: $^{****}p < 0.0001$ y 20 meses: $^{****}p < 0.0001$, respectivamente) (Fig. 2 D). Específicamente, los ratones de 12 y 20 meses pasaron 83,93 ± 14,3 s y 63,48 ± 15,81 s, respectivamente, en el brazo nuevo, en contraste con 135 ± 15,81 s de los

ratones de 2 meses, lo que confirma un efecto dependiente de la edad con respecto a la memoria y aprendizaje (Fig. 2 D).

9.1.2 Reconocimiento de objetos novedosos

El NORT evalúa la memoria de reconocimiento en ratones basándose en la predisposición innata de los roedores a investigar un objeto novedoso durante más tiempo que uno familiar (Fig. 1E) (Antunes and Biala, 2012). Los ratones de los tres grupos de edad demostraron una mayor interacción con el objeto nuevo en comparación con el objeto familiar (Figura 2 F). Sin embargo, el aumento en el tiempo de interacción solo fue significativo en ratones de 2 meses de edad, demostrado por el aumento de interacción con el objeto aumentando hasta un 68% con el objeto novedoso (ANOVA, $F(5,84)=$ ****$p < 0{,}0001$) (Fig. 2 F). Estos resultados confirmaron que el reconocimiento de novedosos en ratones envejecidos es defectuoso, confirmando otro rasgo del deterioro cognitivo, el cual en este caso es asociado a la edad.

9.1.3 Laberinto de Barnes

Se utilizó la prueba del laberinto de Barnes para evaluar la memoria espacial, así como el aprendizaje a corto y largo plazo.

En resumen, los sujetos fueron entrenados como se describió previamente y se cuantificó el número total de errores antes de llegar a la salida de la plataforma, así como la latencia para salir (Fig. 2 G). Se encontró que los ratones de 12 y 20 meses exhiben una memoria a corto plazo defectuosa (STM: evaluada un día después de la última sesión de entrenamiento) evidenciada por cometer más errores al encontrar la salida en comparación con los ratones de 2 meses (ANOVA, $F(5,100)=$ ****$p < 0.0001$ y ****$p < 0.0001$, respectivamente) (Fig. 2 H). De hecho, la STM defectuosa se exacerbó en ratones de 20 meses en contraste con ratones de 12 meses (ANOVA, $F(5,100)=$ **$p < 0{,}002$) (Fig. 2 H). Además, el deterioro en el rendimiento de la memoria se encuentra en etapas posteriores durante la prueba de memoria a largo plazo (LTM: evaluada a los siete días después de la última sesión de entrenamiento) en los ratones de 12 y 20 meses de edad en comparación con los ratones de 2 meses (ANOVA, $F(5,100)=$ ****$p < 0.0001$ y ****$p < 0.0001$, respectivamente) (Fig. 2 H).

También se observó un aumento en el tiempo para ubicar y salir del laberinto de forma edad-dependiente. A los ratones de 12 y 20 meses les tomó más tiempo para encontrar la salida durante las pruebas STM y LTM en comparación con el grupo de 2 meses (ANOVA, F(5,100)= ****p < 0,0001 y ****p < 0,0001, respectivamente) (Fig. 2 I). Estos resultados confirmaron que los ratones de 12 y 20 meses mostraron un rendimiento de memoria espacial comprometido.

9.1.4 Prueba de reconocimiento de ubicación de objetos

El envejecimiento puede causar cambios importantes en la velocidad y la locomoción que podrían sesgar el rendimiento defectuoso encontrado en la prueba del laberinto de Barnes. Para evitar un sesgo, evaluamos, nuevamente, la memoria y el aprendizaje espacial en un pequeño escenario utilizando el OLT (Fig. 2 J). Los ratones de dos meses de edad investigaron los objetos en ubicaciones novedosas significativamente más que los objetos en ubicaciones familiares cuando se probaron usando ambas versiones de la prueba, tanto a corto como a largo plazo, realizadas uno o siete días después del entrenamiento, respectivamente (Figura 2 K - L) (ANOVA, F(5,84)= ****p < 0.0001). En comparación, los ratones de 12 y 20 meses no interactuaron con el objeto en un lugar nuevo significativamente más que en un lugar familiar. Estos resultados confirmaron el deterioro dependiente de la edad en el rendimiento de la memoria espacial en ratones de 12 y 20 meses (Fig. 2 K - L).

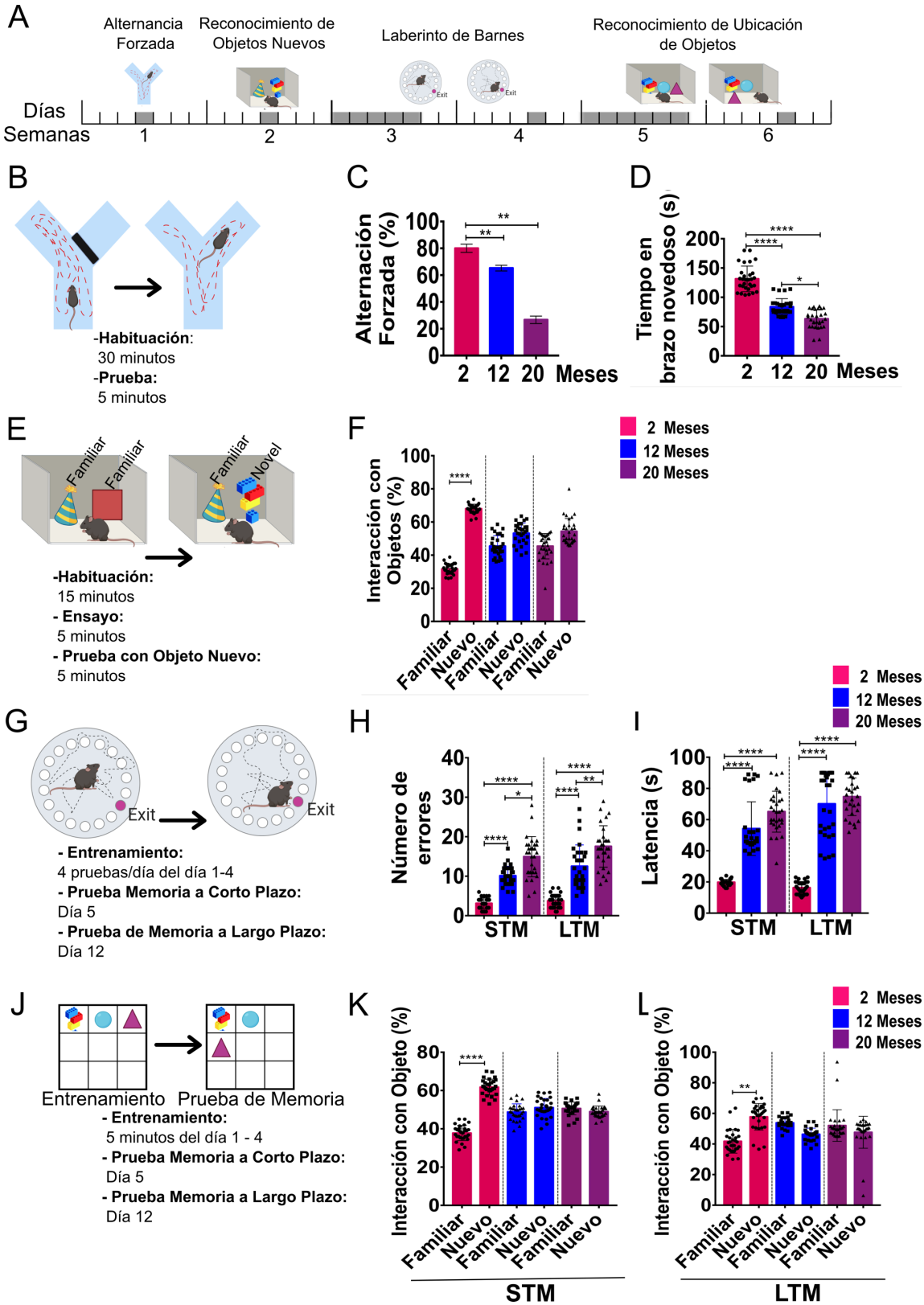

Figura 2. Fenotipado conductual de ratones macho C57BL/6. A) Se utlizaron ratones de 2, 12 y 20 meses de edad en una batería de prueba de comportamiento que constaba de alternancia forzada (laberinto en Y), laberinto de Barnes, NORT y OLT durante un período de 5 semanas. B) En la prueba del laberinto

en Y, los ratones fueron expuestos a una sesión de familiarización durante 5 minutos (T1), luego fueron devueltos a su jaula durante 30 minutos y durante la prueba (T2) se evaluó la alternancia forzada y el tiempo de permanencia en el brazo novedoso en el laberinto Y. C) La prueba de alternancia forzada fue evaluada de acuerdo con el brazo elegido como primera opción en el laberinto en Y durante T2. Los resultados mostraron el porcentaje de alternancia de los diferentes grupos de edad. D) El tiempo de permanencia en el brazo novedoso se realizó 30 minutos después de la sesión de familiarización. Los resultados mostraron el tiempo pasado (s) en el brazo nuevo durante la prueba T2 entre los diferentes grupos. E) El rendimiento de la memoria de reconocimiento se evaluó con la NORT, siguiendo el protocolo ilustrado en la imagen. F) El tiempo pasado con el objeto familiar y el objeto nuevo se representó como % de interacción del objeto. G) La prueba del laberinto de Barnes evaluó la memoria espacial a corto plazo (STM) un día después del último día de entrenamiento y la memoria a largo plazo (LTM) se evaluó 7 días después de la última sesión de entrenamiento. H) El gráfico muestra el número de errores antes de que se encontrara la salida en las pruebas STM y LTM. I) Los resultados muestran la latencia para salir (s) hasta que se encontró la salida, tanto para STM como para LTM. J) También se evaluó STM y LTM con OLT. El tiempo pasado (%) con los objetos en la ubicación conocida (Familiar) se comparó con el objeto en la nueva ubicación (Nuevo). El porcentaje de tiempo dedicado a la interacción del objeto nuevo durante STM (K) y LTM (L). Los resultados se expresan como Media ± SEM seguido de ANOVA post-hoc Tukey n.s= 0.1234, *p= 0.03, **p= 0.002, ***p= 0.0002, ****p <0.0001. n=15/grupo. Creado con BioRender.com

9.2 Alteraciones macroestructurales cerebrales dependientes de la edad

Se realizó un análisis de MRI global para caracterizar selectivamente las alteraciones macroestructurales relacionadas con el volumen cerebral durante el envejecimiento de los ratones.

El análisis mostró diferencias significativas en el volumen local del cerebro completo en los ratones de 12 meses en comparación con el grupo de 2 meses (Fig. 3 A), lo mismo se observó entre los ratones de 12 meses en comparación con ratones de 20 meses (Fig. 3 B) y también, en los ratones de 2 meses en comparación con ratones de 20 meses, todos ellos corregidos por el FDR 5% (Fig. 3 C).

Se identificaron cambios importantes en el volumen local de todo el cerebro en los ratones de 20 meses en comparación con el grupo de 2 meses (Fig. 3 C). Selectivamente, el grupo de 20 meses fue el que mostró más cambios volumétricos en regiones cerebrales selectivas en comparación con el grupo de 2 meses con grupos más localizados (Tabla 2).

En la Tabla 2 se destacan en color rojo las regiones que sufrieron el cambio más drástico, el fórnix y la corteza entorrinal medial izquierda.

Tabla 2. Áreas afectadas por el agrandamiento y contracción del tejido por edad en los grupos de 2 vs 12 y 20 meses

Region Cerebral	Lado	t-stat	Cambio Volumen	Coordenadas			Valor de *p*: 2 vs 12	Valor de *p:* 2 vs 20
Primary visual cortex: monocular area	I	12.85	Higher	2.17	-2.03	3.16	3.50E-06	3.02E-08
Fornix	**I**	**11.82**	**Higher**	**0.17**	**2.41**	**-0.08**	**5.45E-05**	**6.11E-07**
Primary visual cortex	D	11.76	Higher	-3.43	-3.11	1.92	1.60E-05	3.09E-07
Secondary somatosensory cortex	I	4.166	Higher	5.09	0.93	0.24	1.13E-03	4.89E-05
Olfactory bulb: mitral cell layer	I	-12.07	Lower	1.53	4.17	3.32	1.60E-05	3.09E-07
paramedian lobule (lobule 7)	D	-8.538	Lower	-1.31	-5.91	0.36	5.81E-06	2.07E-05
Medial entorhinal cortex	**I**	**-7.839**	**Lower**	**2.85**	**-1.43**	**-2**	**0.00295**	**9.17E-05**
Primary auditory cortex	D	-7.759	Lower	-4.19	-1.11	1.64	5.70E-05	2.61E-05
amygdala	D	-6.086	Lower	-2.43	1.77	-2.52	0.049	0.00464

ANOVA de medidas repetidas a un umbral de p<0,001 (FDR corregido); Prueba t para aumento y disminución de volumen en el grupo de 20 meses en comparación con el grupo de 2 meses.

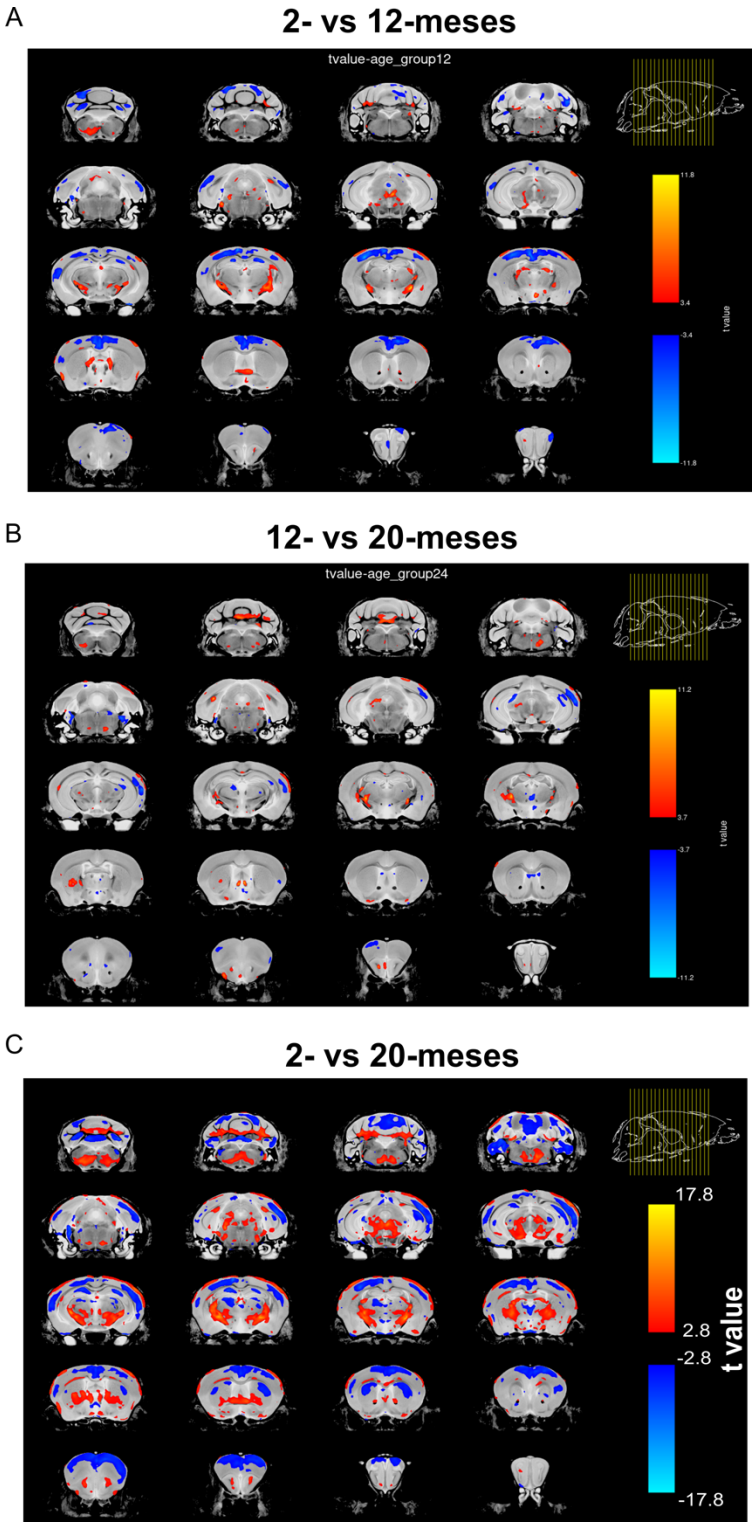

Figura 3. Comparación de volumen cerebral de ratones de 2 y 12 meses y ratones de 12 y 20 meses. Los cambios de volumen se ven representados con un mapa de calor, donde los colores azul-azul claro

indican menor volumen; y los colores rojo-amarillo indican mayor volumen A) DBM de ratones de 2 meses en comparación con el grupo de 12 meses. B) DBM de ratones de 12 meses en comparación con ratones de 20 meses. C) DBM de ratones de 2 meses en comparación con ratones de 20 meses. Los resultados son significativos a FDR 5%. n=12/grupo.

De acuerdo con los resultados de la MRI, se seleccionaron las regiones que mostraron un mayor cambio volumétrico. Con ayuda del Atlas de Cerebro de Ratón Paxinos y Franklin's, se identificó que el fórnix mostraba el mayor aymento de volumen, y la MentC izquierda, el mayor decremento de volumen en los ratones de 20 meses en comparación con los ratones de 2 meses (señalados en rojo en la Tabla 2) (Tabla 2, Fig. 4 A, B).

En particular, se calculó una regresión lineal simple para predecir los jacobianos en fórnix o MEntC izquierdo en función de la edad. Se encontró una ecuación de regresión significativa para predecir el fórnix ($F(2, 37) = 395{,}7$, $^{****}p < 0.0001$), con un R^2 ajustado de 0.952, y para predecir el MEntC izquierdo ($F(2, 37) = 63{,}09$, $^{****}p < 0.0001$), con un R^2 ajustado de 0.761. El fórnix es igual a -0.133 (2 meses) + 0.105 (12 meses) y -0.133 (2 meses) + 0.253 (20 meses) jacobianos. La MEntC izquierda es igual a 0,039 (2 meses) - 0,037 (12 meses) y 0,039 (2 meses) - 0,159 (20 meses) jacobianos. El volumen del fórnix aumenta 0.105 jacobianos a los 12 meses y 0.253 jacobianos a los 20 meses, mientras que el volumen del MEntC izquierdo disminuye -0.037 y -0,159 jacobianos a los 12 y 20 meses, respectivamente (Fig. 3 A, B).

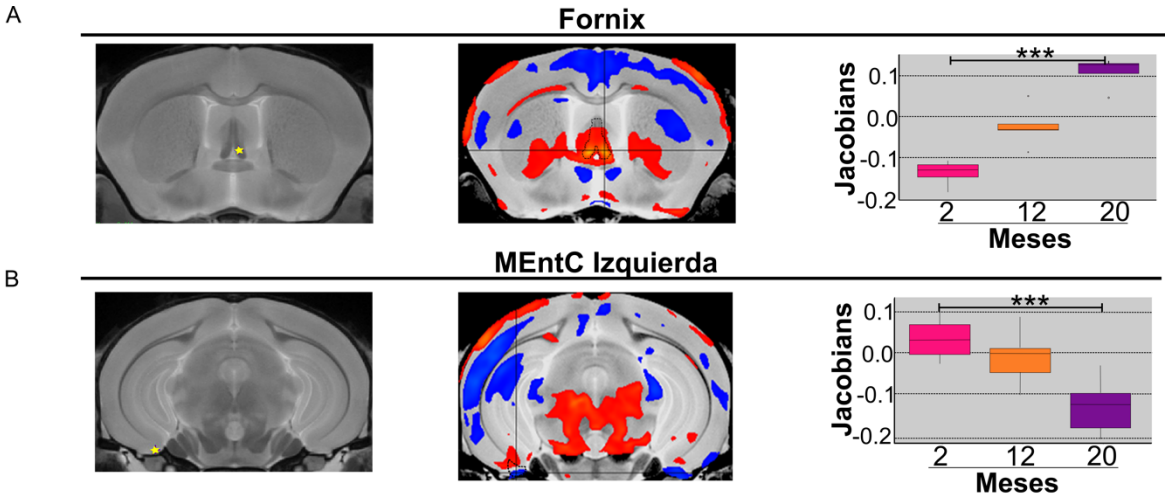

Fig. 4. Comparación del volumen cerebral de ratones C57BL/6 de 2 y 20 meses de edad. A-B) Las primeras imágenes que se observan son de MRI, en las cuales el fórnix y la MEntC izquierda se

encuentran señalados con una estrella amarilla. Seguido de éstas, están los datos de DBM, donde los colores azul-azul claro = menor volumen; rojo-amarillo = mayor volumen. Los resultados son significativos a FDR 5%. Se observa la gráfica demostrando el aumento de volumen relativo en fórnix y el decremento en MEntC izquierda. Los gráficos de barras muestran la media de datos +/- SEM seguido de ANOVA post-hoc Tukey. *p= 0,03, **p= 0,002, ***p= 0,0002. n=15/grupo.

9.3 Los cambios volumétricos en fórnix y MEntC izquierdo correlacionan con la edad y el rendimiento en tareas cognitivas

Se determinó si los cambios de volumen cerebral encontrados en el fórnix y en la MEntC izquierda durante el envejecimiento se correlacionaban con el rendimiento cognitivo y de la memoria. Las correlaciones de Pearson de los cambios de volumen cerebral frente a las tareas cognitivas se representan como mapas de calor (Fig. 5 A-C). Se encontraron correlaciones positivas y negativas entre diferentes áreas del cerebro y diversas tareas cognitivas que se resumen en la Figura 5 A, B, C. En particular, los ratones de 2 meses de edad mostraron una correlación positiva entre el volumen del fórnix y la cantidad de errores (Error_STM) antes de alcanzar la salida en el laberinto de Barnes durante la prueba STM (r = 0.58, *p = 0.02) (Fig. 5 A) y en el desempeño en el NORT (NOR_P) (r = 0.67, ***p = 0,008) (Fig. 5 A). Por el contrario, se encontró una correlación negativa entre el fórnix y el el número de errores en el laberinto de Barnes durante la prueba LTM (Error_LTM) (r = -0.64, **p = 0.01) (Fig. 5 A). También, se encontró una correlación positiva entre el volumen en la MEntC izquierda y el número de errores (Error_LTM) en el laberinto de Barnes durante la prueba LTM (r = 0,63, **p = 0,01) y en el rendimiento durante el OLT en la prueba LTM (OLT_LTM) con relación con el volumen de MEntC izquierda (r = 0,54, *p = 0,04) (Fig. 5 A).

A los 12 meses de edad, el aumento de volumen en el fórnix se correlacionó positivamente con el número de errores durante STM y LTM (Error_STM, Error_LTM) en el laberinto de Barnes (STM: r = 0,58, *p = 0,03; LTM: r = 0,64, *p = 0,04) así como durante la OLT (OLT_STM) en la prueba STM (r = -0,32, **p = 0,01) (Fig. 5 D). Curiosamente, también se encontró una correlación negativa entre MEntC y la cantidad de errores (Error_STM) en el laberinto de Barnes durante LTM (r = -0.48, *p = 0.02) (Fig. 5 B). Asimismo, la disminución de volumen en la MEntC izquierda mostró una correlación negativa con el OLT en la prueba STM (OLT_STM) (r = 0.24, ***p = 2.75x10-5) (Fig. 5 B).

Finalmente, el mayor aumento de volumen en el fórnix encontrado en ratones de 20 meses mostró una correlación positiva con el tiempo transcurrido antes de encontrar la salida (Time_STM) en el laberinto de Barnes durante la prueba STM (r = 0.67, **p* = 0.01), de manera similar durante NORT (NOR_P) (r = 0,55, **p* = 0,05) y OLT durante LTM (OLT_LTM) (r = 0,91, ****p* = 0,0001) (Fig. 5 C). Se encontró una correlación negativa selectiva entre la disminución de MEntC izquierdo con el rendimiento en OLT (OLT_LTM) durante la prueba LTM (MEntC: r = -0.70, ***p = 0.007) (Fig. 5 C).

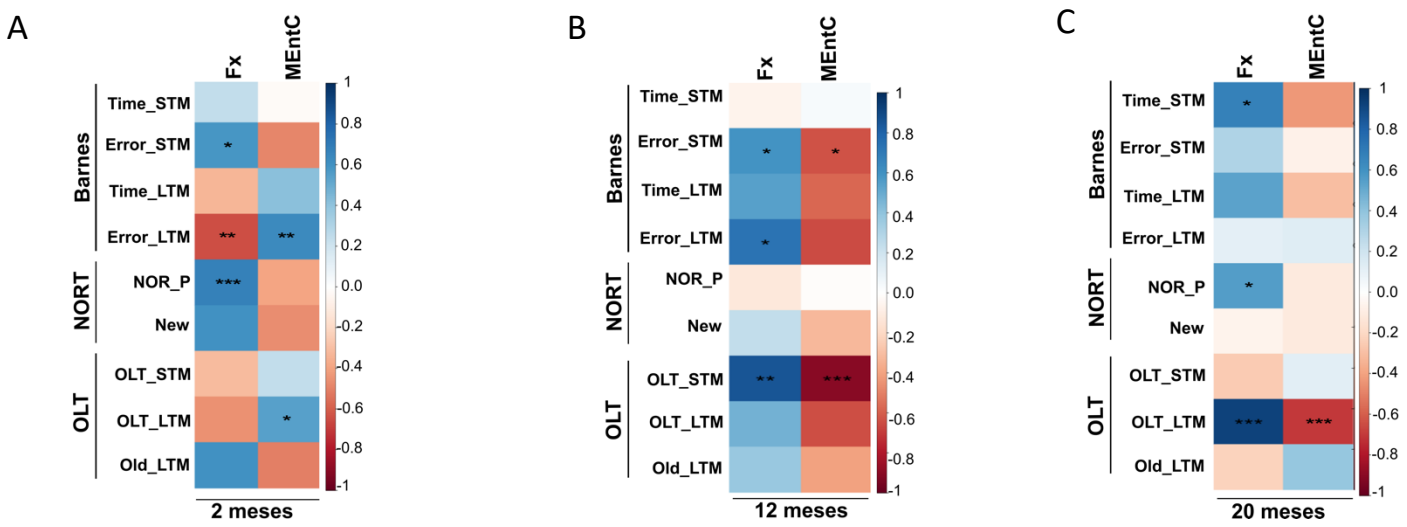

Figura 5. Los cambios volumétricos en fórnix y MEntC izquierdo se correlacionan con la edad y el rendimiento en tareas cognitivas. A-C) Mapas de calor de la prueba de correlación de Pearson entre los cambios volumétricos cerebrales y el rendimiento cognitivo. Correlación de Pearson, **p*= 0,03, ***p*= 0,002, ****p*= 0,0002. n=15/grupo.

9.4 El envejecimiento favorece un perfil de citocinas proinflamatorias en sangre periférica

Uno de los puntos más importantes del proyecto fue evaluar el perfil proinflamatorio en sangre periférica dada su asociación con el deterioro cognitivo durante el envejecimiento (Brombacher et al., 2017; Dubenko et al., 2021; Fossati et al., 2017; Pennisi et al., 2017; Tarkowski et al., 2001; Wyss-Coray, 2016).

La caracterización inicial del aumento en plasma dependiente de la edad de los proinflamatorios mostró un fuerte aumento en citocinas y quimiocinas como: GM-CSF, IFN-γ, IL-6, IL-1 β, IL-4, IL-12p70, IL-13, IL-17, MCP-1 y TNF-α en ratones macho de 20 meses (Fig. 6).

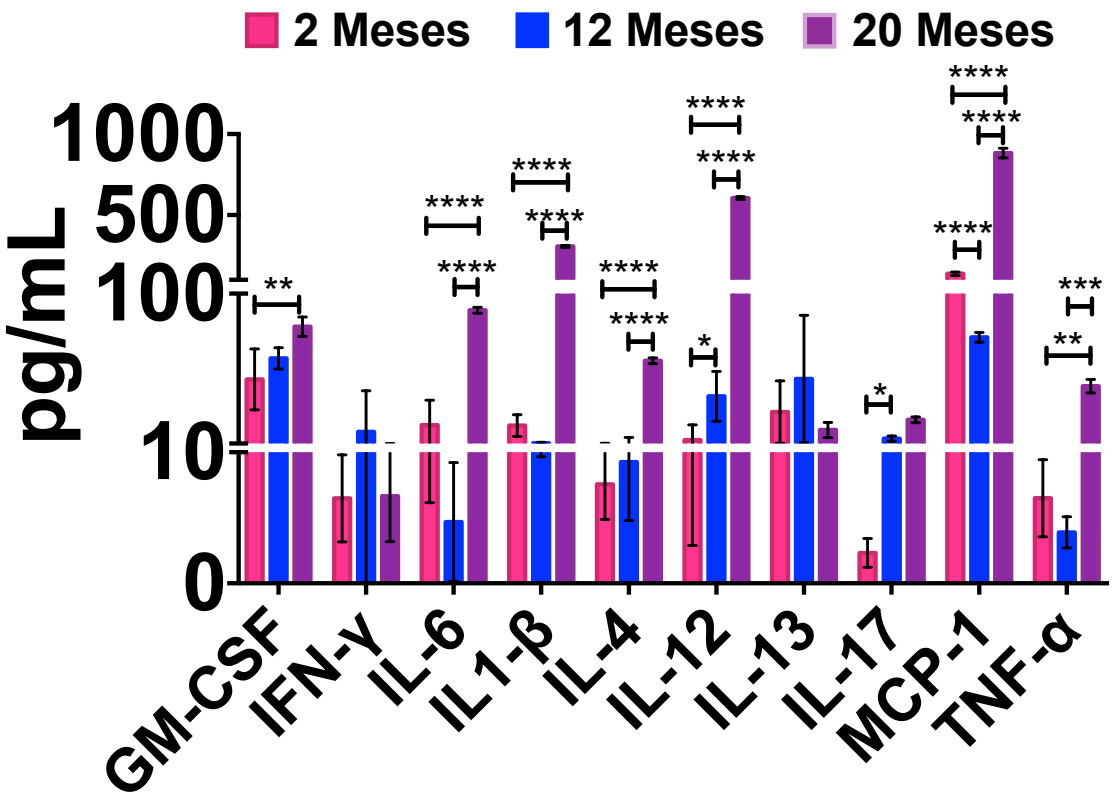

Figura 6. Cuantificación de citocinas en plasma en los grupos de ratones de 2, 12 y 20 meses. El gráfico muestra el análisis de citocinas en plasma. A) Cuantificación de citocinas plasmáticas expresada en pg/mL. La cuantificación de citocinas se midió con la plataforma Bioplex y se muestra en pg/mL. ANOVA post-hoc Tukey n.s= 0,1234, *p= 0,03, **p= 0,002, ***p= 0,0002, ****p= <0,0001. Media ± SEM n=3/grupo).

De acuerdo con los resultados anteriores, se eligieron las citocinas/quimicionas que presentaban los niveles más altos, por los que se decidió proseguir estudiando MCP-1, IL-12p70, TNF-α, IL-1β e IL-6.

En particular, los ratones de 20 meses mostraron aumentos importantes en los niveles plasmáticos de IL12p70, TNF-α, MCP-1 e IL-6 en comparación con el grupo de 2 meses (ANOVA, F(2, 18) = IL12p70: ***p = 0.008, TNF-α: ****p < 0.0001, MCP-1: ****p < 0.0001 e IL-6: ****p < 0.0001) (Fig. 7 A). También encontramos que los ratones de 12 meses mostraron un aumento en los niveles plasmáticos de IL-12p70, TNF-α, IL-1β e IL-6 en comparación con ratones jóvenes de 2 meses (ANOVA, F(2, 18) = IL12p70: **p = 0.002, TNF-α: ****p < 0.0001, IL-1 β: ****p < 0.0001 e IL-6: ****p < 0.0001) (Fig.

7 A). Estos resultados confirman una acumulación dependiente de la edad de IL-12p70, TNF-α, MCP-1, IL-6 e IL-1β en sangre periférica.

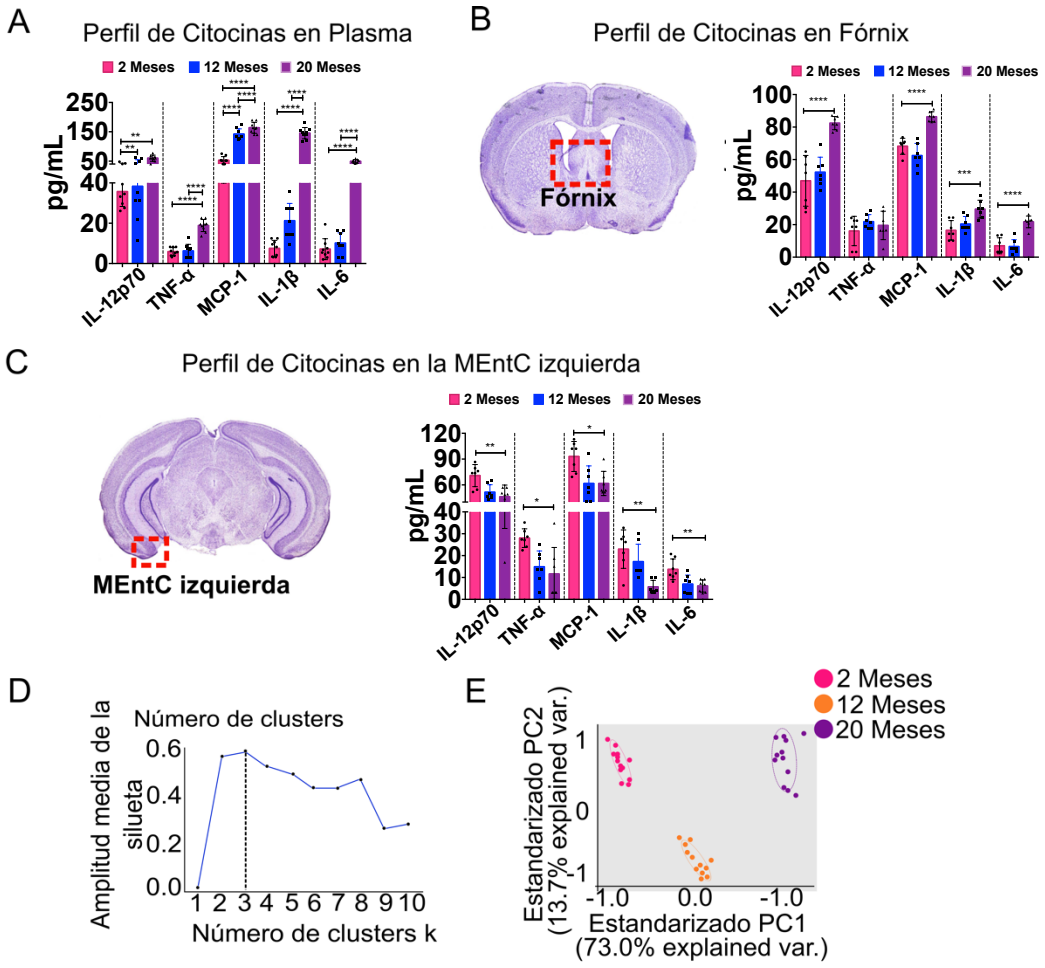

Figura 7. Análisis de cuantificación de citoquinas centrales y periféricas durante el envejecimiento murino. A) Cuantificación de citocinas plasmáticas expresadas en pg/mL en ratones. B) Sección coronal del cerebro representativa del fórnix murino del Atlas de Paxino's del Fornix, el Fornix está resaltado dentro del cuadro rojo. Perfil de citocinas dependiente de la edad en fórnix (pg/mL) de ratones de 2-12 y 20 meses de edad. C) Sección coronal cerebral representativa de la MentC izquierda del Atlas de Paxino's, la MentC se se muestra en el recuadro rojo. Cuantificación de citocinas en MEntC izquierda durante el envejecimiento (pg/ml) de ratones de 2, 12 y 20 meses. D) Análisis de k-media y E) Análisis de componentes principales (PCA) de ratones de 2-12 y 20 meses de edad. Los resultados se expresan como Media ± S.E.M seguido de ANOVA post-hoc Tukey n.s p= 0.1234, *p= 0.03, **p= 0.002, ***p= 0.0002, ****p= 0.0001. n=7-8/grupo.

9.5 Los ratones de edad avanzada muestran un aumento de citocinas proinflamatorias en el fórnix y una disminución en el MEntC izquierdo

De acuerdo con los resultados de MRI, se identificó que el Fornix y la MEntC izquierda experimentaron los cambios volumétricos más dramáticos y antagónicos durante el envejecimiento (Fig. 4 A, B). Se evaluó si los cambios de volumen diferenciales en fórnix y MEntC izquierda correlacionaban con la acumulación de citocinas proinflamatorias. Se encontró que los ratones de 20 meses acumularon IL-12p70, MCP-1, IL-1β e IL-6 en el fórnix en comparación con el grupo de 2 meses (ANOVA, F(2, 18) = IL- 12p70: ****$p < 0.0001$, TNF-α: $p = 0.6884$, MCP-1: ****$p < 0.0001$, IL-1β: ***$p < 0.0008$ e IL-6: ****p < 0.0001) (Fig. 7 B). No se encontraron cambios en TNF-α (ANOVA, F(2, 18) $p= 0.6884$). En particular, los niveles de IL-12p70, TNF-α, MCP-1, IL-1β e IL-6 se redujeron en la MEntC izquierda de ratones de 20 meses en comparación con los ratones de 2 meses (ANOVA, F (2, 18) = IL-12p70: **$p = 0,0031$, TNF-α: *$p = 0,0056$, MCP-1: *$p = 0,0097$, IL-1β: **$p = 0,0007$ e IL-6: **$p = 0,0055$) (Fig. 7 C). Estos resultados confirmaron la acumulación antagonista de IL-12p70, MCP-1, IL-1β e IL-6 en el fórnix y la MEntC izquierda durante el envejecimiento fisiológico.

Después de estas mediciones, se realizó el PCA integrando 38 variables (comportamiento, niveles de citocinas periféricas y cerebrales y volúmenes de regiones cerebrales) para agrupar a los individuos en grupos de acuerdo con sus resultados en comportamiento, perfiles inmunológicos y cambios en el volumen cerebral. El análisis de PCA con k-media identificó tres grupos según la edad de los ratones (Fig. 7 D, E). Como se muestra en la Fig. 7 E, el componente principal 1 (PC1) y el componente principal 2 (PC2) representaron el 73 y el 13,7 % de la varianza total, respectivamente.

9.6 Los niveles de citocinas se correlacionan negativamente con el rendimiento en tareas cognitivas

Se evaluó si la acumulación de citocinas proinflamatorias en sangre periférica, fórnix o MEntC izquierda se correlacionaba con las tareas cognitivas defectuosas en ratones de edad avanzada mediante análisis de Pearson. Se identificaron correlaciones positivas y negativas entre diferentes citocinas y diversas tareas cognitivas que se resumen en la Figura 8 A, B, C. Principalmente, el grupo de dos meses mostró una correlación

negativa de los niveles periféricos de IL-12p70 (IL12p70_P) y MCP1 (MCP1_F) en el fórnix y el tiempo transcurrido antes de encontrar la salida (Time_LTM) en el laberinto de Barnes durante la prueba LTM (IL-12p70: r=-0,67 **p = 0,008; MCP1: r = -0,54, *p = 0,04) (Fig. 3 A). Además, una correlación positiva de la IL-1β periférica (IL1B_P) y el tiempo LTM (Time_LTM) del laberinto de Barnes (r= 0.57, *p = 0.03) (Fig. 8 A). A los 12 meses de edad, los niveles periféricos de IL-6 (IL6_P) se correlacionan negativamente con más tiempo para llegar a la salida en el laberinto de Barnes (Time_STM) durante la prueba STM (r= -0.70 **p = 0.007) (Fig. 8 B). Finalmente, se encontró una correlación negativa en el rendimiento del Laberinto de Barnes y los niveles de IL-1β en el fórnix en ratones de 20 meses (Fig. 8 C).

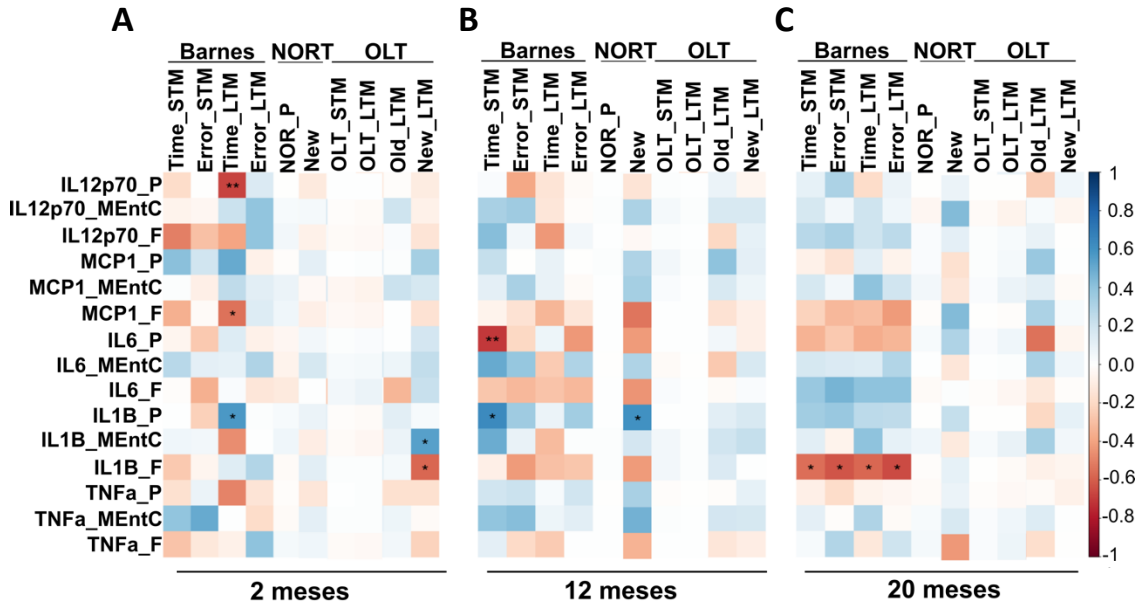

Figura 8. Los niveles de citocinas se correlacionan negativamente con el rendimiento en tareas cognitivas. A-C) Correlaciones de Pearson de los perfiles de citocinas en sangre periférica, fórnix o MEntC izquierda con el desempeño conductual durante el envejecimiento en los tres grupos de edad. Abreviaturas: _P: sangre periférica, _F: fórnix, _MEntC: corteza entorrinal medial izquierda. Para pruebas comportamiento: 1) Barnes, Time_STM: tiempo durante la memoria de tiempo corto, Error_STM: error durante la memoria de tiempo corto, Time_LTM: tiempo durante la memoria de tiempo largo, Error_LTM: error durante la memoria de tiempo largo. 2) NORT: prueba de reconocimiento de objetos novedosos, NOR_P: índice de reconocimiento durante la prueba de reconocimiento de objetos novedosos, New: Tiempo con objeto nuevo durante la prueba de reconocimiento de objetos novedosos. 3) OLT: prueba de ubicación de objetos, OLT_STM: prueba de ubicación de objetos durante la memoria a corto plazo, OLT_LTM: prueba de ubicación de objetos durante la memoria a largo plazo, Old_LTM: tiempo dedicado a la ubicación anterior del objeto durante la prueba de memoria a largo plazo, New_LTM: tiempo dedicado a nueva ubicación del objeto durante la prueba de memoria a largo plazo. n.s p= 0.1234, *p= 0.03, **p= 0.002, ***p= 0.0002, ****p= 0.0001. n=7-8/grupo

9.7 Los niveles de citoquinas no correlacionan con los cambios macroestructurales del cerebro

A continuación, se comprobó si la acumulación central de IL-12p70, TNF-α, MCP-1, IL-1β e IL-6 promovían cambios de volumen en fórnix y MEntC izquierda de los ratones de edad avanzada. Sin embargo, no se encontraron correlaciones significativas entre los niveles de citocinas periféricas o los niveles de citocinas en el fórnix o MEntC izquierda con los cambios cerebrales volumétricos (Fig. 9).

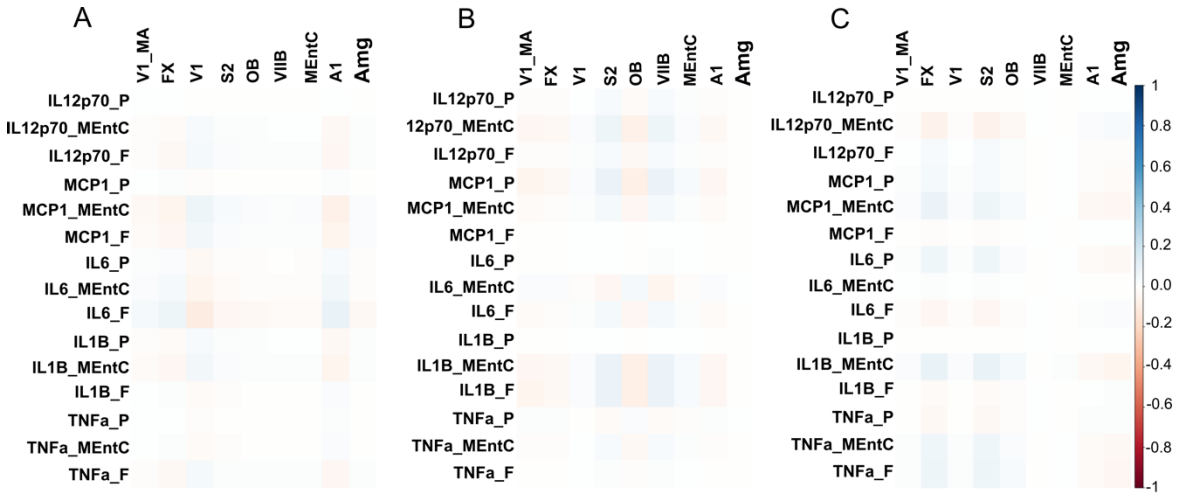

Figura 9. Los niveles de citocinas en plasma, fórnix o MEntC izquierdo no influyen en los cambios volumétricos del cerebro en ratones. A-C) Correlación Pearson de citocinas con cambios volumétricos cerebrales en el cerebro murino. (Abreviaturas: _P= sangre periférica, _F: fórnix, _MEntC: corteza entorrinal medial izquierda; V1_MA: corteza visual primaria, área mononuclear, FX: fórnix, V1: corteza visual primaria, S2: corteza somatosensorial secundaria, OB: bulbo olfativo, VIIB: lóbulo paramediano (lóbulo 7), MEntC: corteza entorrinal medial, A1: corteza auditiva primaria, Amg: amígdala). n=12/grupo.

9.8 El envejecimiento favorece cambios antagónicos en la morfología de la microglía en el Fornix y MEntC izquierdo

Se evaluó la morfología de la microglía en el fórnix y MEntC. Se encontró que durante el envejecimiento aumenta el número total de células Iba-1+ positivas en el fórnix de ratones de 12 y 20 meses en comparación con los de 2 meses (Fig. 10 B, C, ANOVA, $F(2, 6)$ = 2 vs 20: $^{**}p = 0.0014$, 12 vs 20: $^{*}p = 0.0196$). Además, se encontró una disminución significativa en la duración de los procesos de la microglía en el fórnix en ratones de 12 y 20 meses en comparación con los de 2 meses (Fig. 10 D, ANOVA, $F(2, 6)$ = 2 vs 12: $^{**}p = 0.0120$, 12 vs 20: $^{*}p = 0.0075$, 2 vs 20: $^{***}p = 0.0003$). Por otra

parte, la microglía en el fórnix de ratones de 12 meses mostró un aumento en el número de ramificaciones por célula en comparación con los de 2 y 20 meses (Fig. 10 E, ANOVA, F (2, 6) = 2 vs 12: ***p* = 0.0019, 12 vs 20: ****p* = 0.0009).

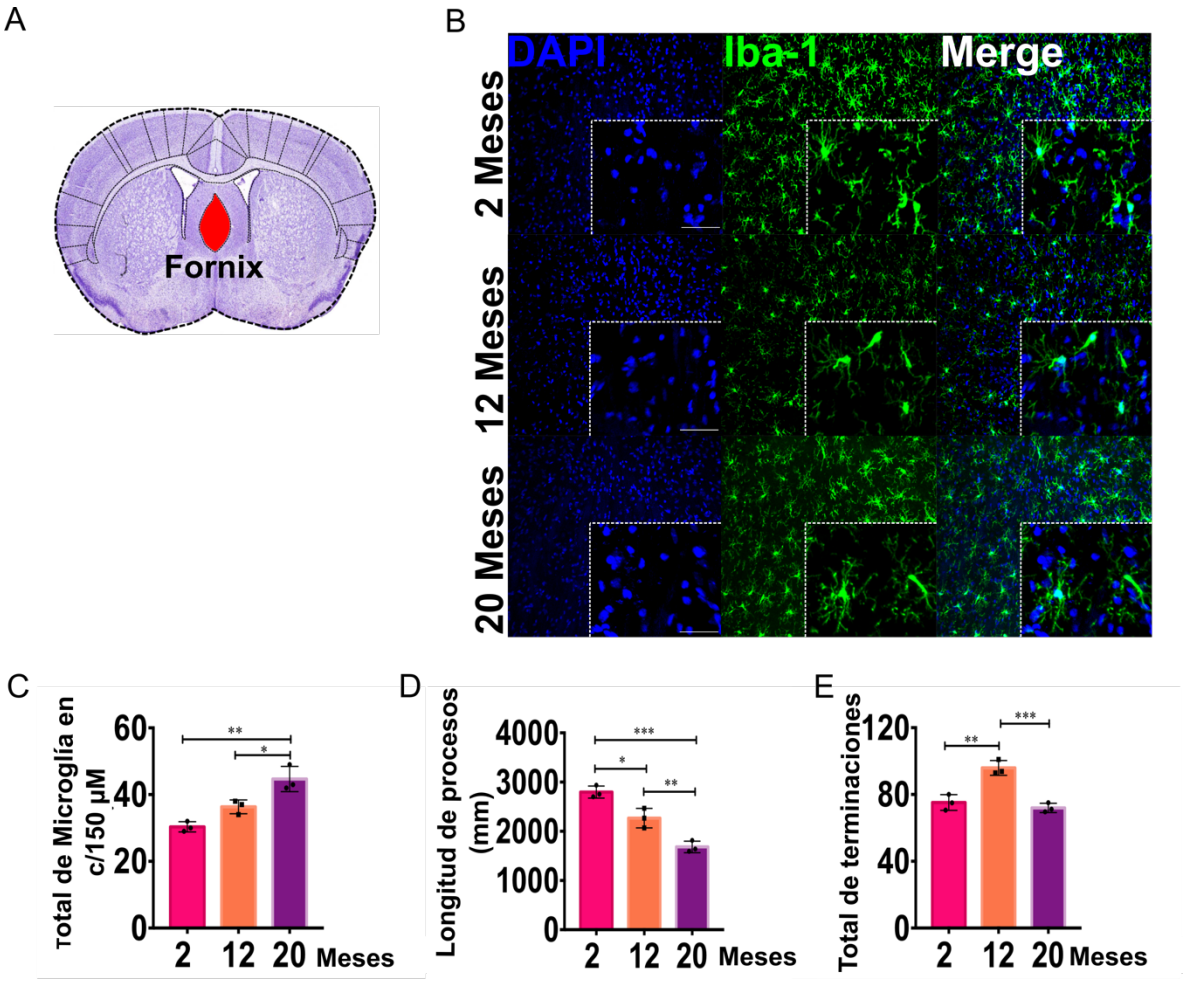

Figura 10. La morfología de la microglía en el fórnix sufre alteraciones durante el envejecimiento. A) Sección coronal representativa del cerebro del fórnix murino del Atlas de Paxinos, el fórnix está resaltado en rojo. B) Inmunofluorescencia para microglía reactiva para Iba-1 en el fórnix durante el envejecimiento. C) Imágenes representativas de la microglía Iba-1+ en el fórnix, se contaron en 5 campos aleatorios. El gráfico muestra el número total de microglía en 150 µm^2 de ratones de 2, 12 y 20 meses de edad. D) El gráfico muestra la longitud de los procesos (µM) de la microglía Iba1+ en el fórnix. E) Gráfica de ramificaciones de microglía Iba1+ por cada célula.

Por el contrario, el envejecimiento disminuyó la inmunotinción de Iba-1+ en el MEntC izquierdo de ratones de 2 y 12 meses, así como en ratones de 2 y 20 meses (ANOVA, F(2, 6) = 2 vs 12: ****p* = 0.0017, 2 vs 20: ****p* = 0.0004; respectivamente) (Fig. 11 B - C). Precisamente, la evaluación de la morfología de la microglía en el MEntC izquierdo

utilizando los complementos de ImageJ AnalyzeSkeleton (2D/3D) identificó un aumento significativo de los procesos de la microglía en los ratones de 20 meses en comparación con los ratones de 2 y 12 meses (***p = 0,0007) (Fig. 11 D) y ramificación celular (Fig. 11 E) en los ratones de 12 y 20 meses en comparación con los de 2 meses (ANOVA, F(2, 6): ***p = 0.0007) (Fig. 11 E, ANOVA, F(2, 6) = 2 vs 12: ****p < 0.0001, 2 vs 20: ***p = 0,0008 y 12 vs 20: **p = 0.0012).

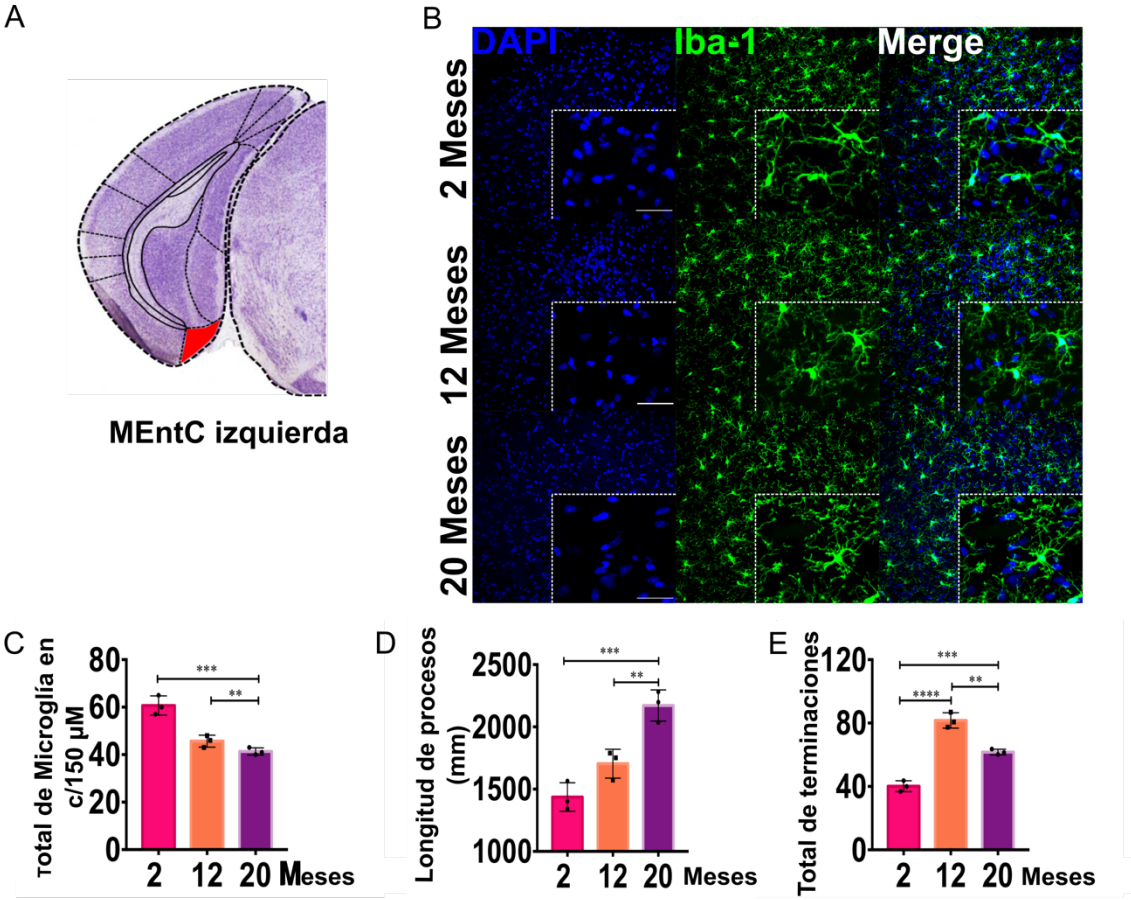

Figura 11. La morfología de la microglía cambia durante el envejecimiento en la MEntC izquierda. A) Sección coronal cerebral representativa de la MEntC izquierda murino del Atlas de Paxinos, la MEntC se muestra en el recuadro rojo. B) Inmunofluorescencia para microglía reactiva Iba-1 en el MEntC izquierdo durante el envejecimiento. C) La inmunotinción de Iba-1 para microglía se contó en 5 campos aleatorios. El gráfico muestra el número de microglía en 150 µm^2 de ratones de 2, 12 y 20 meses de edad. I) El gráfico muestra la longitud de los procesos (µM) de la microglía Iba1+ en la MEntC izquierda. J) Total de terminaciones de microglía Iba1+ por célula.

Finalmente, dada la naturaleza del tejido de la MEntC y todas sus implicaciones en las tareas de memoria y aprendizaje, se decidió evaluar la expresión de sinaptofisina. En particular, el envejecimiento promovió una disminución significativa en la inmunoseñal de sinaptofisina, un marcador proteico de la hendidura sináptica, en la MEntC izquierda

de ratones de 12 y 20 meses en comparación con los de 2 meses (Fig. 12 A, B, ANOVA, F(2, 6) = 2 vs 12: ***p = 0.0009, 2 vs 20: ****p < 0.0001 y 12 vs 20: *p = 0.0109).

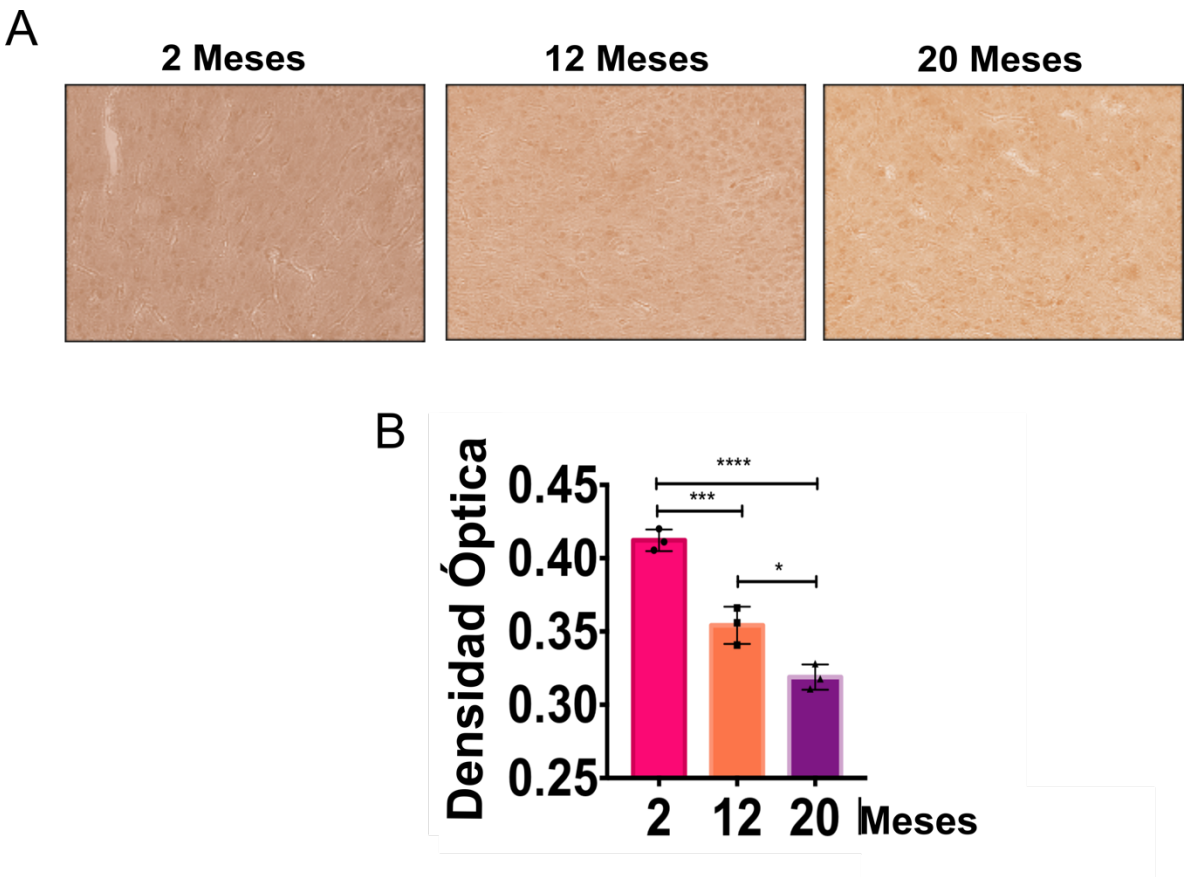

Figura 12. Existen cambios en la expresión de sinaptofisina en el cerebro murino durante el envejecimiento. A) Expresión de sinaptofisina en la MEntC izquierda de ratones de 2, 12 y 20 meses de edad. B) La cuantificación de la densidad óptica para la sinaptofisina se llevó a cabo utilizando la imagen J. Los resultados se expresan como Media ± S.E.M seguido de ANOVA post-hoc Tukey n.sp= 0.1234, *p= 0.03, **p= 0.002, ***p= 0.0002, ****p= 0.0001. n=3/grupo.

9.9 La acumulación de citocinas en el cerebro y el plasma no se correlaciona con la morfología de la microglía en el fórnix o MEntC izquierdo

Se decidió comprobar si la acumulación de citocinas en plasma, fórnix o MEntC izquierda correlacionaba con la plasticidad morfológica de la microglía durante el envejecimiento. Sin embargo, no se encontraron correlaciones significativas entre los niveles de citocinas periféricas o centrales con la morfología de la microglía, es decir, con el número total de microglía por región, la longitud de los procesos y el número de

ramificaciones por célula de los ratones envejecidos a través del análisis de Pearson (Fig. 13).

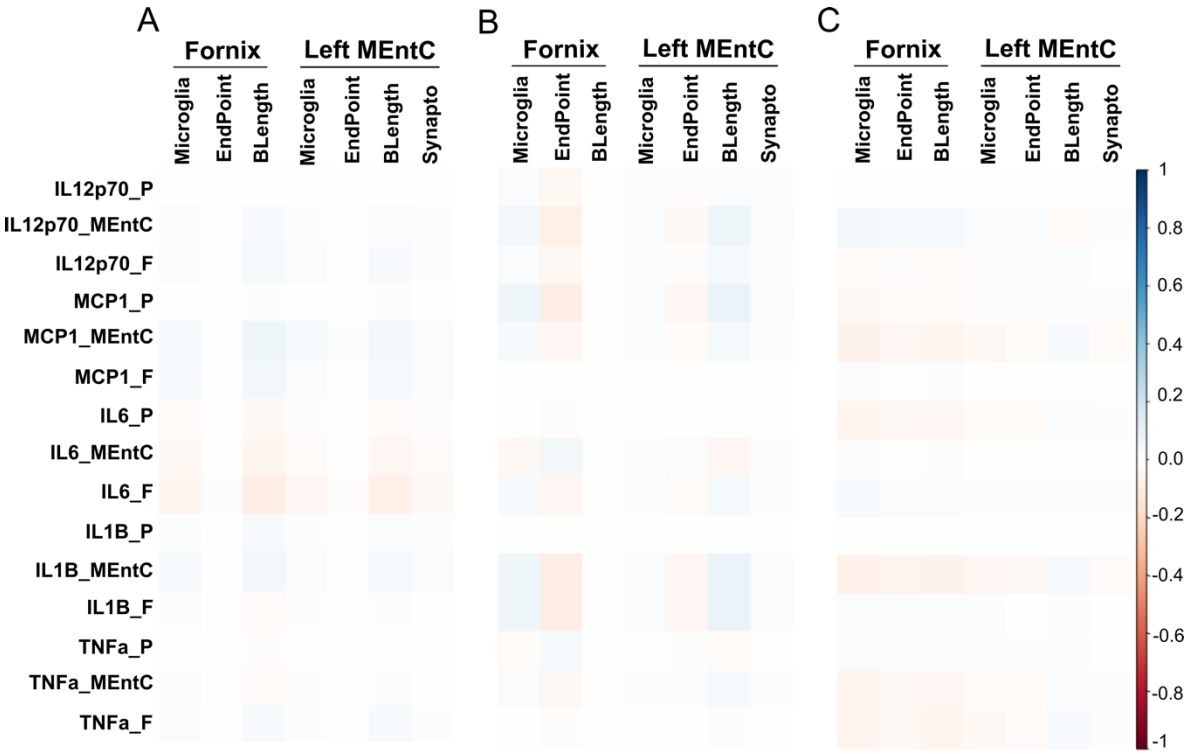

Figura 13. Los niveles de citocinas en plasma, fórnix o MEntC no influyen en la morfología de la microglía en fórnix o MEntC izquierdo. A-C) Correlación de Pearson de citocinas y morfología de la microglía en fórnix y MEntC. (Abreviaturas: _P= sangre periférica, _F: fórnix, _MEntC: corteza entorrinal medial izquierda; Microglia: número de microglia, EndPoint: número de ramificaciones por microglia, BLength: longitud de proceso, Synapto: sinaptofisina). n=15/grupo.

9.10 La morfología de la microglía correlaciona con los cambios de volumen cerebral en el fórnix y el MEntC izquierdo

Se determinó si la plasticidad morfológica de la microglía correlacionaba con cambios volumétricos en fórnix y MEntC izquierda durante el envejecimiento (Figura 14 A, B, C). No se encontraron correlaciones significativas entre la morfología de la microglia (microglia, EndPoint, BLength) y el volumen del fórnix en los ratones macho de 2 y 12 meses de edad (Fig. 14 A, B,). Sin embargo, en los ratones de 2 meses de edad, se observó una correlación positiva en la longitud de la rama de la microglía (BLength) (r = 0,70, **p* = 0.05) y la expresión de sinaptofisina (r = 0,67, **p* = 0.008) con la disminución del volumen en la MEntC izquierda. (Fig. 14 A). Además, a los 12 meses de edad, no

encontramos correlaciones significativas entre la morfología de la microglía y los cambios de volumen de fórnix y MEntC (Fig. 14 B). Finalmente, en los ratones de 20 meses de edad, encontramos una correlación negativa con los puntos finales de la microglía (EndPoint) con el cambio de volumen de MEntC izquierdo (r = -0,85, $**p$ = 0.02) y no hubo correlaciones significativas para la morfología del fórnix y la microglía. (Fig. 14 C).

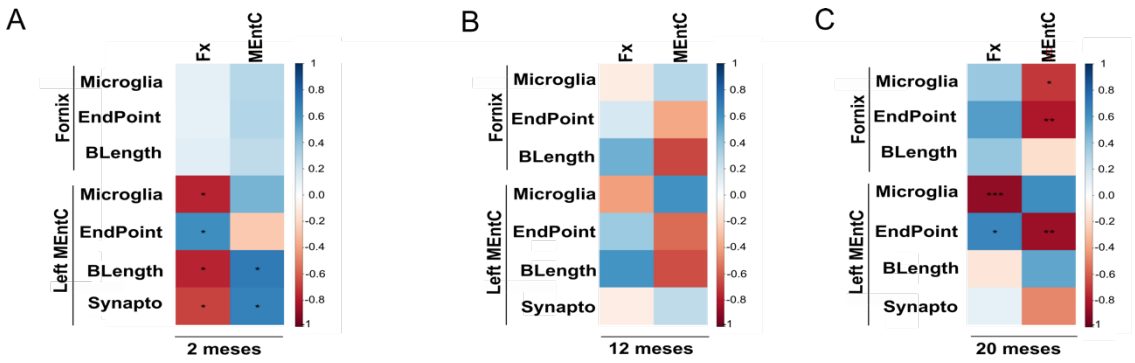

Figura 14. La morfología de la microglía correlaciona con los cambios de volumen cerebral en el fórnix y el MEntC izquierdo. A-C) Correlaciones de Pearson de la morfología de la microglía en fórnix y MEntC izquierda con cambios volumétricos cerebrales. Abreviaturas: Microglia: número de microglia, EndPoint: número de punto final por microglia, BLength: longitud de procesos. Para tareas de comportamiento: 1) Barnes, Time_STM: tiempo durante la memoria de tiempo corto, Error_STM: error durante la memoria de tiempo corto, Time_LTM: tiempo durante la memoria de tiempo largo, Error_LTM: error durante la memoria de tiempo largo. 2) NORT: prueba de reconocimiento de objetos novedosos, NOR_P: índice de reconocimiento durante la prueba de reconocimiento de objetos novedosos, New: Tiempo con objeto nuevo durante la prueba de reconocimiento de objetos novedosos. 3) OLT: prueba de ubicación de objetos, OLT_STM: prueba de ubicación de objetos durante la memoria a corto plazo, OLT_LTM: prueba de ubicación de objetos durante la memoria a largo plazo, Old_LTM: tiempo dedicado a la ubicación anterior del objeto durante la prueba de memoria a largo plazo, New_LTM: tiempo dedicado a nueva ubicación del objeto durante la prueba de memoria a largo plazo. n.s p= 0.1234, *p= 0.03, **p= 0.002, ***p= 0.0002, ****p= 0.0001. n=3/grupo.

9.11 La morfología de la microglía correlaciona con el desempeño en tareas cognitivas durante el envejecimiento

Finalmente, se evaluaron las posibles correlaciones de la morfología de la microglía en el fórnix o en la MEntC izquierda con el rendimiento cognitivo durante el envejecimiento (Fig. 15 A, B, C). A los 2 meses de edad, no se encontraron correlaciones significativas entre la morfología de la microglía con ninguna de las tareas cognitivas evaluadas (Fig. 15 A). Sin embargo, a los 12 meses de edad, se identificaron correlaciones positivas entre la longitud de los procesos de la microglía (BLength) en el

fórnix con el OLT en STM y LTM (OLT_STM, OLT_LTM) (STM: r = 0,72 **p = 0.005; LTM: r = 0.98 ***p = 5.07x10-9) (Fig. 15 B), así como una correlación negativa entre el número de microglía (Microglia) en la MEntC izquierda con el OLT en LTM (LTM: r = - 0,93 **p = 2.1x10-6) (Fig. 15 C). Finalmente, en el grupo de 20 meses se identificó una correlación negativa entre el número de microglía y el desempeño en el NORT (NOR_P) (r = - 0.81 *p = 0.04) y OLT LTM (r = - 0.83 *p = 0,043) (Fig. 15 C).

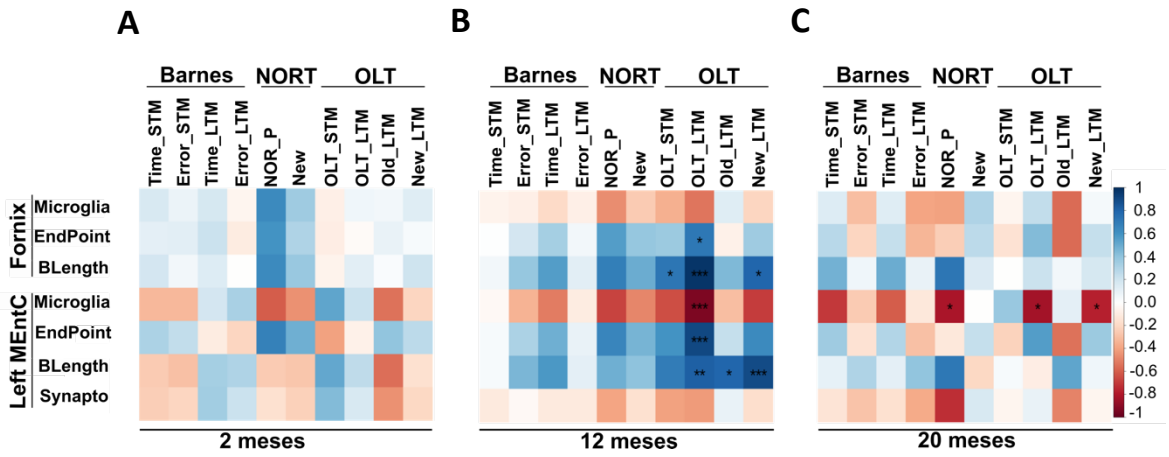

Figura 15. La morfología de la microglía se correlaciona con el desempeño en tareas cognitivas durante el envejecimiento. A-C) Correlación de Pearson de la morfología de la microglía en fórnix y MEntC izquierda con el rendimiento cognitivo durante el envejecimiento. Abreviaturas: Microglia: número de microglia, EndPoint: número de punto final por microglia, BLength: longitud de procesos, Synapto: sinaptofisina, medial, Para tareas de comportamiento: 1) Barnes, Time_STM: tiempo durante la memoria de tiempo corto, Error_STM: error durante la memoria de tiempo corto, Time_LTM: tiempo durante la memoria de tiempo largo, Error_LTM: error durante la memoria de tiempo largo. 2) NORT: prueba de reconocimiento de objetos novedosos, NOR_P: índice de reconocimiento durante la prueba de reconocimiento de objetos novedosos, New: Tiempo con objeto nuevo durante la prueba de reconocimiento de objetos novedosos. 3) OLT: prueba de ubicación de objetos, OLT_STM: prueba de ubicación de objetos durante la memoria a corto plazo, OLT_LTM: prueba de ubicación de objetos durante la memoria a largo plazo, Old_LTM: tiempo dedicado a la ubicación anterior del objeto durante la prueba de memoria a largo plazo, New_LTM: tiempo dedicado a nueva ubicación del objeto durante la prueba de memoria a largo plazo. n.s. p= 0.1234, *p= 0.03, **p= 0.002, ***p= 0.0002, ****p= 0.0001. n=3/grupo.

9.12 El aumento volumétrico del fórnix y la morfología de la microglía predicen un desempeño defectuoso en el reconocimiento de objetos nuevos (NORT) y en la prueba de ubicación de objetos (OLT) en ratones envejecidos

Se calculó un modelo de regresión lineal múltiple para analizar la interacción de los cambios en la morfología y el volumen de la microglía en fórnix y MEntC izquierda que matemáticamente predicen los resultados conductuales durante el envejecimiento. Se consideró Error_LTM y STM durante la prueba de Barnes, NOR_P durante NORT y

OLT_LTM y STM durante OLT como las principales interacciones para realizar el análisis. Particularmente, el análisis de regresión lineal múltiple identificó relaciones significativas entre varias variables con Fornix y no con MentC izquierdo. El análisis de regresión múltiple demostró una interacción negativa significativa entre la longitud de los procesos microgliales y el volumen del fórnix en los ratones de 20 meses y predice significativamente el declive en la preferencia de objetos en NORT y OLT durante LTM; es decir, mientras más cortos los procesos, mayor volumen en fórnix y un peor desempeño en la tarea NORT y OLT durante LTM (Figura 16 A, B). Por el contrario, el análisis demostró una interacción positiva pero no fue significativa entre la longitud de los procesos microgliales y el volumen de MEntC en los ratones de 20 meses (Figura 5 C, D).

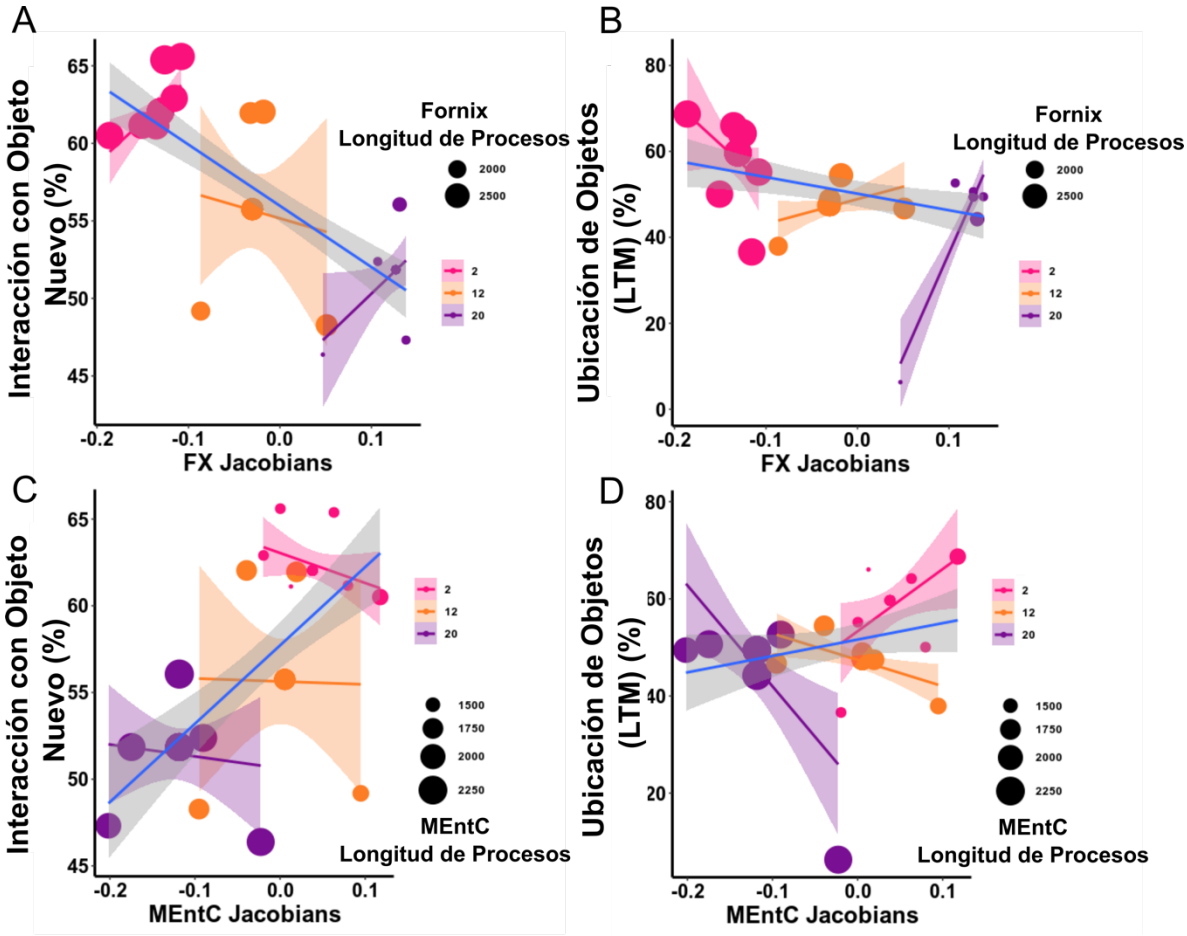

Figura 16. Regresión lineal múltiple de comportamiento (NOR_P y OLT durante LTM, volúmenes cerebrales (jacobianos) y parámetros histológicos (Modelo estadístico de ratones macho de 2, 12 y 20 meses). A) Porcentaje de reconocimiento en el NORT de los tres grupos de edad según el aumento de volumen en el fórnix y la longitud de la rama de la microglía. B) Porcentaje de reconocimiento en el OLT durante LTM de los tres grupos de edad según el aumento de volumen en fórnix y longitud de rama de microglia. C) Porcentaje de reconocimiento en la NORT de los tres grupos de edad según la disminución de volumen en MEntC y longitud de rama de microglia. D) Porcentaje de reconocimiento en el OLT durante LTM de los tres grupos de edad según la disminución de volumen en MEntC y longitud de rama de microglia.

10.DISCUSIÓN

En esta tesis se caracterizaron las alteraciones del volumen cerebral dependientes de la edad en el modelo murino de envejecimiento, mediante MRI junto con un perfil proinflamatorio específico y características morfológicas de la microglía en regiones cerebrales selectivas asociadas con el deterioro cognitivo en ratones macho C57BL/6. Se identificó el fórnix y la MEntC izquierda como las principales estructuras cerebrales que mostraron cambios volumétricos antagónicos dependientes de la edad que se correlacionaron con cambios en la morfológicos de la microglía. Nuestros datos proponen que la plasticidad morfológica de la microglía y el aumento de volumen en el fórnix predicen fallas en las tareas NORT y OLT en ratones machos de edad avanzada.

Se realizó un fenotipado conductual para caracterizar el aprendizaje, la memoria y las deficiencias cognitivas durante el envejecimiento murino. A través de éste, se confirmó un deterioro de la memoria dependiente de la edad en los ratones de 12 y 20 meses en comparación con los ratones de 2 meses. Los ratones machos envejecidos mostraron una pérdida progresiva de la memoria espacial evidenciada por los resultados de la prueba de alternancia forzada, y la latencia y la cantidad de errores durante el laberinto de Barnes, que son consistentes con informes anteriores (Morgan et al., 2018). Además, los ratones viejos no reconocieron la nueva ubicación del objeto en comparación con los ratones jóvenes de 2 meses, lo que confirmó un rendimiento defectuoso de la memoria espacial. Finalmente, la memoria episódica también se vió interrumpida en ratones de 12 y 20 meses durante el paradigma NORT. Esta observación fue consistente con informes previos que han mostrado que la memoria de reconocimiento de objetos se afecta desde los 12 meses de edad (Belblidia et al., 2018; Li et al., 2020).

La primer gran contribución en esta tesis fue la identificación del aumento de volumen en el fórnix durante el envejecimiento en ratones machos. Se utilizó la MRI para caracterizar globalmente las alteraciones cerebrales estructurales durante el envejecimiento como contribuyentes al deterioro cognitivo. Reportes anteriores han documentado que la alteración cerebral estructural contribuye al deterioro cognitivo durante el envejecimiento (Faizy et al., 2020; Filo et al., 2019; Matsuda, 2013). Nuestros resultados muestran que los ratones envejecidos muestran el mayor aumento de volumen en el fórnix y la mayor disminución en la MEntC izquierda. También, se identificó una

pérdida dramática de volumen cerebral en el bulbo olfatorio izquierdo, el lóbulo paramediano derecho, la corteza auditiva primaria derecha y la amígdala derecha en los ratones macho envejecidos.

Los cambios volumétricos encontrados en el fórnix durante el envejecimiento parecen ser controvertidos porque algunos informes han encontrado que disminuyeron durante el envejecimiento (Fletcher et al., 2014, 2013). También, durante el envejecimiento se han reportado disminuciones volumétricas en la materia gris occipital, el hipocampo, la circunvolución occipital media, el polo occipital y el tálamo (Armstrong et al., 2020). Por el contrario, nuestros resultados demostraron que el envejecimiento favorece un aumento de la corteza visual primaria izquierda y la corteza somatosensorial secundaria izquierda. En particular, la reducción en el volumen del hipocampo se reportó como un determinante temprano de la disminución de la memoria (Armstrong et al., 2020; Mungas et al., 2005) y nuestros hallazgos también confirmaron una reducción en el volumen del hipocampo en ratones viejos, sin embargo, esta significancia no sobrevivió la corrección FDR 5%. Con base en las correlaciones encontradas en esta tesis entre los cambios cerebrales de volumen en el fórnix y la MEntC izquierda con las pruebas conductuales como Barnes Maze, OLT y NORT, hemos propuesto que los cambios cerebrales volumétricos antagónicos en el fórnix y la MEntC izquierda durante el envejecimiento contribuyen a la pérdida de la memoria y deterioro cognitivo en ratones.

Los resultados obtenidos sugirieron que las citocinas circulatorias periféricas podrían infiltrarse de manera potencial y selectiva en las regiones del cerebro durante el envejecimiento, promoviendo el deterioro cognitivo. Se identificó que el desempeño en las pruebas de memoria, los cambios volumétricos del cerebro y las variables de inflamación se agruparon en los tres grupos de edad utilizando el análisis PCA. Después de esto, se probó la hipótesis de que la neuroinflamación podría modular los cambios cerebrales volumétricos en el fórnix y la MEntC izquierda en los ratones viejos. El envejecimiento integra un estado proinflamatorio crónico de bajo grado, llamado *inflammageing* (Franceschi et al., 2006) que contribuye significativamente al deterioro cognitivo (Berryer et al., 2016; D'Avila et al., 2018; Feng et al., 2017; López-Otín et al., 2013; Yin et al., 2019). Nuestros resultados confirmaron un perfil de citocinas proinflamatorias dependiente de la edad en plasma, con niveles elevados de IL12p70,

TNF-α, IL-1β, MCP-1 e IL-6, que fueron consistentes con informes previos (Brombacher et al., 2017; Dubenko et al., 2021; Fossati et al., 2017; Pennisi et al., 2017; Tarkowski et al., 2001). De hecho, según el análisis de correlación de Pearson, la acumulación de IL-1β en el fórnix afecta el rendimiento del laberinto de Barnes durante las pruebas STM y LTM. Hasta donde sabemos, no existe evidencia que proponga que la acumulación de IL-1β en el fórnix podría estar asociada con el deterioro de la memoria.

Dado que no encontramos ninguna correlación significativa entre la neuroinflamación y los cambios en el volumen del cerebro, se probó una segunda hipótesis. Según un reporte anterior, la disminución en la expresión de sinaptofisina en el núcleo accumbens podría contribuir potencialmente a los cambios en el volumen cerebral en ratas (Trujillo-Villarreal et al., 2021). De hecho, el plasma de ratones viejos es capaz de disminuir la plasticidad sináptica y perjudicar el aprendizaje espacial y la memoria (Villeda et al., 2014). Los resultados mostraron una disminución en la expresión de sinaptofisina en la MEntC izquierda que también mostró una disminución de volumen en los ratones viejos, lo que respalda que un volumen cerebral más bajo integra la interrupción sináptica. A pesar de todos los resultados, el análisis de Pearson no mostró correlaciones significativas entre los niveles de citocinas en plasma, fórnix o MEntC izquierdo con disminución de volumen en la MEntC izquierda y en el aumento del fórnix. Además, no se encontraron correlaciones significativas entre la expresión de sinaptofisina en la MEntC izquierda con la disminución del volumen en la misma. Por lo tanto, no se pudo concluir que la neuroinflamación esté asociada con cambios de volumen en el fórnix o MEntC.

La segunda contribución más importante de los resultados obtenidos es que la plasticidad selectiva de la microglía en el fórnix y el MEntC izquierdo contribuyen al deterioro cognitivo durante el envejecimiento. Se ha sugerido que la activación de la microglía es un segundo contribuyente potencial a la neuroinflamación durante el envejecimiento (Shahidehpour et al., 2021). De acuerdo a nuestros resultados, el envejecimiento conduce a una disminución en el número de microglía, un aumento en la longitud de los procesos y en las ramificaciones en la MEntC izquierda. Por el contrario, se encontró un aumento en el número de microglía, una disminución en la longitud de los procesos y en las ramificaciones en el fórnix de ratones machos senescentes. La

microglía en la MEntC izquierda parece imitar un "estado de vigilancia" tipificado por una morfología altamente ramificada, con procesos extensos capaces de formar contactos con células y estructuras (Davalos et al., 2005), y permitir un monitoreo continuo del microambiente cerebral. Por el contrario, la microglía en el fórnix parece recapitular el fenotipo de microglía asociado a la enfermedad (DAM) que se encuentra durante el envejecimiento (Davies et al., 2017), mostrando procesos cortos y una morfología ameboidea que también integra la regulación a la baja de varios genes homeostáticos (Keren-Shaul et al., 2017). Sin embargo, de acuerdo a la literatura, esta evidencia de que la morfología de la microglía no confirma la liberación de citocinas. Además, la microglía distrófica que se encuentra en el fórnix de ratones envejecidos se ha observado en cerebros sanos pero envejecidos (Miller and Streit, 2007), y también se ha asociado con enfermedades neurodegenerativas (Shahidehpour et al., 2021). Esta propuesta está de acuerdo con informes anteriores que han demostrado que el envejecimiento se asoció con la aparente plasticidad de la glía pero no con el daño de la densidad de neuritas en el fórnix (Metzler-Baddeley et al., 2019). Sin embargo, queda por aclarar si la microglía distrófica identificada en esta tesis recapitula la microglía senescente asociada con la liberación de citocinas y la neuroinflamación que se convierte en el fenotipo asociado a la enfermedad que se ha encontrado en el envejecimiento.

Finalmente, se realizó un análisis de regresión lineal múltiple para integrar el efecto de la plasticidad morfológica de la microglía con los cambios volumétricos en el fórnix y su asociación con los resultados de las pruebas de memoria durante el envejecimiento. El modelo biológico identificó que una disminución en el índice NORT y OLT está asociada con el tamaño del fórnix y la longitud de los procesos de la microglía en el fórnix de ratones macho senescentes. El fórnix, de acuerdo a su posición anatómica, conecta el hipocampo, el tálamo, el hipotálamo, los núcleos septales y el núcleo accumbens. Por sí mismo, el fórnix es la principal salida del hipocampo y su estimulación mejora la memoria espacial (Hescham et al., 2017). De acuerdo con nuestros datos, las afecciones en el fórnix, como los cambios volumétricos, afectaron procesos dependientes selectivos del hipocampo como NORT y OLT (Broadbent et al., 2010). Por otro lado, se identificó una disminución en el volumen de la MEntC

izquierda. Fisiológicamente, la MEntC también está implicada en la regulación la memoria y el aprendizaje (Bangen et al., 2021; Matuskova et al., 2021), sin embargo, nuestro modelo biológico no demostró su asociación con el rendimiento de NORT y OLT en ratones macho senescentes.

Una de las limitaciones más importantes de esta tesis es la confirmación de una respuesta causa-efecto de la longitud de las ramificaciones de la microglía en los cambios volumétricos del fórnix que afectan el rendimiento cognitivo. Para esto, se requieren experimentos adicionales para demostrar que los cambios morfológicos específicos de la microglía en las regiones cerebrales accesorias que se conectan con el fórnix podrían alterar el rendimiento cognitivo durante el envejecimiento. Finalmente, queda pendiente caracterizar el dimorfismo sexual con respecto al volumen cerebral, los niveles de citocinas y el desempeño conductual en ratones hembra.

11.CONCLUSIONES

Los resultados obtenidos en ésta tesis nos permiten concluir en el modelo murino de envejecimiento utilizado que:

1) La capacidad de aprendizaje y memoria sufre un declive con la edad evidenciada por el mal desempeño en las pruebas de memoria (Laberinto en Y, NORT, Laberinto de Barnes y OLT) a partir de los 12 meses de edad en ratones C57BL/6 macho.
2) El envejecimiento murino se ve acompañado de la presencia de un perfil pro-inflamatorio periférico, en donde destacan los niveles elevados de IL-12p70, TNF-α, MCP-1, IL-1β e IL-6 en el grupo de 12 y 20 meses en comparación con el grupo de 2 meses.
3) Los cambios cerebrales volumétricos mediante MRI muestran el aumento de volumen en el fórnix y el decremento en la MEntC izquierda durante el envejecimiento murino.
4) El fórnix muestra un aumento en la acumulación de citocinas proinflamatorias, mientras que la MEntC izquierda muestra una disminución en el grupo de 20 meses en comparación con el grupo de 2 meses de edad.
5) No existe correlación significativa entre la neuroinflamación y los cambios en el volumétricos encontrados en el cerebro de los ratones en los diferentes grupos de edad.
6) La evaluación morfológica de la microglía confirma un fenotipo activo y distrófico en el fórnix y un fenotipo de vigilancia en la MEntC izquierda.
7) El modelado biológico reveló que el aumento de volumen relacionado con la edad en el fórnix se asoció con microglía distrófica y deterioro cognitivo
8) La disminución en el índice el reconocimiento de objetos está significativamente asociado con el tamaño del fórnix y la longitud de los procesos de la microglía en el fórnix de ratones macho senescentes.
9) La disminución en la expresión de sinaptofisina en la MEntC izquierda también mostró una disminución de volumen en los ratones viejos, lo que respalda que un volumen cerebral bajo puede participar la interrupción sináptica.

10) La plasticidad selectiva de la microglía en el fórnix y la MEntC izquierda contribuyen al deterioro cognitivo durante el envejecimiento.

12.PERSPECTIVAS

- Confirmar una respuesta causa-efecto de la longitud de los procesos de la microglía en los cambios volumétricos del fórnix.
- Modular la activación de la microglía en regiones cerebrales accesorias que se conectan al fórnix y demostrar que el circuito se ve afectado.
- Demostrar de forma directa que los cambios morfológicos específicos de la microglía en el fórnix podrían alterar el rendimiento cognitivo durante el envejecimiento.
- Analizar el dimorfismo sexual en todos los niveles, desde el desempeño en las pruebas de memoria y aprendizaje, los perfiles proinflamatorios y el volumen cerebral.

13.BIBLIOGRAFÍA

Alexander, G.E., Chen, K., Merkley, T.L., Reiman, E.M., Caselli, R.J., Aschenbrenner, M., Santerre-Lemmon, L., Lewis, D.J., Pietrini, P., Teipel, S.J., Hampel, H., Rapoport, S.I., Moeller, J.R., 2006. Regional network of magnetic resonance imaging gray matter volume in healthy aging. Neuroreport 17. https://doi.org/10.1097/01.wnr.0000220135.16844.b6

Antunes, M., Biala, G., 2012. The novel object recognition memory: Neurobiology, test procedure, and its modifications. Cogn. Process. https://doi.org/10.1007/s10339-011-0430-z

Armstrong, N.M., An, Y., Shin, J.J., Williams, O.A., Doshi, J., Erus, G., Davatzikos, C., Ferrucci, L., Beason-Held, L.L., Resnick, S.M., 2020. Associations between cognitive and brain volume changes in cognitively normal older adults. Neuroimage 223. https://doi.org/10.1016/j.neuroimage.2020.117289

Bachstetter, A.D., Ighodaro, E.T., Hassoun, Y., Aldeiri, D., Neltner, J.H., Patel, E., Abner, E.L., Nelson, P.T., 2017. Rod-shaped microglia morphology is associated with aging in 2 human autopsy series. Neurobiol. Aging 52, 98–105. https://doi.org/10.1016/j.neurobiolaging.2016.12.028

Bangen, K.J., Thomas, K.R., Sanchez, D.L., Edmonds, E.C., Weigand, A.J., Delano-Wood, L., Bondi, M.W., 2021. Entorhinal Perfusion Predicts Future Memory Decline, Neurodegeneration, and White Matter Hyperintensity Progression in Older Adults. J. Alzheimer's Dis. 81. https://doi.org/10.3233/JAD-201474

Batterman, K. V., Cabrera, P.E., Moore, T.L., Rosene, D.L., 2021. T Cells Actively Infiltrate the White Matter of the Aging Monkey Brain in Relation to Increased Microglial Reactivity and Cognitive Decline. Front. Immunol. 12. https://doi.org/10.3389/fimmu.2021.607691

Belblidia, H., Leger, M., Abdelmalek, A., Quiedeville, A., Calocer, F., Boulouard, M., Jozet-Alves, C., Freret, T., Schumann-Bard, P., 2018. Characterizing age-related decline of recognition memory and brain activation profile in mice. Exp. Gerontol. 106. https://doi.org/10.1016/j.exger.2018.03.006

Bello-Medina, P.C., Sánchez-Carrasco, L., González-Ornelas, N.R., Jeffery, K.J., Ramírez-Amaya, V., 2013. Differential effects of spaced vs. massed training in long-term object-identity and object-location recognition memory. Behav. Brain Res. 250, 102–113. https://doi.org/10.1016/j.bbr.2013.04.047

Berryer, M.H., Chattopadhyaya, B., Xing, P., Riebe, I., Bosoi, C., Sanon, N., Avoli, M., Hamdan, F.F., Carmant, L., Antoine-bertrand, J., Le, M., Lamarche-vane, N., Lacaille, J., Michaud, J.L., Cristo, G. Di, 2016. The aging systemic milieu negatively regulates neurogenesis and cognitive function. Nature 477, 90–94. https://doi.org/10.1038/nature10357.The

Bettio, L.E.B., Rajendran, L., Gil-Mohapel, J., 2017. The effects of aging in the hippocampus and cognitive decline. Neurosci. Biobehav. Rev. 79, 66–86. https://doi.org/10.1016/J.NEUBIOREV.2017.04.030

Bevins, R.A., Besheer, J., 2006. Object recognition in rats and mice: A one-trial non-matching-to-sample learning task to study "recognition memory." Nat. Protoc. 1, 1306–1311. https://doi.org/10.1038/nprot.2006.205

Broadbent, N.J., Gaskin, S., Squire, L.R., Clark, R.E., 2010. Object recognition memory and the rodent hippocampus. Learn. Mem. 17. https://doi.org/10.1101/lm.1650110

Brombacher, T.M., Nono, J.K., De Gouveia, K.S., Makena, N., Darby, M., Womersley, J., Tamgue, O., Brombacher, F., 2017. IL-13–Mediated Regulation of Learning and Memory. J. Immunol. 198, 2681–2688. https://doi.org/10.4049/jimmunol.1601546

Buckman, L.B., Hasty, A.H., Flaherty, D.K., Buckman, C.T., Thompson, M.M., Matlock, B.K., Weller, K., Ellacott, K.L.J.J., 2014. Obesity induced by a high-fat diet is associated with increased immune cell entry into the central nervous system. Brain. Behav. Immun. 35, 33–42. https://doi.org/10.1016/j.bbi.2013.06.007

Currais, A., 2015. Ageing and inflammation - A central role for mitochondria in brain health and disease. Ageing Res. Rev. 21, 30–42. https://doi.org/10.1016/j.arr.2015.02.001

D'Avila, J.C., Siqueira, L.D., Mazeraud, A., Azevedo, E.P., Foguel, D., Castro-Faria-Neto, H.C., Sharshar, T., Chrétien, F., Bozza, F.A., 2018. Age-related cognitive impairment is associated with long-term neuroinflammation and oxidative stress in a

mouse model of episodic systemic inflammation. J. Neuroinflammation 15. https://doi.org/10.1186/s12974-018-1059-y

Davalos, D., Grutzendler, J., Yang, G., Kim, J. V., Zuo, Y., Jung, S., Littman, D.R., Dustin, M.L., Gan, W.B., 2005. ATP mediates rapid microglial response to local brain injury in vivo. Nat. Neurosci. 8, 752–758. https://doi.org/10.1038/nn1472

Davies, D.S., Ma, J., Jegathees, T., Goldsbury, C., 2017. Microglia show altered morphology and reduced arborization in human brain during aging and Alzheimer's disease. Brain Pathol. 27. https://doi.org/10.1111/bpa.12456

Dubenko, O.E., Chyniak, O.S., Potapov, O.O., 2021. Levels of proinflammatory cytokines IL-17 and IL-23 in patients with alzheimer's disease, mild cognitive impairment and vascular dementia. Wiadomości Lek. 74, 68–71. https://doi.org/10.36740/wlek202101113

Faizy, T.D., Thaler, C., Broocks, G., Flottmann, F., Leischner, H., Kniep, H., Nawabi, J., Schön, G., Stellmann, J.P., Kemmling, A., Reddy, R., Heit, J.J., Fiehler, J., Kumar, D., Hanning, U., 2020. The Myelin Water Fraction Serves as a Marker for Age-Related Myelin Alterations in the Cerebral White Matter – A Multiparametric MRI Aging Study. Front. Neurosci. 14. https://doi.org/10.3389/fnins.2020.00136

Feng, X., Valdearcos, M., Uchida, Y., Lutrin, D., Maze, M., Koliwad, S.K., 2017. Microglia mediate postoperative hippocampal inflammation and cognitive decline in mice. JCI insight 2. https://doi.org/10.1172/jci.insight.91229

Fillmore, P.T., Phillips-meek, M.C., Richards, J.E., Kaye, J., 2015. Age-specific MRI brain and head templates for healthy adults from 20 through 89 years of age 7, 1–14. https://doi.org/10.3389/fnagi.2015.00044

Filo, S., Shtangel, O., Salamon, N., Kol, A., Weisinger, B., Shifman, S., Mezer, A.A., 2019. Disentangling molecular alterations from water-content changes in the aging human brain using quantitative MRI. Nat. Commun. 10. https://doi.org/10.1038/s41467-019-11319-1

Fletcher, E., Carmichael, O., Pasternak, O., Maier-Hein, K.H., DeCarli, C., 2014. Early brain loss in circuits affected by Alzheimer's disease is predicted by fornix microstructure but may be independent of gray matter. Front. Aging Neurosci. 6. https://doi.org/10.3389/fnagi.2014.00106

Fletcher, E., Raman, M., Huebner, P., Liu, A., Mungas, D., Carmichael, O., DeCarli, C., 2013. Loss of fornix white matter volume as a predictor of cognitive impairment in cognitively normal elderly individuals. JAMA Neurol. 70. https://doi.org/10.1001/jamaneurol.2013.3263

Fossati, S., Cejudo, J.R., Debure, L., Pirraglia, E., Glodzik, L., Osorio, R.S., Chen, J., Provost, A., Jeromin, A., Haas, M., Marmar, C., DeLeon, M., 2017. Differential value of plasma tau as a biomarker for alzheimer's disease and chronic traumatic brain injury. Alzheimer's Dement. 13, P1307–P1307. https://doi.org/10.1016/j.jalz.2017.06.1999

Fotenos, A.F., Snyder, A.Z., Girton, L.E., Morris, J.C., Buckner, R.L., 2005. Normative estimates of cross-sectional and longitudinal brain volume decline in aging and AD. Neurology 64, 1032–1039. https://doi.org/10.1212/01.WNL.0000154530.72969.11

Franceschi, C., Bonafè, M., Valensin, S., Olivieri, F., De Luca, M., Ottaviani, E., De Benedictis, G., 2006. Inflamm-aging: An Evolutionary Perspective on Immunosenescence. Ann. N. Y. Acad. Sci. https://doi.org/10.1111/j.1749-6632.2000.tb06651.x

FRANCESCHI, C., BONAFÈ, M., VALENSIN, S., OLIVIERI, F., DE LUCA, M., OTTAVIANI, E., DE BENEDICTIS, G., 2000. Inflamm-aging: An Evolutionary Perspective on Immunosenescence. Ann. N. Y. Acad. Sci. 908, 244–254. https://doi.org/10.1111/j.1749-6632.2000.tb06651.x

Frank, M.G., Barrientos, R.M., Biedenkapp, J.C., Rudy, J.W., Watkins, L.R., Maier, S.F., 2006. mRNA up-regulation of MHC II and pivotal pro-inflammatory genes in normal brain aging. Neurobiol. Aging 27. https://doi.org/10.1016/j.neurobiolaging.2005.03.013

Friedel, M., van Eede, M.C., Pipitone, J., Mallar Chakravarty, M., Lerch, J.P., 2014. Pydpiper: A flexible toolkit for constructing novel registration pipelines. Front. Neuroinform. 8. https://doi.org/10.3389/fninf.2014.00067

Fulop, T., Larbi, A., Dupuis, G., Page, A. Le, Frost, E.H., Cohen, A.A., Witkowski, J.M., Franceschi, C., 2018. Immunosenescence and inflamm-aging as two sides of the same coin: Friends or Foes? Front. Immunol. https://doi.org/10.3389/fimmu.2017.01960

Fung, I.T.H., Sankar, P., Zhang, Y., Robison, L.S., Zhao, X., D'Souza, S.S., Salinero, A.E., Yue, W., Qian, J., Kuentzel, M.L., Chittur, S. V., Temple, S., Zuloaga, K.L., Yang,

Q., 2020. Activation of group 2 innate lymphoid cells alleviates aging-associated cognitive decline. J. Exp. Med. 217. https://doi.org/10.1084/jem.20190915

Galluzzi, S., Beltramello, A., Filippi, M., Frisoni, G.B., 2008. Aging. Neurol.Sci. 29 Suppl 3, 296–300.

Ge, Y., Grossman, R.I., Babb, J.S., Rabin, M.L., Mannon, L.J., Kolson, D.L., 2002. Age-related total gray matter and white matter changes in normal adult brain. Part I: volumetric MR imaging analysis. AJNR. Am. J. Neuroradiol. 23, 1327–1333.

Good, C.D., Johnsrude, I.S., Ashburner, J., Henson, R.N., Friston, K.J., Frackowiak, R.S., 2001. A voxel-based morphometric study of ageing in 465 normal adult human brains. Neuroimage 14, 21–36. https://doi.org/10.1006/nimg.2001.0786

Grieve, S.M., Clark, C.R., Williams, L.M., Peduto, A.J., Gordon, E., 2005. Preservation of limbic and paralimbic structures in aging. Hum. Brain Mapp. 25. https://doi.org/10.1002/hbm.20115

Hescham, S., Temel, Y., Schipper, S., Lagiere, M., Schönfeld, L.M., Blokland, A., Jahanshahi, A., 2017. Fornix deep brain stimulation induced long-term spatial memory independent of hippocampal neurogenesis. Brain Struct. Funct. 222. https://doi.org/10.1007/s00429-016-1188-y

Jeon, H., Mun, G.I., Boo, Y.C., 2012. Analysis of serum cytokine/chemokine profiles affected by aging and exercise in mice. Cytokine 60. https://doi.org/10.1016/j.cyto.2012.07.014

Jernigan, T.L., Archibald, S.L., Fennema-Notestine, C., Gamst, A.C., Stout, J.C., Bonner, J., Hesselink, J.R., 2001. Effects of age on tissues and regions of the cerebrum and cerebellum. Neurobiol. Aging 22. https://doi.org/10.1016/S0197-4580(01)00217-2

Kalpouzos, G., Chételat, G., Baron, J.C., Landeau, B., Mevel, K., Godeau, C., Barré, L., Constans, J.M., Viader, F., Eustache, F., Desgranges, B., 2009. Voxel-based mapping of brain gray matter volume and glucose metabolism profiles in normal aging. Neurobiol. Aging 30. https://doi.org/10.1016/j.neurobiolaging.2007.05.019

Kalueff, A. V., Keisala, T., Minasyan, A., Kuuslahti, M., Tuohimaa, P., 2006. Temporal stability of novelty exploration in mice exposed to different open field tests. Behav. Processes 72, 104–112. https://doi.org/10.1016/j.beproc.2005.12.011

Keren-Shaul, H., Spinrad, A., Weiner, A., Matcovitch-Natan, O., Dvir-Szternfeld, R., Ulland, T.K., David, E., Baruch, K., Lara-Astaiso, D., Toth, B., Itzkovitz, S., Colonna, M., Schwartz, M., Amit, I., 2017. A Unique Microglia Type Associated with Restricting Development of Alzheimer's Disease. Cell 169, 1276-1290.e17. https://doi.org/10.1016/j.cell.2017.05.018

Lee, C.Y.D., Daggett, A., Gu, X., Jiang, L.-L., Langfelder, P., Li, X., Wang, N., Zhao, Y., Park, C.S., Cooper, Y., Ferando, I., Mody, I., Coppola, G., Xu, H., Yang, X.W., 2018. Elevated TREM2 Gene Dosage Reprograms Microglia Responsivity and Ameliorates Pathological Phenotypes in Alzheimer's Disease Models. Neuron 97, 1032-1048.e5. https://doi.org/10.1016/j.neuron.2018.02.002

Lemaître, H., Crivello, F., Grassiot, B., Alpérovitch, A., Tzourio, C., Mazoyer, B., 2005. Age- and sex-related effects on the neuroanatomy of healthy elderly. Neuroimage 26, 900–911. https://doi.org/10.1016/j.neuroimage.2005.02.042

Li, M., Su, S., Cai, W., Cao, J., Miao, X., Zang, W., Gao, S., Xu, Y., Yang, J., Tao, Y.X., Ai, Y., 2020. Differentially Expressed Genes in the Brain of Aging Mice With Cognitive Alteration and Depression- and Anxiety-Like Behaviors. Front. Cell Dev. Biol. 8. https://doi.org/10.3389/fcell.2020.00814

Lo, R.Y., Hubbard, A.E., Shaw, L.M., Trojanowski, J.Q., Petersen, R.C., Aisen, P.S., Weiner, M.W., Jagust, W.J., 2011. Longitudinal change of biomarkers in cognitive decline. Arch. Neurol. 68, 1257–1266. https://doi.org/10.1001/archneurol.2011.123

López-Otín, C., Blasco, M.A., Partridge, L., Serrano, M., Kroemer, G., 2013. The hallmarks of aging. Cell 153. https://doi.org/10.1016/j.cell.2013.05.039

Maldonado-Ruiz, R., Cárdenas-Tueme, M., Montalvo-Martínez, L., Vidaltamayo, R., Garza-Ocañas, L., Reséndez-Perez, D., Camacho, A., 2019. Priming of Hypothalamic Ghrelin Signaling and Microglia Activation Exacerbate Feeding in Rats' Offspring Following Maternal Overnutrition. Nutrients 11. https://doi.org/10.3390/nu11061241

Maldonado-Ruiz, R., Montalvo-Martínez, L., Fuentes-Mera, L., Camacho, A., 2017. Microglia activation due to obesity programs metabolic failure leading to type two diabetes. Nutr. Diabetes. https://doi.org/10.1038/nutd.2017.10

Matsuda, H., 2013. Voxel-based morphometry of brain MRI in normal aging and Alzheimer's disease. Aging Dis. 4, 29–37.

Matuskova, V., Ismail, Z., Nikolai, T., Markova, H., Cechova, K., Nedelska, Z., Laczo, J., Wang, M., Hort, J., Vyhnalek, M., 2021. Mild Behavioral Impairment Is Associated With Atrophy of Entorhinal Cortex and Hippocampus in a Memory Clinic Cohort. Front. Aging Neurosci. 13. https://doi.org/10.3389/fnagi.2021.643271

Metzler-Baddeley, C., Mole, J.P., Sims, R., Fasano, F., Evans, J., Jones, D.K., Aggleton, J.P., Baddeley, R.J., 2019. Fornix white matter glia damage causes hippocampal gray matter damage during age-dependent limbic decline. Sci. Rep. 9, 15164. https://doi.org/10.1038/s41598-019-51737-1

Miller, K.R., Streit, W.J., 2007. The effects of aging, injury and disease on microglial function: A case for cellular senescence, in: Neuron Glia Biology. https://doi.org/10.1017/S1740925X08000136

Morgan, J.A., Singhal, G., Corrigan, F., Jaehne, E.J., Jawahar, M.C., Baune, B.T., 2018. The effects of aerobic exercise on depression-like, anxiety-like, and cognition-like behaviours over the healthy adult lifespan of C57BL/6 mice. Behav. Brain Res. 337. https://doi.org/10.1016/j.bbr.2017.09.022

Mungas, D., Harvey, D., Reed, B.R., Jagust, W.J., DeCarli, C., Beckett, L., Mack, W.J., Kramer, J.H., Weiner, M.W., Schuff, N., Chui, H.C., 2005. Longitudinal volumetric MRI change and rate of cognitive decline. Neurology 65. https://doi.org/10.1212/01.wnl.0000172913.88973.0d

Ober, B.A., 1996. Learning and Memory in Normal Aging, by D.H. Kausler. 1994. New York: Academic Press. 544 pp., $65.00. J. Int. Neuropsychol. Soc. 2. https://doi.org/10.1017/s1355617700001405

Pennisi, M., Crupi, R., Di Paola, R., Ontario, M.L., Bella, R., Calabrese, E.J., Crea, R., Cuzzocrea, S., Calabrese, V., 2017. Inflammasomes, hormesis, and antioxidants in neuroinflammation: Role of NRLP3 in Alzheimer disease. J. Neurosci. Res. https://doi.org/10.1002/jnr.23986

Petersen, R.C., 2016. Mild cognitive impairment. Contin. Lifelong Learn. Neurol. https://doi.org/10.1212/CON.0000000000000313

Resnick, S.M., Pham, D.L., Kraut, M.A., Zonderman, A.B., Davatzikos, C., 2003. Longitudinal magnetic resonance imaging studies of older adults: A shrinking brain. J. Neurosci. 23, 3295–3301. https://doi.org/10.1523/jneurosci.23-08-03295.2003

Salminen, A., Kaarniranta, K., Kauppinen, A., 2012. Inflammaging: Disturbed interplay between autophagy and inflammasomes. Aging (Albany. NY). 4, 166–175. https://doi.org/10.18632/aging.100444

Salter, M.W., Stevens, B., 2017. Microglia emerge as central players in brain disease. Nat. Med. 23, 1018–1027. https://doi.org/10.1038/nm.4397

Santoro, A., Spinelli, C.C., Martucciello, S., Nori, S.L., Capunzo, M., Puca, A.A., Ciaglia, E., 2018. Innate immunity and cellular senescence: The good and the bad in the developmental and aged brain. J. Leukoc. Biol. 1–16. https://doi.org/10.1002/JLB.3MR0118-003R

Sato, K., Taki, Y., Fukuda, H., Kawashima, R., 2003. Neuroanatomical database of normal Japanese brains. Neural Networks 16, 1301–1310. https://doi.org/10.1016/j.neunet.2003.06.004

Shahidehpour, R.K., Higdon, R.E., Crawford, N.G., Neltner, J.H., Ighodaro, E.T., Patel, E., Price, D., Nelson, P.T., Bachstetter, A.D., 2021. Dystrophic microglia are associated with neurodegenerative disease and not healthy aging in the human brain. Neurobiol. Aging 99, 19–27. https://doi.org/10.1016/j.neurobiolaging.2020.12.003

Sheng, J.G., Mrak, R.E., Griffin, W.S.T., 1998. Enlarged and phagocytic, but not primed, interleukin-1α-immunoreactive microglia increase with age in normal human brain. Acta Neuropathol. 95. https://doi.org/10.1007/s004010050792

Sierra, F., 2016. The emergence of geroscience as an interdisciplinary approach to the enhancement of health span and life span. Cold Spring Harb. Perspect. Med. 6. https://doi.org/10.1101/cshperspect.a025163

Smith, C.D., Chebrolu, H., Wekstein, D.R., Schmitt, F.A., Markesbery, W.R., 2007. Age and gender effects on human brain anatomy: A voxel-based morphometric study in healthy elderly. Neurobiol. Aging 28, 1075–1087. https://doi.org/10.1016/j.neurobiolaging.2006.05.018

Soulet, D., Rivest, S., 2014. Microglia. Curr. Biol. 18, 506–508. https://doi.org/10.3389/fncel.2014.00396

Sowell, E.R., Thompson, P.M., Toga, A.W., 2004. Mapping changes in the human cortex throughout the span of life. Neuroscientist. https://doi.org/10.1177/1073858404263960

Suárez, R., Buelvas, N., 2015. El inflamasoma: Mecanismos de activación. Invest. Clin. 56, 74–99.

Sullivan, E. V., Rosenbloom, M., Serventi, K.L., Pfefferbaum, A., 2004. Effects of age and sex on volumes of the thalamus, pons, and cortex. Neurobiol. Aging 25, 185–192. https://doi.org/10.1016/S0197-4580(03)00044-7

Sunyer, B., Patil, S., Höger, H., Luber, G., 2007. Barnes maze, a useful task to assess spatial reference memory in the mice. Nat. Protoc. Exch. 1–12. https://doi.org/10.1038/nprot.2007.390

Taki, Y., Goto, R., Evans, A., Zijdenbos, A., Neelin, P., Lerch, J., Sato, K., Ono, S., Kinomura, S., Nakagawa, M., Sugiura, M., Watanabe, J., Kawashima, R., Fukuda, H., 2004. Voxel-based morphometry of human brain with age and cerebrovascular risk factors. Neurobiol. Aging 25, 455–463. https://doi.org/10.1016/j.neurobiolaging.2003.09.002

Tarkowski, E., Wallin, A., Regland, B., Blennow, K., Tarkowski, A., 2001. Local and systemic GM-CSF increase in Alzheimer's disease and vascular dementia. Acta Neurol. Scand. 103, 166–174. https://doi.org/10.1034/j.1600-0404.2001.103003166.x

Tisserand, D.J., Pruessner, J.C., Sanz Arigita, E.J., Van Boxtel, M.P.J., Evans, A.C., Jolles, J., Uylings, H.B.M., 2002. Regional frontal cortical volumes decrease differentially in aging: An MRI study to compare volumetric approaches and voxel-based morphometry. Neuroimage 17. https://doi.org/10.1016/S1053-8119(02)91173-0

Trujillo-Villarreal, L.A., Romero-Díaz, V.J., Marino-Martínez, I.A., Fuentes-Mera, L., Ponce-Camacho, M.A., Devenyi, G.A., Mallar Chakravarty, M., Camacho-Morales, A., Garza-Villarreal, E.E., 2021. Maternal cafeteria diet exposure primes depression-like behavior in the offspring evoking lower brain volume related to changes in synaptic terminals and gliosis. Transl. Psychiatry 11. https://doi.org/10.1038/s41398-020-01157-x

Villeda, S.A., Plambeck, K.E., Middeldorp, J., Castellano, J.M., Mosher, K.I., Luo, J., Smith, L.K., Bieri, G., Lin, K., Berdnik, D., Wabl, R., Udeochu, J., Wheatley, E.G., Zou, B., Simmons, D.A., Xie, X.S., Longo, F.M., Wyss-Coray, T., 2014. Young blood reverses age-related impairments in cognitive function and synaptic plasticity in mice. Nat. Med. 20, 659–663. https://doi.org/10.1038/nm.3569

von Bernhardi, R., Eugenín-von Bernhardi, L., Eugenín, J., 2015. Microglial cell dysregulation in brain aging and neurodegeneration. Front. Aging Neurosci. 7, 1–21. https://doi.org/10.3389/fnagi.2015.00124

Wolf, A., Bauer, B., Abner, E.L., Ashkenazy-Frolinger, T., Hartz, A.M.S., 2016. A comprehensive behavioral test battery to assess learning and memory in 129S6/ Tg2576 mice. PLoS One 11, 1–23. https://doi.org/10.1371/journal.pone.0147733

Wolfe, H., Minogue, A.M., Rooney, S., Lynch, M.A., 2018. Infiltrating macrophages contribute to age-related neuroinflammation in C57/BL6 mice. Mech. Ageing Dev. 173, 84–91. https://doi.org/10.1016/j.mad.2018.05.003

Wu, M.J., Gao, Y.L., Liu, J.X., Zhu, R., Wang, J., 2019. Principal Component Analysis Based on Graph Laplacian and Double Sparse Constraints for Feature Selection and Sample Clustering on Multi-View Data. Hum. Hered. 84. https://doi.org/10.1159/000501653

Wyss-Coray, T., 2016. Ageing, neurodegeneration and brain rejuvenation. Nature 539, 180–186. https://doi.org/10.1038/nature20411

Yin, P., Wang, X., Wang, S., Wei, Y., Feng, J., Zhu, M., 2019. Maresin 1 Improves Cognitive Decline and Ameliorates Inflammation in a Mouse Model of Alzheimer's Disease. Front. Cell. Neurosci. 13. https://doi.org/10.3389/fncel.2019.00466

Young, K., Morrison, H., 2018. Quantifying microglia morphology from photomicrographs of immunohistochemistry prepared tissue using imagej. J. Vis. Exp. 2018. https://doi.org/10.3791/57648

Zhou, L., Flores, J., Noël, A., Beauchet, O., Sjöström, P.J., Leblanc, A.C., 2019. Methylene blue inhibits Caspase-6 activity, and reverses Caspase-6-induced cognitive impairment and neuroinflammation in aged mice. Acta Neuropathol. Commun. 7. https://doi.org/10.1186/s40478-019-0856-6

RESUMEN BIOGRÁFICO

Marcela Cárdenas Tueme

Candidata para el Grado de
Doctorado en Ciencias con Orientación en Inmunobiología

Tesis: EL AUMENTO VOLUMÉTRICO DEL FÓRNIX Y LA MORFOLOGÍA DE LA MICROGLÍA CONTRIBUYEN A LA AFECTACIÓN DE LA MEMORIA ESPACIAL Y DE RECONOCIMIENTO EN *Mus musculus* DURANTE EL ENVEJECIMIENTO

Campo de Estudio: Neuroinmunología

Datos Personales: Nacida en Monterrey, Nuevo León el 19 de Diciembre de 1989, hija de Carlos Cárdenas Barrera y Marcela Tueme Reséndez.

Educación: Egresada de la Universidad Autónoma de Nuevo León, grado obtenido Lic. en Biotecnología Genómica en 2014.

Experiencia Profesional:

Escuela de Neurociencias CAJAL. Aging Cognition 2021, Bordeaux, Francia.
Curso de Manejo de Animales de Laboratorio. Animod 2019, Varadero, Cuba.
Curso de Microscopía Fluorescente, FluoMicro 2018, ICGEB, Trieste, Italia.
Curso de Neurobiología. Gordon Research Conference, Neurobiology of Brain Disorders, 2018, Barcelona, España.
Responsable de laboratorio de Diagnóstico Molecular en Novogen México, en los años 2014-2015

ARTÍCULOS CIENTÍFICOS PUBLICADOS

frontiers in Neuroscience

REVIEW
published: 04 February 2020
doi: 10.3389/fnins.2020.00013

Neurodegenerative Susceptibility During Maternal Nutritional Programing: Are Central and Peripheral Innate Immune Training Relevant?

*Marcela Cárdenas-Tueme[1], Larisa Montalvo-Martínez[2], Roger Maldonado-Ruiz[2], Alberto Camacho-Morales[2,3] and Diana Reséndez-Pérez[1]**

[1] Departamento de Biología Celular y Genética, Facultad de Ciencias Biológicas, Universidad Autónoma de Nuevo León, San Nicolás de los Garza, Mexico, [2] Departamento de Bioquímica, Facultad de Medicina, Universidad Autónoma de Nuevo León, San Nicolás de los Garza, Mexico, [3] Centro de Investigación y Desarrollo en Ciencias de la Salud, Unidad de Neurometabolismo, Universidad Autónoma de Nuevo León, San Nicolás de los Garza, Mexico

Maternal overnutrition modulates body weight, development of metabolic failure and, potentially, neurodegenerative susceptibility in the offspring. Overnutrition sets a chronic pro-inflammatory profile that integrates peripheral and central immune activation nodes, damaging neuronal physiology and survival. Innate immune cells exposed to hypercaloric diets might experience trained immunity. Here, we address the role of maternal overnutrition as a trigger for central and peripheral immune training and its contribution to neurodegeneration and the molecular nodes implicated in the Nod-like receptor protein 3 (NLRP3) inflammasome pathway leading to immune training. We propose that maternal overnutrition leads to peripheral or central immune training that favor neurodegenerative susceptibility in the offspring.

Keywords: maternal programing, neurodegeneration, inflammation, immune training, cytokines

OPEN ACCESS

Edited by:
Kathleen C. Page, Bucknell University, United States

Reviewed by:
Juan C. Saez, Pontifical Catholic University of Chile, Chile
Nafisa M. Jadavji, Midwestern University, United States

****Correspondence:***
Diana Reséndez-Pérez
diana.resendezpr@uanl.edu.mx;
diaresendez@gmail.com

Specialty section:
This article was submitted to Neuroenergetics, Nutrition and Brain Health, a section of the journal Frontiers in Neuroscience

Received: *18 November 2019*
Accepted: *08 January 2020*
Published: *04 February 2020*

Citation:
Cárdenas-Tueme M, Montalvo-Martínez L, Maldonado-Ruiz R, Camacho-Morales A and Reséndez-Pérez D (2020) Neurodegenerative Susceptibility During Maternal Nutritional Programing: Are Central and Peripheral Innate Immune Training Relevant? Front. Neurosci. 14:13. doi: 10.3389/fnins.2020.00013

INTRODUCTION

According to the World Health Organization, nearly 39% of adults were overweight in 2016, and 13% were obese. Epidemiological data from human catastrophes such as the Dutch famine (1944), the siege of Leningrad (1942–1944), the great Chinese famine (1958–1961), and the Överkalix study (1890-present) propose that changes in nutrient intake such as fasting or overnutrition during pregnancy and lactation are associated with metabolic and behavioral disorders in the offspring (Vaiserman, 2017). Maternal nutritional programing can influence offspring body weight, adiposity, and development of metabolic syndrome in diverse ways (Friedman, 2018; Patro Golab et al., 2018).

For instance, nutritional programing adversely impacts both maternal and offspring health, increasing susceptibility to show metabolic abnormalities later in life such as obesity, dyslipidemia, type 2 diabetes (T2D) mellitus and hypertension, as well as behavioral disorders related to schizophrenia, autism, and compulsive eating (Shapiro et al., 2017; Friedman, 2018; Patro Golab et al., 2018; Derks et al., 2019).

Recent experimental evidence shows that exposure to hypercaloric diets programs the immune nodes that modulate metabolism and neuronal survival during embryogenesis. For instance, the immune response is involved in the balance and maintenance of an adequate metabolic state; however, conditions of altered metabolic demand promote a pro-inflammatory state (Christ et al., 2018). On this context, overnutrition might trigger an epigenetic process called "trained immunity" in innate immune cells, such as microglia in the central nervous system (CNS) and macrophages or natural killer cells in the periphery, which results in enhanced immune responses following infections or immune stimulation. The epigenetic mechanisms that mediate trained immunity are better understood in macrophages and monocytes, and a few have been described in microglia. Wendeln et al. (2018) demonstrated that microglia, just like peripheral macrophages, can be trained to confer long-lasting memory. In microglia, "trained immunity" is dependent on chromatin remodeling and activation of inflammatory signaling pathways (NF-κB, JNK, and ERK1/2). Also, by knocking down Hdac1/2 or Tak1 in long-lived CX3CR1 + cells (most of them microglia) cytokine levels were reduced, suggesting that epigenetic reprograming of inflammatory responses is key to accomplish immune training (Wendeln et al., 2018).

In this review, we address the role of maternal nutritional programing on central and peripheral immune training and crosstalk during positive metabolic scenarios, as well as their potential relevance in neurodegenerative susceptibility in the offspring.

CENTRAL AND PERIPHERAL IMMUNE SYSTEM COMMUNICATION

The innate immune system is the first line of defense against pathogens and tissue damage; it includes physical barriers such as the skin, and specific cell types that modulate the inflammatory response such as macrophages, microglia, and complement proteins. The inflammatory response consists of an innate cellular system and humoral responses that occur during injury to restore homeostasis (Ciaccia, 2010). In this scenario, microglia, play the role of the innate immune system in the brain, infiltrating during early embryogenesis, coordinating neurogenesis, synaptic pruning, connectome establishment, and acting as major antigen-presenting cells (Colonna and Butovsky, 2017; Maldonado-Ruiz et al., 2017). In healthy brains, microglia remain in a ramified stated, and when activated, they enlarge their cell body, change to a phagocytic state, release pro-inflammatory cytokines, and increase antigen presentation and ROS production, leading to neuroinflammation (Colonna and Butovsky, 2017). As shown in **Figure 1**, under an altered physiological scenario, peripheral immune cells infiltrate the brain, become pro-inflammatory and secrete cytokines. This causes an exacerbated immune response by M1-activated microglia which leads to neuroinflammation, favoring protein aggregation and brain damage consistent with neurodegenerative pathologies (Colonna and Butovsky, 2017).

In the past years, the concept of the CNS as an immune-privileged site has changed, and interactions between the peripheral and central immune system have been demonstrated. Furthermore, these interactions are necessary to maintain homeostasis in the CNS, which was once thought to be impossible. For instance, the myeloid cells such as the macrophages and dendritic cells (DCs) in the meninges (dura, arachnoid, and pia mater), choroid plexus, and perivascular spaces in the CNS parenchyma can mount a robust protective and restorative response when necessary.

In addition, there is a strong relationship between inflammation and metabolic disorders in the immune response against infection. It is known that the immune response is involved in the balance and maintenance of an adequate metabolic state; however, it can have adverse effects under conditions of altered metabolic demand (Agrawal, 2014). In this way, positive energy balance during overnutrition promotes an inflammatory state in the CNS. For instance, saturated fatty acids from the diet are considered powerful candidates to trigger immune response in the peripheral system and in the CNS. However, how central immunity communicates with the peripheral immune response during overnutrition remains to be clarified (Maldonado-Ruiz et al., 2017). Based on this complex and delicate regulation, we next address how much the cells of the immune system can be influenced by selective diets.

MATERNAL PROGRAMING BY EXPOSURE TO HIGH-FAT-HIGH-SUGAR DIETS ACTIVATES IMMUNITY AND REGULATES NEURODEGENERATIVE SUSCEPTIBILITY

Experimental data in animal models and humans have contributed to understand the effect of caloric overnutrition during pregnancy on immunity and neurodegenerative susceptibility later in life. The nervous system develops through a sophisticated and precise process from embryonic stages through puberty and adulthood. Proliferation, migration and differentiation of major brain cell types followed by rapid synaptogenesis integrate and establish a selective and efficient brain connectome. The immune system shares a time-dependent development and maturation with the nervous system during embryogenesis and post-natal periods (Estes and McAllister, 2016), which renders these systems extremely responsive to environmental factors, potentially modulating central and peripheral cross-talk and neurodegenerative susceptibility.

Initial experimental evidence in animal models and humans showing defects in glucose homeostasis such as T2D, have

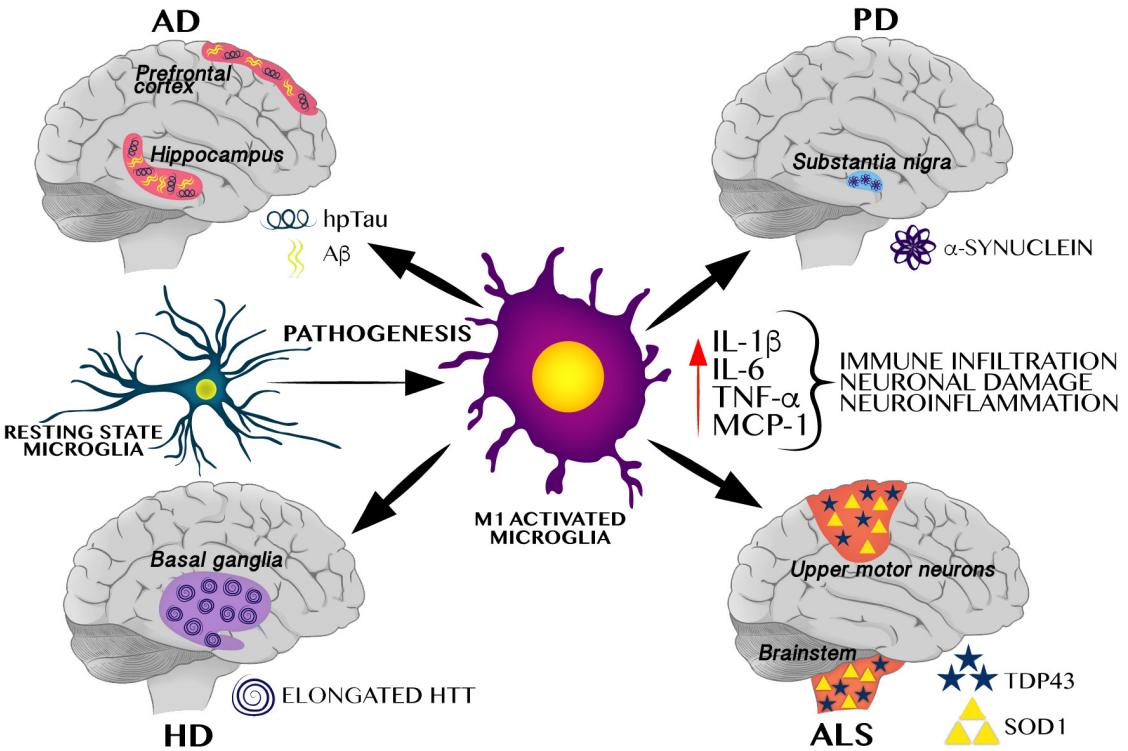

FIGURE 1 | M1 Microglial activation induces a pro-inflammatory cytokines favoring neuroinflammation and protein aggregation-related neurodegenerative pathologies. M1 activated microglia induces a pro-inflammatory profile, including increase of IL-1β, TNF-α, MCP-1, and IL-6, all of these cytokines have been identified in different neurodegenerative pathologies including AD, PD, HD, and ALS. These neurodegenerative pathologies are characterized by selective protein aggregation, including amyloid beta (Aβ) and hyperphosphorylated Tau (hpTau) in AD, α-synuclein in PD, elongated huntingtin (HTT) in HD, and TAR DNA binding protein 43 (TDP43) and superoxide dismutase 1 (SOD1) in ALS.

reported to contribute to neurodegeneration. For instance, rats fed a high-fat/glucose die develop insulin resistance and exhibit impaired spatial learning ability, reduced hippocampal dendritic spine density, and reduced long-term potentiation in the CA1 region due to glucotoxicity or altered insulin signaling (Stranahan et al., 2008). Moreover, Alzheimer's disease (AD) transgenic mice models fed with a high-fat diet showed T2D-like peripheral insulin resistance but also more severe cognitive deficits compared to normoglycemic AD mice (Procaccini et al., 2016), demonstrating the possible interplay between defects in glucose metabolism and AD development. Of note, patients with T2D show two-fold higher risk to develop AD than normal subjects (Ott et al., 1999).

Experimental and clinical data support the hypothesis that inflammation itself might be a risk factor for neurodegeneration during AD (Ott et al., 1999; Bertram et al., 2007; Takahashi et al., 2007; Tartaglione et al., 2016). For instance, Ling Z. et al. (2004) and Ling Z. D. et al. (2004) exposed rats to LPS prenatally and then administered with a subtoxic dose of the dopaminergic (DA) neurotoxin rotenone (1.25 mg/kg per day for 14 days) when 16 months old. Of note, prenatal LPS and postnatal rotenone exposure exacerbate DA cell loss compared with the effects of single LPS or rotenone exposure. Also, initial genomic analysis of AD patients identified several risk genes that encode proteins involved in neural repair and remyelination and in the modulation of microglial responses, including phagocytosis (Bertram et al., 2007; Takahashi et al., 2007).

Obesity or maternal programing by exposure to high-fat-high-sugar diets in animal models and humans is in fact associated with overactivation of the immune system, triggering a process of chronic inflammation named "meta-inflammation" or "metabolic inflammation," which ultimately links central and peripheral immune activation (O'Brien et al., 2017). For instance, maternal overnutrition of high-fat-high-sugar diets during pregnancy in murine models programs metabolic and hormonal settings that modulate neuronal development, axonal pruning, synaptic plasticity and connectome establishment during embryogenesis (Bilbo and Tsang, 2010; Morin et al., 2017; Mucellini et al., 2019). Also, mice born from obese dams have shown significant metabolic alterations including higher body fat, altered serum leptin levels, pancreatic islet hypertrophy, and lower expression of metabolism-related genes (Bilbo and Tsang, 2010; Gomes et al., 2018; Mucellini et al., 2019). In addition, human obesity is associated with the low-grade peripheral immune activation characteristic of an acute phase reaction, including C-reactive protein and serum amyloid A (SAA), an increase of cytokines, such as tumor necrosis factor (TNF-α), IL-1β, and IL-6 in serum, and an increase

in white cell counts (Esser et al., 2014). In fact, systemic immune activation in psoriasis, a skin disorder, efficiently favors neuroinflammation (O'Brien et al., 2017). There are also other evidences in humans verifying that obesity is closely associated with neurodegenerative susceptibility including Alzheimer's, Parkinson's, and Huntington's diseases and nervous system sclerosis (Procaccini et al., 2016), and an increase in the Body Mass Index in healthy mothers is negatively associated with white matter development in their offspring (Ou et al., 2015; Procaccini et al., 2016; Widen et al., 2018). These results suggest that positive energy balance such as during obesity or maternal overnutrition leads to neurodegenerative susceptibility, which potentially involves an immune activation pathway.

Initial reports of maternal programing by overnutrition using murine models identified sex-specific differences in fetal size and gene expression signatures in fetal-brains, showing that male offspring are the most affected. Importantly, the offspring displays a pro-inflammatory gene signature as the top regulated gene pathway (Edlow et al., 2016a). Later on, these results were confirmed in humans in a pilot study that analyzed the amniotic fluid from obese and lean pregnant women on the second trimester; in this study, 205 genes were found differentially regulated, where the lipid regulator, Apolipoprotein D, was the most upregulated gene (9-fold). Also, genes involved in apoptotic cell death were significantly downregulated particularly within pathways involving the cerebral cortex, such as the Serine/threonine kinase 24 ATPase (*STK24*). These biomarkers also correlated with the activation of the transcriptional regulators estrogen receptor, FOS, and STAT3, suggesting a pro-estrogenic, pro-inflammatory milieu (Edlow et al., 2014). In addition, this molecular signature was then confirmed in a prospective case-control study were 701 differentially regulated genes were identified, integrating a neurodegeneration gene signature, including Occludin (*OCLN*), Kinesin Family Member 14 (*KIF14*), and Nuclear receptor subfamily 2, group E, member 1 (*NR2E1*) (Edlow et al., 2016b). Upregulation of *OCLN* and *KIF14* genes have been previously associated to AD and vascular dementia in post-mortem human brain tissue (Romanitan et al., 2007), and in negative regulation of neuron apoptosis and regulation of myelination (Fujikura et al., 2013), respectively. Also, *NR2E1* is implicated in neurogenesis and neuronal differentiation modulating aggressive behavior and fear response (Young et al., 2002). Notably, all of these gene alterations also correlated with a pro-inflammatory signature of upregulated genes: chemokine (C-C motif) receptor 6 (CCR6), O-linked N-acetylglucosamine (GlcNAc) transferase (OGT), chemokine (C-C motif) receptor 2 (CCR2), caspase 4, apoptosis-related cysteine peptidase (CASP4), toll-like receptor 1 (TLR1), nucleoporin 107 kDa (NUP107), decapping enzyme, scavenger (D), among others (Edlow et al., 2016b). Together, maternal nutritional programing by overnutrition activates the central and peripheral immune systems that intimately communicate with each other to modulate neuroinflammation, thus increasing neurodegenerative susceptibility in offspring.

We will now discuss the experimental data addressing the potential role of maternal nutritional programing on the Nod-like receptor protein 3 (NLRP3) inflammasome pathway activation and its effects on neurodegeneration.

POTENTIAL ROLE OF THE NOD-LIKE RECEPTOR PROTEIN 3 INFLAMMASOME PATHWAY ON NEURODEGENERATIVE SUSCEPTIBILITY BY NUTRIENT OVER SUPPLY

The NLRP3- inflammasome pathway is linked to a danger-associated molecular pattern released from damaged or dying neurons that bind and activate the Toll-like receptor (TLR) –dependent myeloid differentiation primary response protein MyD88 (MYD88)–nuclear factor-κB (NF-κB) pathway. At first, the TLR-MYD88-NF-κB pathway positively produces pro-IL-1β and NLRP3 synthesis, activating a positive feedback loop. Then, negative stimuli, including changes in potassium efflux or reactive oxygen species, trigger the inflammasome assembly and processing of pro-IL-1β into IL-1β by caspase 1 activation (Heneka et al., 2018). Finally, the NF-κB transcription factor also regulates a variety of different processes, including stress response and a pro-inflammatory profile activation.

Initial reports by Christ et al. (2018) identified that murine models exposed to high-fat-high-sugar diets set an epigenetic program that primes B lymphocytes into an exacerbated pro-inflammatory phenotype. These, become much more responsive under physiologic stimuli which depend on the NLRP3-inflammasome pathway (Christ et al., 2018). Selective lipid species, such as palmitate and stearate, as well as, carbohydrates have been identified to activate the NLRP3-inflammasome pathway (Wen et al., 2011; Ann et al., 2018). For instance, saturated lipids from diet intake such as palmitic and stearic acids promote IL-1β release from bone marrow-derived macrophages of rodents and humans, respectively (Wen et al., 2011; L'homme et al., 2013), an effect replicated in murine macrophages (Ann et al., 2018). Of note, immune activation by palmitic and stearic acids precisely depends on the NLRP3-inflammasome pathway (Wen et al., 2011; L'homme et al., 2013). Conversely, unsaturated fatty acids, including oleate and linoleate, prevent IL-1β release and are unable to activate the NLRP3-inflammasome pathway in human monocytes/macrophages (L'homme et al., 2013; Sui et al., 2016). Also, a high-fructose diet in mice positively activates the NLRP3-inflammasome pathway and IL-1β release in human macrophage and liver cell lines, which correlates with neutrophil infiltration (Mastrocola et al., 2016; Nigro et al., 2017; Choe and Kim, 2017). Finally, the role of metabolic species regulating the NLRP3-inflammasome and neurodegeneration was recently evidenced by showing that the 25-hydroxycholesterol also activates the NLRP3-inflammasome pathway, promoting progressive neurodegeneration in X-linked adrenoleukodystrophy, a nervous disease with cerebral inflammatory demyelination (Jang et al., 2016). Moreover, the NLRP3 inflammasome pathway has been identified to contribute to PD (Fan et al., 2017;

Gordon et al., 2018; Lee et al., 2018), AD and ALS (Heneka et al., 2013; Johann et al., 2015), HD (Glinsky, 2008), as well as to behavioral alterations in mice at later stages, such as anhedonia (Zhu et al., 2017), anxiety (Lei et al., 2017) and depression-like behavior (Pan et al., 2014; Su et al., 2017).

Altogether, the evidence suggests that overnutrition during pregnancy might promote microglia activation, which correlates with peripheral pro-inflammatory profiles and brain abnormalities in the offspring that are related with neurodegenerative susceptibility. We next discuss the role of diet-induced central and peripheral immune training on neurodegeneration.

DOES CENTRAL AND PERIPHERAL INNATE IMMUNE TRAINING BY NLRP3 INFLAMMASOME CONTRIBUTES TO NEURODEGENERATION?

Trained immunity is a selective innate immune memory that induces an enhanced response to an inflammatory stimulus in innate immune cells (for instance, microglia), with a much stronger effect than that observed in basal conditions. Trained immunity depends of signal imprinting on transcription factors and epigenetic reprograming (**Figure 2A**). At this state, microglia in the CNS, or macrophages, leukocytes, natural killer cells, etc., in the peripheral system undergo apparent changes in their morphology, elevated secretion of cytokines and other inflammatory mediators, as well as substantial epigenetic program settings (Netea et al., 2016). Recent reports in different models and also in humans have confirmed robust innate immune training of myeloid cells following a pro-inflammatory challenge (Arts et al., 2018; Bekkering et al., 2018; Christ et al., 2018; Kaufmann et al., 2018; Mitroulis et al., 2018). For instance, exposure to a brief high-fat diet for 3 days promoted the activation of the NLRP3 inflammasome pathway, leading to central immune training, which potentially associates to deficits in long-term memory formation in mice (Sobesky et al., 2016). Also, peripherally applied inflammatory stimuli induce acute immune training in microglia, which correlates with differential epigenetic reprograming that modulates the microglial Tak1 or Hdac1/2 genes. Notably, microglia immune training persists for at least 6 months and increases neuronal death in an animal model of AD and ischemia (Wendeln et al., 2018). These results support the importance of central immune training as a positive regulator of neurodegenerative susceptibility that, during nutritional programing, depends on the NLRP3 inflammasome pathway, as we mentioned before (Christ et al., 2018).

Major advances demonstrating the role of the NLRP3 inflammasome pathway on neurodegenerative susceptibility have been identified in animal models. In fact, it is believed that the NLRP3 inflammasome pathway goes beyond IL-1β synthesis, activating the function of the NF-κB factor and modulating neurodegenerative susceptibility. At first, experimental studies using murine models propose that NF-κB seems to have a role in the development of synaptic plasticity and neuronal survival (Monje et al., 2003), however, over activation of the IKKβ/NF-kB binomial might set the scenario toward a new pro-inflammatory state involving TNF-α through the paracrine actions modulating neuronal survival (**Figure 2B**). For instance, microglia IKKβ/NF-κB ablation in the hypothalamus reverts cognitive decline in rodents (Zhang et al., 2013), whereas IKKβ/NF-κB activation under long-time exposure to a hypercaloric diet depletes and impairs neuronal differentiation of adult hypothalamic neural stem cells (Li et al., 2012).

In the context of overnutrition, the IKKβ/NF-kB pathway (**Figure 2C**) seems to activate metabolic-related neurodegenerative markers including the suppressor of cytokine signaling 3 (SOCS3), the tyrosine-protein phosphatase non-receptor type 1 (PTP1B), and potentially, the T-cell protein tyrosine phosphatase (TCPTP) (Milanski et al., 2009). SOCS3 is implicated in neuronal damage during aging (Yadav et al., 2005; DiNapoli et al., 2010), and is also activated during Wallerian degeneration in injured peripheral nerves (Girolami et al., 2010; McNamee et al., 2010). The PTP1B marker leads to neuronal damage in the developing brain (Liu et al., 2019) and is actively implicated in apoptotic neuronal death in a high-glucose *in vitro* model (Arroba et al., 2016). Of note, PTP1B inhibition significantly inactivates GSK-3β-suppressing, amyloid β (Aβ)-induced tau phosphorylation and ameliorates spatial learning and memory in an animal model of AD (Kanno et al., 2016). On the other hand, the TCPTP marker was initially identified as a contributor to leptin resistance in the hypothalamus during obesity in rodents (Loh et al., 2011) and as a modulator of the homeostasis of body glucose (Dodd et al., 2015, 2018). Recently, TCPTP was reported to modulate cytokine release by the expression of connexin 30 (CX30) and connexin 43 (CX43) from astrocytes in a reciprocal interplay with PTP1B following LPS administration (Debarba et al., 2018). In fact, connexin43 or pannexin1 in astrocytes has been demonstrated to promote activation of the inflammasome in glial cells (Yi et al., 2016) and, its blockade with boldine, inhibited hemichannel activity in astrocytes and microglia without affecting gap junctional communication in culture and acute hippocampal slices. Also, when tested in animal models, AD mice with long-term oral administration of boldine prevented the increase in glial hemichannel activity, astrocytic Ca^{2+} signal, ATP and glutamate release which in turn, alleviated hippocampal neuronal suffering (Yi et al., 2017). These evidences allow us to propose that the IKKβ/NF-kB pathway activation during overnutrition integrates the PTP1B – TCPTP cross-talk which might be potentially implicated in neuronal survival. Together, given that overnutrition is associated to immune training by regulating the NF-κB activation linked to the NLRP3 inflammasome pathway (Christ et al., 2018), we propose that maternal nutritional programing by exposure to hypercaloric diets during pregnancy might set microglia immune training by activation of the IKKβ/NF-kB pathway, amplifying its effects on the SOCS3, the PTP1B, and the TCPTP (**Figure 2C**). Altogether, these proteins might increase susceptibility to neurodegenerative diseases in the offspring at later stages.

Potential molecular mechanisms that regulate peripheral immune training linked to NLRP3 inflammasome and

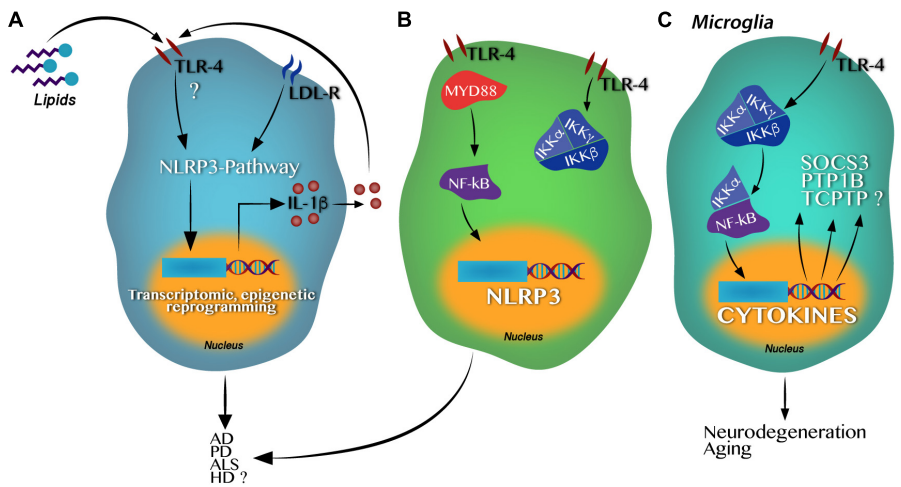

FIGURE 2 | Toll-like receptor 4 activation by hypercaloric diet regulates inflammasome activation in innate cells leading to neurodegeneration. **(A)** In granulocyte monocyte precursor cells lipids activate Toll-like receptor 4 (TLR-4) leading to the inflammasome-pathway (NLRP3) activation, epigenetic, and transcriptomic changes in nucleus and IL-1β synthesis and release. IL-1β itself might stimulate an autocrine loop activating the TLR-4. **(B)** Classic activation of the IKK kinase complex (IKKα and IKKβ) by lipids in granulocyte monocyte precursor cells over supply leads to the NF-κB transcription factor activation and translocation into the nucleus positively regulating the NLRP3 synthesis. Dual activation of the **(A)** and **(B)** pathways result in neuronal death found in AD, PD, HD, and potentially in ALS. **(C)** Activation of the TLR-4 in microglia stimulates the IKK kinase complex following by the NF-κB activation and translocation into the nucleus leading to cytokines, suppressor of cytokine signaling 3 (SOCS3), protein-tyrosine phosphatase 1B (PTP1B) and probably, T-cell protein tyrosine phosphatase (TCPTP) synthesis, which altogether promote neurodegeneration and aging.

neurodegeneration are being elucidated. Qiao et al. (2018) identified that hepatic NLRP3 inflammasome inhibition by *in vivo* siRNA administration decreases the TNF-α, IL-β, IL-12, and IL-18 serum levels. Of note, inhibition of the hepatic NLRP3 inflammasome partially prevents dopaminergic neuronal death in the substantia nigra of a murine Parkinson model by decreasing the pro-inflammatory profile in plasma (Qiao et al., 2018). It seems that immune activation, at least for viral infections, depends on CXCR6, a chemokine receptor of hepatic NK cells involved in the persistence of cellular memory (Netea et al., 2011). This suggests a potential direct link between peripheral immune training in the liver and neuroinflammation that leads to neurodegeneration in the CNS (**Figure 3A**).

Moreover, initial central immune training and its cross-talk with peripheral immunity also seems to be involved in neurodegeneration. For instance, recently, a substantial accumulation of peripheral FOXP3 + regulatory T cells in the mouse brain following ischemic stroke (Ito et al., 2019) was described. Of note, central FOXP3 + regulatory T cells accumulation inhibits neurotoxic astrogliosis by releasing amphiregulin, a low-affinity ligand of the epidermal growth factor receptor (Ito et al., 2019). Central FOXP3 + regulatory T cell accumulation appears to have a binary role on neuronal survival (**Figure 3A**). Transient depletion of FOXP3 + regulatory T cells decrease amyloid-β plaque accumulation, reverts the neuroinflammatory response and improves cognitive performance in the 5XFAD AD mouse model, therefore is beneficial under acute central inflammation (Baruch et al., 2015). Conversely, peripheral immune training in the liver might also be regulated by central immune inflammation (**Figure 3B**). Initial reports show that extracellular vesicles released from astrocytes and microglia during central immune training might be implicated in the peripheral-central immune cross-talk (Wang et al., 2017; Yang et al., 2018). For instance, in murine models, intracerebral injection of IL-1β promotes the release of extracellular vesicles from astrocytes, leading to leukocyte migration into the brain and regulation of the liver cytokines profile by inhibition of the peroxisome proliferator-activated receptor α (Dickens et al., 2017). It is important to mention that extracellular vesicles released by central immune activation depend on glutamine modulation by glutaminase enzyme activation (Dickens et al., 2017; Wang et al., 2017; Wu et al., 2018). In fact, substantial programing of metabolic related pathways coordinates innate immunity. For instance, M1 pro-inflammatory state in macrophages depends largely on glycolytic metabolism, impairment of oxidative phosphorylation and disruption of the Krebs cycle; glycolysis activation during immune training was recently reported to be dependent on the mevalonate pathway (Bekkering et al., 2018). Conversely, macrophages M2 phenotype, which are involved in tissue repair and homeostasis, are dependent on the Krebs cycle (Netea et al., 2011). These results suggest that a shift from oxidative phosphorylation toward glycolysis seems to be a potential metabolic node to regulated immune training. In line with this, the Akt/mTOR/HIF-1α–dependent pathway and the brain neutral sphingomyelin hydrolase 2 have been reported to be

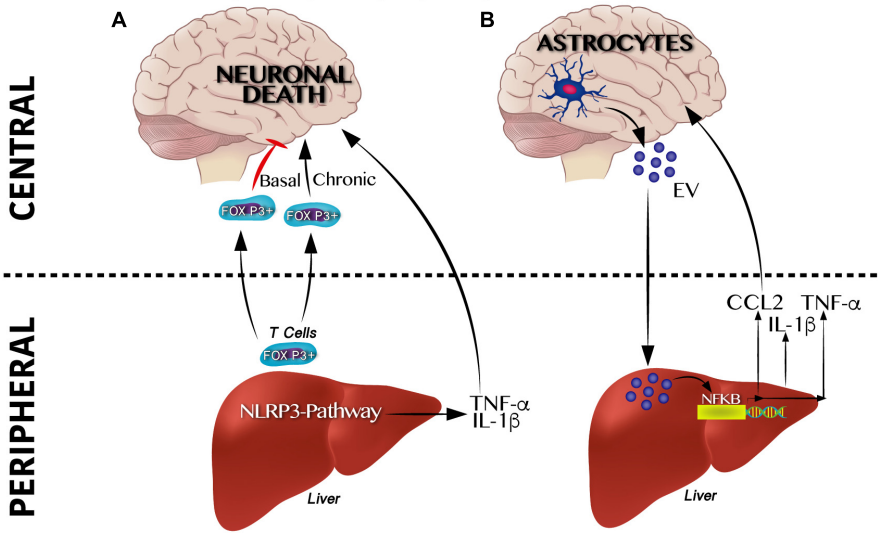

FIGURE 3 | Cross-talk between peripheral and central immune system on neurodegenerative susceptibility. **(A)** Peripheral immune system regulates neurodegeneration. Under a physiological scenario, Foxp3 + T cells are released from the liver to circulation reaching the central nervous system (CNS) positively modulating neuronal survival, whereas soon after a chronic activation Foxp3 + T cells become overactive promoting neuronal death. Likewise, activation of the inflammasome pathway in the liver produces IL-1β and TNF-α which exacerbate neurodegeneration. **(B)** Central immune system regulates neurodegeneration. Astrocytes secrete extracellular vesicles (EV) to the circulation reaching the liver and positively modulating the NF-κB transcriptional activation program, which includes IL-1β, TNF-α and CCL2 synthesis and release. This pro-inflammatory profile has been reported to contribute centrally to neuronal damage.

essential for trained immunity (Cheng et al., 2014; Saeed et al., 2014; Dickens et al., 2017).

A pro-inflammatory profile has been demonstrated to contribute to four major neurodegenerative pathologies and either suppressing or ameliorating this inflammatory process can have a good outcome for these diseases. According to this, we next discuss four of the major neurodegenerative pathologies in which inflammation has been proven to play a key role.

CENTRAL AND PERIPHERAL INFLAMMATORY NODES IN NEURODEGENERATIVE DISEASES

Active Immunity in Alzheimer Disease (AD)

Alzheimer disease is the most common type of senile dementia. Worldwide, approximately 50 million people are living with dementia and this number will triple in the next 40 years (Venigalla et al., 2015). AD is characterized by Aβ aggregation and intracellular bundles of hyperphosphorylated Tau protein (Colonna and Butovsky, 2017), which contribute to cognitive decline (Heneka et al., 2015).

High levels of TNF-α have also been identified in murine models of AD that resemble the classical behavioral abnormalities of the disease in humans (Gabbita et al., 2012; Kinney et al., 2018). Blocking the TNF-α pathway decreases central immune infiltration and prevents AD neurochemical and behavioral phenotypes (Tweedie et al., 2012; Prasad Gabbita et al., 2015), suggesting that central–peripheral cross-talk may be implicated in the disease. Notably, experimental studies using transgenic AD models have demonstrated that non-steroidal anti-inflammatory drugs (NSAIDs) can reduce AD pathology (Kinney et al., 2018). In addition, not only vertebrates seem to have dysregulation of the immune system during AD: In a *D. melanogaster* AD-like model, there is an upregulation of all five antimicrobial peptides (AMPs) related to inflammatory genes, suggesting the activation of innate immunity in AD-like flies. To counteract this neuroinflammation, they fed the flies with *Gardenia jasminoides* extracts (iridoid glycosides and aglycones, such as gardenoside, crocin, geniposide, and genipin) whose components can rescue cognitive deficits in a memory impairment mouse model (Nam and Lee, 2013) and show neuroprotective effect in cell culture (Sun et al., 2014). This experiment demonstrated that even though these extracts did not alter the Aβ concentration, they regulated the expression of immune-related genes (Drosomycin, Diptericine, Attacin, Cecropin, Mtk) in the brain of the flies and ameliorated memory deficits (Wei-Wei et al., 2017). The amelioration of memory loss and the counteraction of inflammation occurs through the modulation of the activity of acetylcholine esterase and the regulation the genes in apoptosis for neuroprotection, which have been recently accounted for in glycosides and aglycones present in *Gardenia jasminoides* extracts (Sun et al., 2014). Moreover, the robust effect of central-peripheral immune activation on AD-like neuropathology is also simulated using prenatal immune activation by the bacterial endotoxin lipopolysaccharide (LPS) or polyinosinic:polycytidylic

acid (PolyI:C) (Chen et al., 2011; Krstic et al., 2012; Giovanoli et al., 2015, 2016) these findings suggest that prenatal immune activation may be an important environmental risk factor that can cause hippocampus-related cognitive and synaptic deficits in the absence of chronic inflammation across aging.

Initial reports in humans have identified a proinflammatory profile of cytokines such as TNF-α, IL-6, and IL-1β in the prefrontal cortex, hippocampus and serum of AD subjects (Cacabelos et al., 1994; Mrak and Griffin, 2005; Calsolaro and Edison, 2016). In fact, the risk for progression from mild cognitive impairment to AD and cognitive decline is higher in subjects with elevated IL-6 and TNF-α levels in the cerebral spinal fluid (Heneka et al., 2015). In the 1980s, when neuroinflammation was described in AD and immune-related cells where described to be close to Aβ plaques, several large epidemiological and observational studies were published concluding that long-term use of NSAIDs showed protective qualities against developing AD. However, recent studies have identified variable outcomes and no convincing evidence regarding the positive effect of NSAIDs in AD (Kinney et al., 2018). Despite these experimental evidences, it is still unknown whether elevated levels of IL-1β, IL-6 and TNF-α lead directly to neurodegeneration in humans (**Figure 1**).

Active Immunity in Parkinson's Disease (PD)

Parkinson's disease is a the second most common neurodegenerative condition, affecting about 1.6% of people over 60 years old; it acts by promoting dopaminergic neuronal death in the substantia nigra pars compacta (Bassani et al., 2015). PD shows intraneuronal aggregates (called Lewy bodies) formed by α-synuclein that contribute to dopaminergic neuronal death in the basal ganglia, leading to the classical parkinsonian motor symptoms (De Virgilio et al., 2016). Neurodegeneration in PD is associated with the activation of microglia (Heneka et al., 2015), increased TNF-α, IL-1β, and IL-6 levels in the midbrain, serum and cerebral spinal fluid (Hofmann et al., 2009; Montgomery and Bowers, 2012) and activation of astrocytes (Wang et al., 2015).

Potential systemic triggers of immune activation in PD have identified that maternal immune activation in murine models reproduces the neurochemical and neuropathological symptoms of the disease (Wang et al., 2009; Vuillermot et al., 2012). Also, TNF-α and IL-6 levels correlate with dopaminergic neuronal death in the PD brain – it seems that both cytokines show a dual role on neurodegeneration and neurophysiology (**Figure 1**). Another *in vivo* example in which neuroinflammation is involved in neurodegeneration is the *D. melanogaster* Rotenone PD-like model. Lakkappa et al. (2018) used a new compound, PTUPB [(4-(5-phenyl-3-3-3-(4-trifluoromethyl-phenyl)-ureido-propyl-pyrazol-1-yl)-benzenesulfonamide)], that inhibited neuroinflammation and in turn prevented the loss of dopaminergic neurons, slightly ameliorating the PD-like pathology.

Similar to the animal models, post-mortem PD patients show infiltration of T-lymphocytes into the substantia nigra (Montgomery and Bowers, 2012). The immune hypothesis as a tentative cause of PD is still active given that, similar to AD genetic risk factors, PD involves the LRRK2, NR4A2, PARK7, and CD74 genes, which are capable of regulating immune function and microglial activation (Pandey et al., 2009). In summary, the involvement of immune responses in PD is not fully understood, but they influence the inflammation response and seem to affect disease progression.

Active Immunity in Huntington's Disease (HD)

Huntington's disease is an autosomal-dominant neurodegenerative disease caused by a CAG trinucleotide repeat expansion that gives place to a polyglutamine region in the huntingtin protein (HTT). HD patients show a positive pro-inflammatory profile (**Figure 1**) correlated with the disease's progression, including increases of IL-1β, IL-6, and TNF-α in the striatum, cerebral spinal fluid and plasma that were also confirmed in mouse models (Rocha et al., 2016). Central immune activation in HD subjects was confirmed using positron emission tomography (PET) and in pre-symptomatic HD-gene carriers (Rocha et al., 2016). Even though pharmacologic immune modulation using the XPro1595 TNF-α inhibitor has shown neuroprotection against the cytokine-induced neurotoxicity in primary R6/2 neurons and human neurons derived from iPSCs of HD patients (Hsiao et al., 2014), the information available is contradictory based on one report describing that neuroinflammation seems a consequence rather than a cause of neurodegeneration in late HD (Vinther-Jensen et al., 2016).

Active Immunity in Amyotrophic Lateral Sclerosis (ALS)

Amyotrophic lateral sclerosis is the most prevalent kind of motor neuron disease in adults, affecting 4–6 per 100,000 people, and is considered a fatal neurodegenerative disease (Filippi and Agosta, 2016). ALS is characterized by the degeneration of motor spinal neurons, brain stem and primary motor cortex mainly associated to a neuroinflammatory response by central (microglial) and peripheral (T-cells) immune activation and infiltration into the affected brain regions (Evans et al., 2013; Filippi and Agosta, 2016). Central immune activation also occurs in patients with either sporadic or familiar ALS, as well as in transgenic models of the disease (Geloso et al., 2017). Immune activation has also been reported in a model of ALS in *D. melanogaster*, in which the flies were supplemented with potent anti-inflammatory natural extracts of *Withania somnifera* (Wse) and *Mucuna pruriens* (Mpe), which significantly rescued climbing impairment (De Rose et al., 2017). Also, ALS patients and mouse models of the disease have elevated levels of TNFα, IL-6, and IL-1β in blood and cerebrospinal fluid. In addition to TNF-α upregulation in ALS, TNFR1, and TNFR2 transcripts have also been found to be overexpressed in ALS patients compared with non-neurological controls (Han et al., 2015; Tortarolo et al., 2017). Similar to Alzheimer, Parkinson and Huntington, modulation of inflammatory cytokine–dependent pathways prevent neuronal death in ALS models. As we commented previously, the contribution of TNFα or IL-6

(**Figure 1**) as etiological causes of ALS pathophysiology remains controversial because of their physiological functions or dual role on the central and peripheral immune activation or as a neurotrophic factors (Tortarolo et al., 2017).

Altogether, these results propose a very new and not-yet-understood pathway that integrates metabolism, central and peripheral immune training and cross-talk which might actively modulate neurodegeneration.

CONCLUSION

Maternal nutritional programing and immune training in microglia or peripheral innate cells are complex and require a profound integration of glycolytic and oxidative metabolism as well as the reprograming of molecular signatures that modulate susceptibility to neuronal damage at earlier stages of development in the offspring. Peripheral or central innate immune training during maternal nutritional programing might integrate a significant node that regulates neurodegenerative susceptibility in the offspring. Potential integration of the NLRP3 inflammasome and the IKKβ/NF-kB pathways in microglia at early stages, and peripheral or central immune cross-talk at later stages, including the FOXP3 + regulatory T cells or the extracellular vesicles, might actively regulate neuroinflammation and neuronal death/survival. This information allows us to propose that maternal nutritional programing leads to peripheral or central immune training, favoring neurodegenerative susceptibility.

AUTHOR CONTRIBUTIONS

MC-T, LM-M, RM-R, AC-M, and DR-P: conceptualization and writing – review and editing. AC-M and DR-P: supervision and visualization.

FUNDING

This work was funded by the National Council of Science and Technology in Mexico (CONACYT), 650620 CONACYT for MC-T, 582196 CONACYT for LM-M, and 573686 CONACYT for RM-R.

ACKNOWLEDGMENTS

We thank Alejandra Arreola-Triana for her support on editing this manuscript and Arlette Yaressi Vinaja-Romero for her figure artworks.

REFERENCES

Agrawal, N. K. (2014). Targeting inflammation in diabetes: newer therapeutic options. *World J. Diabetes* 5, 697–710. doi: 10.4239/wjd.v5.i5.697

Ann, S. J., Kim, K. K., Cheon, E. J., Noh, H. M., Hwang, I., Yu, J. W., et al. (2018). Palmitate and minimally-modified low-density lipoprotein cooperatively promote inflammatory responses in macrophages. *PLoS One* 13:e0193649. doi: 10.1371/journal.pone.0193649

Arroba, A. I., Mazzeo, A., Cazzoni, D., Beltramo, E., Hernández, C., Porta, M., et al. (2016). Somatostatin protects photoreceptor cells against high glucose–induced apoptosis. *Mol. Vis.* 22, 1522–1531.

Arts, R. J. W., Moorlag, S. J. C. F. M., Novakovic, B., Li, Y., Wang, S. Y., Oosting, M., et al. (2018). BCG vaccination protects against experimental viral infection in humans through the induction of cytokines associated with trained immunity. *Cell Host Microbe* 23, 89–100. doi: 10.1016/j.chom.2017.12.010

Baruch, K., Rosenzweig, N., Kertser, A., Deczkowska, A., Sharif, A. M., Spinrad, A., et al. (2015). Breaking immune tolerance by targeting Foxp3+ regulatory T cells mitigates Alzheimer's disease pathology. *Nat. Commun.* 6:7967. doi: 10.1038/ncomms8967

Bassani, T. B., Vital, M. A., and Rauh, L. K. (2015). Neuroinflammation in the pathophysiology of Parkinson's disease and therapeutic evidence of anti-inflammatory drugs. *Arq. Neuropsiquiatr.* 73, 616–623. doi: 10.1590/0004-282X20150057

Bekkering, S., Arts, R. J. W., Novakovic, B., Kourtzelis, I., van der Heijden, C. D. C. C., Li, Y., et al. (2018). Metabolic induction of trained immunity through the mevalonate pathway. *Cell* 172, 135.e9–146.e9. doi: 10.1016/j.cell.2017.11.025

Bertram, L., McQueen, M. B., Mullin, K., Blacker, D., and Tanzi, R. E. (2007). Systematic meta-analyses of Alzheimer disease genetic association studies: the AlzGene database. *Nat. Genet.* 39, 17–23. doi: 10.1038/ng1934

Bilbo, S. D., and Tsang, V. (2010). Enduring consequences of maternal obesity for brain inflammation and behavior of offspring. *FASEB J.* 24, 2104–2115. doi: 10.1096/fj.09-144014

Cacabelos, R., Alvarez, X. A., Fernandez-Novoa, L., Franco, A., Mangues, R., Pellicer, A., et al. (1994). Brain interleukin-1 beta in Alzheimer's disease and vascular dementia. *Methods Find. Exp. Clin. Pharmacol.* 16, 141–151.

Calsolaro, V., and Edison, P. (2016). Neuroinflammation in Alzheimer ' s disease: current evidence and future directions. *Alzheimer's Dement.* 12, 719–732. doi: 10.1016/j.jalz.2016.02.010

Chen, G. H., Wang, H., Yang, Q. G., Tao, F., Wang, C., and Xu, D. X. (2011). Acceleration of age-related learning and memory decline in middle-aged CD-1 mice due to maternal exposure to lipopolysaccharide during late pregnancy. *Behav. Brain Res.* 218, 267–279. doi: 10.1016/j.bbr.2010.11.001

Cheng, S. C., Quintin, J., Cramer, R. A., Shepardson, K. M., Saeed, S., Kumar, V., et al. (2014). MTOR- and HIF-1α-mediated aerobic glycolysis as metabolic basis for trained immunity. *Science* 345:1250684. doi: 10.1126/science.1250684

Choe, J. Y., and Kim, S. K. (2017). Quercetin and ascorbic acid suppress fructose-induced NLRP3 inflammasome activation by blocking intracellular shuttling of TXNIP in human macrophage cell lines. *Inflammation* 40, 980–994. doi: 10.1007/s10753-017-0542-4

Christ, A., Günther, P., Lauterbach, M. A. R., Duewell, P., Biswas, D., Pelka, K., et al. (2018). Western diet Triggers NLRP3-dependent innate immune reprogramming. *Cell* 172, 162.e14–175.e14. doi: 10.1016/j.cell.2017.12.013

Ciaccia, L. (2010). in *Fundamentals of Inflammation*, eds D. W. C. N. Serhan, and P. A. Ward (New York, NY: Cambridge University Press), doi: 10.1097/00000433-198206000-00020

Colonna, M., and Butovsky, O. (2017). Microglia function in the central nervous system during health and neurodegeneration. *Annu. Rev. Immunol.* 35, 441–468. doi: 10.1146/annurev-immunol-051116-052358

De Rose, F., Marotta, R., Talani, G., Catelani, T., Solari, P., Poddighe, S., et al. (2017). Differential effects of phytotherapic preparations in the hSOD1 *Drosophila melanogaster* model of ALS. *Sci. Rep.* 7:41059. doi: 10.1038/srep41059

De Virgilio, A., Greco, A., Fabbrini, G., Inghilleri, M., Rizzo, M. I., Gallo, A., et al. (2016). Parkinson's disease: autoimmunity and neuroinflammation. *Autoimmun. Rev.* 15, 1005–1011. doi: 10.1016/j.autrev.2016.07.022

Debarba, L. K., Vechiato, F. M. V., Veida-Silva, H., Borges, B. C., Jamur, M. C., Antunes-Rodrigues, J., et al. (2018). The role of TCPTP on leptin effects on astrocyte morphology. *Mol. Cell. Endocrinol.* 482, 62–69. doi: 10.1016/j.mce.2018.12.010

Derks, I. P. M., Hivert, M.-F., Rifas-Shiman, S. L., Gingras, V., Young, J. G., Jansen, P. W., et al. (2019). Associations of prenatal exposure to impaired glucose

tolerance with eating in the absence of hunger in early adolescence. *Int. J. Obes.* 43, 1903–1913. doi: 10.1038/s41366-018-0296-296

Dickens, A. M., Tovar-Y-Romo, L. B., Yoo, S. W., Trout, A. L., Bae, M., Kanmogne, M., et al. (2017). Astrocyte-shed extracellular vesicles regulate the peripheral leukocyte response to inflammatory brain lesions. *Sci. Signal.* 10:eaai7696. doi: 10.1126/scisignal.aai7696

DiNapoli, V. A., Benkovic, S. A., Li, X., Kelly, K. A., Miller, D. B., Rosen, C. L., et al. (2010). Age exaggerates proinflammatory cytokine signaling and truncates signal transducers and activators of transcription 3 signaling following ischemic stroke in the rat. *Neuroscience* 170, 633–644. doi: 10.1016/j.neuroscience.2010.07.011

Dodd, G. T., Decherf, S., Loh, K., Simonds, S. E., Wiede, F., Balland, E., et al. (2015). Leptin and insulin act on POMC neurons to promote the browning of white fat. *Cell* 160, 88–104. doi: 10.1016/j.cell.2014.12.022

Dodd, G. T., Lee-Young, R. S., Brüning, J. C., and Tiganis, T. (2018). TCPTP regulates insulin signaling in AgRP neurons to coordinate glucose metabolism with feeding. *Diabetes* 67, 1246–1257. doi: 10.2337/db17-1485

Edlow, A. G., Guedj, F., Pennings, J. L. A., Sverdlov, D., Neri, C., and Bianchi, D. W. (2016a). Males are from Mars, and females are from Venus: sex-specific fetal brain gene expression signatures in a mouse model of maternal diet-induced obesity. *Am. J. Obstet. Gynecol.* 214, 620.e1–620.e4. doi: 10.1016/j.ajog.2016.02.054

Edlow, A. G., Hui, L., Wick, H. C., Fried, I., and Bianchi, D. W. (2016b). Assessing the fetal effects of maternal obesity via transcriptomic analysis of cord blood: a prospective case-control study. *BJOG* 123, 180–189. doi: 10.1111/1471-0528.13795

Edlow, A. G., Vora, N. L., Hui, L., Wick, H. C., Cowan, J. M., and Bianchi, D. W. (2014). Maternal obesity affects fetal neurodevelopmental and metabolic gene expression: a pilot study. *PLoS One* 9:e88661. doi: 10.1371/journal.pone.0088661

Esser, N., Legrand-Poels, S., Piette, J., Scheen, A. J., and Paquot, N. (2014). Inflammation as a link between obesity, metabolic syndrome and type 2 diabetes. *Diabetes Res. Clin. Pract.* 105, 141–150. doi: 10.1016/j.diabres.2014.04.006

Estes, M. L., and McAllister, A. K. (2016). Maternal immune activation: implications for neuropsychiatric disorders. *Science* 353, 772–777. doi: 10.1126/science.aag3194

Evans, M. C., Couch, Y., Sibson, N., and Turner, M. R. (2013). Inflammation and neurovascular changes in amyotrophic lateral sclerosis. *Mol. Cell. Neurosci.* 53, 34–41. doi: 10.1016/j.mcn.2012.10.008

Fan, Z., Liang, Z., Yang, H., Pan, Y., Zheng, Y., and Wang, X. (2017). Tenuigenin protects dopaminergic neurons from inflammation via suppressing NLRP3 inflammasome activation in microglia. *J. Neuroinflammation* 14:256. doi: 10.1186/s12974-017-1036-x

Filippi, M., and Agosta, F. (2016). Does neuroinflammation sustain neurodegeneration in ALS? *Neurology* 87, 2508–2509. doi: 10.1212/WNL.0000000000003441

Friedman, J. E. (2018). Developmental programming of obesity and diabetes in mouse, monkey, and man in 2018: Where are we headed? *Diabetes* 67, 2137–2151. doi: 10.2337/dbi17-0011

Fujikura, K., Setsu, T., Tanigaki, K., Abe, T., Kiyonari, H., Terashima, T., et al. (2013). Kif14 mutation causes severe brain malformation and hypomyelination. *PLoS One* 8:e53490. doi: 10.1371/journal.pone.0053490

Gabbita, S. P., Srivastava, M. K., Eslami, P., Johnson, M. F., Kobritz, N. K., Tweedie, D., et al. (2012). Early intervention with a small molecule inhibitor for tumor nefosis factor-α prevents cognitive deficits in a triple transgenic mouse model of Alzheimer's disease. *J. Neuroinflammation* 9:99.

Geloso, M. C., Corvino, V., Marchese, E., Serrano, A., Michetti, F., and D'Ambrosi, N. (2017). The dual role of microglia in ALS: mechanisms and therapeutic approaches. *Front. Aging Neurosci.* 9:242. doi: 10.3389/fnagi.2017.00242

Giovanoli, S., Notter, T., Richetto, J., Labouesse, M. A., Vuillermot, S., Riva, M. A., et al. (2015). Late prenatal immune activation causes hippocampal deficits in the absence of persistent inflammation across aging. *J. Neuroinflammation* 12:221. doi: 10.1186/s12974-015-0437-y

Giovanoli, S., Weber-Stadlbauer, U., Schedlowski, M., Meyer, U., and Engler, H. (2016). Prenatal immune activation causes hippocampal synaptic deficits in the absence of overt microglia anomalies. *Brain. Behav. Immun.* 55, 25–38. doi: 10.1016/j.bbi.2015.09.015

Girolami, E. I., Bouhy, D., Haber, M., Johnson, H., and David, S. (2010). Differential expression and potential role of SOCS1 and SOCS3 in Wallerian degeneration in injured peripheral nerve. *Exp. Neurol.* 233, 173–182. doi: 10.1016/j.expneurol.2009.06.018

Glinsky, G. V. (2008). SNP-guided microRNA maps (MirMaps) of 16 common human disorders identify a clinically accessible therapy reversing transcriptional aberrations of nuclear import and inflammasome pathways. *Cell Cycle* 7, 3564–3576. doi: 10.4161/cc.7.22.7073

Gomes, R. M., Bueno, F. G., Schamber, C. R., de Mello, J. C. P., de Oliveira, J. C., Francisco, F. A., et al. (2018). Maternal diet-induced obesity during suckling period programs offspring obese phenotype and hypothalamic leptin/insulin resistance. *J. Nutr. Biochem.* 61, 24–32. doi: 10.1016/j.jnutbio.2018.07.006

Gordon, R., Albornoz, E. A., Christie, D. C., Langley, M. R., Kumar, V., Mantovani, S., et al. (2018). Inflammasome inhibition prevents -synuclein pathology and dopaminergic neurodegeneration in mice. *Sci. Transl. Med.* 10:eaah4066. doi: 10.1126/scitranslmed.aah4066

Han, L., Zhang, D., Tao, T., Sun, X., Liu, X., Zhu, G., et al. (2015). The role of N-Glycan modification of TNFR1 in inflammatory microglia activation. *Glycoconj. J.* 32, 685–693. doi: 10.1007/s10719-015-9619-9611

Heneka, M. T., Carson, M. J., Khoury, J., El Gary, E., Brosseron, F., Feinstein, D. L., et al. (2015). Neuroinflammation in Alzheimer's disease. *Lancet Neurol.* 14, 388–405. doi: 10.1016/S1474-4422(15)70016-5.Neuroinflammation

Heneka, M. T., Kummer, M. P., Stutz, A., Delekate, A., Schwartz, S., Vieira-Saecker, A., et al. (2013). NLRP3 is activated in Alzheimer's disease and contributes to pathology in APP/PS1 mice. *Nature* 493, 674–678. doi: 10.1038/nature11729

Heneka, M. T., McManus, R. M., and Latz, E. (2018). Inflammasome signalling in brain function and neurodegenerative disease. *Nat. Rev. Neurosci.* 19, 610–621. doi: 10.1038/s41583-018-0055-7

Hofmann, K. W., Schuh, A. F. S., Saute, J., Townsend, R., Fricke, D., Leke, R., et al. (2009). Interleukin-6 serum levels in patients with Parkinson's disease. *Neurochem. Res.* 34, 1401–1404. doi: 10.1007/s11064-009-9921-z

Hsiao, H.-Y., Chiu, F.-L., Chen, C.-M., Wu, Y.-R., Chen, H.-M., Chen, Y.-C., et al. (2014). Inhibition of soluble tumor necrosis factor is therapeutic in Huntington's disease. *Hum. Mol. Genet.* 23, 4328–4344. doi: 10.1093/hmg/ddu151

Ito, M., Komai, K., Mise-Omata, S., Iizuka-Koga, M., Noguchi, Y., Kondo, T., et al. (2019). Brain regulatory T cells suppress astrogliosis and potentiate neurological recovery. *Nature* 565, 246–250. doi: 10.1038/s41586-018-0824-5

Jang, J., Park, S., Jin Hur, H., Cho, H. J., Hwang, I., Pyo Kang, Y., et al. (2016). 25-hydroxycholesterol contributes to cerebral inflammation of X-linked adrenoleukodystrophy through activation of the NLRP3 inflammasome. *Nat. Commun.* 7:13129. doi: 10.1038/ncomms13129

Johann, S., Heitzer, M., Kanagaratnam, M., Goswami, A., Rizo, T., Weis, J., et al. (2015). NLRP3 inflammasome is expressed by astrocytes in the SOD1 mouse model of ALS and in human sporadic ALS patients. *Glia* 63, 2260–2273. doi: 10.1002/glia.22891

Kanno, T., Tsuchiya, A., Tanaka, A., and Nishizaki, T. (2016). Combination of PKCε activation and PTP1B inhibition effectively suppresses Aβ-induced GSK-3β activation and tau phosphorylation. *Mol. Neurobiol.* 53, 4787–4797. doi: 10.1007/s12035-015-9405-x

Kaufmann, E., Sanz, J., Dunn, J. L., Khan, N., Mendonça, L. E., Pacis, A., et al. (2018). BCG educates hematopoietic stem cells to generate protective innate immunity against tuberculosis. *Cell* 172, 176.e19–190.e19. doi: 10.1016/j.cell.2017.12.031

Kinney, J. W., Bemiller, S. M., Murtishaw, A. S., Leisgang, A. M., Salazar, A. M., and Lamb, B. T. (2018). Inflammation as a central mechanism in Alzheimer's disease. *Alzheimer's Dement. Transl. Res. Clin. Interv.* 4, 575–590. doi: 10.1016/j.trci.2018.06.014

Krstic, D., Madhusudan, A., Doehner, J., Vogel, P., Notter, T., Imhof, C., et al. (2012). Systemic immune challenges trigger and drive Alzheimer-like neuropathology in mice. *J. Neuroinflammation* 9:151. doi: 10.1186/1742-2094-9-151

Lakkappa, N., Krishnamurthy, P. T., Yamjala, K., Hwang, S. H., Hammock, B. D., and Babu, B. (2018). Evaluation of antiparkinson activity of PTUPB by measuring dopamine and its metabolites in *Drosophila melanogaster*: LC–MS/MS method development. *J. Pharm. Biomed. Anal.* 149, 457–464. doi: 10.1016/j.jpba.2017.11.043

Lee, E., Hwang, I., Park, S., Hong, S., Hwang, B., Cho, Y., et al. (2018). MPTP-driven NLRP3 inflammasome activation in microglia plays a central role in dopaminergic neurodegeneration. *Cell Death Differ.* 26, 213–228. doi: 10.1038/s41418-018-0124-5

Lei, Y., Chen, C. J., Yan, X. X., Li, Z., and Deng, X. H. (2017). Early-life lipopolysaccharide exposure potentiates forebrain expression of NLRP3 inflammasome proteins and anxiety-like behavior in adolescent rats. *Brain Res.* 1671, 43–54. doi: 10.1016/j.brainres.2017.06.014

L'homme, L., Esser, N., Riva, L., Scheen, A., Paquot, N., Piette, J., et al. (2013). Unsaturated fatty acids prevent activation of NLRP3 inflammasome in human monocytes/macrophages. *J. Lipid Res.* 54, 2998–3008. doi: 10.1194/jlr.M037861

Li, J., Tang, Y., and Cai, D. (2012). IKKβ/NF-κB disrupts adult hypothalamic neural stem cells to mediate a neurodegenerative mechanism of dietary obesity and pre-diabetes. *Nat. Cell Biol.* 14, 999–1012. doi: 10.1038/ncb2562

Ling, Z., Chang, Q. A., Tong, C. W., Leurgans, S. E., Lipton, J. W., and Carvey, P. M. (2004). Rotenone potentiates dopamine neuron loss in animals exposed to lipopolysaccharide prenatally. *Exp. Neurol.* 190, 373–383. doi: 10.1016/j.expneurol.2004.08.006

Ling, Z. D., Chang, Q., Lipton, J. W., Tong, C. W., Landers, T. M., and Carvey, P. M. (2004). Combined toxicity of prenatal bacterial endotoxin exposure and postnatal 6-hydroxydopamine in the adult rat midbrain. *Neuroscience* 124, 619–628. doi: 10.1016/j.neuroscience.2003.12.017

Liu, B., Ou, G., Chen, Y., and Zhang, J. (2019). Inhibition of protein tyrosine phosphatase 1B protects against sevoflurane-induced neurotoxicity mediated by ER stress in developing brain. *Brain Res. Bull.* 146, 28–39. doi: 10.1016/j.brainresbull.2018.12.006

Loh, K., Fukushima, A., Zhang, X., Galic, S., Briggs, D., Enriori, P. J., et al. (2011). Elevated hypothalamic TCPTP in obesity contributes to cellular leptin resistance. *Cell Metab.* 14, 684–699. doi: 10.1016/j.cmet.2011.09.011

Maldonado-Ruiz, R., Fuentes-Mera, L., and Camacho, A. (2017). Central modulation of neuroinflammation by neuropeptides and energy-sensing hormones during obesity. *Biomed Res. Int.* 2017:7949582. doi: 10.1155/2017/7949582

Mastrocola, R., Collino, M., Penna, C., Nigro, D., Chiazza, F., Fracasso, V., et al. (2016). Maladaptive modulations of nlrp3 inflammasome and cardioprotective pathways are involved in diet-induced exacerbation of myocardial ischemia/reperfusion injury in mice. *Oxid. Med. Cell. Longev.* 2016:3480637. doi: 10.1155/2016/3480637

McNamee, E. N., Ryan, K. M., Griffin, ÉW., González-Reyes, R. E., Ryan, K. J., Harkin, A., et al. (2010). Noradrenaline acting at central β-adrenoceptors induces interleukin-10 and suppressor of cytokine signaling-3 expression in rat brain: implications for neurodegeneration. *Brain. Behav. Immun.* 24, 660–671. doi: 10.1016/j.bbi.2010.02.005

Milanski, M., Degasperi, G., Coope, A., Morari, J., Denis, R., Cintra, D. E., et al. (2009). Saturated fatty acids produce an inflammatory response predominantly through the activation of TLR4 signaling in hypothalamus: implications for the pathogenesis of obesity. *J. Neurosci.* 29, 359–370. doi: 10.1523/JNEUROSCI.2760-08.2009

Mitroulis, I., Ruppova, K., Wang, B., Chen, L. S., Grzybek, M., Grinenko, T., et al. (2018). Modulation of myelopoiesis progenitors is an integral component of trained immunity. *Cell* 172, 147.e12–161.e12. doi: 10.1016/j.cell.2017.11.034

Monje, M. L., Toda, H., and Palmer, T. D. (2003). Inflammatory blockade restores adult hippocampal neurogenesis. *Science* 302, 1760–1765. doi: 10.1126/science.1088417

Montgomery, S. L., and Bowers, W. J. (2012). Tumor necrosis factor-alpha and the roles it plays in homeostatic and degenerative processes within the central nervous system. *J. Neuroimmune Pharmacol.* 7, 42–59. doi: 10.1007/s11481-011-9287-2

Morin, J.-P., Rodríguez-Durán, L. F., Guzmán-Ramos, K., Perez-Cruz, C., Ferreira, G., Diaz-Cintra, S., et al. (2017). Palatable hyper-caloric foods impact on neuronal plasticity. *Front. Behav. Neurosci.* 11:19. doi: 10.3389/fnbeh.2017.00019

Mrak, R. E., and Griffin, W. S. T. (2005). Potential inflammatory biomarkers in Alzheimer's disease. *J. Alzheimers. Dis.* 8, 369–375. doi: 10.3233/jad-2005-8406

Mucellini, A. B., Laureano, D. P., Silveira, P. P., and Sanvitto, G. L. (2019). Maternal and post-natal obesity alters long-term memory and hippocampal molecular signaling of male rat. *Brain Res.* 1708, 138–145. doi: 10.1016/j.brainres.2018.12.021

Nam, Y., and Lee, D. (2013). Ameliorating effect of Zhizi (Fructus Gardeniae) extract and its glycosides on scopolamine-induced memory impairment. *J. Tradit. Chinese Med.* 33, 223–227. doi: 10.1016/s0254-6272(13)60129-6

Netea, M. G., Joosten, L. A. B., Latz, E., Mills, K. H. G., Natoli, G., Stunnenberg, H. G., et al. (2016). Trained immunity: a program of innate immune memory in health and disease. *Science* 352:aaf1098. doi: 10.1126/science.aaf1098

Netea, M. G., Quintin, J., and Van Der Meer, J. W. M. (2011). Trained immunity: a memory for innate host defense. *Cell Host Microbe* 9, 355–361. doi: 10.1016/j.chom.2011.04.006

Nigro, D., Menotti, F., Cento, A. S., Serpe, L., Chiazza, F., Dal Bello, F., et al. (2017). Chronic administration of saturated fats and fructose differently affect SREBP activity resulting in different modulation of Nrf2 and Nlrp3 inflammasome pathways in mice liver. *J. Nutr. Biochem.* 42, 160–171. doi: 10.1016/j.jnutbio.2017.01.010

O'Brien, P. D., Hinder, L. M., Callaghan, B. C., and Feldman, E. L. (2017). Neurological consequences of obesity. *Lancet Neurol.* 16, 465–477.

Ott, A., Stolk, R. P., Van Harskamp, F., Pols, H. A. P., Hofman, A., and Breteler, M. M. B. (1999). Diabetes mellitus and the risk of dementia: the rotterdam study. *Neurology* 53, 1937–1942. doi: 10.1212/wnl.53.9.1937

Ou, X., Thakali, K. M., Shankar, K., Andres, A., and Badger, T. M. (2015). Maternal adiposity negatively influences infant brain white matter development. *Obesity (Silver Spring)* 23, 1047–1054. doi: 10.1002/oby.21055

Pan, Y., Chen, X. Y., Zhang, Q. Y., and Kong, L. D. (2014). Microglial NLRP3 inflammasome activation mediates IL-1β-related inflammation in prefrontal cortex of depressive rats. *Brain. Behav. Immun.* 41, 90–100. doi: 10.1016/j.bbi.2014.04.007

Pandey, A. K., Agarwal, P., Kaur, K., and Datta, M. (2009). MicroRNAs in diabetes: tiny players in big disease. *Cell. Physiol. Biochem.* 23, 221–232. doi: 10.1159/000218169

Patro Golab, B., Santos, S., Voerman, E., Lawlor, D. A., Jaddoe, V. W., Gaillard, R., et al. (2018). Influence of maternal obesity on the association between common pregnancy complications and risk of childhood obesity: an individual participant data meta-analysis. *Lancet Child Adolesc. Heal.* 2, 812–821. doi: 10.1016/S2352-4642(18)30273-6

Prasad Gabbita, S., Johnson, M. F., Kobritz, N., Eslami, P., Poteshkina, A., Varadarajan, S., et al. (2015). Oral TNFα modulation alters neutrophil infiltration, improves cognition and diminishes tau and amyloid pathology in the 3xtgad mouse model. *PLoS One* 10:e0137305. doi: 10.1371/journal.pone.0137305

Procaccini, C., Santopaolo, M., Faicchia, D., Colamatteo, A., Formisano, L., De Candia, P., et al. (2016). Role of metabolism in neurodegenerative disorders. *Metabolism* 65, 1376–1390. doi: 10.1016/j.metabol.2016.05.018

Qiao, C., Zhang, Q., Jiang, Q., Zhang, T., Chen, M., Fan, Y., et al. (2018). Inhibition of the hepatic Nlrp3 protects dopaminergic neurons via attenuating systemic inflammation in a MPTP/p mouse model of Parkinson's disease. *J. Neuroinflammation* 15:193. doi: 10.1186/s12974-018-1236-z

Rocha, N. P., Ribeiro, F. M., Furr-Stimming, E., and Teixeira, A. L. (2016). Neuroimmunology of huntington's disease: revisiting evidence from human studies. *Mediators Inflamm.* 2016:8653132. doi: 10.1155/2016/8653132

Romanitan, M. O., Popescu, B. O., Winblad, B., Bajenaru, O. A., and Bogdanovic, N. (2007). Occludin is overexpressed in Alzheimer's disease and vascular dementia. *J. Cell. Mol. Med.* 11, 569–579. doi: 10.1111/j.1582-4934.2007.00047.x

Saeed, S., Quintin, J., Kerstens, H. H. D., Rao, N. A., Aghajanirefah, A., Matarese, F., et al. (2014). Epigenetic programming of monocyte-to-macrophage differentiation and trained innate immunity. *Science* 345:1251086. doi: 10.1126/science.1251086

Shapiro, A. L. B., Sauder, K. A., Tregellas, J. R., Legget, K. T., Gravitz, S. L., Ringham, B. M., et al. (2017). Exposure to maternal diabetes in utero and offspring eating behavior: the EPOCH study. *Appetite* 116, 610–615. doi: 10.1016/j.appet.2017.05.005

Sobesky, J. L., DAngelo, H. M., Weber, M. D., Anderson, N. D., Frank, M. G., Watkins, L. R., et al. (2016). Glucocorticoids mediate short-term high-fat diet induction of neuroinflammatory priming, the NLRP3 inflammasome, and the danger signal HMGB1. *eNeuro* 3, e0113–e0116. doi: 10.1523/ENEURO.0113-16.2016

Stranahan, A. M., Norma, E. D., Lee, K., Cutler, R. G., Telljohann, R., Egan, J. M., et al. (2008). Diet-induced insulin resistance impairs hippocampal synaptic

plasticity and cognition in middle-aged rats. *Hippocampus* 23, 1–7. doi: 10.1038/jid.2014.371

Su, W. J., Zhang, Y., Chen, Y., Gong, H., Lian, Y. J., Peng, W., et al. (2017). NLRP3 gene knockout blocks NF-κB and MAPK signaling pathway in CUMS-induced depression mouse model. *Behav. Brain Res.* 322(Pt A), 1–8. doi: 10.1016/j.bbr.2017.01.018

Sui, Y. H., Luo, W. J., Xu, Q. Y., and Hua, J. (2016). Dietary saturated fatty acid and polyunsaturated fatty acid oppositely affect hepatic NOD-like receptor protein 3 inflammasome through regulating nuclear factor-kappa B activation. *World J. Gastroenterol.* 22, 2533–2544. doi: 10.3748/wjg.v22.i8.2533

Sun, P., Ding, H., Liang, M., Li, X., Mo, W., Wang, X., et al. (2014). Neuroprotective effects of geniposide in SH-SY5Y cells and primary hippocampal neurons exposed to A β 42. *Biomed Res. Int.* 2014:284314. doi: 10.1155/2014/284314

Takahashi, K., Prinz, M., Stagi, M., Chechneva, O., and Neumann, H. (2007). TREM2-transduced myeloid precursors mediate nervous tissue debris clearance and facilitate recovery in an animal model of multiple sclerosis. *PLoS Med.* 4:e124. doi: 10.1371/journal.pmed.0040124

Tartaglione, A. M., Venerosi, A., and Calamandrei, G. (2016). "Early-life toxic insults and onset of sporadic neurodegenerative diseases—An overview of experimental studies. *Curr. Top. Behav. Neurosci.* 29, 231–264. doi: 10.1007/7854_2015_416

Tortarolo, M., Lo Coco, D., Veglianese, P., Vallarola, A., Giordana, M. T., Marcon, G., et al. (2017). Amyotrophic lateral sclerosis, a multisystem pathology: insights into the role of TNF α. *Mediators Inflamm.* 2017:2985051. doi: 10.1155/2017/2985051

Tweedie, D., Ferguson, R. A., Fishman, K., Frankola, K. A., Van Praag, H., Holloway, H. W., et al. (2012). Tumor necrosis factor-α synthesis inhibitor 3,6'-dithiothalidomide attenuates markers of inflammation, Alzheimer pathology and behavioral deficits in animal models of neuroinflammation and Alzheimer's disease. *J. Neuroinflammation* 9, 575.

Vaiserman, A. M. (2017). Early-life nutritional programming of type 2 diabetes: experimental and quasi-experimental evidence. *Nutrients* 9:e236. doi: 10.3390/nu9030236

Venigalla, M., Gyengesi, E., Sharman, M. J., and Münch, G. (2015). Novel promising therapeutics against chronic neuroinflammation and neurodegeneration in Alzheimer's disease. *Neurochem. Int.* 95, 63–74. doi: 10.1016/j.neuint.2015.10.011

Vinther-Jensen, T., Börnsen, L., Budtz-Jørgensen, E., Ammitzbøll, C., Larsen, I. U., Hjermind, L. E., et al. (2016). Selected CSF biomarkers indicate no evidence of early neuroinflammation in Huntington disease. *Neurol. Neuroimmunol. Neuroinflamm.* 3:e287. doi: 10.1212/NXI.0000000000000287

Vuillermot, S., Joodmardi, E., Perlmann, T., Ove Ogren, S., Feldon, J., and Meyer, U. (2012). Prenatal immune activation interacts with genetic Nurr1 deficiency in the development of attentional impairments. *J. Neurosci.* 32, 436–451. doi: 10.1523/JNEUROSCI.4831-11.2012

Wang, K., Ye, L., Lu, H., Chen, H., Zhang, Y., Huang, Y., et al. (2017). TNF-α promotes extracellular vesicle release in mouse astrocytes through glutaminase. *J. Neuroinflammation* 14:87.

Wang, Q., Liu, Y., and Zhou, J. (2015). Neuroinflammation in Parkinson's disease and its potential as therapeutic target. *Transl. Neurodegener.* 4, 1–9.

Wang, S., Yan, J. Y., Lo, Y. K., Carvey, P. M., and Ling, Z. (2009). Dopaminergic and serotoninergic deficiencies in young adult rats prenatally exposed to the bacterial lipopolysaccharide. *Brain Res.* 1265, 196–204. doi: 10.1016/j.brainres.2009.02.022

Wei-Wei, M., Ye, T., Yan-Ying, W., and I-Feng, P. (2017). Effects of Gardenia jasminoides extracts on cognition and innate immune response in an adult *Drosophila* model of Alzheimer's disease. *Chin. J. Nat. Med.* 15, 899–904. doi: 10.1016/S1875-5364(18)30005-0

Wen, H., Gris, D., Lei, Y., Jha, S., Zhang, L., Huang, M. T. H., et al. (2011). Fatty acid-induced NLRP3-ASC inflammasome activation interferes with insulin signaling. *Nat. Immunol.* 12, 408–415. doi: 10.1038/ni.2022

Wendeln, A., Degenhardt, K., Kaurani, L., Gertig, M., Ulas, T., Jain, G., et al. (2018). Innate immune memory in the brain shapes neurological disease hallmarks. *Nature* 556, 332–338. doi: 10.1038/s41586-018-0023-4

Widen, E. M., Kahn, L. G., Cirillo, P., Cohn, B., Kezios, K. L., and Factor-Litvak, P. (2018). Prepregnancy overweight and obesity are associated with impaired child neurodevelopment. *Matern. Child Nutr.* 14:e12481. doi: 10.1111/mcn.12481

Wu, B., Liu, J., Zhao, R., Li, Y., Peer, J., Braun, A. L., et al. (2018). Glutaminase 1 regulates the release of extracellular vesicles during neuroinflammation through key metabolic intermediate alpha-ketoglutarate. *J. Neuroinflammation* 15:79. doi: 10.1186/s12974-018-1120-x

Yadav, A., Kalita, A., Dhillon, S., and Banerjee, K. (2005). JAK/STAT3 pathway is involved in survival of neurons in response to insulin-like growth factor and negatively regulated by suppressor of cytokine signaling-3. *J. Biol. Chem.* 280, 31830–31840. doi: 10.1074/jbc.M501316200

Yang, Y., Boza-Serrano, A., Dunning, C. J. R., Clausen, B. H., Lambertsen, K. L., and Deierborg, T. (2018). Inflammation leads to distinct populations of extracellular vesicles from microglia. *J. Neuroinflammation* 15:168. doi: 10.1186/s12974-018-1204-7

Yi, C., Ezan, P., Fernández, P., Schmitt, J., Sáez, J. C., Giaume, C., et al. (2017). Inhibition of glial hemichannels by boldine treatment reduces neuronal suffering in a murine model of Alzheimer's disease. *Glia* 65, 1607–1625. doi: 10.1002/glia.23182

Yi, C., Mei, X., Ezan, P., Mato, S., Matias, I., Giaume, C., et al. (2016). Astroglial connexin43 contributes to neuronal suffering in a mouse model of Alzheimer's disease. *Cell Death Differ.* 23, 1691–1701. doi: 10.1038/cdd.2016.63

Young, K. A., Berry, M. L., Mahaffey, C. L., Saionz, J. R., Hawes, N. L., Chang, B., et al. (2002). Fierce: a new mouse deletion of Nr2e1; violent behaviour and ocular abnormalities are background-dependent. *Behav. Brain Res.* 132, 145–158. doi: 10.1016/s0166-4328(01)00413-2

Zhang, G., Li, J., Purkayastha, S., Tang, Y., Zhang, H., Yin, Y., et al. (2013). Hypothalamic programming of systemic ageing involving IKK-β, NF-κB and GnRH. *Nature* 497, 211–216. doi: 10.1038/nature12143

Zhu, W., Cao, F. S., Feng, J., Chen, H. W., Wan, J. R., Lu, Q., et al. (2017). NLRP3 inflammasome activation contributes to long-term behavioral alterations in mice injected with lipopolysaccharide. *Neuroscience* 343, 77–84. doi: 10.1016/j.neuroscience.2016.11.037

Conflict of Interest: The authors declare that the research was conducted in the absence of any commercial or financial relationships that could be construed as a potential conflict of interest.

NeuroImage 252 (2022) 119039

Contents lists available at ScienceDirect

NeuroImage

journal homepage: www.elsevier.com/locate/neuroimage

Fornix volumetric increase and microglia morphology contribute to spatial and recognition-like memory decline in ageing male mice

Marcela Cárdenas-Tueme[a], Luis Ángel Trujillo-Villarreal[b,c], Victor Ramîrez-Amaya[d], Eduardo A. Garza-Villarreal[e], Alberto Camacho-Morales[b,c,*], Diana Reséndez-Pérez[a,*]

[a] Universidad Autónoma de Nuevo León, Facultad de Ciencias Biológicas, Departamento de Biología Celular y Genética, San Nicolás de los Garza, Nuevo León, México
[b] Universidad Autónoma de Nuevo León, Facultad de Medicina, Departamento de Bioquímica, Madero y Dr. Aguirre Pequeño. Col. Mitras Centro. S/N, Monterrey, Nuevo León 64460, México
[c] Universidad Autónoma de Nuevo León, Centro de Investigación y Desarrollo en Ciencias de la Salud, Unidad de Neurometabolismo, Monterrey, Nuevo León, México
[d] Instituto de Investigación Médica Mercedes y Martín Ferreyra INIMEC-CONICET- UNC, Friuli 2434, Colinas de Vélez Sarsfield, Córdoba 5016, Argentina
[e] Instituto de Neurobiología, Universidad Nacional Autónoma de México Campus Juriquilla, Querétaro, México

ARTICLE INFO

Keywords:
Ageing
Neuroinflammation
Microglia
Cognitive decline
Magnetic resonance imageing

ABSTRACT

Ageing displays a low-grade pro-inflammatory profile in blood and the brain. Accumulation of pro-inflammatory cytokines, microglia activation and volumetric changes in the brain correlate with cognitive decline in ageing models. However, the interplay between them is not totally understood. Here, we aimed to globally identify an age-dependent pro-inflammatory profile and microglia morphological plasticity that favors major volume changes in the brain associated with cognitive decline. Cluster analysis of behavioral data obtained from 2-,12- and 20-month-old male C57BL/6 mice revealed age-dependent cognitive decline after the Y-maze, Barnes maze, object recognition (NORT) and object location tests (OLT). Global magnetic resonance imageing (MRI) analysis by deformation-based morphometry (DBM) in the brain identified a volume increase in the fornix and a decrease in the left medial entorhinal cortex (MEntC) during ageing. Notably, the fornix shows an increase in the accumulation of pro-inflammatory cytokines, whereas the left MEntC displays a decrease. Morphological assessment of microglia also confirms an active and dystrophic phenotype in the fornix and a surveillance phenotype in the left MEntC. Finally, biological modeling revealed that age-related volume increase in the fornix was associated with dystrophic microglia and cognitive impairment, as evidenced by failure on tasks examining memory of object location and novelty. Our results propose that the morphological plasticity of microglia might contribute to volumetric changes in brain regions associated with cognitive decline during physiological ageing.

1. Introduction

Ageing is characterized by a progressive loss of physiological integrity and is therefore the primary risk factor for major human pathologies, including cancer, diabetes, cardiovascular disorders, cognitive decline and neurodegenerative diseases (Currais, 2015; López-Otín et al., 2013).

A low-grade pro-inflammatory profile in blood and the brain (Wyss-Coray, 2016) has been previously reported during ageing. Infiltration of peripheral immune cells in the brain account for tissue homeostasis at younger stages, but this infiltration promotes the release of pro-inflammatory cytokines leading to neuroinflammation during ageing (Batterman et al., 2021; Dubenko et al., 2021; Fulop et al., 2018; Jeon et al., 2012). In fact, aged mice show an increase in circulating inflammatory cytokines that correlates with an age-related infiltration of neutrophils and macrophages, allowing for microglial activation in the brain (Wolfe et al., 2018). Microglia become disruptive during ageing, exhibiting morphological plasticity by displaying perinuclear cytoplasm hypertrophy and retracted processes, which are reminiscent of activated microglia (Miller and Streit, 2007; Sheng et al., 1998). Activated microglia in ageing integrate the molecular signatures found in injury or disease states, such as increased expression of major histocompatibility complex II (MHCII) and CD11b (e.g., Iba1, OX6) (Frank et al., 2006). Notably, neuroinflammation and microglia activation promote cognitive decline and increase the susceptibility to neurodegeneration in preclinical and clinical models (Bachstetter et al., 2017; Wolfe et al., 2018; Wyss-Coray, 2016). Congruently, pharmacologic blockage of neuroinflammation improves spatial memory performance in aged mice

* Corresponding authors.
E-mail addresses: alberto.camachomr@uanl.edu.mx (A. Camacho-Morales), diana.resendezpr@uanl.edu.mx (D. Reséndez-Pérez).

https://doi.org/10.1016/j.neuroimage.2022.119039.
Received 13 December 2021; Received in revised form 7 February 2022; Accepted 24 February 2022
Available online 25 February 2022.

(Fung et al., 2020; Zhou et al., 2019). However, the interplay between microglial plasticity and neuroinflammation during ageing, and their role on cognitive decline have not been totally understood.

Volumetric changes in selective brain areas related to cognitive performance have been identified during ageing. Authors report a mean decline in total volume of −0.45% per year from age 18 to 97 (Fotenos et al., 2005), and a persistent linear reduction in cortex and increased ventricular volume beginning at age 20 (Fillmore et al., 2015). Several magnetic resonance imageing (MRI) studies have also reported volumetric reductions of gray matter (GM) in prefrontal, parietal and temporal association cortices, and in the insula, cerebellum, basal ganglia and thalamus of aged humans (Alexander et al., 2006; Good et al., 2001; Grieve et al., 2005; Jernigan et al., 2001; Kalpouzos et al., 2009; Resnick et al., 2003; Sowell et al., 2004; Taki et al., 2004; Tisserand et al., 2002). However, cellular and molecular traits contributing to volumetric brain changes during ageing have not been characterized and in some cases are still misunderstood.

Here, we dissect the contribution of central pro-inflammatory profile and microglial morphological plasticity during ageing and found that they are congruent with volumetric changes in selective regions associated with cognitive decline. We propose that morphological changes in microglia rather than neuroinflammation contribute to volumetric changes in brain regions assisting cognitive decline during physiological ageing.

2. Materials and methods

2.1. Animals and housing

All animal experiments were approved by the Institutional Animal Care and Use Committee of the Universidad Autónoma de Nuevo León (CEIBA-2018-006) and carried out in accordance with Association for Assessment and Acreditation of Laboratory Animal Care International regulations, the US Department of Agriculture Animal Welfare Act, and the Guide for the Care and Use of Laboratory Animals of the NIH. All efforts were made to minimize the number of animals used and their suffering.

Upon arrival, 2-, 12-, and 20-month-old male C57BL/6 mice (n=30/age group) were single-housed in Plexiglas style cages for at least 10 days to acclimatize with *ad libitum* access to standard Chow diet and water, temperature of 23-25° C, and 12:12 h light control. Mice aged 2-, 12-, and 20-month-old were divided into two cohorts of 15 mice each to characterize macro and microplasticity changes using MRI, immunofluorescence and immunohistochemistry, and brain morphological analysis (cohort 1), and Bioplex analysis for central and peripheral pro-inflammatory markers (cohort 2). We performed the behavioral phenotyping of both cohorts as described below.

2.2. Behavioral phenotyping

The behavioral test battery was performed in the two cohorts of male mice by exposing them to four memory tests in the following order: Y-maze forced alternation, NORT, Barnes maze and OLT (Fig. 1, Fig. S1). We followed a specific order to conduct the tests so that the mice could have several resting days between the tasks and to avoid carryover effects from prior tests (Fig. 1A). Visual cues were placed on the walls of the testing area for all tests except the NORT. All mice were habituated to the testing room for 1-hour before each test day. All behavioral tests were conducted by the same experimenter to avoid extra stress on the animals, which was blinded from the groups. During the trials, mice were not able to see the experimenter, as they were separated by a glass wall. A detailed description of the methodological procedures and rationale of inclusion are found in the Supplemental Information.

2.3. Ex-vivo fixation and MRI analysis by DBM

Male mice from the cohort 1 (2-month-old n=15, 12-month-old n=15, and 20-month-old n=15) were allocated to perform MRI analysis, however after preprocessing and quality control of the MRI images those that had artifacts in the acquisition were excluded. Finally, an n = 12 for the 2-month, 12-month and 20-month-old mice was reported.

A dermal dissection was performed from the abdominal region to the upper part of the thoracic cage, exposing the heart. Then, left ventricle of the heart was punctured following its apex and a cut was made in the right atrium to open the circulatory system. Mice were transcardially perfused with 0.1M PBS + Heparin (10 U/ml) + Prohance wash solution (4 mM) using an infusion pump (Fisher Scientific GP1000) at a flow rate of 10 ml/min. Subsequently, the washing solution was changed to the fixing solution including 4% paraformaldehyde (PFA) in 0.1M PBS + 4 mM Prohance for 25 min, following the same flow, as previously reported (Trujillo-Villarreal et al., 2021). The brain protected by the skull was collected and samples were stored at 4°C in 4% PFA + 4 mM Prohance for 24 hours and then the solution was changed to 0.1M PBS + 0.02% sodium azide until further analysis of MRI.

For MRI acquisition, the skulls were submerged and fixed inside plastic tubes filled with Fomblin (a chemically inert perfluoropolyether fluorocarbon; Solvay Solexis, Inc.). Imageing was performed in a 16 cm bore 7 T Bruker scanner (Pharmascan 70/16) using a Paravision 6.0.1 system and a Tx/Rx volume coil for mice with a 72 mm inner diameter. We then acquired a T1w Bruker FLASH sequence name: 3D_FLASH_Mn_Garza, TR/TE = 32.88/8.64 ms, flip angle = 20 degrees, averages = 1, matrix = 256 × 256 × 256, spacing = 0.050 mm, Pixel bandwidth = 108.507 Hz, FOV = 12.8 × 12.8 × 12.8 mm, no. of slices = 255. The resolution of the final MRI images was 0.05 mm isotropic. Morphological analysis was performed by converting DICOM to MINC format, and then preprocessed using an in-house pipeline based on MINC-Tools (https://github.com/CoBrALab/minc-toolkit-extras/blob/master/mouse-preprocessing-v5.sh) and the pydpiper pipeline (https://github.com/Mouse-Imageing-Centre/pydpiper). All analyses were performed using pydpiper version 1.8 (Friedel et al., 2014), R studio version 3.6.3 (Rstudio, 2020), and the RMINC version 1.5.2.2 (Lerch, J., 2017) and tidyverse version 1.3.1 (Wickham, H., 2017) packages.

All images were converted from DICOM to MINC format, and then preprocessed using an in-house pipeline based on MINC-Tools and ANTs, which performed the following steps: center image, full mask and N4 Bias Field Correction. We then used an image registration-based approach to assess anatomical differences between groups. Image registration finds a smooth spatial transformation that best aligns one image to another such that corresponding anatomical features are superimposed. We used an automated intensity-based group-wise registration approach (Lerch, JP., 2011) to align all brains in the study into a common coordinate system, yielding an average image of the 45 T1w scans. The deformation that aligns the images becomes a summary of how they differ. To assess volume differences between groups, we performed DBM as it provides a continuous voxel by voxel definition of volume changes (expansion/contraction) related to their age. Deformations were then mapped from the individual scans back to the average image. The final deformation fields were computed with a greedy symmetric diffeomorphic registration (the SyN algorithm in ANTS) (Avants, B. et al., 2008; Bird, S. et al., 2009) then inverted and blurred with a 0.1 mm FWHM Gaussian smoothing kernel. The Jacobian determinants of these deformations were extracted, giving a measure of local volume expansion/contraction at every voxel in the brain. Log-transformed Jacobian relative determinants (blurred 0.2 mm) were used to assess differences between groups because they better estimate a normal distribution.

2.4. Histological analysis

Brains from the MRI analysis (cohort 1) (n = 4) were randomly collected, dissected from the skull and incubated in 10%, 20% and 30%

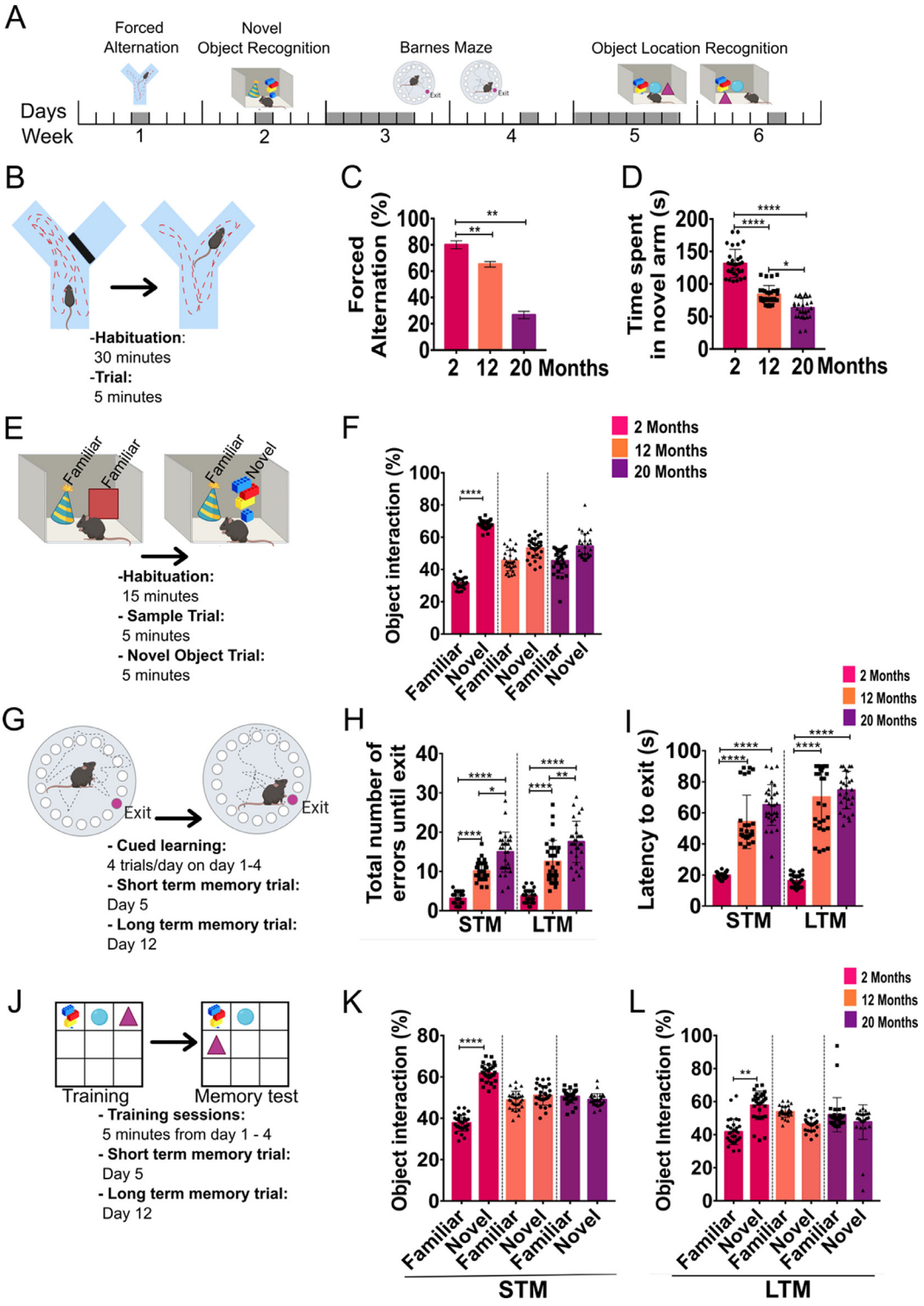

Fig 1. Behavioral phenotyping of male C57BL/6 mice. A) 2-,12- and 20-month-old mice were tested in a behavioral test battery consisting of forced alternation (Y-maze), Barnes maze, NORT and OLT over a period of 5 weeks**. B)** In the Y-maze test, mice were exposed to a familiarization session for 5 minutes (T1), afterwards they were returned to their cage for 30 minutes and then during the trial (T2) forced alternation and time spent in the novel arm was assessed in the Y maze. **C)** Forced alternation test was evaluated according to the arm chosen as the first option in the Y maze during T2. Results show the percentage of alternation between groups. **D)** Time spent in the novel arm was conducted 30 min after the familiarization session. Results show time spent (s) in the novel arm during the retrieval trial between groups**. E)** Recognition memory performance was evaluated with the NORT, following the protocol illustrated in the picture. **F)** Time spent with the familiar object and novel object is represented as % of object interaction. **G)** Barnes maze test evaluated spatial short-term (STM) memory by one day after the last training day and long-term memory (LTM) was evaluated 7 days later after the last training session. **H)** The graph shows the number of errors before the exit was found in the STM and LTM tests. **I)** Results show latency to exit (s) until the exit was found, for both STM and LTM. **J)** Spatial STM and LTM were also evaluated with OLT, with this test mouse speed bias was avoided. Time spent (%) with the objects in the known location (Familiar) was compared with the object in the new location (Novel). Percentage of time spent during the novel object interaction during STM (K) and LTM (L). Results are expressed as Mean ± S.E.M followed by ANOVA *post-hoc* Tukey n.s= 0.1234, *p= 0.03, **p= 0.002, ***p= 0.0002, ****p <0.0001. n=15/group. Created with BioRender.com

sucrose + 0.1 M PBS and 30 μm coronal sections for two regions, fornix (Fornix, Bregma 4.28 mm to – 0.14 mm) and left Medial entorhinal cortex (left MEntC, Bregma 4.04 mm to – .22mm), were obtained in a cryostat. Anatomical limits of each brain region were identified using the mice brain atlas (Paxinos and Franklin, 2001).

2.5. Immunohistochemistry for synaptophysin

The immunohistochemistry of brains from the cohort 1 was performed as we reported (Trujillo-Villarreal et al., 2021). The slices of 2-,12-, and 20-month-old male mice (n=4/group of age) were 2 x washed with 0.1 M PBS + 0.1% TritonX-100, incubated with the peroxidase blocker for 10 minutes (Abcam, Cat. AB64264), washed with 0.1M PBS + 0.1% TritonX-100 and incubated with the protein blocker for 10 minutes (Abcam, Cat. AB64264). Sections were incubated with 0.1M PBS + 0.1% TritonX-100, following by the primary anti-synaptophysin antibody (4 μg/mL, Genscript Cat. A01307) at 4°C overnight. Finally, sections were exposed to biotinylated goat anti-rabbit IgG secondary antibody for 10 minutes, following by streptavidin (10 min) and diaminobenzidine chromogen solution (30μL in 1.5mL of substrate) for 10 minutes. Assembly of the cut was performed with mounting solution on coverslips. Negative controls were prepared by omission of primary antibodies and no densitometry signal was identified.

2.6. Immunofluorescence for Iba-1

The immunofluorescence of brains from the cohort 1 was performed as we previously reported (Maldonado-Ruiz et al., 2019). Free floating sections of 30 μm of 2-,12-, and 20-month-old mice (n=4/group of age) were washed three times for 5 min with 1X PBS + 0.1% TritonX-100 (PBST) and were blocked in PBST + 10% goat serum + 10% horse serum at room temperature (RT) for an hour. Subsequently, sections were incubated with the primary antibody anti-Iba1 1:200 (ab178847, abcam, Cambridge, MA, USA) at 4°C for 48 h. Two days later, the sections were washed in PBST three times and then incubated for two hours with the secondary antibody Alexa fluor anti-rabbit 1:1000 (A-11034, Invitrogen) diluted in PBST + 1% goat serum + 1% horse serum. Afterwards, brain sections were washed three times with PBST and air-dried at RT. Finally, brain sections were mounted using Vectashield with DAPI (Vector Laboratories, Burlingame, CA, USA) on coverslips.

2.7. Microglia morphological analysis

Microglia morphology was analyzed in brains from the cohort 1 as previously described (Young and Morrison, 2018) using the free software Fiji: an open-source platform for biological-image analysis. In brief, Iba1 positive cells in the brain tissue were obtained and images were converted into 8-bit and into grayscale. Images were adjusted to the minimum or maximum sliders as needed, up to the edges of the histogram but no further followed by an Unsharp mask filter. Afterwards, we performed a despeckle to eliminate all the salt and pepper noise, converted into binary and used the remove outliers function. Subsequently, the images were saved separately and by using the plugin Skeleton we measured microglia branches length and the number of end points. Finally, the results were graphed and analyzed according to their protocol.

2.8. Cytokine quantification in peripheral blood, fornix and left MEntC

Male mice from cohort 2 were anesthetized with 500 μL i.p. pentobarbital (PiSA Agropecuaria) overdose and peripheral blood was collected through cardiac puncture and kept in pharmaceutical-grade Heparin BD Vacutainer^{TM} Heparin Plasma Tubes (BD 368480), and brains were dissected, collected and frozen (-80° C) for further use.

Blood tubes were centrifuged at 2500 rpm for 20 minutes and plasma was collected. According to the MRI analysis, we selected the fornix and left MEntC because they displayed the largest volume changes with age. To selectively isolate the fornix and the left MEntC, we started off by obtaining in the cryostat coronal sections of 40 μm of the fornix (Bregma 4.28 mm to – 0.14 mm) and left MEntC (Bregma 4.04 mm to – 0.22mm). Then, using the mouse brain atlas (Paxinos and Franklin, 2001) and under the dissecting stereoscope (Leica, ez4) with a scalpel the selective regions were cut and collected in 0.1 mL tubes.

Cytokine profile in plasma, fornix and the left MEntC was identified using the MILLIPLEX MAP Kit Mouse Cytokine/Chemokine Magnetic Bead Panel (Millipore corporation, MCY-TOMAG-70K), following the manufacturer's instructions. In brief, for cytokine analysis in the brain, Fornix or left MEntC were incubated in 70 μL cell signaling Lysis buffer for Multiplexing (Millipore corporation, 43-040), homogenized by sonication (amplitude 20% 3 pulses/second 10 times), followed by centrifugation at 10,000 RMP/4°C and then the supernatant was isolated.

Reads from the plasma, fornix and the left MEntC supernatant samples were performed employing the Luminex® 200^{TM} Multiplexing Instrument (Luminex Corporation, LX200-XPON3.1). We measured the pro-inflammatory cytokines IL-1β, IL-4, IL-6, IL-12, IL-13, IL-17- GM-CSF, INF-γ, TNF-α, and MCP-1.

2.9. Principal component analysis (PCA)

PCA involves 2D matrix composition of data as an effective dimension-reducing tool retaining the information of the original data as much as possible (Wu et al., 2019). In this study, we integrated 38 variables (behavior, peripheral and brain cytokine levels and brain region volumes), for PCA analysis. PCA was performed to provide an indication of the capacity of variables to cluster individuals according to their behavioural test performance, cytokine levels, and brain volume. Variables contributions to PCA analysis can be found in the Supplemental Information (Fig. S6, S7 and Table S3).

2.10. Statistical analysis

Data are presented as mean ± SEM for all data. All statistical analyses including testing the normality of data distribution were performed using GraphPad Prism 7.01 and IBM SPSS statistics version 22 software and a corrected p value <0.05 was considered as significant. All results were tested for normality using Shapiro-Wilk test. For differences between the 3 groups in the behavioral tests, one-way ANOVA followed by Tukey's multiple comparison test was used and effect size was calculated in R language. Significant differences in cognitive performance during behavioral phenotyping data are shown as the mean ± SEM and significant differences at $p < 0.05$. The statistical analysis on DBM was performed using the log transformed Jacobian determinants as the dependent variable, "age group" as the independent variable (between subjects) and "weight" as covariate (mouse weight at euthanasia). We compared the three groups using a general lineal model and analyses were corrected for multiple comparisons using the false-discovery rate (FDR) at 5%. Furthermore, we extracted the jacobians values from significant peaks at V1: primary visual cortex, FX: fornix, S2: secondary somatosensory cortex, OB: olfactory bulb, VIIB: paramedian lobule (lobule 7), MEntC: medial entorhinal cortex, A1: primary auditory cortex, Amg: Amygdala. Jacobians from regions of interest were correlated with the behavior, cytokines and histology data to explore their association pattern using Pearson correlation and corrected using the FDR at 5%. These analyses were performed in R studio version 3.6.3.

3. Results

3.1. Ageing disrupts cognitive and memory performance in male mice

Individual behavioral phenotyping was performed in two cohorts of subjects to determine the effect of ageing on cognitive decline.

3.1.1. Forced alternation

We found an age-dependent effect on working memory in male C57BL/6 mice. Ageing decreased the forced alternation percentage between the 12- and 20-month-old mice (ANOVA, $F_{(2,42)}$= 12-month-old: $^{**}p = 0.0049$ and 20-month-old: $^{**}p = 0.0018$, respectively) when compared to 2-month-old mice (Fig. 1 B, C, and D). Selectively, about 60% of the 12-month-old mice and about 20% of the 20-month-old mice performing the forced alternation test recognized the blocked arm as novel and chose it as their first choice when compared with the 2-month-old mice which showed a preference of 80% for the novel arm (Fig. 1 C). Also, 12- and 20-month-old mice allocated less time in the novel arm when compared with the 2-month-old mice (ANOVA, $F_{(2,42)}$= 12-month-old: $^{****}p < 0.0001$ and 20-month-old: $^{****}p < 0.0001$, respectively) (Fig. 1 D). More specifically, 12 and 20-month-old mice spent 83.93 ± 14.3 s and 63.48 ± 15.81 s, respectively in the novel arm, in contrast to 135 ± 15.81 s in 2-month-old mice, confirming an age-dependent effect on preference and recognition performance (Fig. 1 D).

3.1.2. Novel object recognition

The NORT evaluates recognition memory in mice based on the innate predisposition of rodents to investigate a novel object longer than a familiar one (Fig. 1E) (Antunes and Biala, 2012). Male mice in all three age groups demonstrated increased interaction with the novel object as compared to the familiar object (Figure 1 F). However, the increase in interaction time was only significant in 2-month-old mice, whereby % object interaction during each trial increased from approximately 31% with the familiar object to 68% with the novel object. (ANOVA, $F_{(5,84)}$= $^{****}p < 0.0001$) (Fig. 1F). These results confirm defective novel item recognition and interaction in aged mice.

3.1.3. Barnes maze

The Barnes maze test was used to assess spatial memory and learning in the short and long term. In brief, subjects were trained as described and we scored the total number of errors before reaching the exit from the platform as well as latency to exit (Fig. 1 G). We found that 12- and 20-month-old mice exhibit defective short-term memory (STM: evaluated at one day after the last training session) evidenced by more errors finding the exit when compared with the 2-month-old (ANOVA, $F_{(5,100)}$= $^{****}p < 0.0001$ and $^{****}p < 0.0001$, respectively) (Fig. 1 H). In fact, defective STM was exacerbated in 20-month-old mice in contrast to 12-month-old mice (ANOVA, $F_{(5,100)}$= $^{**}p < 0.002$) (Fig. 1 H). In addition, impairment in memory performance is found at later stages during the long-term memory (LTM: evaluated at seven days after the last training session) test in the 12- and 20-month-old mice when compared with the 2-month-old (ANOVA, $F_{(5,100)}$= $^{****}p < 0.0001$ and $^{****}p < 0.0001$, respectively) (Fig. 1 H).

An increase in the time needed to locate and exit the maze was also seen with age. Mice aged 12- and 20-month experience longer time to find the exit during the STM and LTM tests when compared with the 2-month-old group (ANOVA, $F_{(5,100)}$= $^{****}p < 0.0001$ and $^{****}p < 0.0001$, respectively) (Fig. 1 I). These results confirm that 12- and 20-month-old male mice display a compromised spatial memory performance.

3.1.4. Object location recognition test

Ageing can cause major changes in speed and locomotion that could potentially bias the defective performance found in the Barnes maze test. In order to avoid a bias, we evaluated spatial memory and learning in a small arena using the OLT (Fig. 1 J). Two-month-old mice investigated objects at novel locations significantly more than objects at familiar locations when tested using both short-term and long-term versions of the test, conducted at one- or seven-days post-training, respectively (Figure 1 K - L) (ANOVA, $F_{(5,84)}$= $^{****}p < 0.0001$). In comparison, 12- and 20-month-old mice did not interact with the object in a novel location significantly more than that in a familiar location. These results confirm age-dependent impairment in spatial memory performance in 12- and 20-month-old mice (Fig. 1 K - L).

3.2. Age-dependent brain macrostructural alterations

We performed global MRI analysis to selectively characterize regional volume-related macrostructural brain alterations during ageing. The pairwise analysis showed significant whole-brain local volume differences in the 12-month-old mice compared with the 2-month-old group (Supplemental Information Fig. S2 A), 12-month-old mice compared with 20-month-old mice (Supplemental Information Fig. S2 B) and also, 2-month-old mice compared with 20-month-old mice, all of them corrected by the FDR 5% (Supplemental information Fig. S2 C). Major whole-brain local volume changes were identified in the 20-month-old mice when compared with 2-month-old group (Fig. S2 C). Selectively, the 20-month-old group showed lower and higher local volume of selective brain regions compared with the 2-month-old group with more localized clusters (Supplemental Information Table S1). By using the Paxinos and Franklin's Mouse Brain in Stereotaxic Coordinates Atlas, we identified that the fornix displayed the higher and the left MEntC displayed the lowest local volume change in the 20-month-old mice when compared with 2-month-old mice (Table S1, Fig. 2A, B). Notably, a simple linear regression was calculated to predict jacobians on fornix or left MEntC based on age. A significant regression equation was found to predict fornix ($F_{(2, 37)}$ = 395.7, $^{****}p < 0.0001$), with an adjusted R^2 of 0.952, and to predict the left MEntC ($F_{(2, 37)}$ = 63.09, $^{****}p < 0.0001$), with an adjusted R^2 of 0.761. Predicted fornix is equal to -0.133 (2-month) + 0.105 (12-months) and -0.133 (2-month) + 0.253 (20-months) jacobian value. Predicted left MEntC is equal to 0.039 (2-month) - 0.037 (12-months) and 0.039 (2-month) - 0.159 (20-months) jacobians. Fornix volume increases 0.105 for 12 months and 0.253 for 20 months, whereas left MEntC volume decreases -0.037 and -0.159 jacobians for 12 and 20 months, respectively (Fig. 2 A, B).

3.3. Antagonistic volumetric changes in fornix and left MEntC correlate with age and performance in cognitive tasks

We tested whether brain volume changes found in the fornix and left MEntC during ageing correlated with cognitive and memory performance. Pearson correlations of brain volume changes vs cognitive tasks are pictured as heatmaps (Fig. 2 C-E). We found positive and negative correlations among different brain areas and diverse cognitive tasks that were summarized in Table S2 A, B, C. In particular, 2-month-old mice showed a positive correlation between fornix volume and number of errors (Error_STM) before reaching the exit in the Barnes maze during the STM test (r = 0.58, $^{*}p = 0.02$) (Fig. 2 C, Table S2 A) and in the performance in the NORT (NOR_P) (r = 0.67, $^{***}p = 0.008$) (Fig. 2 C, Table S2 A). Conversely, a negative correlation was found between fornix and behavior before reaching the exit in the Barnes maze during the LTM test (Error_LTM) (r = -0.64, $^{**}p = 0.01$) (Fig. 2 C, Table S2 A). We also found a positive correlation between the volume in the left MEntC and the number of errors (Error_LTM) in the Barnes maze during the LTM test (r = 0.63, $^{**}p = 0.01$) and in the performance during the OLT in the LTM test (OLT_LTM) for the left MEntC volume (r = 0.54, $^{*}p = 0.04$) (Fig. 2C, Table S2 A).

At 12 months of age, increased volume in the fornix positively correlates with the number of errors during STM and LTM (Error_STM, Error_LTM) in the Barnes maze (STM: r = 0.58, $^{*}p = 0.03$; LTM: r = 0.64, $^{*}p = 0.04$) as well as during the OLT (OLT_STM) in the STM test (r = -0.32, $^{**}p = 0.01$) (Fig. 2 D, Table S2 B). Interestingly, we also found a negative correlation between MEntC and the number of errors (Error_STM) in the Barnes maze during LTM (r = -0.48, $^{*}p = 0.02$) (Fig. 2 D, Table S2 B). Likewise, decreased volume in the left MEntC displays a negative correlation with (Fig. 2 D, Table S2 B) the OLT in the STM test (OLT_STM) (r = 0.24, $^{***}p = 2.75 \times 10^{-5}$) (Fig. 2 D, Table S2 B).

Finally, major volume increase in the fornix found in 20-month-old mice shows a positive correlation with the time spent before finding the exit (Time_STM) in the Barnes maze during the STM test (r = 0.67, $^{*}p = 0.01$), similarly during the NORT (NOR_P) (r = 0.55, $^{*}p = 0.05$) and

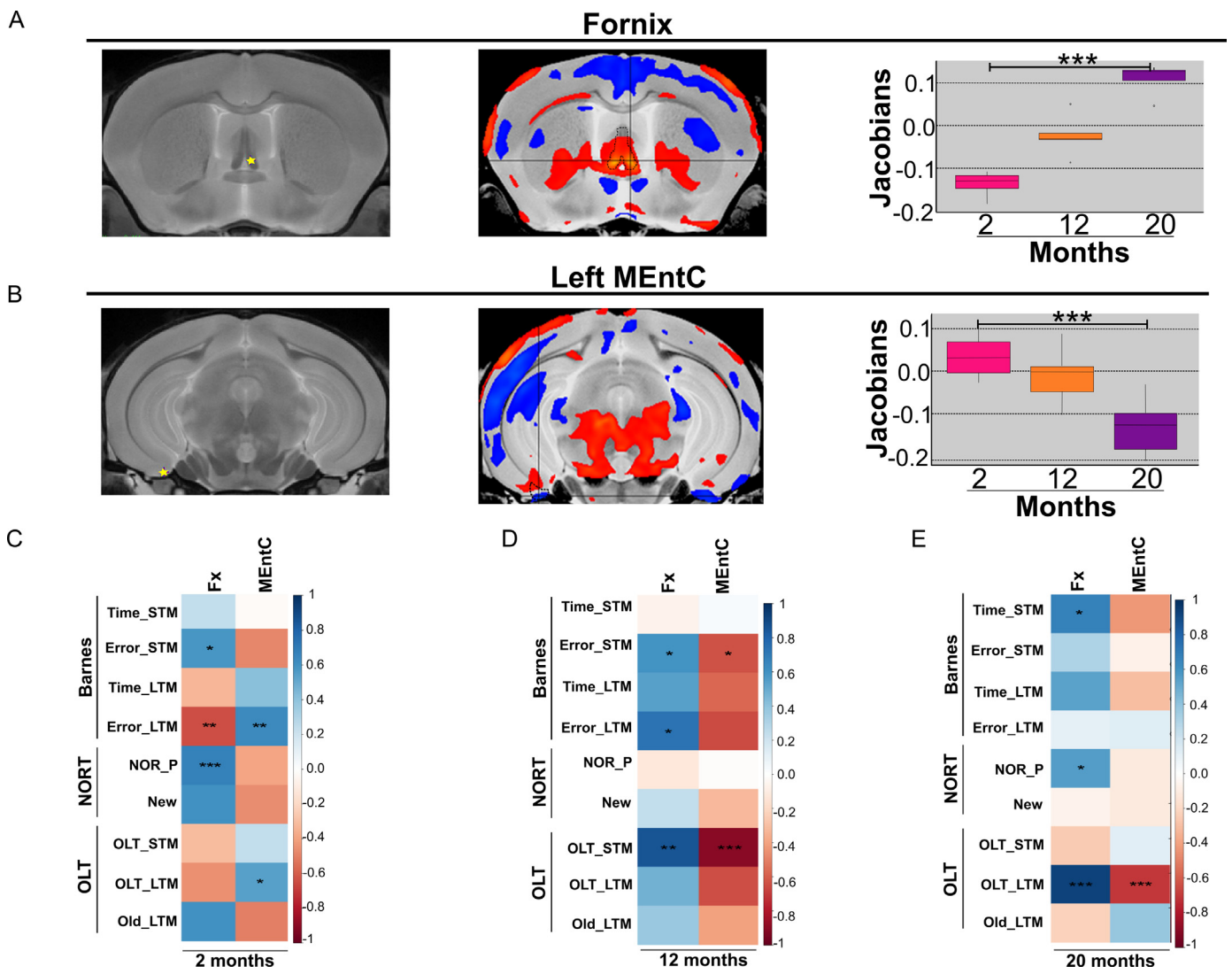

Fig 2. DBM of brain volume comparison of 2- and 20-month-old male C57BL/6 mice. A-B) MRI images of DBM data of 2- compared with 20-month-old mice. ROI = Fornix or Left MEntC plot of relative volume peak (right) and DBM (Left), box plot of relative volume peak (right). Blue-light blue = lower volume; red-yellow = higher volume. Results are significant at FDR 5%. Boxplots show the relative volume (y axis = Jacobians) in each group (x axis) across age in significant peaks. **C-E)** Heatmaps of Pearson correlation test between brain volumetric changes and cognitive performance. Bar graphs display data mean +/- SEM followed by ANOVA post-hoc Tukey. *p= 0.03, **p= 0.002, ***p= 0.0002. n=15/group.

OLT during the LTM (OLT_LTM) (r = 0.91, $^{***}p = 0.0001$) (Fig 2 E, Table S2 C). A selective negative correlation was found between decrease in left MEntC with the performance in the OLT (OLT_LTM) during the LTM test (MEntC: r = -0.70, $^{***}p = 0.007$) (Fig. 2 E, Table S2 C).

3.4. Ageing favors a pro-inflammatory cytokine profile in peripheral blood

We were interested in evaluating the pro-inflammatory profile in peripheral blood given their associations to cognitive decline during ageing (Brombacher et al., 2017; Dubenko et al., 2021; Fossati et al., 2017; Pennisi et al., 2017; Tarkowski et al., 2001). Initial characterization of age-dependent increase in plasma of the pro-inflammatory shown a robust increase in cytokines and chemokines such as: GM-CSF, IFN- γ, IL-6, IL-1 β, IL-4, IL-12p70, IL-13, IL-17, MCP-1 and TNF-α in 20-month-old male mice (Fig. S3). Notably, 20-month-old mice show major increases in IL12p70, TNF-α, MCP-1 and IL-6 plasma levels when compared with the 2-month-old group (ANOVA, $F_{(2, 18)}$ = IL12p70: $^{***}p = 0.008$, TNF-α: $^{****}p$ <0.0001, MCP-1: $^{****}p < 0.0001$ and IL-6: $^{****}p < 0.0001$) (Fig. 3 A). We also found that 12-month-old mice display an increase in IL-12p70, TNF-α, IL-1β and IL-6 plasma levels when compare to young 2-month-old mice (ANOVA, $F_{(2, 18)}$ = IL12p70: $^{**}p = 0.002$, TNF-α: $^{****}p$ <0.0001, IL-1 β: $^{****}p < 0.0001$ and IL-6: $^{****}p < 0.0001$) (Fig. 3 A). These results confirm an age-dependent accumulation of IL-12p70, TNF-α, MCP-1, IL-6 and IL-1β in peripheral blood.

3.5. Aged male mice show increased pro-inflammatory cytokines in the fornix and decreased in the left MEntC

According to our MRI analyses, we identified that the Fornix and the left MEntC experienced the major and antagonistic volumetric changes during ageing (Fig. 2 A, B). We evaluated whether differential volume changes in fornix and left MEntC correlate with pro-inflammatory cytokines accumulation. We found that 20-month-old mice accumulate IL-12p70, MCP-1, IL-1β and IL-6 in the fornix when compared with the 2-month-old group (ANOVA, $F_{(2, 18)}$ = IL-12p70: $^{****}p < 0.0001$, TNF-α: $p = 0.6884$, MCP-1: $^{****}p < 0.0001$, IL-1β: $^{***}p < 0.0008$ and IL-6: $^{****}p < 0.0001$) (Fig. 3 B). No changes were found in TNF-α (ANOVA, $F_{(2, 18)}$ = p= 0.6884). Notably, levels of the IL-12p70, TNF-α, MCP-1, IL-1β and IL-6 were reduced in the left MEntC of 20-month-old mice in comparison with 2-month-old mice (ANOVA, $F_{(2, 18)}$ = IL-

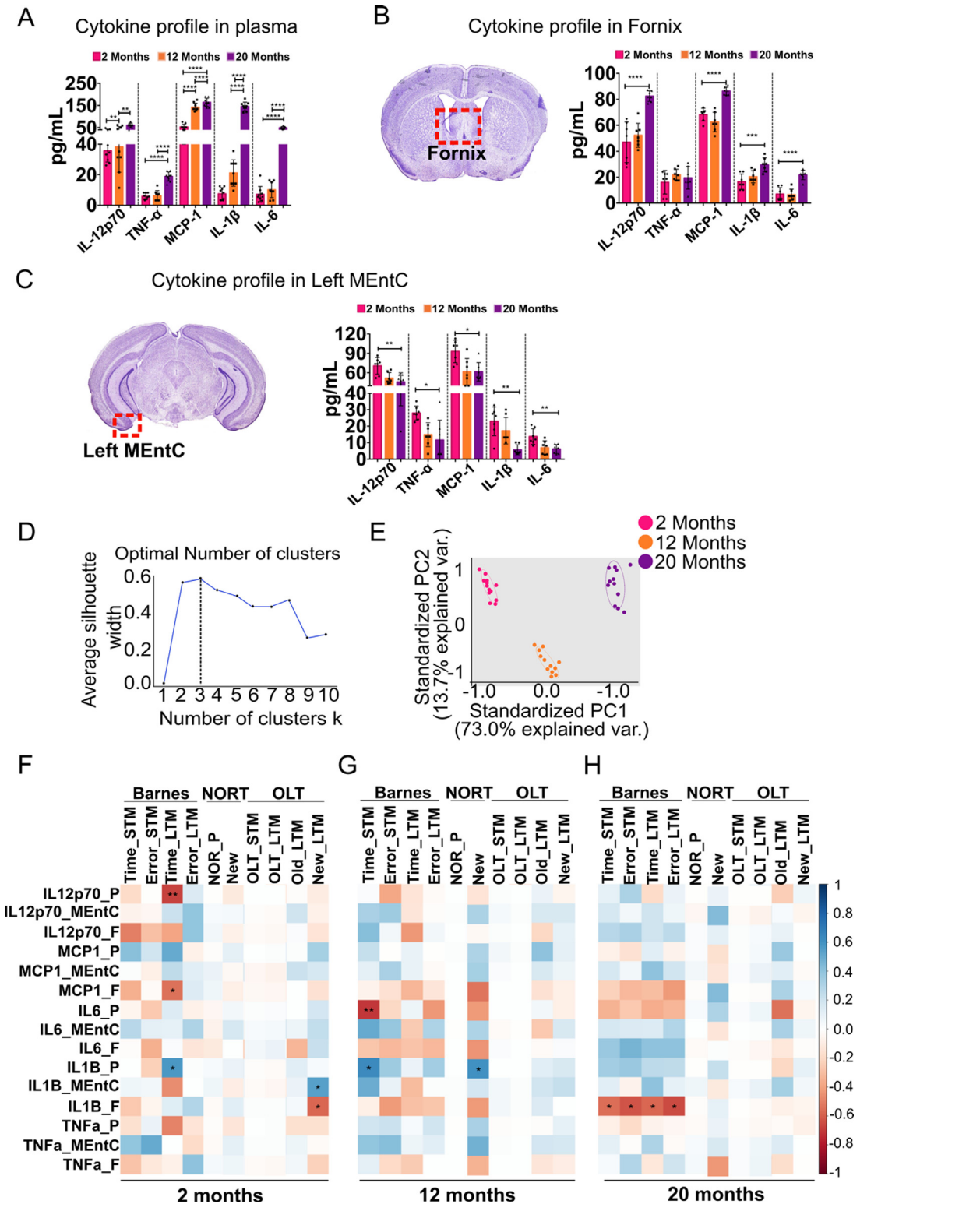

Fig 3. Central and peripheral cytokine quantification analysis. A) Plasmatic cytokine quantification expressed in pg/mL in aged male mice. **B)** Representative brain coronal sections of the Paxino's Atlas of the murine Fornix, the Fornix is highlighted within the red box. Age-dependent cytokine profile in Fornix (pg/mL) of 2-12-, and 20-month-old mice. **C)** Representative brain coronal section of the Paxino's Atlas of the murine Left MEnt, it is shown in the red box**.** Cytokines quantification in Left MEntC during ageing (pg/mL) of 2-12-, and 20-month-old-mice. **D)** k-mean analysis and **E)** Principal component analysis (PCA) of 2-12-, and 20-month-old-mice. **F-H)** Pearson correlation of cytokines profiles in peripheral blood, fornix or left MEntC with behavioral performance during ageing. Abbreviations: _P: peripheral blood, _F: fornix, _MEntC: left Medial entorhinal cortex. For behavioural tasks: 1) Barnes, Time_STM: time during short time memory, Error_STM: error during short time memory, Time_LTM: time during long time memory, Error_LTM: error during long time memory. 2) NORT: novel object recognition test, NOR_P: recognition index during the novel object recognition test, New: Time with new object during the novel object recognition test. 3) OLT: object location test, OLT_STM: object location test during the short time memory, OLT_LTM: object location test during long term memory, Old_LTM: time spent with object's old location during the long-term memory test, New_LTM: time spent with object's new location during the long-term memory test. Results are expressed as Mean ± S.E.M followed by ANOVA *post-hoc* Tukey $^{n.s}$ p= 0.1234, *p= 0.03, **p= 0.002, ***p= 0.0002, ****p= 0.0001. n=7-8/group.

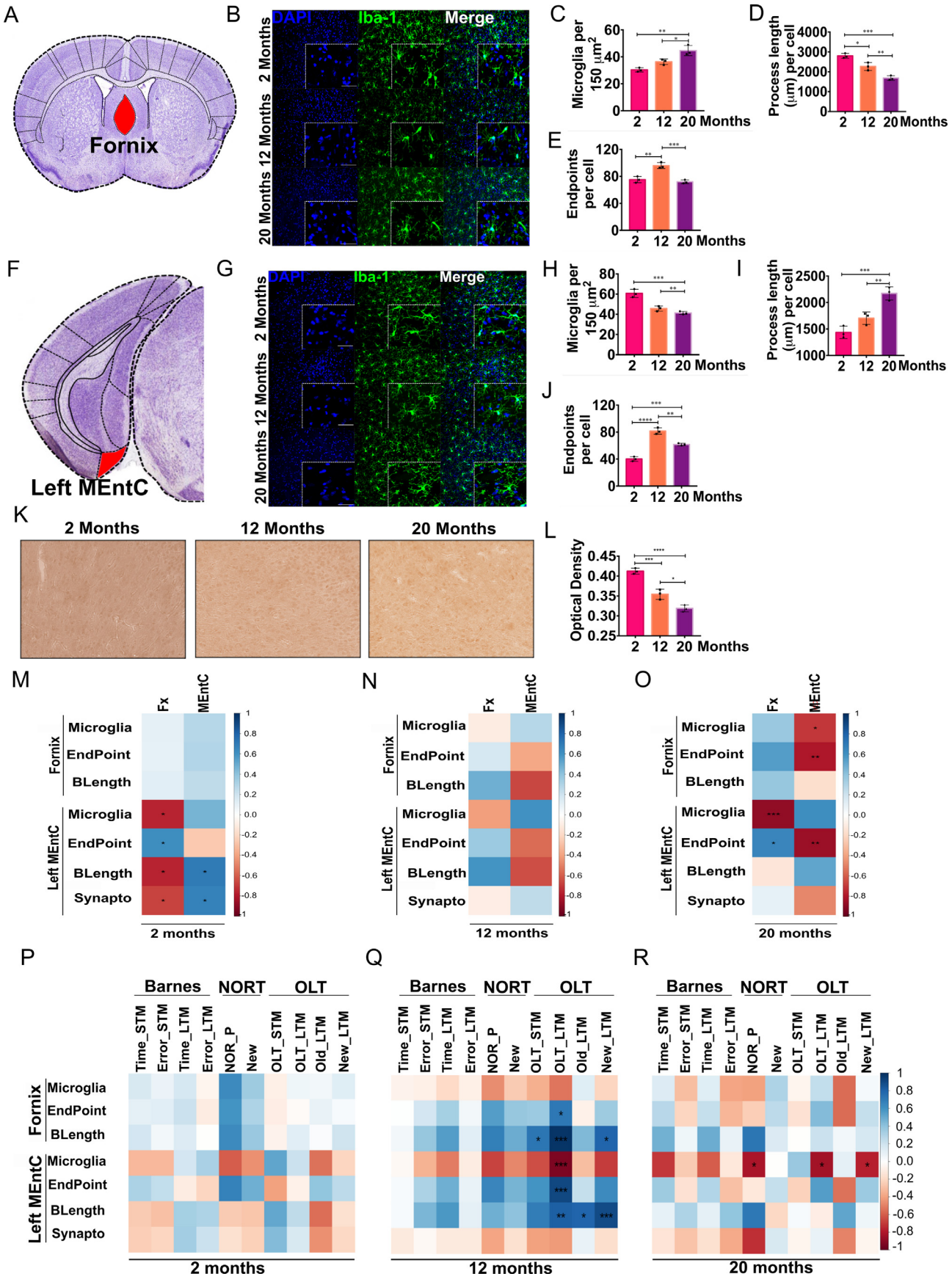

Fig 4. Fornix and left MEntC integrate changes in microglia morphology during ageing. A) Representative brain coronal sections of the Paxino's Atlas of the murine Fornix, the Fornix is highlighted in red. **B)** Immunofluorescence for Iba-1 reactive microglia in the fornix during ageing. **C)** Representative images for Iba-1+ microglia in the fornix, these were counted in 5 random fields. The graph shows the number of microglia in 150 μm^2 of 2-,12- and 20-month-old-mice. **D)** The graph shows processes length (μM) of Iba1+ microglia in the fornix. **E)** Iba1+ microglia endpoint per cell. **F)** Representative brain coronal section of the Paxino's

12p70: $^{**}p = 0.0031$, TNF-α: $^{*}p = 0.0056$, MCP-1: $^{*}p = 0.0097$, IL-1β: $^{**}p = 0.0007$ and IL-6: $^{**}p = 0.0055$) (Fig. 3 C). These results confirm antagonistic IL-12p70, MCP-1, IL-1β and IL-6 accumulation in the fornix and left MEntC during physiological ageing.

PCA was performed by integrating 38 variables (behavior, peripheral and brain cytokines levels and brain region volumes) to cluster individuals into groups according to their results in behavior, immune profiles and brain volume changes. PCA analysis with k-mean identified three clusters according to mice age (Fig. 3D). As shown in Fig. 3E, principal component 1 (PC1) and principal component 2 (PC2) accounted for 73 and 13.7% of the total variance, respectively (Fig. S6, S7 and Table S3).

3.6. Cytokine levels negatively correlate to performance in cognitive tasks

We assessed whether pro-inflammatory cytokine accumulation in peripheral blood, fornix or left MEntC correlate with defective cognitive tasks in aged male mice by Pearson analysis. We identified positive and negative correlations among different cytokines and diverse cognitive tasks that were summarized in Table S4 A, B, C. Two-month-old group shows a negative correlation of peripheral IL-12p70 (IL12p70_P) and MCP1 levels (MCP1_F) in the fornix and the time spent before finding the exit (Time_LTM) in the Barnes maze during the LTM test (IL-12p70: r=-0.67 $^{**}p = 0.008$; MCP1: r = -0.54, $^{*}p = 0.04$) (Fig. 3 F). Also, a positive correlation of peripheral IL-1β (IL1B_P) and time LTM (Time_LTM) of the Barnes maze (r= 0.57, $^{*}p = 0.03$) (Fig. 3 F, Table S4 A). By 12 months of age, peripheral IL-6 levels (IL6_P) negatively correlates with more time spent reaching the exit in Barnes maze (Time_STM) during the STM test (r= -0.70 $^{**}p = 0.007$) (Fig. 3 G, Table S4 B). Finally, a negative correlation was found in performance of the Barnes Maze and levels of IL-1β in the fornix in 20-month-old mice (Fig. 3 H, Table S4 C).

3.7. Cytokine levels do not correlate with brain macrostructural changes

Next, we tested whether the central accumulation of IL-12p70, TNF-α, MCP-1, IL-1β and IL-6 promote volume changes in fornix and left MEntC of aged male mice. We found no significant correlations between peripheral cytokine levels or cytokine levels in the fornix or left MEntC with volumetric brain changes (Table S5 A, B, C) (Fig. S4).

3.8. Ageing favors antagonistic changes in microglia morphology in the Fornix and left MEntC

Microglia morphology in the fornix and MEntC was evaluated. Ageing increases the total number positive Iba-1 cells in the fornix of 12- and 20-month-old male mice when compared with the 2-month-old (Fig 4 A – E, ANOVA, $F_{(2, 6)} = 2$ vs 20: $^{**}p = 0.0014$, 12 vs 20: $^{*}p = 0.0196$). Also, a significant decrease in the length of microglial processes in the fornix was found in 12- and 20-month-old mice when compared with the 2-month-old (Fig. 4 D, ANOVA, $F_{(2, 6)} = 2$ vs 12: $^{**}p = 0.0120$, 12 vs 20: $^{*}p = 0.0075$, ***2 vs 20: $p = 0.0003$). Microglia in the fornix of 12-month-old mice shows increase in the number of end points per cell when compared with the 2-and 20-month-old (Fig. 4 E, ANOVA, $F_{(2, 6)} = 2$ vs 12: $^{**}p = 0.0019$, 12 vs 20: $^{***}p = 0.0009$).

In contrast, ageing decreases the Iba-1 immunostaining (microglia marker) in the left MEntC of 2- and 12-month-old mice as well as for the 2- and 20-month-old mice (ANOVA, $F_{(2, 6)} = 2$ vs 12: $^{***}p = 0.0017$, 2 vs 20: $^{***}p = 0.0004$; respectively) (Fig. 4 F - H). Precisely, evaluation of microglia morphology in the left MEntC using ImageJ plugins AnalyzeSkeleton (2D/3D) identified significant enlargement of microglia processes in the 20-month-old mice when compared with the 2- and 12-month-old mice ($^{***}p = 0.0007$) (Fig. 4 I) and cell ramification in the 12- and 20-month-old mice when compared with the 2-month-old (ANOVA, $F_{(2, 6)} = {}^{***}p = 0.0007$) (Fig. 4 J, ANOVA, $F_{(2, 6)} = 2$ vs 12: $^{****}p < 0.0001$, 2 vs 20: $^{***}p = 0.0008$ and 12 vs 20: $^{**}p = 0.0012$). Finally, we previously reported that volume decrease in the right nucleus accumbens (NAc) core of rats correlates with lower expression of synaptophysin (Trujillo-Villarreal et al., 2021). Notably, ageing promotes significant decrease in synaptophysin immunosignal, a protein marker of the synaptic cleft, in the left MEntC of 12- and 20-month-old mice when compared with the 2-month-old (Fig 4 K, L, ANOVA, $F_{(2, 6)} = 2$ vs 12: $^{***}p = 0.0009$, 2 vs 20: $^{****}p < 0.0001$ and 12 vs 20: $^{*}p = 0.0109$).

3.9. Brain and plasma cytokine accumulation does not correlate with microglia morphology in the fornix or left MEntC

We tested whether cytokines accumulation in plasma, fornix or left MEntC correlate with morphological plasticity of microglia during ageing. We found no significant correlations between peripheral or central cytokine levels with the number of microglia, length of processes, and number of end points per cell in aged male mice in the Pearson analysis (Table S6 A, B, C) (Fig. S5).

3.10. Microglia morphology correlates with brain volume changes in fornix and left MEntC

We were interested in determining whether morphological plasticity in microglia correlates to volumetric changes in fornix and left MEntC during ageing (Table S6 A, B, C). No significant correlations between microglia morphology (microglia, EndPoint, BLength) and fornix volume in the 2- and 12-month-old male mice were found (Fig. 4 M, N, Table S7 A, B). However, in the 2-month-old mice a positive correlation in microglia branch length (BLength) (r = 0.70, $^{*}p = 0.05$) and synaptophysin expression (r = 0.67, $^{*}p = 0.008$) with volume decrease in the left MEntC was found (Fig. 4 M, Table S7 A). Furthermore, at 12-month-old we found no significant correlations between microglia morphology and fornix and MEntC volume changes (Fig. 4 N, Table S7 B). Finally, in the 20-month-old mice we found a negative correlation with microglia end-points (EndPoint) with the left MEntC volume change (r = -0.85, $^{**}p = 0.02$) and no significant correlations for fornix and microglia morphology (Fig. 4 O, Table S7 C).

Atlas of the murine Left MEntC, MEntC is shown in the red zone. **G)** Immunofluorescence for Iba-1 reactive microglia in the left MEntC during ageing. **H)** Iba-1 immunostaining for microglia was counted in 5 random fields. The graph shows the number of microglia in 150 μm^2 of 2-,12- and 20-month-old-mice. **I)** The graph shows processes length (μM) of Iba1+ microglia in the left MEntC**. J)** Iba1+ microglia endpoint per cell. **K)** Synaptophysin expression in the left MEntC from 2-,12- and 20-month-old mice. **L)** Optical density quantification for synaptophysin was carried out using Image J. **M-O)** Pearson correlation of microglia morphology in fornix and left MEntC and brain volumetric changes. **P-R)** Pearson correlation of microglia morphology in fornix and left MEntC with cognitive performance during ageing. Abbreviations: Microglia: # number of microglia, EndPoint: number of end-point per microglia, BLength: branch length, Synapto: synaptophysin, V1_MA: primary visual cortex, mononuclear area, FX: fornix, V1: primary visual cortex, S2: secondary somatosensory cortex, OB: olfactory bulb, VIIB: paramedian lobule (lobule 7), MEntC: medial entorhinal cortex, A1: primary auditory cortex, Amg: Amygdala. For behavioural tasks: 1) Barnes, Time_STM: time during short time memory, Error_STM: error during short time memory, Time_LTM: time during long time memory, Error_LTM: error during long time memory. 2) NORT: novel object recognition test, NOR_P: recognition index during the novel object recognition test, New: Time with new object during the novel object recognition test. 3) OLT: object location test, OLT_STM: object location test during the short time memory, OLT_LTM: object location test during long term memory, Old_LTM: time spent with object's old location during the long-term memory test, New_LTM: time spent with object's new location during the long-term memory test. Results are expressed as Mean ± S.E.M following by ANOVA *post-hoc* Tukey $^{n.s}$p= 0.1234, *p= 0.03, **p= 0.002, ***p= 0.0002, ****p= 0.0001. n=3/group.

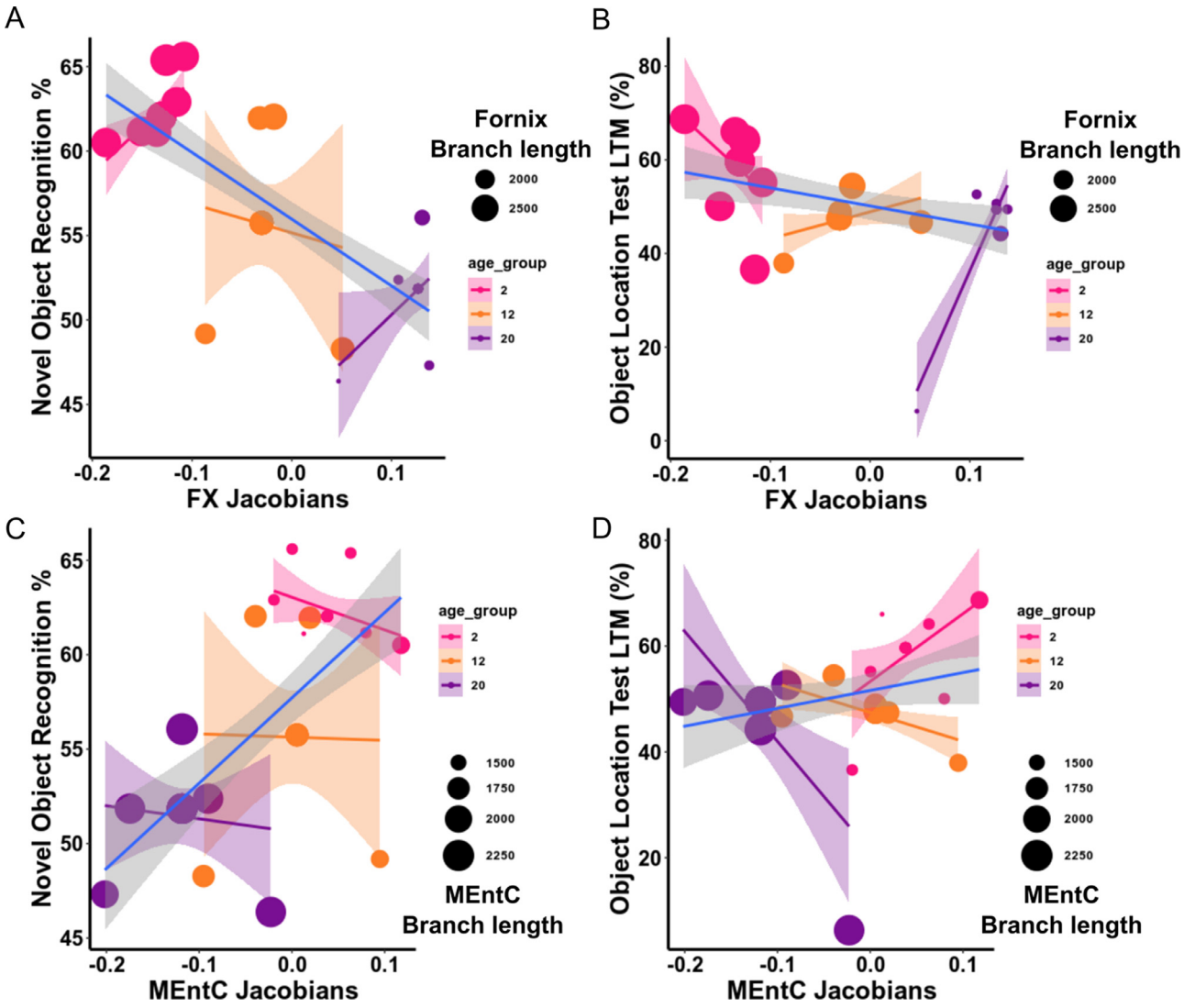

Fig. 5. Multiple linear regression of behavior (NOR_P and OLT during LTM, brain volumes (jacobians) and histology parameters (Statistical model from 2, 12 and 20-months-old male mice). A) Recognition percentage in the NORT of the three groups of age according to the volume increase in fornix and microglia branch length. **B)** Recognition percentage in the OLT during LTM of the three groups of age according to the volume increase in fornix and microglia branch length. **C)** Recognition percentage in the NORT of the three groups of age according to the volume decrease in MEntC and microglia branch length. **D)** Recognition percentage in the OLT during LTM of the three groups of age according to the volume decrease in MEntC and microglia branch length.

3.11. Microglia morphology correlates with the performance in cognitive tasks during ageing

Finally, we evaluated potential correlations of microglia morphology in the fornix or in the left MEntC with cognitive performance during ageing (Fig 4 P – R, Table S8 A, B, C). At 2-months-old we found no significant correlations between microglia morphology with none of the cognitive tasks evaluated (Fig 4 P, Table S8 A). However, by 12-months-old, we identified positive correlations between microglia branch length (BLength) in the fornix with the OLT in STM and LTM (OLT_STM, OLT_LTM) (STM: $r = 0.72$ $^{**}p = 0.005$; LTM: $r = 0.98$ $^{***}p = 5.07 \times 10^{-9}$) (Fig. 4 Q, Table S8 B), as well as a negative correlation of microglia number (Microglia) in the left MEntC with the OLT in LTM (LTM: $r = -0.93$ $^{**}p = 2.1 \times 10^{-6}$) (Fig. 4Q, Table S8 B). Finally, in the 20-month-old group a negative correlation between the number of microglia and the performance in the NORT (NOR_P) ($r = -0.81$ $^{*}p = 0.04$) and OLT LTM was identified ($r = -0.83$ $^{*}p = 0.043$) (Fig 4 R, Table S8 C).

3.12. Fornix volumetric increase and microglia morphology predicts defective novel object recognition (NORT) and object location (OLT) memory in aged male mice

A multiple linear regression model was calculated to analyze the interaction of changes in microglia morphology and volume in fornix and left MEntC predicting behavioral outcomes during ageing. We consider Error_LTM and STM during the Barnes test, NOR_P during NORT and OLT_LTM and STM during the OLT as the major interactions to perform the analysis. Notably, the multiple linear regression analysis identified significant relationships among several variables with Fornix and not in left MentC (Table S9). Our multiple regression analysis demonstrated a negative interaction between microglial branch length and fornix volume that is evident in the 20-month-old mice and significantly predicts object preference in the NORT and OLT during LTM (Figure 5 A, B) (Table S9). Conversely, our analysis demonstrated a positive interaction between microglial branch length and MEntC volume that is evident in

the 20-month-old mice and significantly predicts object preference in the NORT and OLT during LTM (Figure 5 C, D) (Table S9).

4. Discussion

In the current study, we globally characterized age-dependent brain volume alterations using MRI coupled to selective pro-inflammatory profile and microglia morphological features in selective brain regions associated with cognitive decline in male C57BL/6 mice. We identified the fornix and left MEntC as the major brain structures showing age-dependent antagonistic volumetric changes which correlated with changes in microglia morphology. Our data propose that morphological plasticity of microglia and volume increase in the fornix predicts failure in the NORT and OLT tasks in aged male mice.

Behavioral phenotyping was performed to characterize learning, memory and cognitive impairments during ageing. We confirmed an age-dependent memory impairment in the 12- and 20-month-old mice compared with the 2-month-old mice. Aged male mice showed progressive loss in spatial memory evidenced by the results of the Forced Alternation Test, and latency and number of errors during the Barnes Maze, that are consistent with previous reports (Morgan et al., 2018). Also, aged mice are not able to recognize the novel location of the object when compared with the young 2-month-old mice, confirming defective spatial memory performance. Finally, episodic-like memory is also disrupted in 12- and 20-month-old mice during the NORT paradigm. This observation was consistent with previous reports showing that the object recognition memory seemed to be impaired as early as the age of 12 months (Belblidia et al., 2018; Li et al., 2020).

Our first major contribution in this proposal is the identification of volume increase in fornix during ageing in male mice. We used MRI analysis to globally characterize structural brain alterations during ageing as a contributor to cognitive impairment. Previous reports documented that structural brain alteration contributes to cognitive decline during ageing (Faizy et al., 2020; Filo et al., 2019; Matsuda, 2013). Here, we reported that aged mice show the highest volume increase in the fornix and the greatest decrease in the left MEntC. We also identified a dramatic loss of brain volume in the left olfactory bulb, the right paramedian lobule, the right primary auditory cortex and the right amygdala in aged male mice. Volumetric changes in the fornix during ageing seem to be controversial because some reports have found it decreased during ageing (Fletcher et al., 2014, 2013). Volumetric declines have also been reported in occipital grey matter, hippocampus, middle occipital gyrus, occipital pole, and thalamus (Armstrong et al., 2020). In contrast, our results demonstrated that ageing favors an increase in the left primary visual cortex and the left secondary somatosensory cortex. Notably, reduction in hippocampal volume was reported as an early determinant for memory decline (Armstrong et al., 2020; Mungas et al., 2005) and our findings also confirm a reduction in the hippocampal volume in aged mice, however it did not survive the FDR 5% correction. Based on correlations found in our study between volume brain changes in the fornix and left MEntC with the behavioral tasks such as the Barnes Maze, OLT and NORT, we propose that antagonistic volumetric brain changes in the fornix and the left MEntC during ageing contribute to memory and cognitive decline in mice.

Our experiments suggested that peripheral circulatory cytokines might potentially and selectively infiltrate brain regions during ageing, assisting cognitive decline. We identified that behavior, brain volumetric changes and inflammation variables clustered into the three groups of age using the PCA analysis. Following this, we tested the hypothesis that neuroinflammation might modulate volumetric brain changes in the fornix and the left MEntC in aged mice. Ageing integrates a low-grade chronic pro-inflammatory state, called inflammageing (FRANCESCHI et al., 2000) which significantly contributes to cognitive decline (Berryer et al., 2016; D'Avila et al., 2018; Feng et al., 2017; López-Otín et al., 2013; Yin et al., 2019). Our results confirmed an age-dependent pro-inflammatory cytokine profile in plasma, with increased levels of IL12p70, TNF-α, IL-1β, MCP-1 and IL-6, which are consistent with previous reports (Brombacher et al., 2017; Dubenko et al., 2021; Fossati et al., 2017; Pennisi et al., 2017; Tarkowski et al., 2001). In fact, according to the Pearson correlation analysis the IL-1β accumulation in the fornix disrupts the performance of the Barnes Maze during the STM and LTM tests. To our knowledge no evidence has been reported to propose that IL-1β accumulation in the fornix could be associated to memory impairment.

Since we did not find any significant correlation between neuroinflammation and brain volume changes we tested a second proposal. According to our previous report, a decrease in synaptophysin expression in the right NAc core could be a potential contributor to brain volume changes in rats (Trujillo-Villarreal et al., 2021). In fact, plasma from old mice is able to decrease synaptic plasticity and impair spatial learning and memory (Villeda et al., 2011). In the current study, we identified a decreased in synaptophysin expression in the left MEntC which also shows a volume decrease in aged mice, supporting that lower brain volume integrates synaptic disruption. Despite all the results, the Pearson analysis does not show significant correlations between cytokines levels in plasma, fornix or left MEntC with volume decrease in left MEntC and increase in the fornix. Also, no significant correlations between synaptophysin expression in the left MEntC with volume decrease in left MEntC were found. Therefore, we cannot conclude that neuroinflammation is associated with volume changes in the fornix or MEntC.

A second major contribution of our study is that selective microglia plasticity in the fornix and left MEntC contribute to cognitive decline during ageing. Microglia activation has been suggested as a second potential contributor to neuroinflammation during ageing (Shahidehpour et al., 2021). We found that ageing leads to a decrease in the number of microglia, an increase in branch length, and and in ramified morphology in the left MEntC. Conversely, an increase in the number of microglia, a decrease in branch length and in ramified morphology were found in the fornix of aged male mice. Microglia in the left MEntC seems to imitate a "surveillance state" typified by a highly ramified morphology, with extended processes capable of forming contacts with cells and structures (Davalos et al., 2005), and enabling a continuous monitoring of the brain microenvironment. In contrast, microglia in the fornix seems to recapitulate the disease-associated microglia (DAM) phenotype found during ageing (Davies et al., 2017), showing short processes, and amoeboid morphology that also integrates downregulation of various homeostatic genes (Keren-Shaul et al., 2017). However, this evidence from microglia morphology does not confirm cytokine release. Also, dystrophic microglia found in the fornix of aged mice have been observed in healthy but aged brains (Miller and Streit, 2007), and they have also been associated with neurodegenerative disease (Shahidehpour et al., 2021). This proposal agrees with previous reports demonstrating that ageing was associated with apparent glia plasticity but not neurite density damage in the fornix (Metzler-Baddeley et al., 2019). It remains to be clarified whether the dystrophic microglia identified in our study, recapitulates senescent microglia associated with cytokine release and neuroinflammation which become the disease-associated phenotype found in ageing.

We performed a multiple linear regression analysis to integrate the effect of microglia morphological plasticity on volumetric changes in fornix and their association to behavioral outcomes during ageing. Biological modeling identified that a decrease in the NORT and OLT index is associated with fornix size and microglia branch length in fornix of aged male mice. The fornix connects the hippocampus, the thalamus, the hypothalamus, the septal nuclei and the nucleus accumbens. By itself, the fornix is the major output of the hippocampus and its stimulation improves spatial memory (Hescham et al., 2017). In accordance with our data, afflictions in the fornix, such as volumetric changes affect selective hippocampal dependent processes such as NORT and OLT (Broadbent et al., 2010). On the other hand, we identified a decrease in the volume of the left MEntC. Physiologically, the MEntC also regulates memory and learning (Bangen et al., 2021; Matuskova et al., 2021),

however, our biological model did not demonstrate its association with the performance of NORT and OLT performance in aged male mice.

A potential limitation of our study is to confirm a cause-effect response of microglia branch length in the volumetric changes of fornix affecting the cognitive performance. Additional experiments are required to demonstrate that specific microglia morphological changes in accessory brain regions connecting to the fornix which might disrupt cognitive performance during ageing. Finally, the sexual dimorphism regarding brain volume, cytokine levels and behavioral performance in female mice must be characterized.

Conclusions

Our findings identified global volumetric and cellular brain changes emerging during physiological ageing. We highlight an age-dependent microglia morphological plasticity modulating volume increase in fornix which are associated with failure in the NORT and OLT in aged male mice. Peripheral and central factors assisting cognitive decline in murine models of physiological ageing offer the opportunity to dissect major molecular pathways for efficient therapeutic or preventive personalized treatments. We conceive that our experimental findings add scientific evidence supporting micro and macrostructural brain disruptions which might provide a rationale for the etiology of cognitive impairment during ageing.

Data and code availability statement

https://doi.org/10.5281/zenodo.5329351

This doi link contains the files of the preprocessed structural T1 resonances and the relative volumes of each subject

https://github.com/LuisTrujillo11/Aging.git

This link contains the code in created in Rstudio used for the general lineal model of Deformation Based Morphometry. It also contains the database in an Excel file where the behavior, weight and group data of each subject can be found. It also contains Atlas DSUR 2016, mask and tmap.

Declaration of Competing Interest

The authors declare no conflict of interests.

Credit authorship contribution statement

Marcela Cárdenas-Tueme: Investigation, Formal analysis, Methodology, Writing – original draft. **Luis Ángel Trujillo-Villarreal:** Investigation, Formal analysis, Methodology, Writing – original draft. **Victor Ramírez-Amaya:** Formal analysis, Resources, Supervision, Writing – review & editing. **Eduardo A. Garza-Villarreal:** Funding acquisition, Formal analysis, Resources, Software, Supervision, Writing – review & editing. **Alberto Camacho-Morales:** Conceptualization, Funding acquisition, Formal analysis, Project administration, Resources, Supervision, Writing – original draft, Writing – review & editing. **Diana Reséndez-Pérez:** Conceptualization, Funding acquisition, Formal analysis, Project administration, Resources, Supervision, Writing – review & editing.

Acknowledgments

This research was enabled in part by support provided by M. Mallar Chakravarty and Gabriel A. Devenyi at the Computational Brain Anatomy Lab (CoBrA Lab) (http://cobralab.ca), CIC, Douglas Research Centre, Montreal and Compute Canada (www.computecanada.ca). Also, we thank to M.C. Juan José Ortíz Retana and Dr. Luis Concha from for the Laboratorio Nacional de Imagenología por Resonancia Magnética, UNAM, México. This work was supported by the National Council of Science and Technology in Mexico (CONACYT, Grant number: 255317), 650620 CONACYT for M. Cárdenas-Tueme and 781759 CONACYT for L.A. Trujillo-Villarreal. We also would like to thank M.Sc. Alejandra Arreola-Triana for her support in editing this manuscript. This research was funded by: This Grant: PAPIIT-IA202120 for E.A. Garza-Villarreal. Grant: PAICYT: CN1184-20 for D. Reséndez-Pérez. Grant: IBRO-LARC for A. Camacho-Morales. This study received support from Luis Aguilar of the Laboratorio Nacional de Visualización Científica Avanzada (LAVIS). To my dad CCB (1953-2021) with all my love and dedication. I will forever love and miss you.

Supplementary materials

Supplementary material associated with this article can be found, in the online version, at doi:10.1016/j.neuroimage.2022.119039.

References

Alexander, G.E., Chen, K., Merkley, T.L., Reiman, E.M., Caselli, R.J., Aschenbrenner, M., Santerre-Lemmon, L., Lewis, D.J., Pietrini, P., Teipel, S.J., Hampel, H., Rapoport, S.I., Moeller, J.R., 2006. Regional network of magnetic resonance imageing gray matter volume in healthy ageing. Neuroreport 17. doi:10.1097/01.wnr.0000220135.16844.b6.

Antunes, M., Biala, G., 2012. The novel object recognition memory: neurobiology, test procedure, and its modifications. Cogn. Process. doi:10.1007/s10339-011-0430-z.

Armstrong, N.M., An, Y., Shin, J.J., Williams, O.A., Doshi, J., Erus, G., Davatzikos, C., Ferrucci, L., Beason-Held, L.L., Resnick, S.M., 2020. Associations between cognitive and brain volume changes in cognitively normal older adults. Neuroimage 223. doi:10.1016/j.neuroimage.2020.117289.

Bachstetter, A.D., Ighodaro, E.T., Hassoun, Y., Aldeiri, D., Neltner, J.H., Patel, E., Abner, E.L., Nelson, P.T., 2017. Rod-shaped microglia morphology is associated with ageing in 2 human autopsy series. Neurobiol. Ageing 52, 98–105. doi:10.1016/j.neurobiolageing.2016.12.028.

Bangen, K.J., Thomas, K.R., Sanchez, D.L., Edmonds, E.C., Weigand, A.J., Delano-Wood, L., Bondi, M.W., 2021. Entorhinal perfusion predicts future memory decline, neurodegeneration, and white matter hyperintensity progression in older adults. J. Alzheimer's Dis. 81. doi:10.3233/JAD-201474.

Batterman, K.V., Cabrera, P.E., Moore, T.L., Rosene, D.L., 2021. T cells actively infiltrate the white matter of the ageing monkey brain in relation to increased microglial reactivity and cognitive decline. Front. Immunol. 12. doi:10.3389/fimmu.2021.607691.

Belblidia, H., Leger, M., Abdelmalek, A., Quiedeville, A., Calocer, F., Boulouard, M., Jozet-Alves, C., Freret, T., Schumann-Bard, P., 2018. Characterizing age-related decline of recognition memory and brain activation profile in mice. Exp. Gerontol. 106. doi:10.1016/j.exger.2018.03.006.

Berryer, M.H., Chattopadhyaya, B., Xing, P., Riebe, I., Bosoi, C., Sanon, N., Avoli, M., Hamdan, F.F., Carmant, L., Antoine-bertrand, J., Le, M., Lamarche-vane, N., Lacaille, J., Michaud, J.L., Cristo, G.Di, 2016. The ageing systemic milieu negatively regulates neurogenesis and cognitive function. Nature 477, 90–94. doi:10.1038/nature10357.The.

Brombacher, T.M., Nono, J.K., De Gouveia, K.S., Makena, N., Darby, M., Womersley, J., Tamgue, O., Brombacher, F., 2017. IL-13–mediated regulation of learning and memory. J. Immunol. 198, 2681–2688. doi:10.4049/jimmunol.1601546.

Currais, A., 2015. Ageing and inflammation - A central role for mitochondria in brain health and disease. Ageing Res. Rev. 21, 30–42. doi:10.1016/j.arr.2015.02.001.

D'Avila, J.C., Siqueira, L.D., Mazeraud, A., Azevedo, E.P., Foguel, D., Castro-Faria-Neto, H.C., Sharshar, T., Chrétien, F., Bozza, F.A., 2018. Age-related cognitive impairment is associated with long-term neuroinflammation and oxidative stress in a mouse model of episodic systemic inflammation. J. Neuroinflamm. 15. doi:10.1186/s12974-018-1059-y.

Davalos, D., Grutzendler, J., Yang, G., Kim, J.V., Zuo, Y., Jung, S., Littman, D.R., Dustin, M.L., Gan, W.B., 2005. ATP mediates rapid microglial response to local brain injury in vivo. Nat. Neurosci. 8, 752–758. doi:10.1038/nn1472.

Davies, D.S., Ma, J., Jegathees, T., Goldsbury, C., 2017. Microglia show altered morphology and reduced arborization in human brain during ageing and Alzheimer's disease. Brain Pathol 27. doi:10.1111/bpa.12456.

Dubenko, O.E., Chyniak, O.S., Potapov, O.O., 2021. Levels of proinflammatory cytokines IL-17 and IL-23 in patients with alzheimer's disease, mild cognitive impairment and vascular dementia. Wiadomości Lek 74, 68–71. doi:10.36740/wlek202101113.

Faizy, T.D., Thaler, C., Broocks, G., Flottmann, F., Leischner, H., Kniep, H., Nawabi, J., Schön, G., Stellmann, J.P., Kemmling, A., Reddy, R., Heit, J.J., Fiehler, J., Kumar, D., Hanning, U., 2020. The myelin water fraction serves as a marker for age-related myelin alterations in the cerebral white matter – a multiparametric MRI ageing study. Front. Neurosci. 14. doi:10.3389/fnins.2020.00136.

Feng, X., Valdearcos, M., Uchida, Y., Lutrin, D., Maze, M., Koliwad, S.K., 2017. Microglia mediate postoperative hippocampal inflammation and cognitive decline in mice. JCI insight 2. doi:10.1172/jci.insight.91229.

Fillmore, P.T., Phillips-meek, M.C., Richards, J.E., 2015. Age-specific MRI brain and head templates for healthy adults from 20 through 89 years of age. Kaye, J., 7, 1–14. doi:10.3389/fnagi.2015.00044.

Filo, S., Shtangel, O., Salamon, N., Kol, A., Weisinger, B., Shifman, S., Mezer, A.A., 2019. Disentangling molecular alterations from water-content changes in the ageing human brain using quantitative MRI. Nat. Commun. 10. doi:10.1038/s41467-019-11319-1.

Fletcher, E., Carmichael, O., Pasternak, O., Maier-Hein, K.H., DeCarli, C., 2014. Early brain loss in circuits affected by Alzheimer's disease is predicted by fornix microstructure but may be independent of gray matter. Front. Ageing Neurosci. 6. doi:10.3389/fnagi.2014.00106.

Fletcher, E., Raman, M., Huebner, P., Liu, A., Mungas, D., Carmichael, O., DeCarli, C., 2013. Loss of fornix white matter volume as a predictor of cognitive impairment in cognitively normal elderly individuals. JAMA Neurol 70. doi:10.1001/jamaneurol.2013.3263.

Fossati, S., Cejudo, J.R., Debure, L., Pirraglia, E., Glodzik, L., Osorio, R.S., Chen, J., Provost, A., Jeromin, A., Haas, M., Marmar, C., DeLeon, M., 2017. Differential value of plasma tau as a biomarker for alzheimer's disease and chronic traumatic brain injury. Alzheimer's Dement 13, P1307. doi:10.1016/j.jalz.2017.06.1999, –P1307.

Fotenos, A.F., Snyder, A.Z., Girton, L.E., Morris, J.C., Buckner, R.L., 2005. Normative estimates of cross-sectional and longitudinal brain volume decline in ageing and AD. Neurology 64, 1032–1039. doi:10.1212/01.WNL.0000154530.72969.11.

FRANCESCHI, C., BONAFÈ, M., VALENSIN, S., OLIVIERI, F., DE LUCA, M., OTTAVIANI, E., DE BENEDICTIS, G., 2000. Inflamm-ageing: an evolutionary perspective on immunosenescence. Ann. N. Y. Acad. Sci. 908, 244–254. doi:10.1111/j.1749-6632.2000.tb06651.x.

Frank, M.G., Barrientos, R.M., Biedenkapp, J.C., Rudy, J.W., Watkins, L.R., Maier, S.F., 2006. mRNA up-regulation of MHC II and pivotal pro-inflammatory genes in normal brain ageing. Neurobiol. Ageing 27. doi:10.1016/j.neurobiolageing.2005.03.013.

Friedel, M., van Eede, M.C., Pipitone, J., Mallar Chakravarty, M., Lerch, J.P., 2014. Pydpiper: A flexible toolkit for constructing novel registration pipelines. Front. Neuroinform. 8. doi:10.3389/fninf.2014.00067.

Fulop, T., Larbi, A., Dupuis, G., Page, A.Le, Frost, E.H., Cohen, A.A., Witkowski, J.M., Franceschi, C., 2018. Immunosenescence and inflamm-ageing as two sides of the same coin: friends or foes? Front. Immunol. doi:10.3389/fimmu.2017.01960.

Fung, I.T.H., Sankar, P., Zhang, Y., Robison, L.S., Zhao, X., D'Souza, S.S., Salinero, A.E., Yue, W., Qian, J., Kuentzel, M.L., Chittur, S.V., Temple, S., Zuloaga, K.L., Yang, Q., 2020. Activation of group 2 innate lymphoid cells alleviates ageing-associated cognitive decline. J. Exp. Med. 217. doi:10.1084/jem.20190915.

Good, C.D., Johnsrude, I.S., Ashburner, J., Henson, R.N., Friston, K.J., Frackowiak, R.S., 2001. A voxel-based morphometric study of ageing in 465 normal adult human brains. Neuroimage 14, 21–36. doi:10.1006/nimg.2001.0786.

Grieve, S.M., Clark, C.R., Williams, L.M., Peduto, A.J., Gordon, E., 2005. Preservation of limbic and paralimbic structures in ageing. Hum. Brain Mapp 25. doi:10.1002/hbm.20115.

Hescham, S., Temel, Y., Schipper, S., Lagiere, M., Schönfeld, L.M., Blokland, A., Jahanshahi, A., 2017. Fornix deep brain stimulation induced long-term spatial memory independent of hippocampal neurogenesis. Brain Struct. Funct. 222. doi:10.1007/s00429-016-1188-y.

Jeon, H., Mun, G.I., Boo, Y.C., 2012. Analysis of serum cytokine/chemokine profiles affected by ageing and exercise in mice. Cytokine 60. doi:10.1016/j.cyto.2012.07.014.

Jernigan, T.L., Archibald, S.L., Fennema-Notestine, C., Gamst, A.C., Stout, J.C., Bonner, J., Hesselink, J.R., 2001. Effects of age on tissues and regions of the cerebrum and cerebellum. Neurobiol. Ageing 22. doi:10.1016/S0197-4580(01)00217-2.

Kalpouzos, G., Chételat, G., Baron, J.C., Landeau, B., Mevel, K., Godeau, C., Barré, L., Constans, J.M., Viader, F., Eustache, F., Desgranges, B., 2009. Voxel-based mapping of brain gray matter volume and glucose metabolism profiles in normal ageing. Neurobiol. Ageing 30. doi:10.1016/j.neurobiolageing.2007.05.019.

Keren-Shaul, H., Spinrad, A., Weiner, A., Matcovitch-Natan, O., Dvir-Szternfeld, R., Ulland, T.K., David, E., Baruch, K., Lara-Astaiso, D., Toth, B., Itzkovitz, S., Colonna, M., Schwartz, M., Amit, I., 2017. A unique microglia type associated with restricting development of Alzheimer's disease. Cell 169, 1276–1290. doi:10.1016/j.cell.2017.05.018, e17.

Li, M., Su, S., Cai, W., Cao, J., Miao, X., Zang, W., Gao, S., Xu, Y., Yang, J., Tao, Y.X., Ai, Y., 2020. Differentially expressed genes in the brain of ageing mice with cognitive alteration and depression- and anxiety-like behaviors. Front. Cell Dev. Biol. 8. doi:10.3389/fcell.2020.00814.

López-Otín, C., Blasco, M.A., Partridge, L., Serrano, M., Kroemer, G., 2013. The hallmarks of ageing. Cell 153. doi:10.1016/j.cell.2013.05.039.

Maldonado-Ruiz, R., Cárdenas-Tueme, M., Montalvo-Martínez, L., Vidaltamayo, R., Garza-Ocañas, L., Reséndez-Perez, D., Camacho, A., 2019. Priming of hypothalamic ghrelin signaling and microglia activation exacerbate feeding in rats' offspring following maternal overnutrition. Nutrients 11. doi:10.3390/nu11061241.

Matsuda, H., 2013. Voxel-based morphometry of brain MRI in normal ageing and Alzheimer's disease. Ageing Dis 4, 29–37.

Matuskova, V., Ismail, Z., Nikolai, T., Markova, H., Cechova, K., Nedelska, Z., Laczo, J., Wang, M., Hort, J., Vyhnalek, M., 2021. Mild behavioral impairment is associated with atrophy of entorhinal cortex and hippocampus in a memory clinic cohort. Front. Ageing Neurosci. 13. doi:10.3389/fnagi.2021.643271.

Metzler-Baddeley, C., Mole, J.P., Sims, R., Fasano, F., Evans, J., Jones, D.K., Aggleton, J.P., Baddeley, R.J., 2019. Fornix white matter glia damage causes hippocampal gray matter damage during age-dependent limbic decline. Sci. Rep. 9, 15164. doi:10.1038/s41598-019-51737-1.

Miller, K.R., Streit, W.J., 2007. The effects of ageing, injury and disease on microglial function: a case for cellular senescence. Neuron Glia Biology doi:10.1017/S1740925X08000136.

Morgan, J.A., Singhal, G., Corrigan, F., Jaehne, E.J., Jawahar, M.C., Baune, B.T., 2018. The effects of aerobic exercise on depression-like, anxiety-like, and cognition-like behaviours over the healthy adult lifespan of C57BL/6 mice. Behav. Brain Res. 337. doi:10.1016/j.bbr.2017.09.022.

Mungas, D., Harvey, D., Reed, B.R., Jagust, W.J., DeCarli, C., Beckett, L., Mack, W.J., Kramer, J.H., Weiner, M.W., Schuff, N., Chui, H.C., 2005. Longitudinal volumetric MRI change and rate of cognitive decline. Neurology 65. doi:10.1212/01.wnl.0000172913.88973.0d.

Pennisi, M., Crupi, R., Di Paola, R., Ontario, M.L., Bella, R., Calabrese, E.J., Crea, R., Cuzzocrea, S., Calabrese, V., 2017. Inflammasomes, hormesis, and antioxidants in neuroinflammation: role of NRLP3 in Alzheimer disease. J. Neurosci. Res. doi:10.1002/jnr.23986.

Resnick, S.M., Pham, D.L., Kraut, M.A., Zonderman, A.B., Davatzikos, C., 2003. Longitudinal magnetic resonance imageing studies of older adults: A shrinking brain. J. Neurosci. 23. doi:10.1523/jneurosci.23-08-03295.2003.

Rstudio, T., 2020. RStudio: Integrated Development for R. Rstudio Team, PBC, Boston, MA URL http://www.rstudio.com/ doi:10.1145/3132847.3132886.

Shahidehpour, R.K., Higdon, R.E., Crawford, N.G., Neltner, J.H., Ighodaro, E.T., Patel, E., Price, D., Nelson, P.T., Bachstetter, A.D., 2021. Dystrophic microglia are associated with neurodegenerative disease and not healthy ageing in the human brain. Neurobiol. Ageing 99, 19–27. doi:10.1016/j.neurobiolageing.2020.12.003.

Sheng, J.G., Mrak, R.E., Griffin, W.S.T., 1998. Enlarged and phagocytic, but not primed, interleukin-1α-immunoreactive microglia increase with age in normal human brain. Acta Neuropathol 95. doi:10.1007/s004010050792.

Sowell, E.R., Thompson, P.M., Toga, A.W., 2004. Mapping changes in the human cortex throughout the span of life. Neuroscientist doi:10.1177/1073858404263960.

Taki, Y., Goto, R., Evans, A., Zijdenbos, A., Neelin, P., Lerch, J., Sato, K., Ono, S., Kinomura, S., Nakagawa, M., Sugiura, M., Watanabe, J., Kawashima, R., Fukuda, H., 2004. Voxel-based morphometry of human brain with age and cerebrovascular risk factors. Neurobiol. Ageing 25, 455–463. doi:10.1016/j.neurobiolageing.2003.09.002.

Tarkowski, E., Wallin, A., Regland, B., Blennow, K., Tarkowski, A., 2001. Local and systemic GM-CSF increase in Alzheimer's disease and vascular dementia. Acta Neurol. Scand. 103, 166–174. doi:10.1034/j.1600-0404.2001.103003166.x.

Tisserand, D.J., Pruessner, J.C., Sanz Arigita, E.J., Van Boxtel, M.P.J., Evans, A.C., Jolles, J., Uylings, H.B.M., 2002. Regional frontal cortical volumes decrease differentially in ageing: An MRI study to compare volumetric approaches and voxel-based morphometry. Neuroimage 17. doi:10.1016/S1053-8119(02)91173-0.

Trujillo-Villarreal, L.A., Romero-Díaz, V.J., Marino-Martínez, I.A., Fuentes-Mera, L., Ponce-Camacho, M.A., Devenyi, G.A., Mallar Chakravarty, M., Camacho-Morales, A., Garza-Villarreal, E.E., 2021. Maternal cafeteria diet exposure primes depression-like behavior in the offspring evoking lower brain volume related to changes in synaptic terminals and gliosis. Transl. Psychiatry 11. doi:10.1038/s41398-020-01157-x.

Villeda, S.A., Luo, J., Mosher, K.I., Zou, B., Britschgi, M., Bieri, G., Stan, T.M., Fainberg, N., Ding, Z., Eggel, A., Lucin, K.M., Czirr, E., Park, J.S., Couillard-Després, S., Aigner, L., Li, G., Peskind, E.R., Kaye, J.A., Quinn, J.F., Galasko, D.R., Xie, X.S., Rando, T.A., Wyss-Coray, T., 2011. The ageing systemic milieu negatively regulates neurogenesis and cognitive function. Nature 477, 90–96. doi:10.1038/nature10357.

Wolfe, H., Minogue, A.M., Rooney, S., Lynch, M.A., 2018. Infiltrating macrophages contribute to age-related neuroinflammation in C57/BL6 mice. Mech. Ageing Dev. 173, 84–91. doi:10.1016/j.mad.2018.05.003.

Wu, M.J., Gao, Y.L., Liu, J.X., Zhu, R., Wang, J., 2019. Principal component analysis based on graph laplacian and double sparse constraints for feature selection and sample clustering on multi-view data. Hum. Hered. 84. doi:10.1159/000501653.

Wyss-Coray, T., 2016. Ageing, neurodegeneration and brain rejuvenation. Nature 539, 180–186. doi:10.1038/nature20411.

Yin, P., Wang, X., Wang, S., Wei, Y., Feng, J., Zhu, M., 2019. Maresin 1 improves cognitive decline and ameliorates inflammation in a mouse model of Alzheimer's disease. Front. Cell. Neurosci. 13. doi:10.3389/fncel.2019.00466.

Young, K., Morrison, H., 2018. Quantifying microglia morphology from photomicrographs of immunohistochemistry prepared tissue using imagej. J. Vis. Exp. doi:10.3791/57648, 2018.

Zhou, L., Flores, J., Noël, A., Beauchet, O., Sjöström, P.J., Leblanc, A.C., 2019. Methylene blue inhibits Caspase-6 activity, and reverses Caspase-6-induced cognitive impairment and neuroinflammation in aged mice. Acta Neuropathol. Commun. 7. doi:10.1186/s40478-019-0856-6.

Received: 31 May 2020 | Revised: 12 July 2020 | Accepted: 27 July 2020

DOI: 10.1111/jnc.15141

REVIEW

Journal of Neurochemistry JNC The Official Journal of the International Society for Neurochemistry WILEY

Potential role of primed microglia during obesity on the mesocorticolimbic circuit in autism spectrum disorder

Luis A- Trujillo Villarreal[1,2] | Marcela Cárdenas-Tueme[3] | Roger Maldonado-Ruiz[1,2] | Diana Reséndez-Pérez[3] | Alberto Camacho-Morales[1,2]

[1]Departamento de Bioquímica, Facultad de Medicina, Universidad Autónoma de Nuevo León, San Nicolas de los Garza, México

[2]Unidad de Neurometabolismo, Centro de Investigación y Desarrollo en Ciencias de la Salud, Universidad Autónoma de Nuevo León, San Nicolas de los Garza, México

[3]Departamento de Biología Celular y Genética, Facultad de Ciencias Biológicas, Universidad Autónoma de Nuevo León, San Nicolas de los Garza, México

Correspondence
Alberto Camacho-Morales, Departamento de Bioquímica, Facultad de Medicina, Universidad Autónoma de Nuevo León, Francisco I. Madero y Dr. Aguirre Pequeño. Col. Mitras Centro, S/N. Monterrey, San Nicolas de los Garza, N.L. C.P. 64460, México.
Email: acm590@hotmail.com; alberto.camachomr@uanl.edu.mx

Funding information
National Council of Science and Technology in Mexico (CONACYT), Grant/Award Number: 781759, 573686 and 650620; IBRO-PROLAB

Abstract

Autism spectrum disorder (ASD) is a complex neurodevelopmental disease which involves functional and structural defects in selective central nervous system (CNS) regions that harm function and individual ability to process and respond to external stimuli. Individuals with ASD spend less time engaging in social interaction compared to non-affected subjects. Studies employing structural and functional magnetic resonance imaging reported morphological and functional abnormalities in the connectivity of the mesocorticolimbic reward pathway between the nucleus accumbens and the ventral tegmental area (VTA) in response to social stimuli, as well as diminished medial prefrontal cortex in response to visual cues, whereas stronger reward system responses for the non-social realm (e.g., video games) than social rewards (e.g., approval), associated with caudate nucleus responsiveness in ASD children. Defects in the mesocorticolimbic reward pathway have been modulated in transgenic murine models using D2 dopamine receptor heterozygous (D2+/−) or dopamine transporter knockout mice, which exhibit sociability deficits and repetitive behaviors observed in ASD phenotypes. Notably, the mesocorticolimbic reward pathway is modulated by systemic and central inflammation, such as primed microglia, which occurs during obesity or maternal overnutrition. Therefore, we propose that a positive energy balance during obesity/maternal overnutrition coordinates a systemic and central inflammatory crosstalk that modulates the dopaminergic neurotransmission in selective brain areas of the mesocorticolimbic reward pathway. Here, we will describe how obesity/maternal overnutrition may prime microglia, causing abnormalities in dopamine neurotransmission of the mesocorticolimbic reward pathway, postulating a possible immune role in the development of ASD.

KEYWORDS

autism, maternal programming, microglial priming, neuroimaging, obesity

Abbreviations: ACC, anterior cingulate cortex; Amy, amygdala; ASD, autism spectrum disorder; CNS, central nervous system; D1DR, dopamine receptor 1; D2DR, dopamine receptor 2; DAT, dopamine transporter; DS, dorsal striatum; HIP, hippocampus; MIA, maternal immune activation; mPFC, medial prefrontal cortex; NAc, nucleus accumbens; OFC, orbitofrontal cortex; PFC, prefrontal cortex; TLR4, Toll-like receptor 4.

1 | INTRODUCTION

Autism spectrum disorder (ASD) is a neurodevelopmental disease that impairs the function of the central nervous system (CNS) and efficient responses to sensory external stimuli (American Psychiatric Association, 2000). Since 2012, ASD prevalence has increased from 1 in 150 to 1 in 68 cases per births. Boys are notably the most affected, showing 23.6 cases per 1,000 births, whereas the prevalence in girls is 5.3 cases per 1,000 births (Christensen et al., 2016). Despite technological, scientific, and epidemiological advances, etiological causes of ASD have not been precisely clarified, suggesting that environmental, genetic, epigenetic, immune, and metabolic related-nutritional factors might modulate ASD susceptibility (Tremblay & Jiang, 2019).

ASD appearance shows functional and structural defects in selective CNS regions, such as the prefrontal cortex (PFC), the amygdala (Amy), the hippocampus (HIP), and the cerebellum. Individuals with ASD spend less time engaged in social interaction compared to non-ASD subjects, a behavioral criteria reproduced in both humans and animal models (Maldonado-Ruiz, Garza-Ocañas, & Camacho, 2019). Of note, children diagnosed with ASD do not attribute enough value to potential social interactions and prefer other environmental stimuli which seems to them more highly valued (Kishida et al., 2019), suggesting defects in the mesocorticolimbic reward system. Functional integration of the mesocorticolimbic reward system actively develops by dopaminergic innervations which arise from the ventral tegmental area (VTA) to the ventral striatum, including both the nucleus accumbens (NAc) and the olfactory tubercle, and to the PFC. On its own, dopaminergic tone to target brain areas is finely modulated by transmembrane-coupled related dopamine transporter (DAT). Studies employing imaging and functional magnetic resonance imaging of ASD subjects report structural and functional connectivity abnormalities of the mesocorticolimbic reward pathway between the VTA and the NAc (Supekar et al., 2018), as well as diminished ventro mPFC response to visual cues to valued social interaction (Kishida et al., 2019). Also, ASD adolescents display stronger responses for the non-social realm in the caudate nucleus (e.g., video games) than for social rewards (e.g., approval; Kohls, Antezana, Mosner, Schultz, & Yerys, 2018). This evidence strongly suggests a causal relationship between the mesocorticolimbic reward system and ASD-related behaviors such as social avoidance.

Immunity has recently been proposed as a potential molecular pathway modulating ASD susceptibility. Initial epidemiological reports identified an increased rate of children born with ASD from mothers exposed to infection during pregnancy (Atladottir, Henriksen, Schendel, & Parner, 2012; Atladóttir et al., 2010). For instance, high levels of pro-inflammatory cytokines in the amniotic fluid, placenta, and mesocorticolimbic reward-related regions were found in both mothers and children with ASD (Abdallah et al., 2013; Li et al., 2009; Vargas, Nascimbene, Krishnan, Zimmerman, & Pardo, 2005). In the pathogenic scenario known as maternal programming, systemic immune activation in pregnant women with autoimmune disease primes neurodevelopmental changes in the fetus, showing increased risk of attention-deficit/hyperactivity disorders in children (Nielsen, Benros, & Dalsgaard, 2017). Mechanistically, cytokines closely interact and coordinate proper CNS development and ASD susceptibility by modulating microglia and neuronal plasticity (Maldonado-Ruiz, Garza-Ocañas, et al., 2019), potentially controlling brain structure and connectome establishment. Of note, pharmacological activation of inflammatory immune response by lipopolysaccharides disrupts dopaminergic signaling (D3DR; Wang et al., 2018), favoring TNF-α, IL-1β, and IL-6 accumulation and microglial activation in mesocorticolimbic regions of murine models (Wang et al., 2019). Genetic ablation of the D2DR correlates with sociability deficits and repetitive behavior during adulthood after early life stress (DiCarlo et al., 2019; Lee & Han, 2019). These lines of evidence support the notion that a pro-inflammatory profile and microglial activation might negatively regulate the mesocorticolimbic reward pathway priming ASD traits.

Finally, epidemiologic studies have identified that children born from obese mothers show an increased risk of ASD (Edlow, 2018). Obesity itself integrates a state of chronic low-level immune activation (Gregor & Hotamisligil, 2011) and pregnancy is associated with increased levels of certain pro-inflammatory cytokines (Christian & Porter, 2014), suggesting a potential immune activation in pregnant obese mothers. Here, we propose that obesity/maternal overnutrition coordinates a systemic and central inflammatory crosstalk that modulates the dopaminergic neurotransmission in selective brain areas of the mesocorticolimbic circuit. We will add experimental data corroborating the potential interplay between obesity/maternal overnutrition and microglial activation on morphological and functional brain abnormalities. We will focus on the dopamine neurotransmission of the mesocorticolimbic reward pathway to propose potential immune routes of ASD occurrence primed by obesity during pregnancy.

2 | ROLE OF THE MESOCORTICOLIMBIC REWARD PATHWAY ON DEFECTIVE SOCIAL BEHAVIOR IN ASD

Social interaction helps humans to constantly adapt to environmental and social demands. Humans and animals have a strong motivation to seek and permanently stablish social ties, and the mutual support offered by these relationships helps us face difficulties, care for the needs of others and preserve our species. From an evolutionary perspective, socialization and reproduction are mediated by the mesocorticolimbic reward circuit (Rademacher, Schulte-Rüther, Hanewald, & Lammertz, 2016).

The mesocorticolimbic circuit arises from dopaminergic neurons located in the VTA that project to the NAc, ventral striatum and innervate several regions of the PFC, central Amy, basolateral Amy, HIP, and dopamine neurons in the substantia nigra (SN) that project further on to the dorsal striatum. Functionally, the dopaminergic input from the VTA to NAc and ventral striatum regulates goal-oriented behaviors, whereas the VTA to dorsal striatum has been

TABLE 1 Defective mesocorticolimbic reward pathway favors social avoidance or ASD

Citation	Model	Origin of population	Age (years)	Phenotype	Stimulus during task	Brain changes
Ernst et al. (1997)	Human	American	13–14	Autism		Fluorine–18-labeled fluorodopa ratio was reduced by 39% in the anterior mPFC of ASD
Rogers et al. (2004)	Human	American-European	23–25	Autism	Monetary	Increased activation of the ACC
Greene et al. (2018)	Human	American	10–17	Autism	Monetary	Increased activation of the ACC
Dichter, Richey, et al. (2012), Delmonte et al. (2012), Kohls et al. (2013) and Kohls et al. (2014)	Human	American-European	14–26	Autism	Monetary	Increased activation in the medial and ventro mPFC, in the NAc, Amy, caudate and putamen
Schmitz et al. (2008)	Human	European	20–50	Autism	Monetary	Activation of the left ACC and left middle, superior frontal gyrus and the right superior parietal lobe
Delgado et al. (2000)	Human	African-American, Asian, Caucasian	18–40	Autism	Monetary	Activation in NAc, ventral striatum (VS), thalamus, OFC, putamen and caudate regions
Di Martino et al. (2011)	Human	American	10–12	Autism		Hyperconnectivity in the superior temporal gyrus, insula, and brainstem areas
Li et al. (2019) and Fu et al. (2020)	Human	American	0.5, 1, and 2	Autism		Enlargement in the Amy and CA1–3 of HIP by 6 months of age and in subiculum by 24 months
Duan et al. (2020)	Human	American	0.5, 1, and 2	Autism		Volume decrease in bilateral NAc and globus pallidus
Shams et al. (2018)	Zebra fish	Fish	Adult	Social avoidance		Decreased dopamine levels in whole-brain
Bariselli et al. (2016)	Mouse C57BL/6J	Mouse	Adult	Social avoidance		Reduced neuronal dopaminergic activity in the VTA
DiCarlo et al. (2019)	Mouse C57BL/6	Mouse	Adult	Social avoidance		Anomalous dopamine accumulation in striatum
Gunaydin et al. (2014) and Tickerhoof et al. (2020)	Mouse C57BL/6	Mouse	Adult	Social avoidance		Disruption of D1DR activation
DiCarlo et al. (2019)	Mouse C57BL/6	Mouse	Adult	Social avoidance		Disruption of D2DR activation
Yu et al. (2020)	Mouse C57BL/6	Mouse C57BL/6	Adult	Social avoidance		Deficient functional connectivity in mPFC, bed nucleus of the stria terminalis, Amy, hypothalamus, thalamus, piriform area, anterior cingulate, and periaqueductal gray
Yamaguchi et al. (2017)	Japanese macaques *Macaca fuscata*	Japanese macaques	Adult	Social avoidance		Disruption of D2DR activation

Abbreviations: ACC, anterior cingulate cortex; Amy, amygdala; ASD, Autism spectrum disorder; D1DR, dopamine receptor 1; D2DR, dopamine receptor 2; HIP, hypothalamus; mPFC, medial prefrontal cortex; NAc, nucleus accumbens; OFC, orbitofrontal cortex; PFC, prefrontal cortex.

associated with acquisition of habits (Russo & Nestler, 2013; Volkow, Wise, & Baler, 2017). Also, dopamine, on its own, finely integrates the function of the mesocorticolimbic reward circuit by activating the dopamine receptor 1 and 2 (D1DR and D2DR) at post-synaptic densities of the target brain regions. Following dopamine receptor activation, dopamine is time-dependently translocated into the pre-synaptic terminal by DAT.

According to the social motivation hypothesis, ASD is a motivation disorder where people prefer to explore and learn from the non-social environment at the expense of the social world (Clements et al., 2018; Kohls et al., 2018). In others words, ASD individuals find social stimuli less rewarding compared with non-affected individuals (Clements et al., 2018; Kohls et al., 2018). Initial reports using positron emission tomographic scanning identified a decrease in the accumulation of fluorine-18-labeled fluorodopa in the anterior medial prefrontal cortex of autistic people (Ernst, Zametkin, Matochik, Pascualvaca, & Cohen, 1997). Genomic analysis has supported potential gene targets in the mesocorticolimbic circuit as contributors to social avoidance in ASD. For instance, initial genetic reports identified de novo mutation in the human DAT gene (*SLC6A3*) as a candidate in ASD susceptibility (Bowton et al., 2014; Neale et al., 2012), which seems to promote dopamine efflux affecting normal social behavior. In addition, gene polymorphisms of dopamine receptor 3 and 4 have also been identified in people with ASD (Gadow, Devincent, Olvet, Pisarevskaya, & Hatchwell, 2010; Staal, Langen, Dijk, Mensen, & Durston, 2015). Likewise, a genome-wide multiphenotypic association analysis identified the deleted colorectal cancer gene, which encodes the transmembrane protein netrin 1 receptor, involved in the neuronal growth cones (Vosberg et al., 2018; Ye et al., 2020). Notably, the deleted colorectal cancer haploinsufficiency in humans displays correlation with social defects found in ASD individuals (Vosberg et al., 2018; Table 1).

Animal models have also confirmed that deficient function of the mesocorticolimbic circuit positively leads to social avoidance. For instance, social interaction in rats shows differential gene expression of the reward gene-related interactome including opioid, serotonin, and dopamine systems (Alugubelly et al., 2019). Genetic mouse models, replicating mutations in the DAT or SHANK3 protein found in humans, lead to anomalous dopamine accumulation or reduced neuronal dopaminergic activity in the mesocorticolimbic brain regions favoring social avoidance (Bariselli et al., 2016; DiCarlo et al., 2019). Also, decreased dopamine levels in zebra fish set a model of social isolation (Shams, Amlani, Buske, Chatterjee, & Gerlai, 2018), confirming an evolutionary conserved pathway. Conversely, a pharmacological increase in the dopamine concentration or blocking the dopamine receptor with Risperidone in people with ASD improves social preferences (Behmanesh, Moghaddam, Mohammadi, & Akhondzadeh, 2019; Eisenegger et al., 2013; Table 1).

Dopamine innervation to target areas is temporally and spatially regulated during social avoidance, suggesting that the phasic firing from the VTA to NAc promotes dopamine release at the synaptic cleft and endorses social avoidance in mice (Gunaydin et al., 2014). In vivo recordings in the NAc activity have identified that the medium spiny neurons efficiently respond to VTA input (Lobo & Nestler, 2011; Moratalla, Xu, Tonegawa, & Graybiel, 1996). Notably, increasing dopamine signaling in the NAc favors social play in adolescent rats, whereas antagonism of either D1 or D2DR decreases it (Manduca et al., 2016). Also, it seems that the VTA to NAc pathway programs subject specific social avoidance, whereas some subjects are resilient (Cao et al., 2010), which suggest subject-selective effects on social behavior.

Defects in the mesocorticolimbic circuit leading to social avoidance are also identified at postsynaptic level, precisely during the D1DR and D2DR activation. D1DR plays an important role in the VTA-NAc dopaminergic response, and interestingly it only happens in adult female mice (Gunaydin et al., 2014). Moreover, administration of intrastriatal D1DR antagonists led to a reduction of spontaneous stereotypies in mice (Presti, Mikes, & Lewis, 2003), demonstrating an important role of dopamine signaling anomalies involved in defective social behavior. Experimental data confirm that pharmacological or optogenetic activation in the D1DR leads social behavior in murine models, whereas its inhibition prevents it (Gunaydin et al., 2014; Lewis, Tanimura, Lee, & Bodfish, 2007; Lobo & Nestler, 2011; Presti et al., 2003). Selectively, pharmacological activation of D1DR signaling in the median Amy actively increases social avoidance (Tickerhoof, Hale, Butler, & Smith, 2020). In fact, favoring D1DR expression in the NAc using neutrophil inhibitory factor promotes social behavior in male rats (Kopec, Smith, Ayre, Sweat, & Bilbo, 2018). Conversely, injection of neutrophil inhibitory factor into the NAc did not alter D1DR levels nor social behavior in females (Kopec et al., 2018). A potential explanation to this discrepancy might be related to the fact that additional neuromodulatory systems, such as opioids, endo-cannabinoids, serotonin, oxytocin, and vasopressin, assist adolescent social behavior without involving the immune system (Argue et al., 2017; Dölen, Darvishzadeh, Huang, & Malenka, 2013; Smith, Ratnaseelan, & Veenema, 2018; Smith, Wilkins, Mogavero, & Veenema, 2015; Veenema, Bredewold, & De Vries, , 2012), and there is evidence that receptor expression for these various systems also changes over the course of development (Smith et al., 2017, 2018). In fact, pro-social behavior has also been described as oxytocin dependent: oxytocin innervation from the paraventricular nucleus of the hypothalamus to the VTA increases VTA neuron excitability and initiates dopamine release into the NAc, which in turn promotes social behavior in murine models (Hung et al., 2017). These lines of evidence contribute to explain the role for mesocorticolimbic circuit refinement during development by proposing that D1DR activation promotes social behavior. On its own, disruption of the D2DR signaling has been associated with social isolation and repetitive behavior (DiCarlo et al., 2019; Lee & Han, 2019). Recapitulating this scenario, pharmacological inhibition/activation of the D2DR leads/prevents to social isolation in macaques (Yamaguchi, Lee, Kato, Jas, & Goto, 2017; Table 1).

Together, these lines of evidence support the notion that deficient in the mesocorticolimbic reward circuit leading social avoidance (Pavăl, 2017) relies on the following three major targets: (a)

defective dopamine synaptic release, (b) failure in DAT and D2DR functionality, and (c) increase in the D1DR activation (Figure 1).

3 | DEFECTS IN FUNCTIONAL AND STRUCTURAL ENGRAMS OF THE MESOCORTICOLIMBIC CIRCUIT ENCODE SOCIAL AVOIDANCE IN ASD

Functional and structural MRI have supported the characterization of brain abnormalities underlying major behavioral traits in people with ASD. MRI analysis has enabled researchers to search for neuroanatomical biomarkers and attempt to develop MRI-based classification algorithms and computer-aided diagnostic systems to aid diagnosis and predict major behavioral traits in people with ASD (Richards et al., 2020; Yang et al., 2016). Although MRI analysis has provided information about selective neurodevelopmental characteristics and behavioral criteria for ASD diagnosis, they still do not completely validate whether neuroanatomical biomarkers can predict ASD in the entire population. Based on this, we will focus on brain abnormalities correlated with reward defects in the mesocorticolimbic structures identified by functional MRI (fMRI) analysis to confirm failure in connectivity patterns (Esteban et al., 2019; Mohammad-Rezazadeh, Frohlich, Loo, & Jeste, 2016), and also, in structural MRI reports focused on volumetric and morphometric analyses to give evidence of abnormal brain anatomy in people with ASD (Lerch, Sled, & Henkelman, 2011). By functionality, fMRI is a reliable and efficient experimental approach based on time series of blood oxygenation level-dependent signals coupled to statistical modeling able to measure functional connectivity between two brain areas (Herold, Aye, Lehmann, Taubert, & Müller, 2020; Jiang & Zuo, 2016). From a neurobiology perspective, cognitive tasks trigger brain connectivity by selective hemodynamic integration of higher neuronal energy metabolism in brain areas, which results on a positive correlation of major energetic demands, oxygen consumption, and blood oxygenation level-dependent signal contrast (Forouzannezhad et al., 2019; Herold et al., 2020; Sumiyoshi, Keeley, & Lu, 2019).

Classical studies using MRI approaches by Dawson et al. (2004), Dawson, Webb, and McPartland (2005) hypothesized that people with ASD have social motivation deficits, including failure in reward to social information (Dawson et al., 2004, 2005), contributing to the social motivation hypothesis for ASD (Chevallier, Kohls, Troiani, Brodkin, & Schultz, 2012). Neurobiologically, connections in frontostriatal and frontolimbic circuits mediate the reward feedback between emotional and cognitive stimulus (Lockwood & Wittmann, 2018). For instance, studies in monkeys and humans reported that the anterior cingulate cortex (ACC) relays signals that motivate socialization and reward (Lockwood & Wittmann, 2018; Rigney, Koski, & Beer, 2018; Rudebeck, Buckley, Walton, & Rushworth, 2006). In this context, people with ASD exposed to a non-social rewards show increased activation of the ACC, which correlates with increased severity of ASD symptoms (Greene et al., 2018; Rogers et al., 2004). Also, increased activation in the ventral and dorsal striatum, ventro mPFC, ACC, and orbitofrontal cortex (OFC) were found in individuals with ASD following a response to social or monetary rewards (Delmonte et al., 2012; Dichter, Richey, Rittenberg, Sabatino, & Bodfish, 2012; Kohls et al., 2013, 2014). Furthermore, individuals with ASD show activation of the left ACC and left middle, superior frontal gyrus, and the right superior parietal lobe (Schmitz et al., 2008) for the monetary reward achievement. Conversely, the ventro mPFC response is attenuated in children with ASD who were shown a favorite face, compared to non-ASD children (Kishida et al., 2019). Besides, mesocorticolimbic areas such the VTA, ventral HIP, hypothalamus, and NAc are widely reported to project to the ventro mPFC and regulate social motivation and anxiety in rodents (Allsop, Vander Weele, Wichmann, & Tye, 2014; Yu et al., 2020). In this context, evaluation of the social motivation hypothesis of autism using fMRI, Clements C. et al. reported large clusters of reward circuitry hypoactivation in the bilateral caudate, right HIP, lateral occipital cortex, inferior frontal gyrus and ACC regions for the ASD group, whereas hyperactivation was observed in the right insula, putamen, the right temporal occipital fusiform cortex, and the left superior temporal gyrus/planum temporale (Clements et al., 2018). Also, reward response to monetary incentives suggests that the anticipatory rewarding clusters for money in people with ASD integrates the activation in NAc, ventral striatum (VS), thalamus, OFC, putamen and caudate regions, whereas monetary outcomes recruit activation in medial and ventro mPFC, in the NAc, Amy, caudate and putamen (Delgado, Nystrom, Fissell, Noll, & Fiez, 2000; Forbes et al., 2009; Wacker, Dillon, & Pizzagalli, 2009). In fact, using the MeCP2 transgenic murine model of autism has reported deficient functional connectivity in mPFC, bed nucleus of the stria terminalis, Amy, hypothalamus, thalamus, piriform area, anterior cingulate, and periaqueductal gray, which were reversed by normalizing the MeCP2 levels in the mPFC (Yu et al., 2020), suggesting that the VTA–mPFC or vHIP–mPFC circuits participates in the regulation of social recognition in rodents, which it is still to be proven in humans. Conversely, fMRI analysis of people with ASD exposed to a monetary reward display hypoactivation in the left NAc, as well as the right frontal pole and right insular cortex, but not in the ventro mPFC; however, people with ASD demonstrated relatively greater activation in a number of cortical regions outside of classic reward circuits (Dichter, Damiano, & Allen, 2012). In addition, hyperconnectivity has also been identified in the superior temporal gyrus, insula, and brainstem areas (Di Martino et al., 2011), and in the cingulate cortex and inferior and superior frontal gyri, as well as other specific areas (Lynch et al., 2013; Uddin et al., 2013). These lines of evidence demonstrated hyper- and hypoconnectivity patterns of neuronal activity of the mesocorticolimbic circuit of people with ASD during social motivation. However, in a more realistic view, a single cognitive or neural cluster does not explain development and maintenance of all ASD traits in all individuals, so social and non-social rewards might be actively depending for each outcome. In fact, children at risk to develop ASD might show atypical incentive exploration and more attention to objects than other people as young as 12 months

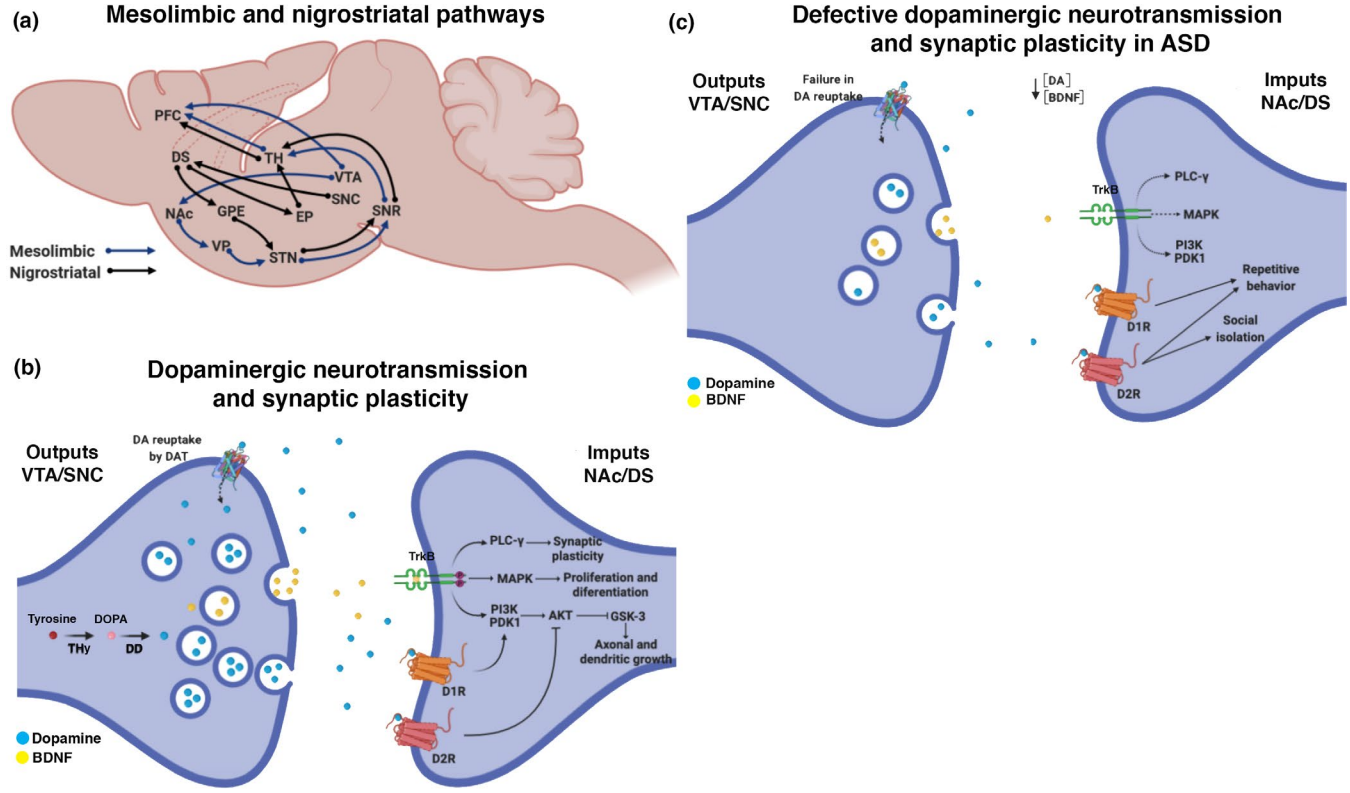

FIGURE 1 Defective mesocorticolimbic reward pathway regulates ASD occurrence. (a) Mesolimbic and nigrostriatal circuit regulate social interaction in humans and animals. The mesolimbic pathway integrates dopaminergic inputs into the PFC and NAc, which arise from the VTA. Also, mesolimbic innervation from the SNR to TH assists PFC activation. SNR integrates a mesolimbic input feedback from the NAc, VP, and STN relays. The nigrostriatal circuit also includes TH inputs from the SNR and EP. Also, SNC innervates dorsal striatum (DS) which sends inputs to EP linking EP-TH connection. Finally, SNR also integrates a nigrostriatal input feedback from the DS, GPe, and STN relays (Rademacher et al., 2016; Russo & Nestler, 2013; Volkow et al., 2017). (b) Mesolimbic or nigrostriatal circuits including the VTA and SNC outputs to NAc and DS, respectively, regulating dopaminergic neurotransmission. Pre-synaptic dopamine synthesis from tyrosine at the VTA and SNC are released by exocytosis at NAc and DS synaptic clefts allowing dopamine accumulation and extrasynaptic dopamine diffusion away from the post-synaptic density. Dopamine binds to the D1DR and D2DR subtypes activating and antagonizing, respectively, the phosphatidylinositol 3-kinase-AKT pathway. AKT promotes axonal and dendritic growth by blocking the GSK-3 activity. Synaptic BDNF release binds to TrKB receptors at post-synaptic terminals favoring intracellular phosphorylation of Tyr490, Tyr515, and Tyr816 sites activating the MAPK and PLC-gamma pathways and synaptic plasticity and neuronal proliferation and differentiation, respectively (Rademacher et al., 2016; Russo & Nestler, 2013; Volkow et al., 2017). Finally, time-dependent D1DR and D2DR activation is precisely modulated by sodium-dependent pre-synaptic DAT allowing a fine-tuning modulation of neuronal function (Rademacher et al., 2016; Russo & Nestler, 2013; Volkow et al., 2017). (c) Defective dopaminergic neurotransmission has been reported in ASD subjects (Ernst et al., 1997; Pavăl, 2017). Dopamine synthesis at pre-synaptic terminals is impaired in the VTA and SNC potentially impairing D1DR and D2DR activation at post-synaptic terminals of NAc and DS of murine models, respectively (Bariselli et al., 2016; DiCarlo et al., 2019). Dopamine uptake at the pre-synaptic terminals by the DAT is also disrupted by decreasing dopamine accumulation into pre-synaptic vesicles (Bariselli et al., 2016; DiCarlo et al., 2019). Also, reports have shown a decrease in brain-derived neurotrophic factor accumulation in synaptic clefts and absence of the MAPK, PLC-gamma, and phosphatidylinositol 3-kinase activation and defective synaptic plasticity and neuronal proliferation and differentiation. Notably, D1DR and D2DR activation at NAc and DS regions associate with repetitive behavior and social isolation. Abbreviations: AKT, Protein kinase B; BDNF, Brain-derived Neurotrophic Factor; DA, dopamine; DAT, dopamine transporter; DD, dopamine decarboxylase; D1DR, dopamine receptor 1; D2DR, dopamine receptor 2; EP, entopedincullar nucleus; GSK-3, Glycogen synthase kinase 3; GPe, globus pallidum externus; DS, dorsal striatum; MAPK, mitogen-activated protein kinase; NAc, nucleus accumbens; PDK1, Phosphoinositide-dependent kinase-1; PFC, prefrontal cortex; PI3K, phosphatidylinositol 3-kinase; PLC-gamma, Phospholipase C-gamma; SNC, substantia nigra pars compacta; SNR, substantia nigra pars reticulata; STN, subthalamic nucleus; TH, thalamus; THy, tyrosine hydroxylase; TrKB, Brain-Derived Neurotrophic Factor Receptor; VP, ventral pallidum, VTA, ventral tegmental area. Created with BioRender.com

old (Elison et al., 2014; Ozonoff et al., 2008), which agree with a time-dependent neural dysconnectivity as a leading node of ASD traits (Jack, 2018; Chakravarty, 2018; Figure 2).

Experimental evidence applying structural MRI analysis in people with ASD has found common structural abnormalities affecting the mesocorticolimbic circuit among ASD patients. Genetic approach using MANCOVA analysis showed an association between alleles of the SNP rs167771 and the total striatum volume and greater caudate nucleus volume, correlated with ASD behavioral traits (Staal et al., 2015). Initial analysis of 6-month-old high-risk

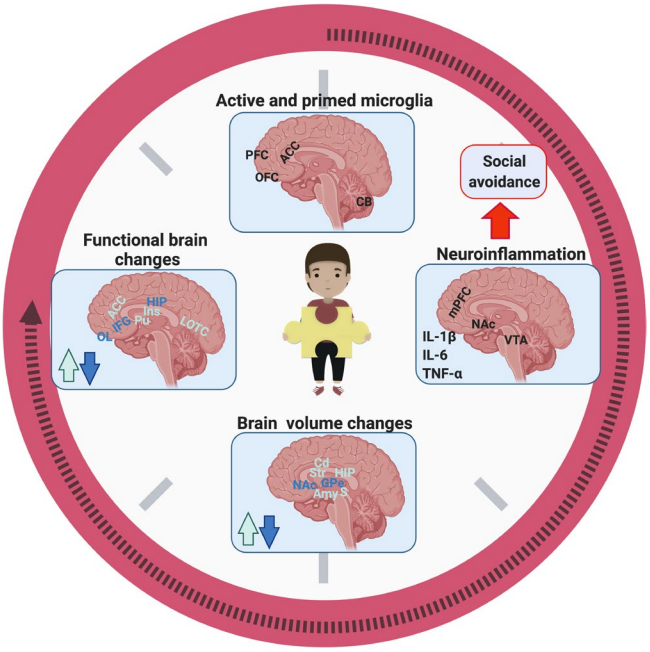

FIGURE 2 Structural and functional brain defects, active microglia, and neuroinflammation in ASD subjects. This figure integrates a potential time-dependent role of primed microglia assisting brain neuroinflammation in mesocortical and nigrostriatal regions during ASD occurrence. Active and primed microglia was detected in PFC, ACC, OFC, and CB regions of ASD subjects (Suzuki et al., 2013). Also, neuroinflammatory markers including IL-1-beta, IL-6, and TNF-alpha have been identified in mPFC, NAc, and VTA of autistic peers (Li et al., 2009; Singer et al., 2006; Singh & Rivas, 2004; Vargas et al., 2005). Structural and/or functional defects including brain volume or connectivity increase or decrease have been reported in ASD subjects. Volume increases in Amy, Cd, HIP, S, and Str (Fu et al., 2020; Li et al., 2019), whereas a volume decreases in NAc and GPe (Duan et al., 2020) were characterized. Finally, functional changes including hyperactivation in ACC, Ins, LOTC, and Pu (Kishida et al., 2019), whereas hypoactivation in IFG, HIP, and OL brain regions (Delmonte et al., 2012; Dichter, Richey, et al., 2012; Kohls et al., 2013, 2014). Abbreviations: ACC, anterior cingulate cortex; Amygdala, Amy; Cd, caudate nucleus, EP, entopedincullar nucleus; IFG, inferior frontal gyrus; GPe, globus pallidum externus; HIP, hippocampus; Ins, insula; LOTC, lateral occipito-temporal gyrus; NAc, nucleus accumbens; OL, olfactory lobe; Pu, Putamen; PFC, prefrontal cortex; mPFC, medial prefrontal cortex; S, subiculum; Str, Striatum; VTA, ventral tegmental area; Gray arrows: increase; Blue arrows: decrease. Created with BioRender.com

infants compared with autistic siblings and low-risk infants found no differences in total brain volume, (Hazlett et al., 2011), consistent with the hypothesis that structural brain alterations might be a postnatal event in young children with ASD. In fact, a longitudinal study showed enlargement in the Amy and CA1-3 of HIP by 6 months of age and in subiculum by 24 months of age in people with ASD (Fu et al., 2020; Li et al., 2019). Conversely, Duan et al. (2020) reported a significant volume decrease in bilateral mesocorticolimbic circuit-related regions such as NAc and globus pallidus in ASD compared with controls (Duan et al., 2020). In addition, structural analysis using the diffusion tensor imaging technology to assess in vivo microstructure of white matter tracts in the brain (Tohyama, Walker, Sammartino, Krishna, & Hodaie, 2020) reported alterations in the fractional anisotropy, a measurement of axon directionality. Diffusion tensor imaging analysis of ASD brains shows a bilateral fractional anisotropy reduction in mesocorticolimbic circuit regions compared to non-ASD individuals (Haigh, Keller, Minshew, & Eack, 2020). Precisely, a significant lower fractional anisotropy in left inferior fronto-occipital fasciculus, left superior longitudinal fasciculus, left inferior longitudinal fasciculus, and in the right Amy was found in the less-cognitively affected ASD people compared with controls (Im et al., 2018). Also, an increase in fractional anisotropy in large areas such as bilateral corticospinal tract, corona radiata, cingulum, anterior thalamic radiation, forceps major, forceps minor, internal capsule, external capsule, corpus callosum, SLF, inferior longitudinal fasciculus, and inferior fronto-occipital fasciculus were found in ASD patients (Fu et al., 2020), suggesting defects in language processing, sociality, and cognition (Simon et al., 2020). Finally, genetic contribution to ASD pathology such as deleted colorectal cancer haploinsufficiency displays defects in mesocorticolimbic connectivity, structural volume alterations, and social avoidance, which is also reproducible in murine models, except that striatal volumetric reductions were found ventrally in mice and more dorsally in humans (Vosberg et al., 2018; Figure 2).

Together, these experimental evidence confirm that defects in functional and structural engrams of the mesocorticolimbic circuit determine social avoidance in people with ASD and open a potential future research to characterize selective age-dependent changes of severity for intervention (Im et al., 2018; Tohyama et al., 2020).

4 | SYSTEMIC AND CENTRAL PRO-INFLAMMATORY PROFILES REGULATE THE MESOCORTICOLIMBIC CIRCUIT DURING ASD

Initial characterization of central pro-inflammatory profile in people with ASD has identified serum antibodies, TGF-β1, TNF-α, IFN-γ, and IL-6 markers in post-mortem samples of anterior cingulate gyrus, cortex, and PFC (Li et al., 2009; Singer et al., 2006; Singh & Rivas, 2004; Vargas et al., 2005). Also, microglial activation and density has been identified by positron emission tomography imaging (Suzuki et al., 2013) and Iba-1 immunosignal in post-mortem PFC region of people with ASD (Morgan et al., 2010, 2012). Experimental evidence has proposed that the pro-inflammatory profile found in ASD might be potentially related to an autoimmune disease. While this proposal might be taken carefully and probably reflects selective phenotypes worldwide, initial reports show correlation between a third hypervariable region and the C4 complement alleles with ASD susceptibility (Gesundheit et al., 2013). Also, a positive correlation was found between ASD susceptibility and maternal autoimmune disorder (Edmiston, Jones, Vu, Ashwood, & Van de Water, 2018; Jones & Van de Water, 2019). For instance, a systemic pro-inflammatory profile including circulating antibodies targeting

lymphocyte antigens was identified in serum of mothers with ASD children (Edmiston et al., 2018), which positively correlates with an increase in the susceptibility to ASD after birth (Chen et al., 2016). In fact, serum autoantibodies against fetal neuronal migration and neural network brain targets, including the collapsin response mediator proteins 1 and 2 (CRMP1 and CRMP2), cypin, and the Y-box binding protein 1 and the *N*-methyl-D-aspartate receptor for glutamatergic neurotransmission, have been identified in mothers of people with ASD (Brimberg, Sadiq, Gregersen, & Diamond, 2013; Edmiston et al., 2018; Fox-Edmiston & Van de Water, 2015; Gréa et al., 2017). Notably, in a recent exploratory study, Krakowiak, Walker, Tancredi, Hertz-Picciotto, and Van de Water (2017) reported that metabolic failure related to gestational diabetes was associated with an up to 3.2-fold increase in anti-fetal brain autoantibodies (Krakowiak et al., 2017), suggesting a potential interplay between metabolism and immune activation during development. Together, these lines of evidence support the potential role of maternal autoimmunity regulating ASD susceptibility in the offspring.

By definition, during autoimmunity our body recognizes, neutralizes, or destroys selective targets of the body itself by integrating a finely and controlled systemic and central pro-inflammatory state. In fact, maternal immune activation (MIA) by fever diagnosed during pregnancy is associated with ASD development in the offspring (Brucato et al., 2017). Notably, epidemiological data have suggested that children whose mothers reported a history of immune activation (allergies and asthma) developed severe social impairment (Patel et al., 2018). MIA itself has been replicated in murine models by exposing mothers to influenza virus inoculation during pregnancy, and reporting up to 12% increases for ASD risk (Jiang et al., 2016). Notably, pharmacological MIA models in human and non-human primates and murine models set a systemic pro-inflammatory signature including IL-2, IFN-γ, IL-6, IL-4, IL-17A, and TNF-α in plasma, amniotic fluid, and placenta as well as lymphocyte proliferation and maturation (Careaga, Murai, & Bauman, 2017), which leads to ASD susceptibility in the offspring (Careaga et al., 2017; Graham et al., 2018; Kim et al., 2017; Rudolph et al., 2018; Shin Yim et al., 2017). Also, we have reported that positive inflammatory profile during MIA might be programmed by maternal overnutrition (Maldonado-Ruiz, Garza-Ocañas, et al., 2019) affecting mesocorticolimbic pathway functionality and favoring ASD-like (Maldonado-Ruiz, Garza-Ocañas, et al., 2019) or addiction-like behavior in the offspring (Montalvo-Martínez, Maldonado-Ruiz, Cárdenas-Tueme, Reséndez-Pérez, & Camacho, 2018). It seems that a pro-inflammatory profile sets a sex-dependent effect on ASD susceptibility, given that higher levels of IL-8 increased ASD severity in females, whereas increased IL-15 and reduced IL-8, IL-1β, and macrophage inflammatory protein-1α and TGF-β1 levels were found in males (Hu et al., 2018; Masi et al., 2017). In any case, a precise scenario of integrating selective pro-inflammatory candidates as a potential pharmacologic therapeutic avenue to prevent or revert ASD susceptibility has not been identified. Two recent meta-analysis identified the pro- and anti-inflammatory cytokines signatures of IFN-γ, IL-1β, IL-6, and TNF-α, and IL-10 and IL-1Ra in people with ASD compared with control subjects, respectively (Saghazadeh et al., 2019a, 2019b). These meta-analyses suggest that ethnicity, age, and gender contribute to different inflammatory profiles in people with ASD (Saghazadeh et al., 2019a, 2019b). However, perhaps the most reliable cytokine recently reported to closely modulate ASD susceptibility is the IL-17A (Kim et al., 2017; Reed et al., 2020; Shin Yim et al., 2017). The IL-17A–IL-17 receptor interaction integrates peripheral and central immunity, a node modulating neuronal activity during neurodevelopment, efficiently preventing ASD (Reed et al., 2020). Mechanistically, an increase in IL-17A during MIA in rodents positively promotes sociability in the offspring by direct neuronal activation of the primary somatosensory cortex (Reed et al., 2020). Notably, it seems that the effect of the IL-17A–IL-17 pathway is centrally selected, given that, in contrast to promote sociability traits during brain activation, the IL-17A–IL-17 activation in peripheral monocytes enhances oxidative inflammation of Autistic children (Nadeem et al., 2018). However, despite substantial scientific evidence linking MIA and ASD, most maternal infections in humans do not lead to ASD in the offspring (Selten & Morgan, 2010), proposing that ASD consolidation probably requires a "second hit" external stimuli (Picci & Scherf, 2015). For instance, no correlation was found in peripheral and cerebrospinal fluid pro-inflammatory markers in people with ASD (Pardo et al., 2017), suggesting that peripheral markers might not optimally reflect the immune status of the CNS. In fact, basic research addressing the role of MIA in murine models supports the notion that behavioral and immunological effects during MIA are selectively dependent on the animal's strain (Schwartzer et al., 2013) and selective pro-inflammatory trigger (Glass, Norton, Fox, & Kusnecov, 2019; Oskvig, Elkahloun, Johnson, Phillips, & Herkenham, 2012). We expect that such scenario might be recapitulated in people with ASD (Figures 2 and 3; Table 2).

Additionally, a positive pro-inflammatory profile closely regulates social motivation behavior by modulating the mesocorticolimbic circuit. As we stated before, genetic analyses in humans have confirmed that genomic defects in the dopaminergic neurotransmission integrates social avoidance (Bowton et al., 2014; Gadow et al., 2010; Neale et al., 2012; Staal et al., 2015; Vosberg et al., 2018). Notably, maternal IL-6 increases during pregnancy are associated with deficient newborn brain connectivity and future working memory in offspring aged 2 (Rudolph et al., 2018). Substantial evidence using murine models has confirmed that MIA by LPS exposure or pharmacological simulation of viral infection by Poly I:C inoculation efficiently primes defects in dopaminergic neurotransmission in the offspring, recapitulating ASD traits. For instance, LPS and Poly I:C exposure promotes a decrease in the dopamine levels, in the D1DR and D2DR number and in the DAT in NAc, PFC and striatum of people with ASD (Kirsten, Taricano, Flório, Palermo-Neto, & Bernardi, 2010; Meyer et al., 2008; Ozawa et al., 2006; Romero, Guaza, Castellano, & Borrell, 2010; Soto et al., 2013; Vuillermot, Weber, Feldon, & Meyer, 2010). Also, deletion in the dopamine receptor 3 gene in mice displays high levels of TNF-α, IL-1β, and IL-6, and notably, microglial activation in selected brain regions of the mesocorticolimbic circuit (Wang et al., 2019). Defects in dopamine receptor 3 and in the

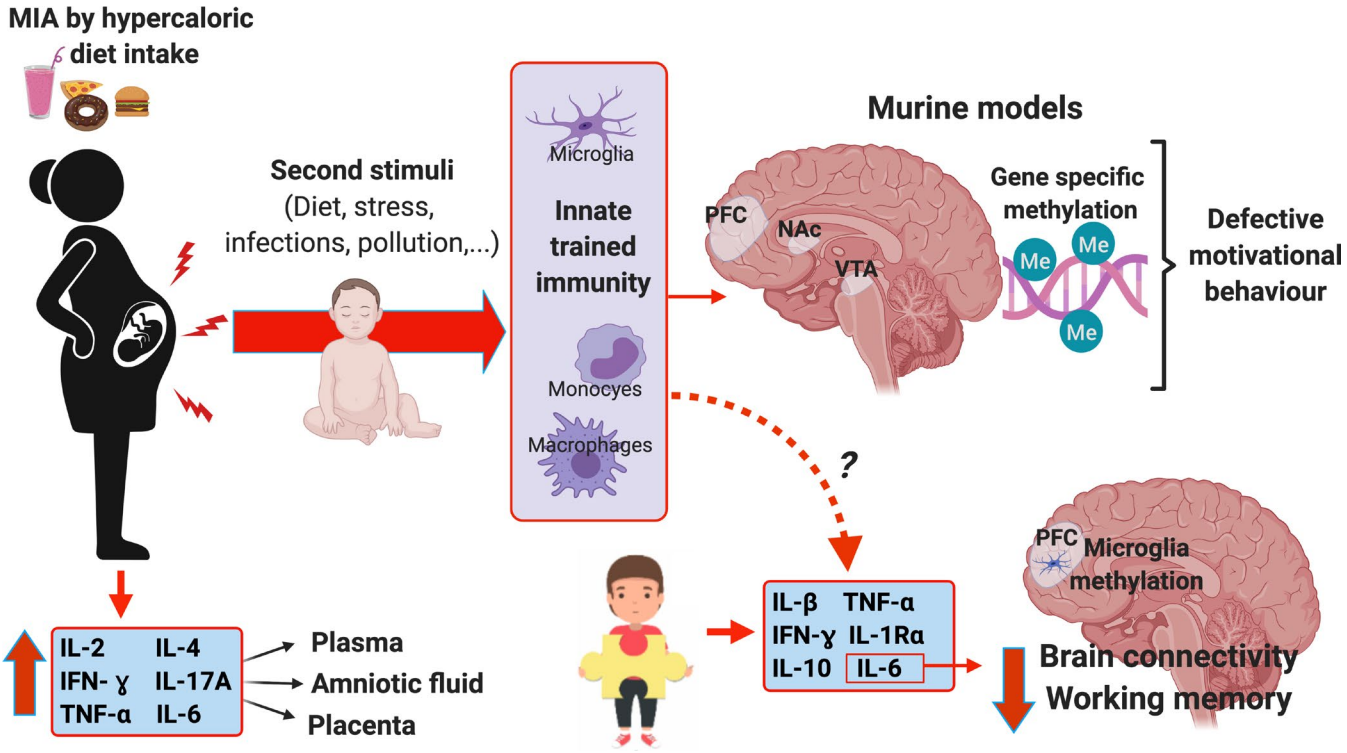

FIGURE 3 MIA of innate trained immunity and social avoidance. Hypercaloric diet intake during pregnancy might activates a pro-inflammatory profile including plasma, amniotic fluid, and placenta including IL-2, IL-4, IL-6, IL-17A, IFN-γ, and TNF-α increase (Careaga et al., 2017; Graham et al., 2018; Kim et al., 2017; Rudolph et al., 2018; Shin Yim et al., 2017), which sets a defective neurodevelopmental program of the fetus. Hypothetically, offspring might be exposed to a second stimuli (diet, stress, infections, environment) which consolidate the innate trained immunity phenotype of microglia, monocytes, and macrophages (Selten & Morgan, 2010). At this stage, ASD subjects show plasma increase in IL-1β, IL-6, IL-10, IL-1Rα, IFN-γ, and TNF-α (Li et al., 2009; Singer et al., 2006; Singh & Rivas, 2004; Vargas et al., 2005). Precisely, IL-6 increase has been associated with defective brain connectivity and working memory in in 3-year-old subjects from mothers exposed to pregnancy infections (Rudolph et al., 2018). Innate trained immunity also correlates with methylation signatures in mesocorticolimbic regions in the offspring of maternal programed models. Enhance in DNA methylation has been identified in VTA, PFC, and NAc regions which associates with defective motivational behavior (Cruz-Carrillo et al., 2020; Ganu et al., 2012; Grissom et al., 2015; Vucetic et al., 2010). It is still to be tested if obesity or maternal overnutrition associate with systemic and central pro-inflammatory profile favoring methylation signatures in microglia of the mesocorticolimbic circuit. Abbreviations: GABA, gaba-aminobutiric acid; MIA, maternal immune activation. Created with BioRender.com

GluR1 AMPA receptor subunit in the VTA, mPFC, and NAc have been reported to occur following LPS administration in murine models, showing a depression-like behavior phenotype (Sekio & Seki, 2015; Wang et al., 2018). Conversely, pharmacologic activation of GluR1 and dopamine receptor 3 revert LPS-induced depression-like behavior by preventing changes in pro-inflammatory cytokine profile (Sekio & Seki, 2015; Wang et al., 2018). On its own, dopamine displays potent anti-inflammatory effects suppressing the action of cytokines iNOS and the NLRP3 activation in the RAW264.7 macrophage cell line (Liu & Shifang, 2019) and by blocking the nuclear NF-κB p65 translocation in microglial cells (Yoshioka et al., 2020). Also, granulocyte colony-stimulating factor, an immune cell-derived molecule, decrease brain TNF-α gene expression and enhances pre-synaptic dopamine release in the NAc of the mesocorticolimbic circuit (Kutlu et al., 2018), and promotes motivation (Calipari et al., 2018). The nuclear NF-κB p65 transcription factor has also been closely associated with metabolic alterations induced by fatty acids, such as insulin resistance on neurons and microglial activation, a pathological scenario reported during positive energy balance such as during obesity or overnutrition (Delint-Ramirez et al., 2015; Maldonado-Ruiz, Montalvo-Martínez, Fuentes-Mera, & Camacho, 2017), and hyperphagia (Maldonado-Ruiz, Cárdenas-Tueme, et al., 2019).

Together, these lines of evidence point out that inflammatory response, microglial activation, and complement-mediated immune signaling modulate selective reward-dependent regions for social interaction and ASD traits. Major contributors of a positive pro-inflammatory profile during ASD susceptibility have not been totally clarified and it integrates an active and open field of research. We conceive that a chronic low-grade pro-inflammatory profile such as happens during obesity/overnutrition might activate central microglia and favors deficient brain connectivity in the mesocorticolimbic circuit during neurodevelopment. Next, we add major findings of the role of central microglial activation by maternal obesity and/or maternal overnutrition and its effects on ASD appearance.

TABLE 2 Maternal programming of pro-inflammatory profile and defective behavior in the offspring

Citation	Model	Dietary manipulation	Offspring age (months)	Phenotype	Brain changes in the offspring
Pro-inflammatory profile and microglia activation in the offspring					
Grayson *et al.* (2010)	Maternal programming in Japanese macaques *Macaca fuscata*	High-fat exposure	48		Increased in IL–1-beta and IL–1 type 1 receptor, and microglia activation in the hypothalamus
Edlow et al. (2019)	Maternal programming in C57Bl/6 mice	High-fat exposure	Embryonic day 8.5–17.5		Recruitment of CD11b + placental macrophages, microglia activation and TNF-α production in brain
Maldonado-Ruiz, Cárdenas-Tueme, et al. (2019)	Maternal programming in Wistar rats	High-fat and sugar exposure	3	Depression-like behavior	Microglia activation in hypothalamus
de la Garza et al. (2019)	Maternal programming in Wistar rats	High-fat and sugar exposure	3	Depression-like behavior	Increased in TANK binding kinase 1 in the hippocampus
Defective behavior and changes in the mesocorticolimbic circuit in the offspring					
Naef *et al.* (2008)	Maternal programming in Sprague–Dawley rats	High-fat exposure	2–3	Decrease locomotion and behavioral sensitization to amphetamine	Increased tyrosine hydroxylase expression in the VTA and NAc
Ong *et al.* (2011)	Maternal programming in Sprague–Dawley rats	High-fat exposure	1–3		Decreased dopamine transporter in the VTA and NAc
Naef et al. (2011)	Maternal programming in Sprague–Dawley rats	High-fat exposure	3	Addiction-like behavior	Altered dopamine transmission in the NAc and D2DR decrease in the VTA
Camacho et al. (2017)	Maternal programming in Wistar rats	High-fat and sugar exposure	3	Addiction-like behavior	Upregulation of mGlur 2,3 receptor and NR1 subunit in the NAc shell and PFC

Abbreviations: NAc, nucleus accumbens; PFC, prefrontal cortex.

5 | MATERNAL OBESITY PRIMES MICROGLIAL ACTIVATION AND SYSTEMIC PRO-INFLAMMATORY PROFILE MODULATING THE MESOCORTICOLIMBIC CIRCUIT IN ASD

Several clinical studies have identified that maternal obesity leads to up to 1.39% and 1.59% of ASD cases and a greater likelihood of having a child with ASD compared with their lean counterparts (Andersen, Thomsen, Nohr, & Lemcke, 2018; Bilder et al., 2013; Krakowiak et al., 2012; Li et al., 2016; Reynolds, Inder, Neil, Pineda, & Rogers, 2014). Notably, active microglia was found in mesocorticolimbic and accessory brain regions of people with ASD, including cerebellum, PFC (Fatemi et al., 2012; Morgan et al., 2010, 2012; Selten & Morgan, 2010; Tetreault et al., 2012), ACG, and OFC (Suzuki et al., 2013). Neurobiological evidence has described that microglia actively modulates proper neurodevelopment by regulating neurogenesis, synaptic plasticity, and synaptic striping, and also, it is the major antigen presenting cells in brain (Cárdenas-Tueme, Montalvo-Martínez, Maldonado-Ruiz, Camacho-Morales, & Reséndez-Pérez, 2020; Jiang, Cowan, Moonah, & Petri, 2018; Paolicelli et al., 2011). However, based on the inaccessibility of living human brains for molecular characterization and ethical and technological limitations to test microglial function in human brains, it is still unknown whether microglial activation is significantly relevant to favor social avoidance in ASD subjects. In any case, perhaps the most realistic confirmation of the physiological role of microglia assisting brain neurodevelopment and disease in humans was reported

recently by Bennet's research group (Oosterhof et al., 2019). Dr. Bennet identified that homozygous mutations in the colony-stimulating factor 1 receptor promotes leukoencephalopathy and substantial decreases in microglia (Oosterhof et al., 2019). Magnetic resonance imaging and post-mortem brain histopathological analysis demonstrated the absence of corpus callosum and cingulate sulcus, dystrophic basal ganglia, thalamus, hippocampus, and reduced white/gray ratio in brain, extensive axonal degeneration with numerous spheroids, and intraparenchymal calcifications associated with brain tissue degeneration and gliosis (Oosterhof et al., 2019). Notably, locally depleted microglial numbers might reflect a key role of the colony-stimulating factor 1 receptor signaling on microglial maturation during embryonic development (Chitu & Stanley, 2006; Ginhoux et al., 2010). Unfortunately, potential effects of microglial depletion on social avoidance in ASD individuals were not characterized given that the subject carrying the colony-stimulating factor 1 receptor mutation died at 10 months of age from streptococcal bacteremia. Animal models have contributed to major advances on the neurobiology impact of microglia providing striking similarities and reproducing the observed behavioral traits exhibit by ASD subjects, including social avoidance. We next described major findings supporting the role of microglia on social avoidance in animal models of maternal obesity and/or maternal overnutrition of hypercaloric diets.

Recent evidence identified that hypercaloric diet exposure primes an immunity phenotype by reprograming the innate cells toward an enhanced immune response at later stages (Christ et al., 2018). For instance, cells of the innate immune system might exhibit adaptive cellular responses to an external stimulus, which primes a selective response to a second stimulus, a molecular mechanism termed "trained immunity" (Netea et al., 2020; Netea, Quintin, Meer, & van der Meer, 2011). Notably, the adaptive innate phenotype has also been reported in microglia (Wendeln et al., 2018). For a detailed review of microglial priming in brain see Neher and Cunningham, (2019). Of importance, it is known that reprogramming of innate immunity integrates metabolic flexible networks including glucose and fat-dependent pathways which assist the setting of innate immune training (Neher & Cunningham, 2019). For instance, initial reports have identified that macrophages express the classical insulin signaling pathway for immunological training (Ieronymaki, Theodorakis, et al., 2019) and efficiently depends on glycolysis for development the M1 pro-inflammatory phenotype (See Ieronymaki, Daskalaki, Lyroni, & Tsatsanis, 2019, for details). In specific, the insulin-like growth factor 1 receptor and mTOR pathway coordinates immune priming in monocytes (Bekkering et al., 2018). Notably, microglia is also able to secrete the insulin-like growth factor 1 which allowing neuronal survival and synaptic "stripping" by the C1q-C3 binding receptor in target synapsis during neurodevelopment (Salter & Stevens, 2017), confirming active insulin signaling assisting physiological homeostasis, such as reported during glucose balance (Maldonado-Ruiz, Montalvo-Martínez, et al., 2017). This evidence suggest that microglia integrates insulin-related pathways favoring long-lasting reprogramming of immunity and suggest that metabolic compromised such as happened during obesity might negatively disrupt physiological immune training.

Obesity and/or maternal overnutrition of hypercaloric diets also integrates a pathological chronic low-grade pro-inflammatory profile in the brain, in part promoted by the interaction of fatty acids from diet with toll-like receptors, known as metabolic inflammation (Cai & Khor, 2019; Milanski et al., 2009). Reports have identified that exposure to hypercaloric diets in murine models efficiently induces IgG accumulation in hypothalamic microglia (Yi, Tschop, Woods, & Hofmann, 2012). Also, hypercaloric diet-induced obesity reproduces the metabolic inflammation, favoring defects in social novelty (Zilkha, Kuperman, & Kimchi, 2017), and suppressing social interactions (Veniaminova et al., 2017). Mechanistically, metabolic inflammation in the CNS activates the pro-inflammatory pathway toll-like receptor 4 (TLR4)/IKK/NF-κB in microglia (De Souza et al., 2005; Milanski et al., 2009), and we have reported that obese murine models show up-regulation of the TBK1-related IKK marker (Delint-Ramirez et al., 2015; Diaz et al., 2015). A potential scenario sets that TLR4/IKK/NF-κB pathway allows IL-1β secretion, astrocyte activation in the choroid plexus, integrating peripheral B and T cells and a macrophage response by secreting chemo-attractant molecules (Maldonado-Ruiz, Fuentes-Mera, & Camacho, 2017). In fact, selective depletion of TLR2 and TLR4 reestablishes social interaction in a mice model of repeated social defeat stress by decreasing microglial activation in the PFC (Nie et al., 2018), suggesting that maternal hypercaloric diet primes PFC microglia and social avoidance in the offspring by TLR-dependent signaling.

Mice exposed to maternal hypercaloric diet during pregnancy have confirmed microglial priming (Banik et al., 2017; Maldonado-Ruiz, Cárdenas-Tueme, et al., 2019) and defective mesocorticolimbic activity to a natural reward and depression-like behaviour in the offspring (Camacho, Montalvo-Martinez, Cardenas-Perez, Fuentes-Mera, & Garza-Ocañas, 2017; de la Garza et al., 2019; Naef et al., 2011). Also, maternal obesity has shown altered regulation of NAc dopamine transmission and D2DR decrease in the VTA of the offspring (Naef et al., 2011). In fact, it seems that maternal programming by caloric exposure contributes to microglial activation and ASD appearance at early stages of life. In this context, brain microglia initially originated from the yolk sac during embryogenesis have an estimated median life span of >15 months in the mouse cortex (Askew et al., 2017; Füger et al., 2017; Tay et al., 2017), and of 4 years in humans, with some reports identifying a life span of 20 years (Réu et al., 2017). This selective long-lived identity benefits microglia by preserving its embryogenic phagocytic, immune, and pro-inflammatory profiles; however, they also might be compromised, favoring negative outcomes in adulthood if they were negatively primed during embryogenesis. Hence, if we assume that active microglia regulate a proper activity and experience-dependent refinement, setting a mature mesocorticolimbic connectome during neurodevelopment (Schafer & Stevens, 2015; Walport, 2001), it is conceivable that, in people with ASD, external pro-inflammatory stimuli during maternal obesity/overnutrition might prime microglial cells to disrupt the neuronal connectome. This would favor abnormal behavioral traits at earlier years of life. On this context,

recent reports have identified that fetal brain microglia from obese mothers displays a pro-inflammatory cytokine in response to immune LPS challenge (Edlow et al., 2019), a similar pattern of response was identified in glucose-deprived microglial cells, a pathological state included in diabetes (Churchward, Tchir, & Todd, 2018). We also reported that primed microglia from mothers programmed by exposure to western diet display major active profile followed by intrahypothalamic LPS administration (Maldonado-Ruiz, Cárdenas-Tueme, et al., 2019). In fact, microglial depletion still shows a pro-inflammatory and molecular signatures of aged microglia (O'Neil, Witcher, McKim, & Godbout, 2018) and shows hyperactivity after repopulation (Weber et al., 2019), suggesting that primed microglia conserve their original molecular signature when reaching adulthood. Notably, central accumulation of inflammatory monocytes in anxious mice was associated with microglial priming (McKim et al., 2016; Weber et al., 2019), which confirm the existence of a central microglial training favoring monocyte recruitment into the brain and defective behavior in the offspring. It is still open to debate whether maternal obesity primes the fetal brain microglia to show a pro-inflammatory profile and central recruitment of monocytes followed by a "second hit" stimuli in the offspring (Figures 2 and 3). Thus, an hypothetical pro-inflammatory stimuli during maternal obesity or exposure to maternal hypercaloric diet might set the MIA phenotype, favoring microglial priming to display enhanced, suppressed or unresponsive states to subsequent stimuli in the offspring (Picci & Scherf, 2015; Figure 3; see Table 2).

Finally, molecular identity of pathways assisting a direct link of microglial priming in maternal obese/overnutrition states to social avoidance in the offspring have not been totally stablished. Experimental evidence supports the notion that MIA might favor epigenetic modulation of DNA and genomic signatures during embryonic development which become mutually dependent by the host and fetus. Recent reports show that fetal programming by caloric exposure during development primes an epigenetic signature of gene expression which might persist even after long periods in the offspring, leading to aberrant behavioral phenotypes (Kereliuk, Brawerman, & Dolinsky, 2017; Maldonado-Ruiz, Garza-Ocañas, et al., 2019; Montalvo-Martínez et al., 2018). Epigenetic signatures including methylation, histone modification, and micro RNAs have been recently reported to closely set major molecular mechanism of innate immune training and metabolism during embryonic development. At this final stage of the manuscript, we add experimental evidence found in animal models addressing diet-induced methylation signatures as a molecular mechanism coordinating microglial priming and neuroinflammation and its potential role on social avoidance.

6 | METHYLOMIC SIGNATURES PRIME MICROGLIAL ACTIVATION IN THE MESOCORTICOLIMBIC CIRCUIT OF ASD SUBJECTS

Substantial experimental evidence has reported selective methylation changes in mesocorticolimbic regions in animal models and ASD subjects (See review for details of epigenetics on immune system in ASD (Nardone & Elliott, 2016). DNA methylation is a physiological molecular mechanism catalyzed by a family of closely related DNA methyltransferases. DNA methylation covers the modification of cytosine residues in the CpG dinucleotides within the gene sequences and histone methylation. In a general view, methylated DNA can recruit proteins from the methyl-CpG-binding domain Kaiso, MeCP2 (methyl-CpG-binding protein 2), and members of the MBD (Methyl-CpG-binding domain) family, which recognize 5-methylcytosines in CpG islands and participate in chromatin silencing (McCabe, Brandes, & Vertino, 2009). Perhaps the most elegant confirmation of the effect of hypercaloric diet on epigenetic immunological training was reported by Christ et al., 2018 (Christ et al., 2018), showing a selective epigenomic reprogramming of leukocytes in opened enhancer regions of ten-eleven 2 enzyme and in the TLR4. Notably, the ten-eleven enzymes function as DNA demethylases which relay on intracellular metabolic cues including the 2-oxoglutarate metabolite (Blaschke et al., 2013). This molecular mechanism represents a relatively new scientific field showing an interplay between metabolism and epigenetic reprogramming of immunity induced by caloric diets. Of importance, hypercaloric diets exposure in pregnant mice mothers are able to set epigenetic reprogramming including DNA hypomethylation and enhanced expression in the hypothalamic proopiomelanocortin (POMC) and melanocortin receptor 4 (MC4R) gene in the offspring (Zheng et al., 2015). Remarkably, fetal programmed mice by high-fat diet showed DNA methylation of the dopamine reuptake transporter in the VTA, PFC, and NAc regions (Ganu, Harris, Collins, & Aagaard, 2012; Vucetic, Kimmel, Totoki, Hollenbeck, & Reyes, 2010), and we have recently reported that mice fed with a CAF during pregnancy promotes an increase in methylation in the NAc of the offspring leading to defective motivation for rewards (Cruz-Carrillo et al., 2020). Also, mice fed with a high-fat diet during pregnancy overexpressed DNA methyltransferase 1 in the PFC which leads to a decrease in motivation for rewards in the offspring (Grissom, Herdt, Desilets, Lidsky-Everson, & Reyes, 2015). Consistently, these lines of evidence confirm that maternal exposure to hypercaloric formula in murine models sets selective methylation signatures in mesocorticolimbic regions modulating motivation for rewards in the offspring.

Substantial evidence in ASD subjects has supported the role of differential methylation signatures including hyper-and hypomethylation correlating with major behavioral traits of the disease (this topic was elegantly addressed by)). Precisely, differential methylation signatures have been identified for genes related to complement response in cell sorting-sorted neurons isolated from PFC of ASD subjects (Nardone, Sams, Zito, Reuveni, & Elliott, 2017). Differential methylation signatures within open chromatin regions in microglia were also enrichened in the PFC of ASD subjects (Vogel Ciernia et al., 2020). However, it is still unconfirmed if methylation accounts to activate microglial priming leading to neuroinflammation and its role on social avoidance. In vitro studies using microglial cells have tested this hypothesis by showing that pharmacologic inhibition of methylation favors IL-1β increases gene expression

(Cruz-Carrillo et al., 2020; Matt, Lawson, & Johnson, 2016), and phagocytic activity induced by lipopolysaccharide and palmitic acid stimulation (Cruz-Carrillo et al., 2020), suggesting that hypomethylation blocks pro-inflammatory profile and phagocytic activity in microglia. Together, it still remains to be determined whether hypercaloric diets do promote methylation signatures in microglia favoring a pro-inflammatory/phagocytic profile in mesocorticolimbic regions promoting social avoidance in ASD subjects.

Despite the strong experimental evidence previously commented, it is hard to be conclusive regarding potential and selective external stimuli performing microglial priming during maternal obesity/overnutrition. A potential molecular scenario would be that microglial response efficiently to hypercaloric diets to induce methylation marks and regulate immune training. Given that if the fetal pool origin of microglia is preserved up to 20 years (Réu et al., 2017), initial fetal microglial priming during pregnancy of obese mothers might overrespond to postnatal immune challenges, increasing the risk for social avoidance in people with ASD. In any case, a precise characterization of subjects born from obese mothers is necessary to categorize aberrant microglial activation and the risk to develop ASD. However, this strategy must integrate sophisticated platforms of direct assay molecular arrays during the normal brain development in an ongoing pregnancy or after birth. Potentially, these data will represent an initial step toward selective biomarker identity of microglial priming during pregnancy, the effect of maternal diet and pregnancy interactome, and the fetal neuroimmune activation that leads to aberrant brain development and disease susceptibility.

7 | CONCLUSION

Children with ASD exhibit social avoidance traits regulated by defective activity of the mesocorticolimbic reward pathway. Differences in brain neurochemical and immune components, and structural and functional mesocorticolimbic connectivity have been reported to encode social isolation. We propose that a positive energy balance during obesity/maternal overnutrition coordinates a systemic and central inflammatory crosstalk that modulates the dopaminergic neurotransmission in selective brain areas of the mesocorticolimbic reward pathway. However, a combination of post-mortem tissue analysis coupled to spatial and temporal resolution neuroimaging studies might be useful to confirm a potential role of maternal obesity/overnutrition linked to methylation signatures favoring microglial priming and social avoidance in ASD offspring subjects. Such approaches allow us to deconstruct the conceptions of ASD deeply to where they can be grounded in biology.

ACKNOWLEDGMENTS

The authors thank M.S. Alejandra Arreola-Triana for her support on editing this manuscript. The authors also thank María Fernanda García-Morales for her contribution on the figures design. This work was funded by the National Council of Science and Technology in Mexico (CONACYT), 781759 CONACYT for Luis Trujillo-Villarreal, 573686 CONACYT for Roger Maldonado-Ruiz, 650620 CONACYT for Marcela Cárdenas-Tueme. Also, IBRO-PROLAB 2020 for ACM.

CONFLICT OF INTEREST

The authors declare that the research was conducted in the absence of any commercial or financial relationships that could be construed as a potential conflict of interest.

ORCID

Luis A- Trujillo Villarreal https://orcid.org/0000-0002-8246-3054
Marcela Cárdenas-Tueme https://orcid.org/0000-0003-4259-6781
Roger Maldonado-Ruiz https://orcid.org/0000-0002-2093-0219
Diana Reséndez-Pérez https://orcid.org/0000-0002-4709-7677
Alberto Camacho-Morales https://orcid.org/0000-0002-2588-9489

REFERENCES

Abdallah, M. W., Larsen, N., Grove, J., Nørgaard-Pedersen, B., Thorsen, P., Mortensen, E. L., & Hougaard, D. M. (2013). Amniotic fluid inflammatory cytokines: Potential markers of immunologic dysfunction in autism spectrum disorders. *The World Journal of Biological Psychiatry*, *14*, 528–538.

Allsop, S. A., Vander Weele, C. M., Wichmann, R., & Tye, K. M. (2014). Optogenetic insights on the relationship between anxiety-related behaviors and social deficits. *Frontiers in Behavioural Neurosciences*, *8*, 1–14.

Alugubelly, N., Mohammed, A. N., Edelmann, M. J., Nanduri, B., Sayed, M., Park, J. W., & Carr, R. L. (2019). Adolescent rat social play: Amygdalar proteomic and transcriptomic data. *Data in Brief*, *27*, 104589–https://doi.org/10.1016/j.dib.2019.104589

American Psychiatric Association (2000). *Diagnostic and Statistical Manual of Mental Disorders, Fourth Edition, Text Revision*.

Andersen, C. H., Thomsen, P. H., Nohr, E. A., & Lemcke, S. (2018). Maternal body mass index before pregnancy as a risk factor for ADHD and autism in children. *European Child and Adolescent Psychiatry*, *27*, 139–148.

Argue, K. J., VanRyzin, J. W., Falvo, D. J., Whitaker, A. R., Yu, S. J., & McCarthy, M. M. (2017). Activation of both CB1 and CB2 endocannabinoid receptors is critical for masculinization of the developing medial amygdala and juvenile social play behavior. *Eneuro*, *4*, 1–20. https://doi.org/10.1523/ENEURO.0344-16.2017

Askew, K., Li, K., Olmos-Alonso, A., Garcia-Moreno, F., Liang, Y., Richardson, P., … Gomez-Nicola, D. (2017). Coupled proliferation and apoptosis maintain the rapid turnover of microglia in the adult brain. *Cell Reports*, *18*, 391–405. https://doi.org/10.1016/j.celrep.2016.12.041

Atladottir, H. O., Henriksen, T. B., Schendel, D. E., & Parner, E. T. (2012). Autism after infection, febrile episodes, and antibiotic use during pregnancy: An exploratory study. *Pediatrics*, *130*, e1447–e1454. https://doi.org/10.1542/peds.2012-1107

Atladóttir, H. Ó., Thorsen, P., Østergaard, L., Schendel, D. E., Lemcke, S., Abdallah, M., & Parner, E. T. (2010). Maternal infection requiring hospitalization during pregnancy and autism spectrum disorders. *Journal of Autism and Developmental Disorders*, *40*, 1423–1430.

Banik, A., Kandilya, D., Ramya, S., Stünkel, W., Chong, Y., & Dheen, S. (2017). Maternal factors that induce epigenetic changes contribute

to neurological disorders in offspring. *Genes (Basel)*, *8*, 150. https://doi.org/10.3390/genes8060150

Bariselli, S., Tzanoulinou, S., Glangetas, C., Prévost-Solié, C., Pucci, L., Viguié, J., … Bellone, C. (2016). SHANK3 controls maturation of social reward circuits in the VTA. *Nature Neuroscience*, *19*, 926–934.

Behmanesh, H., Moghaddam, H. S., Mohammadi, M. R., & Akhondzadeh, S. (2019). Risperidone combination therapy with propentofylline for treatment of irritability in autism spectrum disorders: A randomized, double-blind, placebo-controlled clinical trial. *Clinical Neuropharmacology*, *42*, 189–196. https://doi.org/10.1097/WNF.0000000000000368

Bekkering, S., Arts, R. J. W., Novakovic, B., Kourtzelis, I., van der Heijden, C. D. C. C., Li, Y., … Netea, M. G. (2018). Metabolic induction of trained immunity through the mevalonate pathway. *Cell*, *172*, 135–146.e9. https://doi.org/10.1016/j.cell.2017.11.025

Bilder, D. A., Bakian, A. V., Viskochil, J., Clark, E. A. S., Botts, E. L., Smith, K. R., … Coon, H. (2013). Maternal prenatal weight gain and autism spectrum disorders. *Pediatrics*, *132*, e1276–e1283. https://doi.org/10.1542/peds.2013-1188

Blaschke, K., Ebata, K. T., Karimi, M. M., Zepeda-Martínez, J. A., Goyal, P., Mahapatra, S., … Lorincz, M. C. (2013). Vitamin C induces Tet-dependent DNA demethylation and a blastocyst-like state in ES cells. *Nature*, *500*, 222–226.

Bowton, E., Saunders, C., Reddy, I. A., Campbell, N. G., Hamilton, P. J., Henry, L. K., … Galli, A. (2014). SLC6A3 coding variant Ala559Val found in two autism probands alters dopamine transporter function and trafficking. *Translational Psychiatry*, *4*, e464. https://doi.org/10.1038/tp.2014.90

Brimberg, L., Sadiq, A., Gregersen, P. K., & Diamond, B. (2013). Brain-reactive IgG correlates with autoimmunity in mothers of a child with an autism spectrum disorder. *Molecular Psychiatry*, *18*, 1171–1177.

Brucato, M., Ladd-Acosta, C., Li, M., Caruso, D., Hong, X., Kaczaniuk, J., … Wang, X. (2017). Prenatal exposure to fever is associated with autism spectrum disorder in the Boston birth cohort. *Autism Research*, *10*, 1878–1890. https://doi.org/10.1002/aur.1841

Cai, D., & Khor, S. (2019). "Hypothalamic Microinflammation" paradigm in aging and metabolic diseases. *Cell Metabolism*, *30*, 19–35.

Calipari, E. S., Godino, A., Peck, E. G., Salery, M., Mervosh, N. L., Landry, J. A., … Kiraly, D. D. (2018). Granulocyte-colony stimulating factor controls neural and behavioral plasticity in response to cocaine. *Nature Communications*, *9*, 9.

Camacho, A., Montalvo-Martinez, L., Cardenas-Perez, R. E., Fuentes-Mera, L., & Garza-Ocañas, L. (2017). Obesogenic diet intake during pregnancy programs aberrant synaptic plasticity and addiction-like behavior to a palatable food in offspring. *Behavioral Brain Research*, *330*, 46–55.

Cao, J.-L., Covington, H. E., Friedman, A. K., Wilkinson, M. B., Walsh, J. J., Cooper, D. C., … Han, M.-H. (2010). Mesolimbic dopamine neurons in the brain reward circuit mediate susceptibility to social defeat and antidepressant action. *Journal of Neuroscience*, *30*, 16453–16458. https://doi.org/10.1523/JNEUROSCI.3177-10.2010

Cárdenas-Tueme, M., Montalvo-Martínez, L., Maldonado-Ruiz, R., Camacho-Morales, A., & Reséndez-Pérez, D. (2020). Neurodegenerative susceptibility during maternal nutritional programing: Are central and peripheral innate immune training relevant? *Frontiers in Neuroscience*, *14*, 1–12.

Careaga, M., Murai, T., & Bauman, M. D. (2017). Maternal immune activation and autism spectrum disorder: From rodents to nonhuman and human primates. *Biological Psychiatry*, *81*, 391–401.

Chen, S. W., Zhong, X. S., Jiang, L. N., Zheng, X. Y., Xiong, Y. Q., Ma, S. J., … Chen, Q. (2016). Maternal autoimmune diseases and the risk of autism spectrum disorders in offspring: A systematic review and meta-analysis. *Behavioral Brain Research*, *296*, 61–69.

Chevallier, C., Kohls, G., Troiani, V., Brodkin, E. S., & Schultz, R. T. (2012). The social motivation theory of autism. *Trends in Cognitive Sciences*, *16*, 231–239.

Chitu, V., & Stanley, E. R. (2006). Colony-stimulating factor-1 in immunity and inflammation. *Current Opinion in Immunology*, *18*, 39–48.

Christ, A., Günther, P., Lauterbach, M. A. R., Duewell, P., Biswas, D., Pelka, K., … Latz, E. (2018). Western diet triggers NLRP3-dependent innate immune reprogramming. *Cell*, *172*, 162–175.e14. https://doi.org/10.1016/j.cell.2017.12.013

Christensen, D. L., Baio, J., Braun, K. V. N., Bilder, D., Charles, J., Constantino, J. N., … Yeargin-Allsopp, M. (2016). Prevalence and characteristics of autism spectrum disorder among children aged 8 years — Autism and Developmental Disabilities Monitoring Network, 11 Sites, United States, 2012. *MMWR Surveillance Summary*, *65*, 1–23. https://doi.org/10.15585/mmwr.ss6503a1

Christian, L. M., & Porter, K. (2014). Longitudinal changes in serum proinflammatory markers across pregnancy and postpartum: Effects of maternal body mass index. *Cytokine*, *70*, 134–140. https://doi.org/10.1016/j.cyto.2014.06.018

Churchward, M. A., Tchir, D. R., & Todd, K. G. (2018). Microglial function during glucose deprivation: Inflammatory and neuropsychiatric implications. *Molecular Neurobiology*, *55*, 1477–1487. https://doi.org/10.1007/s12035-017-0422-9

Clements, C. C., Zoltowski, A. R., Yankowitz, L. D., Yerys, B. E., Schultz, R. T., & Herrington, J. D. (2018). Evaluation of the social motivation hypothesis of autism a systematic review and meta-analysis. *JAMA Psychiatry*, *75*, 797–808. https://doi.org/10.1001/jamapsychiatry.2018.1100

Cruz-Carrillo, G., Montalvo-Martínez, L., Cárdenas-Tueme, M., Bernal-Vega, S., Maldonado-Ruiz, R., Reséndez-Pérez, D., … Camacho-Morales, A. (2020). Fetal programming by methyl donors modulates central inflammation and prevents food addiction-like behavior in rats. *Frontiers in Neuroscience*, *14*, 1–15.

Dawson, G., Toth, K., Abbott, R., Osterling, J., Munson, J., Estes, A., & Liaw, J. (2004). Early social attention impairments in autism: Social orienting, joint attention, and attention to distress. *Developmental Psychology*, *40*, 271–283. https://doi.org/10.1037/0012-1649.40.2.271

Dawson, G., Webb, S. J., & McPartland, J. (2005). Understanding the nature of face processing impairment in autism: Insights from behavioral and electrophysiological studies. *Developmental Neuropsychology*, *27*, 403–424. https://doi.org/10.1207/s15326942dn2703_6

de la Garza, A., Garza-Cuellar, M., Silva-Hernandez, I., Cardenas-Perez, R., Reyes-Castro, L., Zambrano, E., … Camacho, A. (2019). Maternal flavonoids intake reverts depression-like behaviour in rat female offspring. *Nutrients*, *11*, 572. https://doi.org/10.3390/nu11030572

De Souza, C. T., Araujo, E. P., Bordin, S., Ashimine, R., Zollner, R. L., Boschero, A. C., … Velloso, L. A. (2005). Consumption of a fat-rich diet activates a proinflammatory response and induces insulin resistance in the hypothalamus. *Endocrinology*, *146*, 4192–4199. https://doi.org/10.1210/en.2004-1520

Delgado, M. R., Nystrom, L. E., Fissell, C., Noll, D. C., & Fiez, J. A. (2000). Tracking the hemodynamic responses to reward and punishment in the striatum. *Journal of Neurophysiology*, *84*, 3072–3077. https://doi.org/10.1152/jn.2000.84.6.3072

Delint-Ramirez, I., Maldonado, R. R., Torre-Villalvazo, I., Fuentes-Mera, L., Garza, O. L., Tovar, A., & Camacho, A. (2015). Genetic obesity alters recruitment of TANK-binding kinase 1 and AKT into hypothalamic lipid rafts domains. *Neurochemistry International*, *80*, 23–32.

Delmonte, S., Balsters, J. H., McGrath, J., Fitzgerald, J., Brennan, S., Fagan, A. J., & Gallagher, L. (2012). Social and monetary reward processing in autism spectrum disorders. *Molecular Autism*, *3*, 1.

Di Martino, A., Kelly, C., Grzadzinski, R., Zuo, X.-N., Mennes, M., Mairena, M. A., … Milham, M. P. (2011). Aberrant striatal functional connectivity in children with autism. *Biological Psychiatry*, *69*, 847–856.

Diaz, B., Fuentes-Mera, L., Tovar, A., Montiel, T., Massieu, L., Martínez-Rodríguez, H. G., & Camacho, A. (2015). Saturated lipids decrease mitofusin 2 leading to endoplasmic reticulum stress activation and insulin resistance in hypothalamic cells. *Brain Research*, *1627*, 80–89. https://doi.org/10.1016/j.brainres.2015.09.014

DiCarlo, G. E., Aguilar, J. I., Matthies, H. J. G., Harrison, F. E., Bundschuh, K. E., West, A., … Galli, A. (2019). Autism-linked dopamine transporter mutation alters striatal dopamine neurotransmission and dopamine-dependent behaviors. *Journal of Clinical Investigation*, *129*(8), 3407–3419. https://doi.org/10.1172/JCI127411

Dichter, G. S., Damiano, C. A., & Allen, J. A. (2012) Reward circuitry dysfunction in psychiatric and neurodevelopmental disorders and genetic syndromes: Animal models and clinical findings. *Journal of Neurodevelopmental Disorders*, *4*(1), https://doi.org/10.1186/1866-1955-4-19

Dichter, G. S., Richey, J. A., Rittenberg, A. M., Sabatino, A., & Bodfish, J. W. (2012). Reward circuitry function in autism during face anticipation and outcomes. *Journal of Autism and Developmental Disorders*, *42*, 147–160. https://doi.org/10.1007/s10803-011-1221-1

Dölen, G., Darvishzadeh, A., Huang, K. W., & Malenka, R. C. (2013). Social reward requires coordinated activity of nucleus accumbens oxytocin and serotonin. *Nature*, *501*, 179–184. https://doi.org/10.1038/nature12518

Duan, X., Wang, R., Xiao, J., Li, Y. A., Huang, X., Guo, X., … Chen, H. (2020). Subcortical structural covariance in young children with autism spectrum disorder. *Progress in Neuro-Psychopharmacology and Biological Psychiatry*, *99*. https://doi.org/10.1016/j.pnpbp.2020.109874

Edlow, A. G. (2018). Maternal obesity and neurodevelopmental and psychiatric disorders in offspring. *Prenatal Diagnosis*, *37*, 95–110.

Edlow, A. G., Glass, R. M., Smith, C. J., Tran, P. K., James, K., & Bilbo, S. (2019). Placental macrophages: A window into fetal microglial function in maternal obesity. *International Journal of Developmental Neuroscience*, *77*, 60–68.

Edmiston, E., Jones, K. L., Vu, T., Ashwood, P., & Van de Water, J. (2018). Identification of the antigenic epitopes of maternal autoantibodies in autism spectrum disorders. *Brain, Behavior, and Immunity*, *69*, 399–407.

Eisenegger, C., Pedroni, A., Rieskamp, J., Zehnder, C., Ebstein, R., Fehr, E., & Knoch, D. (2013). DAT1 polymorphism determines L-DOPA effects on learning about others' prosociality. *PLoS One*, *8*(7), e67820. https://doi.org/10.1371/journal.pone.0067820

Elison, J. T., Wolff, J. J., Reznick, J. S., Botteron, K. N., Estes, A. M., Gu, H., … Piven, J. (2014). Repetitive behavior in 12-month-olds later classified with autism spectrum disorder. *Journal of the American Academy of Child and Adolescent Psychiatry*, *53*, 1216–1224.

Ernst, M., Zametkin, A. J., Matochik, J. A., Pascualvaca, D., & Cohen, R. M. (1997). Low medial prefrontal dopaminergic activity in autistic children. *Lancet*, *350*, 638. https://doi.org/10.1016/S0140-6736(05)63326-0

Esteban, O., Markiewicz, C. J., Blair, R. W., Moodie, C. A., Isik, A. I., Erramuzpe, A., … Oya, H. (2019). fMRIPrep: A robust preprocessing pipeline for functional MRI. *Nature Methods*, *16*, 111–116.

Fatemi, S. H., Aldinger, K. A., Ashwood, P., Bauman, M. L., Blaha, C. D., Blatt, G. J., … Welsh, J. P. (2012). Consensus paper: pathological role of the cerebellum in autism. *The Cerebellum*, *11*, 777–807. https://doi.org/10.1007/s12311-012-0355-9

Forbes, E. E., Hariri, A. R., Martin, S. L., Silk, J. S., Moyles, D. L., Fisher, P. M., … Dahl, R. E. (2009). Altered striatal activation predicting real-world positive affect in adolescent major depressive disorder. *American Journal of Psychiatry*, *166*, 64–73.

Forouzannezhad, P., Abbaspour, A., Fang, C., Cabrerizo, M., Loewenstein, D., Duara, R., & Adjouadi, M. (2019). A survey on applications and analysis methods of functional magnetic resonance imaging for Alzheimer's disease. *Journal of Neuroscience Methods*, *317*, 121–140.

Fox-Edmiston, E. & Van de Water, J. (2015). Maternal anti-fetal brain IgG autoantibodies and autism spectrum disorder: Current knowledge and its implications for potential therapeutics. *CNS Drugs*, *29*, 715–724. https://doi.org/10.1007/s40263-015-0279-2

Fu, L., Wang, Y., Fang, H., Xiao, X., Xiao, T., Li, Y., … Ke, X. (2020). Longitudinal study of brain asymmetries in autism and developmental delays aged 2–5 years. *Neuroscience*, *432*, 137–149.

Füger, P., Hefendehl, J. K., Veeraraghavalu, K., Wendeln, A.-C., Schlosser, C., Obermüller, U., … Thunemann, M. (2017). Microglia turnover with aging and in an Alzheimer's model via long-term in vivo single-cell imaging. *Nature Neuroscience*, *20*, 1371–1376.

Gadow, K. D., Devincent, C. J., Olvet, D. M., Pisarevskaya, V., & Hatchwell, E. (2010). Association of DRD4 polymorphism with severity of oppositional defiant disorder, separation anxiety disorder and repetitive behaviors in children with autism spectrum disorder. *European Journal of Neuroscience*, *32*, 1058–1065.

Ganu, R. S., Harris, R. A., Collins, K., & Aagaard, K. M. (2012). Early origins of adult disease: Approaches for investigating the programmable epigenome in humans, nonhuman primates, and rodents. *ILAR Journal*, *53*, 306–321. https://doi.org/10.1093/ilar.53.3-4.306

Gesundheit, B., Rosenzweig, J. P., Naor, D., Lerer, B., Zachor, D. A., Procházka, V., … Ashwood, P. (2013). Immunological and autoimmune considerations of autism spectrum disorders. *Journal of Autoimmunity*, *44*, 1–7. https://doi.org/10.1016/j.jaut.2013.05.005

Ginhoux, F., Greter, M., Leboeuf, M., Nandi, S., See, P., Gokhan, S., … Samokhvalov, I. M. (2010). Fate mapping analysis reveals that adult microglia derive from primitive macrophages. *Science*, *330*, 841–845.

Glass, R., Norton, S., Fox, N., & Kusnecov, A. W. (2019). Maternal immune activation with staphylococcal enterotoxin A produces unique behavioral changes in C57BL/6 mouse offspring. *Brain, Behavior, and Immunity*, *75*, 12–25.

Graham, A. M., Rasmussen, J. M., Rudolph, M. D., Heim, C. M., Gilmore, J. H., Styner, M., … Buss, C. (2018). Maternal systemic interleukin-6 during pregnancy is associated with newborn amygdala phenotypes and subsequent behavior at 2 years of age. *Biological Psychiatry*, *83*, 109–119.

Grayson, B. E., Levasseur, P. R., Williams, S. M., Smith, M. S., Marks, D. L., & Grove, K. L. (2010). Changes in melanocortin expression and inflammatory pathways in fetal offspring of nonhuman primates fed a high-fat diet. *Endocrinology*, *151*(4), 1622-1632.

Gréa, H., Scheid, I., Gaman, A., Rogemond, V., Gillet, S., Honnorat, J., … Bouvard, M. (2017). Clinical and autoimmune features of a patient with autism spectrum disorder seropositive for anti-NMDA-receptor autoantibody. *Dialogues in Clinical Neuroscience*, *19*, 65–70.

Greene, R. K., Spanos, M., Alderman, C., Walsh, E., Bizzell, J., Mosner, M. G., … Sikich, L. (2018). The effects of intranasal oxytocin on reward circuitry responses in children with autism spectrum disorder. *Journal of Neurodevelopmental Disorders*, *10*, 1–16.

Gregor, M. F., & Hotamisligil, G. S. (2011). Inflammatory mechanisms in obesity. *Annual Review of Immunology*, *29*, 415–445. https://doi.org/10.1146/annurev-immunol-031210-101322

Grissom, N. M., Herdt, C. T., Desilets, J., Lidsky-Everson, J., & Reyes, T. M. (2015). Dissociable deficits of executive function caused by gestational adversity are linked to specific transcriptional changes in the prefrontal cortex. *Neuropsychopharmacology*, *40*, 1353–1363. https://doi.org/10.1038/npp.2014.313

Gunaydin, L. A., Grosenick, L., Finkelstein, J. C., Kauvar, I. V., Fenno, L. E., Adhikari, A., … Deisseroth, K. (2014). Natural neural projection dynamics underlying social behavior. *Cell*, *157*, 1535–1551. https://doi.org/10.1016/j.cell.2014.05.017

Haigh, S. M., Keller, T. A., Minshew, N. J., & Eack, S. M. (2020). Reduced white matter integrity and deficits in neuropsychological functioning in adults with autism spectrum disorder. *Autism Research*, *13*(5), 702–714. https://doi.org/10.1002/aur.2271

Hazlett, H., Poe, M., Greig, G., Styner, M., Chappell, C., Smith, R. G., … Piven, J. (2011). Early brain overgrowth in autism associated with an increase in cortical surface area before age 2. *Archives of General Psychiatry*, *68*, 467–476.

Herold, F., Aye, N., Lehmann, N., Taubert, M., & Müller, N. G. (2020). The contribution of functional magnetic resonance imaging to the understanding of the effects of acute physical exercise on cognition. *Brain Sciences*, *10*(3), 175. https://doi.org/10.3390/brainsci10030175

Hu, C.-C., Xu, X., Xiong, G.-L., Xu, Q., Zhou, B.-R., Li, C.-Y., … Yu, X. (2018). Alterations in plasma cytokine levels in chinese children with autism spectrum disorder. *Autism Research*, *11*, 989–999. https://doi.org/10.1002/aur.1940

Hung, L. W., Neuner, S., Polepalli, J. S., Beier, K. T., Wright, M., Walsh, J. J., … Malenka, R. C. (2017). Gating of social reward by oxytocin in the ventral tegmental area. *Science*, *357*, 1406–1411.

Ieronymaki, E., Daskalaki, M. G., Lyroni, K., & Tsatsanis, C. (2019). Insulin signaling and insulin resistance facilitate trained immunity in macrophages through metabolic and epigenetic changes. *Frontiers in Immunology*, *10*, 1–8. https://doi.org/10.3389/fimmu.2019.01330

Ieronymaki, E., Theodorakis, E. M., Lyroni, K., Vergadi, E., Lagoudaki, E., Al-Qahtani, A., … Tsatsanis, C. (2019). Insulin resistance in macrophages alters their metabolism and promotes an M2-like phenotype. *The Journal of Immunology*, *202*, 1786–1797. https://doi.org/10.4049/jimmunol.1800065

Im, W. Y., Ha, J. H., Kim, E. J., Cheon, K. A., Cho, J., & Song, D. H. (2018). Impaired white matter integrity and social cognition in high-function autism: Diffusion tensor imaging study. *Psychiatry Investigation*, *15*, 292–299. https://doi.org/10.30773/pi.2017.08.15

Jack, A. (2018). Neuroimaging in neurodevelopmental disorders: Focus on resting-state fMRI analysis of intrinsic functional brain connectivity. *Current Opinion in Neurology*, *31*, 140–148. https://doi.org/10.1097/WCO.0000000000000536

Jiang, H. Y., Xu, L. L., Shao, L., Xia, R. M., Yu, Z. H., Ling, Z. X., … Ruan, B. (2016). Maternal infection during pregnancy and risk of autism spectrum disorders: A systematic review and meta-analysis. *Brain, Behavior, and Immunity*, *58*, 165–172.

Jiang, L., & Zuo, X. N. (2016). Regional homogeneity: A multimodal, multiscale neuroimaging marker of the human connectome. *Neuroscientist*, *22*, 486–505. https://doi.org/10.1177/1073858415595004

Jiang, N. M., Cowan, M., Moonah, S. N., & Petri, W. A. (2018). The impact of systemic inflammation on neurodevelopment. *Trends in Molecular Medicine*, *24*, 794–804.

Jones, K. L., & Van de Water, J. (2019). Maternal autoantibody related autism: Mechanisms and pathways. *Molecular Psychiatry*, *24*, 252–265.

Kereliuk, S., Brawerman, G., & Dolinsky, V. (2017). Maternal macronutrient consumption and the developmental origins of metabolic disease in the offspring. *International Journal of Molecular Sciences*, *18*, 1451.

Kim, S., Kim, H., Yim, Y. S., Ha, S., Atarashi, K., Tan, T. G., … Huh, J. R. (2017). Maternal gut bacteria promote neurodevelopmental abnormalities in mouse offspring. *Nature*, *549*, 528–532. https://doi.org/10.1038/nature23910

Kirsten, T. B., Taricano, M., Flório, J. C., Palermo-Neto, J., & Bernardi, M. M. (2010). Prenatal lipopolysaccharide reduces motor activity after an immune challenge in adult male offspring. *Behavioral Brain Research*, *211*, 77–82.

Kishida, K. T., Asis-Cruz, J., De, T.-D., Liebenow, B., Beauchamp, M. S., & Montague, P. R. (2019). Diminished single-stimulus response in vmPFC to favorite people in children diagnosed with autism spectrum disorder. *Biological Psychology*, *145*, 174–184.

Kohls, G., Antezana, L., Mosner, M. G., Schultz, R. T., & Yerys, B. E. (2018). Altered reward system reactivity for personalized circumscribed interests in autism. *Molecular Autism*, *9*, 1–12.

Kohls, G., Schulte-Rüther, M., Nehrkorn, B., Müller, K., Fink, G. R., Kamp-Becker, I., … Konrad, K. (2013). Reward system dysfunction in autism spectrum disorders. *Social Cognitive and Affective Neuroscience*, *8*, 565–572.

Kohls, G., Thönessen, H., Bartley, G. K., Grossheinrich, N., Fink, G. R., Herpertz-Dahlmann, B., & Konrad, K. (2014). Differentiating neural reward responsiveness in autism versus ADHD. *Developmental Cognitive Neuroscience*, *10*, 104–116.

Kopec Ashley M., Smith Caroline J., Ayre Nathan R., Sweat Sean C., Bilbo Staci D. (2018). Microglial dopamine receptor elimination defines sex-specific nucleus accumbens development and social behavior in adolescent rats. *Nature Communications*, *9*, (1), 1–16. http://dx.doi.org/10.1038/s41467-018-06118-z.

Krakowiak, P., Walker, C. K., Bremer, A. A., Baker, A. S., Ozonoff, S., Hansen, R. L., & Hertz-Picciotto, I. (2012). Maternal metabolic conditions and risk for autism and other neurodevelopmental disorders. *Pediatrics*, *129*, e1121–e1128. https://doi.org/10.1542/peds.2011-2583

Krakowiak, P., Walker, C. K., Tancredi, D., Hertz-Picciotto, I., & Van de Water, J. (2017). Autism-specific maternal anti-fetal brain autoantibodies are associated with metabolic conditions. *Autism Research*, *10*, 89–98. https://doi.org/10.1002/aur.1657

Kutlu, M. G., Brady, L. J., Peck, E. G., Hofford, R. S., Yorgason, J. T., Siciliano, C. A., … Calipari, E. S. (2018). Granulocyte colony stimulating factor enhances reward learning through potentiation of mesolimbic dopamine system function. *The Journal of Neuroscience*, *38*(41), 8845–8859. https://doi.org/10.1523/JNEUROSCI.1116-18.2018

Lee, Y., & Han, P. L. (2019). Early-life stress in D2 heterozygous mice promotes autistic-like behaviors through the downregulation of the BDNF-TrkB pathway in the dorsal striatum. *Experimental Neurobiology*, *28*(3), 337–351. https://doi.org/10.5607/en.2019.28.3.337

Lerch, J. P., Sled, J. G., & Henkelman, R. M. (2011) MRI phenotyping of genetically altered mice. *Methods in molecular biology (Clifton, N.J.)*, *711*, 349–361.https://doi.org/10.1007/978-1-61737-992-5_17.

Lewis, M., Tanimura, Y., Lee, L., & Bodfish, J. (2007). Animal models of restricted repetitive behavior in autism. *Behavioral Brain Research*, *176*, 66–74.

Li, G., Chen, M.-H., Li, G., Wu, D., Lian, C., Sun, Q., … Wang, L. (2019). A longitudinal MRI study of amygdala and hippocampal subfields for infants with risk of autism. *Graph Learning in Medical Imaging*, *11849*, 164–171.

Li, M., Fallin, M. D., Riley, A., Landa, R., Walker, S. O., Silverstein, M., … Hong, X. (2016). The association of maternal obesity and diabetes with autism and other developmental disabilities. *Pediatrics*, *137*, e20152206.

Li, X., Chauhan, A., Sheikh, A. M., Patil, S., Chauhan, V., Li, X.-M., … Malik, M. (2009). Elevated immune response in the brain of autistic patients. *Journal of Neuroimmunology*, *207*, 111–116. https://doi.org/10.1016/j.jneuroim.2008.12.002

Liu, A., & Shifang, D. (2019). Anti-inflammatory effects of dopamine in lipopolysaccharide (LPS)-stimulated RAW264.7 cells via inhibiting NLRP3 inflammasome activation. *Annals of Clinical and Laboratory Science*, *3*, 353–360.

Lobo, M. K., & Nestler, E. J. (2011). The striatal balancing act in drug addiction: Distinct roles of direct and indirect pathway medium spiny neurons. *Frontiers in Neuroanatomy*, *5*, 1–11. https://doi.org/10.3389/fnana.2011.00041

Lockwood, P. L., & Wittmann, M. K. (2018). Ventral anterior cingulate cortex and social decision-making. *Neuroscience and Biobehavioral Reviews*, *92*, 187–191.

Lynch, C. J., Uddin, L. Q., Supekar, K., Khouzam, A., Phillips, J., & Menon, V. (2013). Default mode network in childhood autism: Posteromedial cortex heterogeneity and relationship with social deficits. *Biological Psychiatry*, *74*, 212–219.

Maldonado-Ruiz, R., Cárdenas-Tueme, M., Montalvo-Martínez, L., Vidaltamayo, R., Garza-Ocañas, L., Reséndez-Perez, D., & Camacho, A. (2019). Priming of hypothalamic ghrelin signaling and microglia

activation exacerbate feeding in rats' offspring following maternal overnutrition. *Nutrients*, *11*. https://doi.org/10.3390/nu11061241

Maldonado-Ruiz, R., Fuentes-Mera, L., & Camacho, A. (2017). Central modulation of neuroinflammation by neuropeptides and energy-sensing hormones during obesity. *BioMed Research International*, *2017*, 1–12. https://doi.org/10.1155/2017/7949582

Maldonado-Ruiz, R., Garza-Ocañas, L., & Camacho, A. (2019). Inflammatory domains modulate autism spectrum disorder susceptibility during maternal nutritional programming. *Neurochemistry International*, *126*, 109–117. https://doi.org/10.1016/j.neuint.2019.03.009

Maldonado-Ruiz, R., Montalvo-Martínez, L., Fuentes-Mera, L., & Camacho, A. (2017). Microglia activation due to obesity programs metabolic failure leading to type two diabetes. *Nutrition and Diabetes*, *7*, e254. https://doi.org/10.1038/nutd.2017.10

Manduca, A., Servadio, M., Damsteegt, R., Campolongo, P., Vanderschuren, L. J., & Trezza, V. (2016). Dopaminergic neurotransmission in the nucleus accumbens modulates social play behavior in rats. *Neuropsychopharmacology*, *41*, 2215–2223. https://doi.org/10.1038/npp.2016.22

Masi, A., Breen, E. J., Alvares, G. A., Glozier, N., Hickie, I. B., Hunt, A., … Whitehouse, A. J. (2017). Cytokine levels and associations with symptom severity in male and female children with autism spectrum disorder. *Molecular Autism*, *8*, 63.

Matt, S. M., Lawson, M. A., & Johnson, R. W. (2016). Aging and peripheral lipopolysaccharide can modulate epigenetic regulators and decrease IL-1β promoter DNA methylation in microglia. *Neurobiology of Aging*, *47*, 1–9.

McCabe, M. T., Brandes, J. C., & Vertino, P. M. (2009). Cancer DNA methylation: Molecular mechanisms and clinical implications. *Clinical Cancer Research*, *15*, 3927–3937. https://doi.org/10.1158/1078-0432.CCR-08-2784

McKim, D. B., Patterson, J. M., Wohleb, E. S., Jarrett, B. L., Reader, B. F., Godbout, J. P., & Sheridan, J. F. (2016). Sympathetic release of splenic monocytes promotes recurring anxiety following repeated social defeat. *Biological Psychiatry*, *79*, 803–813.

Meyer, U., Nyffeler, M., Schwendener, S., Knuesel, I., Yee, B. K., & Feldon, J. (2008). Relative prenatal and postnatal maternal contributions to schizophrenia-related neurochemical dysfunction after in utero immune challenge. *Neuropsychopharmacology*, *33*, 441–456. https://doi.org/10.1038/sj.npp.1301413

Milanski, M., Degasperi, G., Coope, A., Morari, J., Denis, R., Cintra, D. E., … Velloso, L. A. (2009). saturated fatty acids produce an inflammatory response predominantly through the activation of TLR4 signaling in hypothalamus: Implications for the pathogenesis of obesity. *Journal of Neuroscience*, *29*, 359–370. https://doi.org/10.1523/JNEUROSCI.2760-08.2009

Mohammad-Rezazadeh, I., Frohlich, J., Loo, S. K., & Jeste, S. S. (2016). Brain connectivity in autism spectrum disorder. *Current Opinion in Neurology*, *29*, 137–147.

Montalvo-Martínez, L., Maldonado-Ruiz, R., Cárdenas-Tueme, M., Reséndez-Pérez, D., & Camacho, A. (2018). Maternal overnutrition programs central inflammation and addiction-like behavior in offspring. *BioMed Research International*, *2018*, 8061389.

Moratalla, R., Xu, M., Tonegawa, S., & Graybiel, A. M. (1996). Cellular responses to psychomotor stimulant and neuroleptic drugs are abnormal in mice lacking the D1 dopamine receptor. *Proceedings of the National Academy of Sciences of the United States of America*, *93*, 14928–14933.

Morgan, J. T., Chana, G., Abramson, I., Semendeferi, K., Courchesne, E., & Everall, I. P. (2012). Abnormal microglial–neuronal spatial organization in the dorsolateral prefrontal cortex in autism. *Brain Research*, *1456*, 72–81. https://doi.org/10.1016/j.brainres.2012.03.036

Morgan, J. T., Chana, G., Pardo, C. A., Achim, C., Semendeferi, K., Buckwalter, J., … Everall, I. P. (2010). Microglial activation and increased microglial density observed in the dorsolateral prefrontal cortex in autism. *Biological Psychiatry*, *68*, 368–376.

Nadeem, A., Ahmad, S. F., Attia, S. M., Bakheet, S. A., Al-Harbi, N. O., & AL-Ayadhi L. Y. (2018). Activation of IL-17 receptor leads to increased oxidative inflammation in peripheral monocytes of autistic children. *Brain, Behavior, and Immunity*, *67*, 335–344.

Naef, L., Moquin, L., Dal Bo, G., Giros, B., Gratton, A., & Walker, C.-D. (2011). Maternal high-fat intake alters presynaptic regulation of dopamine in the nucleus accumbens and increases motivation for fat rewards in the offspring. *Neuroscience*, *176*, 225–236. https://doi.org/10.1016/j.neuroscience.2010.12.037

Naef, L., Srivastava, L., Gratton, A., Hendrickson, H., Owens, S. M., & Walker, C. D. (2008). Maternal high fat diet during the perinatal period alters mesocorticolimbic dopamine in the adult rat offspring: reduction in the behavioral responses to repeated amphetamine administration. *Psychopharmacology*, *197*(1), 83-94.

Nardone, S., & Elliott, E. (2016). The interaction between the immune system and epigenetics in the etiology of autism spectrum disorders. *Frontiers in Neuroscience*, *10*, 1–9. https://doi.org/10.3389/fnins.2016.00329

Nardone, S., Sams, D. S., Zito, A., Reuveni, E., & Elliott, E. (2017). Dysregulation of cortical neuron DNA methylation profile in autism spectrum disorder. *Cerebral Cortex*, *27*, 5739–5754. https://doi.org/10.1093/cercor/bhx250

Neale, B. M., Kou, Y., Liu, L. I., Ma'ayan, A., Samocha, K. E., Sabo, A., … Daly, M. J. (2012). Patterns and rates of exonic de novo mutations in autism spectrum disorders. *Nature*, *485*, 242–245. https://doi.org/10.1038/nature11011

Neher, J. J., & Cunningham, C. (2019). Priming microglia for innate immune memory in the brain. *Trends in Immunology*, *40*, 358–374. https://doi.org/10.1016/j.it.2019.02.001

Netea, M. G., Domínguez-Andrés, J., Barreiro, L. B., Chavakis, T., Divangahi, M., Fuchs, E., … Latz, E. (2020). Defining trained immunity and its role in health and disease. *Nature Reviews Immunology*, *20*(6), 375–388. https://doi.org/10.1038/s41577-020-0285-6

Netea, M. G., Quintin, J., & van der Meer, J. W. M. (2011). Trained immunity: A memory for innate host defense. *Cell Host and Microbe*, *9*, 355–361. https://doi.org/10.1016/j.chom.2011.04.006

Nie, X., Kitaoka, S., Tanaka, K., Segi-Nishida, E., Imoto, Y., Ogawa, A., … Furuyashiki, T. (2018). The innate immune receptors TLR2/4 mediate repeated social defeat stress-induced social avoidance through prefrontal microglial activation. *Neuron*, *99*, 464–479.e7. https://doi.org/10.1016/j.neuron.2018.06.035

Nielsen, P. R., Benros, M. E., & Dalsgaard, S. (2017). Associations between autoimmune diseases and attention-deficit/hyperactivity disorder: A Nationwide Study. *Journal of the American Academy of Child and Adolescent Psychiatry*, *56*, 234–240.e1.

O'Neil, S. M., Witcher, K. G., McKim, D. B., & Godbout, J. P. (2018). Forced turnover of aged microglia induces an intermediate phenotype but does not rebalance CNS environmental cues driving priming to immune challenge. *Acta Neuropathologica Communications*, *6*, 129.

Oosterhof, N., Chang, I. J., Karimiani, E. G., Kuil, L. E., Jensen, D. M., Daza, R., … Demmers, J. (2019). Homozygous mutations in CSF1R cause a pediatric-onset leukoencephalopathy and can result in congenital absence of microglia. *American Journal of Human Genetics*, *104*, 936–947.

Oskvig, D. B., Elkahloun, A. G., Johnson, K. R., Phillips, T. M., & Herkenham, M. (2012). Maternal immune activation by LPS selectively alters specific gene expression profiles of interneuron migration and oxidative stress in the fetus without triggering a fetal immune response. *Brain, Behavior, and Immunity*, *26*, 623–634.

Ozawa, K., Hashimoto, K., Kishimoto, T., Shimizu, E., Ishikura, H., & Iyo, M. (2006). Immune activation during pregnancy in mice leads to dopaminergic hyperfunction and cognitive impairment in the offspring:

A neurodevelopmental animal model of schizophrenia. *Biological Psychiatry*, *59*, 546–554.

Ozonoff, S., Macari, S., Young, G. S., Goldring, S., Thompson, M., & Rogers, S. J. (2008). Atypical object exploration at 12 months of age is associated with autism in a prospective sample. *Autism*, *12*, 457–472.

Paolicelli, R. C., Bolasco, G., Pagani, F., Maggi, L., Scianni, M., Panzanelli, P., … Ragozzino, D. (2011). Synaptic pruning by microglia is necessary for normal brain development. *Science*, *333*, 1456–1458.

Pardo, C. A., Farmer, C. A., Thurm, A., Shebl, F. M., Ilieva, J., Kalra, S., & Swedo, S. (2017). Serum and cerebrospinal fluid immune mediators in children with autistic disorder: A longitudinal study. *Molecular Autism*, *8*, 1.

Park, M. T. M., Raznahan, A., Shaw, P., Gogtay, N., Lerch, J. P., & Chakravarty, M. M. (2018). Neuroanatomical phenotypes in mental illness: Identifying convergent and divergent cortical phenotypes across autism, ADHD and schizophrenia. *Journal of Psychiatry and Neuroscience*, *43*, 201–212. https://doi.org/10.1503/jpn.170094

Patel, S., Masi, A., Dale, R. C., Whitehouse, A. J. O., Pokorski, I., Alvares, G. A., … Guastella, A. J. (2018). Social impairments in autism spectrum disorder are related to maternal immune history profile. *Molecular Psychiatry*, *23*, 1794–1797.

Pavăl, D. (2017). A dopamine hypothesis of autism spectrum disorder. *Developmental Neuroscience*, *39*, 355–360.

Picci, G., & Scherf, K. S. (2015). A two-hit model of autism. *Clinical Psychological Science*, *3*, 349–371.

Presti, M. F., Mikes, H. M., & Lewis, M. H. (2003). Selective blockade of spontaneous motor stereotypy via intrastriatal pharmacological manipulation. *Pharmacology, Biochemistry and Behavior*, *74*, 833–839.

Rademacher, L., Schulte-Rüther, M., Hanewald, B., & Lammertz, S. (2016). Reward: From basic reinforcers to anticipation of social cues. *Current Topics in Behavioral Neurosciences*.*30*, 207–221. https://doi:10.1007/7854_2015_429.

Reed, M. D., Yim, Y. S., Wimmer, R. D., Kim, H., Ryu, C., Welch, G. M., … Choi, G. B. (2020). IL-17a promotes sociability in mouse models of neurodevelopmental disorders. *Nature*, *577*, 249–253. https://doi.org/10.1038/s41586-019-1843-6

Réu, P., Khosravi, A., Bernard, S., Mold, J. E., Salehpour, M., Alkass, K., … Frisén, J. (2017). The lifespan and turnover of microglia in the human brain. *Cell Reports*, *20*, 779–784. https://doi.org/10.1016/j.celrep.2017.07.004

Reynolds, L. C., Inder, T. E., Neil, J. J., Pineda, R. G., & Rogers, C. E. (2014). Maternal obesity and increased risk for autism and developmental delay among very preterm infants. *Journal of Perinatology*, *34*, 688–692. https://doi.org/10.1038/jp.2014.80

Richards, R., Greimel, E., Kliemann, D., Koerte, I. K., Schulte-Körne, G., Reuter, M., & Wachinger, C. (2020). Increased hippocampal shape asymmetry and volumetric ventricular asymmetry in autism spectrum disorder. *NeuroImage Clinical*, *26*, 102207. https://doi.org/10.1016/j.nicl.2020.102207

Rigney, A. E., Koski, J. E., & Beer, J. S. (2018). The functional role of ventral anterior cingulate cortex in social evaluation: Disentangling valence from subjectively rewarding opportunities. *Social Cognitive and Affective Neuroscience*, *13*, 14–21.

Rogers, R. D., Ramnani, N., Mackay, C., Wilson, J. L., Jezzard, P., Carter, C. S., & Smith, S. M. (2004). Distinct portions of anterior cingulate cortex and medial prefrontal cortex are activated by reward processing in separable phases of decision-making cognition. *Biological Psychiatry*, *55*, 594–602.

Romero, E., Guaza, C., Castellano, B., & Borrell, J. (2010). Ontogeny of sensorimotor gating and immune impairment induced by prenatal immune challenge in rats: Implications for the etiopathology of schizophrenia. *Molecular Psychiatry*, *15*, 372–383.

Rudebeck, P. H., Buckley, M. J., Walton, M. E., & Rushworth, M. F. S. (2006). A role for the macaque anterior cingulate gyrus in social valuation. *Science*, *313*, 1310–1312.

Rudolph, M. D., Graham, A. M., Feczko, E., Miranda-Dominguez, O., Rasmussen, J. M., Nardos, R., … Fair, D. A. (2018). Maternal IL-6 during pregnancy can be estimated from newborn brain connectivity and predicts future working memory in offspring. *Nature Neuroscience*, *21*, 765–772.

Russo, S. J., & Nestler, E. J. (2013). The brain reward circuitry in mood disorders. *Nature Reviews Neuroscience*, *14*(9), 609–625. https://doi.org/10.1038/nrn3381

Saghazadeh, A., Ataeinia, B., Keynejad, K., Abdolalizadeh, A., Hirbod-Mobarakeh, A., & Rezaei, N. (2019a). A meta-analysis of pro-inflammatory cytokines in autism spectrum disorders: Effects of age, gender, and latitude. *Journal of Psychiatric Research*, *115*, 90–102. https://doi.org/10.1016/j.jpsychires.2019.05.019

Saghazadeh, A., Ataeinia, B., Keynejad, K., Abdolalizadeh, A., Hirbod-Mobarakeh, A., & Rezaei, N. (2019b). Anti-inflammatory cytokines in autism spectrum disorders: A systematic review and meta-analysis. *Cytokine*, *123*, 154740. https://doi.org/10.1016/j.cyto.2019.154740

Salter, M. W., & Stevens, B. (2017). Microglia emerge as central players in brain disease. *Nature Medicine*, *23*, 1018–1027.

Schafer, D. P., & Stevens, B. (2015). Microglia function in central nervous system development and plasticity. *Cold Spring Harbor Perspectives in Biology*, *7*, a020545. https://doi.org/10.1101/cshperspect.a020545

Schmitz, N., Rubia, K., Amelsvoort, T., Van, D. E., Smith, A., & Murphy, D. G. M. (2008). Neural correlates of reward in autism. *British Journal of Psychiatry*, *192*, 19–24.

Schwartzer, J. J., Careaga, M., Onore, C. E., Rushakoff, J. A., Berman, R. F., & Ashwood, P. (2013). Maternal immune activation and strain specific interactions in the development of autism-like behaviors in mice. *Translational Psychiatry*, *3*, e240–e249. https://doi.org/10.1038/tp.2013.16

Sekio, M., & Seki, K. (2015). Lipopolysaccharide-induced depressive-like behavior is associated with α1-adrenoceptor dependent downregulation of the membrane GluR1 subunit in the mouse medial prefrontal cortex and ventral tegmental area. *International Journal of Neuropsychopharmacology*, *18*, 1–12. https://doi.org/10.1093/ijnp/pyu005

Selten, J. P., & Morgan, V. A. (2010). Prenatal exposure to influenza and major affective disorder. *Bipolar Disorders*, *12*, 753–754. https://doi.org/10.1111/j.1399-5618.2010.00849.x

Shams, S., Amlani, S., Buske, C., Chatterjee, D., & Gerlai, R. (2018). Developmental social isolation affects adult behavior, social interaction, and dopamine metabolite levels in zebrafish. *Developmental Psychobiology*, *60*(1), 43–56. https://doi.org/10.1002/dev.21581

Shin Yim, Y., Park, A., Berrios, J., Lafourcade, M., Pascual, L. M., Soares, N., … Choi, G. B. (2017). Reversing behavioural abnormalities in mice exposed to maternal inflammation. *Nature*, *549*(7673), 482–487. https://doi.org/10.1038/nature23909

Simon, M., Campbell, E., Genest, F., MacLean, M. W., Champoux, F., & Lepore, F. (2020). The impact of early deafness on brain plasticity: A systematic review of the white and gray matter changes. *Frontiers in Neuroscience*, *14*, https://doi.org/10.3389/fnins.2020.00206

Singer, H. S., Morris, C. M., Williams, P. N., Yoon, D. Y., Hong, J. J., & Zimmerman, A. W. (2006). Antibrain antibodies in children with autism and their unaffected siblings. *Journal of Neuroimmunology*, *178*, 149–155. https://doi.org/10.1016/j.jneuroim.2006.05.025

Singh, V. K., & Rivas, W. H. (2004). Prevalence of serum antibodies to caudate nucleus in autistic children. *Neuroscience Letters*, *355*, 53–56.

Smith, C. J. W., Poehlmann, M. L., Li, S., Ratnaseelan, A. M., Bredewold, R., & Veenema, A. H. (2017). Age and sex differences in oxytocin and vasopressin V1a receptor binding densities in the rat brain: Focus on the social decision-making network. *Brain Structure and Function*, *222*, 981–1006. https://doi.org/10.1007/s00429-016-1260-7

Smith, C. J. W., Ratnaseelan, A. M., & Veenema, A. H. (2018). Robust age, but limited sex, differences in mu-opioid receptors in the rat brain: Relevance for reward and drug-seeking behaviors in juveniles. *Brain Structure and Function*, *223*, 475–488. https://doi.org/10.1007/s00429-017-1498-8

Smith, C. J. W., Wilkins, K. B., Mogavero, J. N., & Veenema, A. H. (2015). Social novelty investigation in the juvenile rat: modulation by the μ-opioid system. *Journal of Neuroendocrinology*, *27*, 752–764. https://doi.org/10.1111/jne.12301

Soto, A. M. S., Kirsten, T. B., Reis-Silva, T. M., Martins, M. F. M., Teodorov, E., Flório, J. C., … Bondan, E. F. (2013). Single early prenatal lipopolysaccharide exposure impairs striatal monoamines and maternal care in female rats. *Life Sciences*, *92*, 852–858. https://doi.org/10.1016/j.lfs.2013.03.003

Staal, W. G., Langen, M., Van Dijk, S., Mensen V. T., & Durston, S. (2015). DRD3 gene and striatum in autism spectrum disorder. *British Journal of Psychiatry*, *206*, 431–432.

Sumiyoshi, A., Keeley, R. J., & Lu, H. (2019). Physiological considerations of functional magnetic resonance imaging in animal models. *Biological Psychiatry: Cognitive Neuroscience and Neuroimaging*, *4*, 522–532.

Supekar, K., Kochalka, J., Schaer, M., Wakeman, H., Qin, S., Padmanabhan, A., & Menon, V. (2018). Deficits in mesolimbic reward pathway underlie social interaction impairments in children with autism. *Brain*, *141*, 2795–2805. https://doi.org/10.1093/brain/awy191

Suzuki, K., Sugihara, G., Ouchi, Y., Nakamura, K., Futatsubashi, M., Takebayashi, K., … Mori, N. (2013). Microglial activation in young adults with autism spectrum disorder. *JAMA Psychiatry*, *70*, 49. https://doi.org/10.1001/jamapsychiatry.2013.272

Tay, T. L., Mai, D., Dautzenberg, J., Fernández-Klett, F., Lin, G., Sagar, D. M., … Margineanu, A. (2017). A new fate mapping system reveals context-dependent random or clonal expansion of microglia. *Nature Neuroscience*, *20*, 793–803.

Tetreault, N. A., Hakeem, A. Y., Jiang, S., Williams, B. A., Allman, E., Wold, B. J., & Allman, J. M. (2012). Microglia in the cerebral cortex in autism. *Journal of Autism and Developmental Disorders*, *42*, 2569–2584.

Tickerhoof, M. C., Hale, L. H., Butler, M. J., & Smith, A. S. (2020). Regulation of defeat-induced social avoidance by medial amygdala DRD1 in male and female prairie voles. *Psychoneuroendocrinology*, *113*, 104542. https://doi.org/10.1016/j.psyneuen.2019.104542

Tohyama, S., Walker, M. R., Sammartino, F., Krishna, V., & Hodaie, M. (2020). The utility of diffusion tensor imaging in neuromodulation: Moving beyond conventional magnetic resonance imaging. *Neuromodulation*, *23*(4), 427–435. https://doi.org/10.1111/ner.13107

Tremblay, M. W., & Jiang, Y. (2019). DNA methylation and susceptibility to autism spectrum disorder. *Annual Review of Medicine*, *70*, 151–166. https://doi.org/10.1146/annurev-med-120417-091431

Uddin, L. Q., Supekar, K., Lynch, C. J., Khouzam, A., Phillips, J., Feinstein, C., … Vinod, M. P. (2013). Salience network-based classification and prediction of symptom severity in children with autism. *JAMA Psychiatry*, *70*, 869–879. https://doi.org/10.1001/jamapsychiatry.2013.104

Vargas, D. L., Nascimbene, C., Krishnan, C., Zimmerman, A. W., & Pardo, C. A. (2005). Neuroglial activation and neuroinflammation in the brain of patients with autism. *Annals of Neurology*, *57*, 67–81.

Veenema, A. H., Bredewold, R., & De Vries, G. J. (2012). Vasopressin regulates social recognition in juvenile and adult rats of both sexes, but in sex- and age-specific ways. *Hormones and Behavior*, *61*, 50–56.

Veniaminova, E., Cespuglio, R., Cheung, C. W., Umriukhin, A., Markova, N., Shevtsova, E., … Strekalova, T. (2017). Autism-like behaviours and memory deficits result from a western diet in mice. *Neural Plasticity*, *2017*, 1–14. https://doi.org/10.1155/2017/9498247

Vogel Ciernia, A., Laufer, B. I., Hwang, H., Dunaway, K. W., Mordaunt, C. E., Coulson, R. L., … LaSalle, J. M. (2020). Epigenomic convergence of neural-immune risk factors in neurodevelopmental disorder cortex. *Cerebral Cortex*, *30*, 640–655. https://doi.org/10.1093/cercor/bhz115

Volkow, N. D., Wise, R. A., & Baler, R. (2017). The dopamine motive system: Implications for drug and food addiction. *Nature Reviews Neuroscience*, *18*, 741–752.

Vosberg, D. E., Zhang, Y., Menegaux, A., Chalupa, A., Manitt, C., Zehntner, S., … Dagher, A. (2018). Mesocorticolimbic connectivity and volumetric alterations in dcc mutation carriers. *Journal of Neuroscience*, *38*, 4655–4665.

Vucetic, Z., Kimmel, J., Totoki, K., Hollenbeck, E., & Reyes, T. M. (2010). Maternal high-fat diet alters methylation and gene expression of dopamine and opioid-related genes. *Endocrinology*, *151*, 4756–4764. https://doi.org/10.1210/en.2010-0505

Vuillermot, S., Weber, L., Feldon, J., & Meyer, U. (2010). A longitudinal examination of the neurodevelopmental impact of prenatal immune activation in mice reveals primary defects in dopaminergic development relevant to schizophrenia. *Journal of Neuroscience*, *30*, 1270–1287. https://doi.org/10.1523/JNEUROSCI.5408-09.2010

Wacker, J., Dillon, D. G., & Pizzagalli, D. A. (2009). The role of the nucleus accumbens and rostral anterior cingulate cortex in anhedonia: Integration of resting EEG, fMRI, and volumetric techniques. *NeuroImage*, *46*, 327–337. https://doi.org/10.1016/j.neuroimage.2009.01.058

Walport, M. J. (2001). Complement. *New England Journal of Medicine*, *344*, 1140–1144.

Wang, J., Jia, Y., Li, G., Wang, B., Zhou, T., Zhu, L., … Chen, Y. (2018). The dopamine receptor D3 regulates lipopolysaccharide-induced depressive-like behavior in mice. *International Journal of Neuropsychopharmacology*, *21*(5), 448–460. https://doi.org/10.1093/ijnp/pyy005

Wang, J., Lai, S., Li, G., Zhou, T., Wang, B., Cao, F., … Chen, Y. (2019). Microglial activation contributes to depressive-like behavior in dopamine D3 receptor knockout mice. *Brain, Behavior, and Immunity*, *83*, 226–238. https://doi.org/10.1016/j.bbi.2019.10.016

Weber, M. D., McKim, D. B., Niraula, A., Witcher, K. G., Yin, W., Sobol, C. G., … Godbout, J. P. (2019). The influence of microglial elimination and repopulation on stress sensitization induced by repeated social defeat. *Biological Psychiatry*, *85*, 667–678.

Wendeln, A.-C., Degenhardt, K., Kaurani, L., Gertig, M., Ulas, T., Jain, G., … Neher, J. J. (2018). Innate immune memory in the brain shapes neurological disease hallmarks. *Nature*, *556*, 332–338. https://doi.org/10.1038/s41586-018-0023-4

Yamaguchi, Y., Lee, Y. A., Kato, A., Jas, E., & Goto, Y. (2017). The roles of dopamine d2 receptor in the social hierarchy of rodents and primates. *Scientific Reports*, *7*(1), 1–10. https://doi.org/10.1038/srep43348.

Yang, D., Pelphrey, K. A., Sukhodolsky, D. G., Crowley, M. J., Dayan, E., Dvornek, N. C., … Ventola, P. (2016). Brain responses to biological motion predict treatment outcome in young children with autism. *Translational Psychiatry*, *6*, e948. https://doi.org/10.1038/tp.2016.213

Ye, J., Liu, L., Xu, X., Wen, Y., Li, P., Cheng, B., … Liang, C. (2020). A genome-wide multiphenotypic association analysis identified candidate genes and gene ontology shared by four common risky behaviors. *Aging*, *12*, 3287–3297.

Yi, C.-X., Tschop, M. H., Woods, S. C., & Hofmann, S. M. (2012). High-fat-diet exposure induces IgG accumulation in hypothalamic microglia. *Disease Models and Mechanisms*, *5*, 686–690.

Yoshioka, Y., Sugino, Y., Shibagaki, F., Yamamuro, A., Ishimaru, Y., & Maeda, S. (2020). Dopamine attenuates lipopolysaccharide-induced expression of proinflammatory cytokines by inhibiting the nuclear translocation of NF-κB p65 through the formation of dopamine

quinone in microglia. *European Journal of Pharmacology*, *866*, 172826. https://doi.org/10.1016/j.ejphar.2019.172826

Yu, B., Yuan, B. O., Dai, J.-K., Cheng, T.-L., Xia, S.-N., He, L.-J., … Qiu, Z.-L. (2020). Reversal of social recognition deficit in adult mice with MECP2 duplication via normalization of MeCP2 in the medial prefrontal cortex. *Neuroscience Bulletin*, *36*(6), 570–584. https://doi.org/10.1007/s12264-020-00467-w

Zheng, J., Xiao, X., Zhang, Q., Yu, M., Xu, J., Wang, Z., … Wang, T. (2015). Maternal and post-weaning high-fat, high-sucrose diet modulates glucose homeostasis and hypothalamic POMC promoter methylation in mouse offspring. *Metabolic Brain Disease*, *30*, 1129–1137. https://doi.org/10.1007/s11011-015-9678-9

Zilkha, N., Kuperman, Y., & Kimchi, T. (2017). High-fat diet exacerbates cognitive rigidity and social deficiency in the BTBR mouse model of autism. *Neuroscience*, *345*, 142–154. https://doi.org/10.1016/j.neuroscience.2016.01.070

How to cite this article: Trujillo Villarreal LA-, Cárdenas-Tueme M, Maldonado-Ruiz R, Reséndez-Pérez D, Camacho-Morales A. Potential role of primed microglia during obesity on the mesocorticolimbic circuit in autism spectrum disorder. *J. Neurochem*. 2021;156:415–434. https://doi.org/10.1111/jnc.15141

frontiers in Neuroscience

ORIGINAL RESEARCH
published: 03 June 2020
doi: 10.3389/fnins.2020.00452

Fetal Programming by Methyl Donors Modulates Central Inflammation and Prevents Food Addiction-Like Behavior in Rats

*Gabriela Cruz-Carrillo[1,2], Larisa Montalvo-Martínez[1,2], Marcela Cárdenas-Tueme[3], Sofia Bernal-Vega[3], Roger Maldonado-Ruiz[1,2], Diana Reséndez-Pérez[3], Dalia Rodríguez-Ríos[4], Gertrud Lund[4], Lourdes Garza-Ocañas[5] and Alberto Camacho-Morales[1,2]**

[1] Department of Biochemistry, College of Medicine, Universidad Autónoma de Nuevo León, San Nicolás de los Garza, Mexico, [2] Neurometabolism Unit, Center for Research and Development in Health Sciences, Universidad Autónoma de Nuevo León, San Nicolás de los Garza, Mexico, [3] Department of Cell Biology and Genetics, College of Biological Sciences, Universidad Autónoma de Nuevo León, San Nicolás de los Garza, Mexico, [4] Department of Genetic Engineering, CINVESTAV Irapuato Unit, Irapuato, Mexico, [5] Department of Pharmacology and Toxicology, College of Medicine, Universidad Autónoma de Nuevo León, San Nicolás de los Garza, Mexico

OPEN ACCESS

Edited by:
Gustavo Pacheco-Lopez, Autonomous Metropolitan University, Mexico

Reviewed by:
Emmanuel N. Pothos, Tufts University School of Medicine, United States
Margarita Curras-Collazo, University of California, Riverside, United States

***Correspondence:**
Alberto Camacho-Morales
acm590@hotmail.com;
alberto.camachomr@uanl.edu.mx

Specialty section:
This article was submitted to Neuroenergetics, Nutrition and Brain Health, a section of the journal Frontiers in Neuroscience

Received: 13 December 2019
Accepted: 14 April 2020
Published: 03 June 2020

Citation:
Cruz-Carrillo G, Montalvo-Martínez L, Cárdenas-Tueme M, Bernal-Vega S, Maldonado-Ruiz R, Reséndez-Pérez D, Rodríguez-Ríos D, Lund G, Garza-Ocañas L and Camacho-Morales A (2020) Fetal Programming by Methyl Donors Modulates Central Inflammation and Prevents Food Addiction-Like Behavior in Rats. Front. Neurosci. 14:452. doi: 10.3389/fnins.2020.00452

Fetal programming by hypercaloric intake leads to food addiction-like behavior and brain pro-inflammatory gene expression in offspring. The role of methylome modulation during programming on central immune activation and addiction-like behavior has not been characterized. We employed a nutritional programming model exposing female Wistar rats to chow diet, cafeteria (CAF), or CAF-methyl donor's diet from pre-pregnancy to weaning. Addiction-like behavior in offspring was characterized by the operant training response using Skinner boxes. Food intake in offspring was determined after fasting–refeeding schedule and subcutaneous injection of ghrelin. Genome-wide DNA methylation in the nucleus accumbens (NAc) shell was performed by fluorescence polarization, and brain immune activation was evaluated using real-time PCR for pro-inflammatory cytokines (IL-1β, TNF-1α, and IL-6). Molecular effects of methyl modulators [S-adenosylmethionine (SAM) or 5-azatidine (5-AZA)] on pro-inflammatory cytokine expression and phagocytosis were identified in the cultures of immortalized SIM-A9 microglia cells following palmitic acid (100 μM) or LPS (100 nM) stimulation for 6 or 24 h. Our results show that fetal programming by CAF exposure increases the number of offspring subjects and reinforcers under the operant training response schedule, which correlates with an increase in the NAc shell global methylation. Notably, methyl donor's diet selectively decreases lever-pressing responses for reinforcers and unexpectedly decreases the NAc shell global methylation. Also, programmed offspring by CAF diet shows a selective IL-6 gene expression in the NAc shell, which is reverted to control values by methyl diet exposure. *In vitro* analysis identified that LPS and palmitic acid activate IL-1β, TNF-1α, and IL-6 gene expression, which is repressed by the methyl donor SAM. Finally, methylation actively represses phagocytosis activity of SIM-A9 microglia cells induced by LPS and palmitic acid stimulation. Our *in vivo* and *in vitro* data suggest that fetal programming by methyl donors actively decreases addiction-like

behavior to palatable food in the offspring, which correlates with a decrease in NAc shell methylome, expression of pro-inflammatory cytokine genes, and activity of phagocytic microglia. These results support the role of fetal programming in brain methylome on immune activation and food addiction-like behavior in the offspring.

Keywords: programming, methylome, addiction, nucleus accumbens, inflammation

INTRODUCTION

Maternal obesity or maternal hypercaloric intake in humans and murine models is associated with an increased risk of systemic and central pathologies early in life. We and others have published that maternal overnutrition programs negative metabolic and immune profiles (Cardenas-Perez et al., 2018; Maldonado-Ruiz et al., 2019), and addiction (Camacho, 2017; Sarker et al., 2018), as well as depression-like behavior phenotypes in the offspring (de la Garza et al., 2019). Excessive high-energy food consumption seems to modulate positively or negatively a hedonic phenotype in humans and animal models. Several neurotransmitter-related hypotheses were proposed to explain unhealthy eating; for instance, the hypothesis of the reward deficiency states that in the context of high caloric overfeeding or obesity, uncontrolled food intake is activated in order to compensate for a deficient reward effect of food consumption due to failure in the dopaminergic activity (Kenny, 2011; Land and DiLeone, 2012; Barry et al., 2018; Courtney et al., 2018; Gold et al., 2018; van Galen et al., 2018; DiFeliceantonio and Small, 2019; Ducrocq et al., 2019). Under this scenario, impulsiveness for unhealthy eating and caloric overconsumption as a reward is developed (Volkow et al., 2011; Dietrich et al., 2014; Bongers et al., 2015). Classically, reward and incentive salience are integrated to the nucleus accumbens (NAc), whereas preoccupation/anticipation including craving, impulsivity, and executive function involve the prefrontal cortex (PFC) (Volkow and Wise, 2005; Volkow et al., 2013; Koob and Volkow, 2016).

Potential molecular or cellular mechanism leading to addiction-like behavior during maternal hypercaloric exposure is not totally understood. Hypercaloric diets themselves stimulate central and peripheral inflammatory nodes. For instance, exposure to saturated fatty acids during pregnancy activate the Toll-like type 4 receptor signaling (TLR4) in adipocytes and macrophages (Shi et al., 2006) and promotes substantial activation of microglia in the hypothalamus (Maldonado-Ruiz et al., 2019). Systemic and central immune activation pathways regulate abnormal behaviors including depression (Wohleb et al., 2016), schizophrenia (Yuan et al., 2019), and addiction (Alfonso-Loeches et al., 2010; Pascual et al., 2011; Hofford et al., 2018). Conversely, systemic treatment of the anti-inflammatory drug minocycline to methamphetamine-addicted rats reverted addiction-like behavior (Snider et al., 2013; Attarzadeh-Yazdi et al., 2014). Of note, morphine binds to the TLR4 directly, which increases the risk of drug-induced reinstatement (Schwarz and Bilbo, 2013), and blocking the TLR4 pathway in the VTA of rats reduces cocaine and morphine-primed drug seeking (Tanda et al., 2016; Chen et al., 2017; Brown et al., 2018), which seems to depend on microglia activation (Northcutt et al., 2015). Physiologically, TLR4 signaling regulates glutamatergic stimulation in the NAc shell (Kashima and Grueter, 2017); however, repeated cocaine administration activates striatal microglia, leading to TNF-α production and disrupting glutamatergic synaptic strength in the NAc shell (Lewitus et al., 2016). These data suggest that microglia activation and TLR4 signaling positively modulate reinstatement for drug-seeking behavior. It is unknown if addiction-like behavior primed by maternal hypercaloric programming sets a TLR4-like inflammatory profile in NAc capable of regulating addiction-like behavior in the offspring.

Exposure to hypercaloric diet in mice sets a higher proliferation and immune response of myeloid progenitor cells by activating an epigenetic reprogramming mechanism (Christ et al., 2018), known as trained immunity (Netea, 2013). Physiologically, epigenetic modulation, such as DNA methylation, positively activates neuronal differentiation in mammals (Mohn et al., 2008), regulates synaptic plasticity in the hippocampus (Levenson et al., 2006), and, by its own neuronal activity induced by external cues, closely modulates DNA methylation (Maag et al., 2017). For instance, chronic exposure to amphetamine, ecstasy, or MDMA favors a positive global DNA methylation and pro-inflammatory profile in the NAc shell of rats (Mychasiuk et al., 2013), and shows an increase in tri-methylation of lysine 4 in histone H3 (H3K4me3) on the pronociceptin, prodynorphin, and neuropsin promoters, while decreasing the acetylation of lysine 9 in Histone H3 (H3K9ac) in the nociceptin/orphaninFQ (pN/OFQ) (Caputi et al., 2016). Also, maternal care of rat offspring blocks drug-induced reinstatement of morphine by decreasing the methylation of the IL-10 promoter in NAc shell (Schwarz et al., 2011). These evidences support a potential role of the brain proinflammatory profile and drug addiction susceptibility actively modulated by methylation and/or acetylation of histones and/or DNA. Overall, we hypothesized that maternal programming by caloric diet exposure primes DNA methylation changes and a pro-inflammatory profile in NAc favoring addiction-like behavior for natural rewards in the offspring.

The present study aimed to explore the role of maternal nutritional programming and its effects on DNA methylation, pro-inflammatory profile, and susceptibility to addiction-like behavior in the offspring.

MATERIALS AND METHODS

Animals and Housing

All the experiments were performed using 2-month-old wild-type female Wistar rats (initial body weight, 200–250 g). Animals

were handled according to the NIH Guide for the Care and Use of Laboratory Animals (NIH Publications No. 80–23, revised in 1996). We followed the Basel Declaration to implement the ethical principles of Replacement, Reduction, and Refinement of experimental animal models. Our study was approved by the local Animal Care Committee (BI0002) at the Universidad Autónoma de Nuevo León, Mexico. Rats were housed individually in Plexiglas-style cages, maintained at 20–23°C in a temperature-controlled room with a 12-h light/dark cycle. Water was available *ad libitum* in the home cage. Food availability is described below.

Diets

- The standard chow diet formula contained 57% carbohydrates, 13% lipids, and 30% proteins, and 290 mg of sodium, caloric density = 3.35 kcal/g (LabDiet, St. Louis, MO 63144, 5001, United States). Cafeteria (CAF) diet was made of liquid chocolate, biscuits, bacon, fried potatoes, standard chow diet, and pork paté at a 1:1:1:1:1:1:2 ratio, including 39% carbohydrates, 49% lipids, 12% proteins, and 290 mg of sodium, caloric density = 3.72 kcal/g, as we reported (Camacho, 2017; Cardenas-Perez et al., 2018; Maldonado-Ruiz et al., 2019). CAF diet with methyl donors consisted of CAF formula enriched with betaine (5 g/kg of diet), choline (5,37 g/kg of diet), folic acid (5,5 mg/kg of diet), and vitamin B12 (0.5 mg/kg of diet). Total fiber available for CAF diet and standard chow diet is similar and can be found in **Supplementary Table S1** in **Supplementary Material**.

Maternal Programming Model

Animals were acclimated to the animal facility 7 days before being exposed to the diet. A total of 27 10-week-old female Wistar rats (initial body weight, 200–250 g) were housed in standard conditions as described above with *ad libitum* access to food and water. Females were randomized into three different dietary groups: standard chow diet (C, $n = 8$), CAF diet ($n = 14$), and CAF + methyl donor supplemented (CAF + Met, $n = 5$) and were exposed *ad libitum* to them for 9 weeks, including 3 weeks before mating, 3 weeks during gestation, and 3 weeks during lactation. Rats were mated with age-matched Wistar males for 2 days, after which males were removed from the home cage. Pregnancy diagnosis was performed after mating by vaginal plug. Female rats lacking plugs were returned to the home cage for a second mating. Pregnant rats were transferred to individual cages and were kept on the same diet until birth and lactation. Pregnant females might have uneven litter load during gestation; however, litters were adjusted to 10 pups per mother after birth. After 21 days of lactation, male offspring were exposed to a control diet until 2 months of age before the operant training test protocol (see below for details and **Figure 1A** for experimental design). We chose male offspring based on the potential hormone sensitive-behavioral effects in females. In any case, in order to follow the ethical principles of Replacement, Reduction, and Refinement of experimental animal models, we allocated all female offspring to a second experimental behavioral protocol, which is currently under investigation.

Operant Training Test

We followed the operant training protocol using the Skinner box as reported before (Camacho, 2017), with slight modifications.

Rat Acclimation and Food Restriction

Upon arrival, offspring rats from the three dietary groups: chow diet, CAF, and CAF + Met were group-housed for at least 7 days to acclimatize with *ad libitum* access to standard chow diet and water. After acclimation, rats were subsequently single-housed, and food was restricted by lowering to 70% their daily chow food intake until they lost 5–10% of total body weight at 7 days. This manipulation allowed acquisition of efficient lever-press responding during training. Upon reaching desired weight, we adjusted daily food intake to stabilize their weights for the remainder of the training period.

Fixed Ratio (FR)-1 Schedule

Rats were trained to press the lever on a fixed ratio (FR)-1 reinforcement schedule where a single lever press delivers a food pellet to the receptacle. Only one lever is designated as "active," showing a 5-s timeout (TO) to the FR1 schedule (FR1/TO-5), during which additional lever pressing does not result in the delivery of a food pellet. Each FR training session lasts 1 h or when 100 pellets have been delivered. Training on the FR1 schedule lasted 3 days.

Fixed Ratio (FR)-5 Schedule

We established the FR5/TO-5 seconds schedule where five active lever presses triggered the delivery of the food pellet. Training on the FR5 schedule lasted 4 days. As for FR1/TO-5, schedule rats were exposed to *ad libitum* access to standard chow and water.

Progressive Ratio (PR) Schedule

The PR testing was calculated as per Richardson and Roberts (1996) using the following formula (rounded to the nearest integer): = [5e (R × 0.2)]−5, where R is equal to the number of food rewards already earned plus 1 (i.e., next reinforcer). Thus, the number of responses required to earn a food reward follow the order: 1, 2, 4, 6, 9, 12, 15, 20, 25, 32, 40, 50, 62, 77, 95, and so on. The PR session lasts a maximum of 1 h per day. Failure to press the lever in any 10-min period results in termination of the session. We also verified performance on the PR schedule by documenting the stable reinforcement for food when the number of rewards earned in a 1-h session deviates by $\leq$10% for at least 3 consecutive days. Like in the FR1/TO-5 and FR5/TO-5 schedule, rats were exposed to *ad libitum* access to standard chow and water. Training on the PR schedule lasted 5 days.

Calculation of Motivation and Intake Scores

Addiction-like and non-addiction-like behavior in the offspring subjects was diagnosed by integrating lever presses during the FR5 and PR schedules, as reported (Bock et al., 2013; Le et al., 2017). We use the $\times = \frac{X_i - \overline{X}}{s.d}$, where X_i is the behavior value for each rat, $\overline{X}$ is the mean behavior value for all the rats, and *s.d.* is the standard deviation of the population behavior value. We identified addiction-like and non-addiction-like behavior in the offspring by the FR5/PR ratio by setting a +0.5 or −0.5 score at

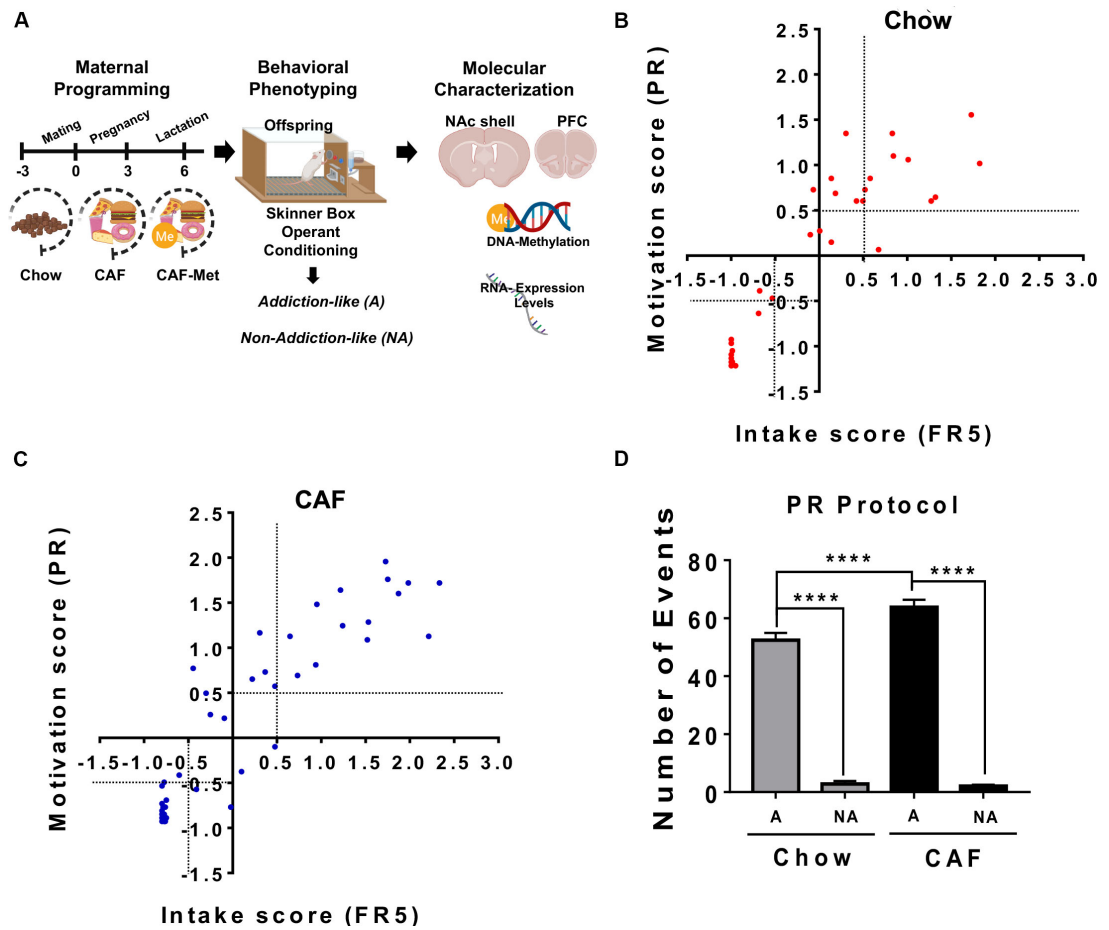

FIGURE 1 | Maternal programming by CAF diet primes addiction-like behavior in offspring. **(A)** Maternal programming model. We fed female Wistar rats for 9 weeks including pre-pregnancy, pregnancy, and lactation with standard chow diet (C, n = 8) or CAF diet (n = 14). Offspring was fed with control diet after weaning until 2 months of age and was trained in the operant training test protocol to diagnosed non-addiction and addiction-like behavior. Molecular characterization of pro-inflammatory expression and global DNA methylome in the NAc shell were performed in non-addiction and addiction-like behavior subjects. **(B,C)** To diagnose addiction-like and non-addiction-like behavior phenotypes in the offspring subjects, we calculated the intake and motivation scores by integrating lever presses during the FR5 and PR schedules, respectively, as reported (Bock et al., 2013; Le et al., 2017). We identified addiction-like and non-addiction-like behavior in the offspring by the FR5/PR ratio by setting a +0.5 or –0.5 score at "x" and "y" axis to characterize the addiction or non-addiction-like behavior subjects, respectively. Motivation (based on PR) or intake (based on FR5) scores in the offspring programmed by chow or CAF, respectively. Graphs show mean ± SEM. Chow, n = 53; CAF, n = 36. **(D)** Number of events during PR protocol of subjects exposed to chow or CAF diet during programming. Graphs show mean ± SEM. Chow diet programmed, addict = 10, non-addict = 14; CAF diet programmed, addict = 10, non-addict = 27. Statistical significance after using one-way ANOVA, followed by a Bonferroni's *post hoc* test. The differences between the groups of operant training test were tested by two-way repeated measures ANOVA. ****$p < 0.0001$. A, Addiction-like; NA, Non-addiction-like.

"x" (intake score) and "y" (motivation score) to characterize the addiction- or non-addiction-like behavior subjects, respectively. This analysis allows one to set the intake and motivation scores for each subject to classify them as high and low responses (addiction- or non-addiction-like behavior) to operant training for natural rewards during the FR5 and PR schedules.

Dams after lactation and offspring after addiction-like and non-addiction-like behavior characterization were sacrificed using decapitation according to the NORMA Oficial Mexicana NOM-062-ZOO-1999. We used decapitation to preserve DNA/RNA integrity. Also, we allocated all female offspring to a second experimental behavioral protocol, which is currently under investigation.

Microglia Cell Culture and Treatments

SIM-A9 (CRL-3265) mouse microglia cells were purchased from ATCC (Manassas, VA, United States) and were expanded in Corning® T75 cm^2 flasks with Dulbecco's modified Eagle's medium (DMEM high glucose 4.5 g/L, Caisson Labs, EE.UU, Utah) supplemented with 10% (vol/vol) 5% heat-inactivated horse serum and heat-inactivated fetal bovine serum 10% (Sigma Aldrich, EE.UU, Missouri), 50 units/ml penicillin, and 50 μg/ml streptomycin (Penicillin/Streptomycin, Sigma Aldrich, EE.UU, Missouri) in a 5% CO_2 incubator at 37°C. The cells were split when they reached 70–90% confluence (plate ratio of 1:4) using a PBS/EDTA/EGTA/GLUCOSE solution

(1 × /1 mM/1 mM/1 mg/ml) at 37°C for 1–5 min, followed by washing/resuspension in growth medium.

After confluence, cells were plated in 6-well plates and 96-well plates, at 200,000 and 5000 cells per well accordingly and pre-incubated with 5-Aza-2′-deoxycytidine (5-AZA) (Sigma Aldrich, A3656) or S-(5′-adenosyl)-L-methionine (SAM) (Sigma-Aldrich, A2408) for 24 h and cell viability was evaluated as described below. Based on cell viability assay in some experiments, we used preincubation of 250 μM SAM or 75 nM 5-AZA or 0.1% DMSO (Control) for 24 h followed by 500 ng lipopolysaccharide (LPS) (stock 1 μg/ml) (Sigma-Aldrich, L3023) or 100 μM palmitic acid (PAL) (Sigma-Aldrich, P9767) stimulation for the next 6 and 24 h. PAL was first solubilized in DMEM containing 10% of free fatty acid bovine serum albumin and then administered in each well.

Cell Viability Analysis

Cell survival was determined using the MTT (Cell proliferation kit I, Roche Diagnostics, Mannheim, Germany) following manufacturer instructions by adding MTT (3-[4,5-dimethylthiazol-2-yl]-2,5-diphenyl tetrazolium bromide) for 1 h at 37°C in a CO_2 chamber. Cell viability was quantified at 570 nm wavelength. Results are expressed as percentage of MTT reduction relative to control cells treated with 0.1% DMSO.

Quantitative Phagocytosis Assay in Microglia Cells

Phagocytosis in microglia cells was determined using the green fluorescent latex beads (Sigma, L1030-1ML), which were pre-opsonized in fetal bovine serum (FBS) (1:5 ratio) for 1 h at 37°C. Subsequently, the FBS with the beads was added to the wells to obtain a final concentration of beads = 0.1% (v/v) as previously reported in Lian et al. (2016). After the cell treatment described previously, cells were incubated with the beads during 6 h at 37°C. We also incubated the experiment at 4°C for 6 h as a negative control.

The percentage of phagocytosis of the microglia was analyzed using a flow cytometer (BD Acuri C6 Plus). After the 6-h incubation ended, the culture medium containing the beads was discarded and the cells were washed twice with sterile 1 × PBS at 37°C. Cells were detached using 1 ml of the PBS/EDTA/EGTA/GLUCOSE solution (1 × /1 mM/1 mM/1 mg/ml) and resuspended in 100 μl of 1 × PBS for analysis in the BD Acuri C6 Plus flow cytometer in the channel FL1-A.

Qualitative Phagocytosis Assay in Microglia Cells

To visualize phagocytosis under conditions of proinflammatory LPS and PAL stimulation and its modulation by 5-AZA and SAM methylation modulators, we used confocal microscopy. SIM-A9 cells were seeded on sterile coverslips in six-well plates covered with 0.01% poly-L-lysine solution (Sigma, p4707). After treatment, cells were fixed by adding 4% paraformaldehyde (PAF) (Sigma, 158127) for 10 min, washed three times with 1 × PBS, and were permeabilized with PBS solution 1 × + 0.1% Triton X-100 (PBST) (Sigma, × 100) for 10 min. Next, the cells were blocked in PBST + 10% goat serum (GIBCO, 16210064) for 30 min and washed three times with 1 × PBS. Microglia immunodetection was performed by overnight primary antibody anti-mouse Iba-1 (1:200) (Abcam, ab178847) incubation at 4°C followed by goat anti-rabbit IgG coupled to Alexa Fluor 546 (1:1000) (Invitrogen, A-11035). Finally, cells were washed 3 × with 1 × PBS and mounted in VECTASHIELD mounting medium with DAPI (Vector Laboratories, H-1000-10). Fluorescent signals were detected by confocal-laser microscopy using an Olympus BX61W1 microscope with an FV1000 module with diode laser. Finally, the images were processed with ImageJ software.

NAc Shell and PFC Isolation and DNA/RNA Extraction

Brains were isolated from addiction-like and non-addiction-like behavior of subjects from the three dietary groups: chow diet, CAF, and CAF + Met and were frozen on dry ice and stored at −80°C until the collection of tissue. NAc shell and *PFC* of each brain were surgically isolated following stereotaxic coordinates according to Paxinos and Watson (2007) and total DNA/RNA extraction was performed by utilizing a purification kit (Qiagen) according to the manufacturer's instructions.

Quantitative Real-Time RT-PCR

We used 200 ng of total RNA for cDNA retro transcription using Applied Biosystems™ High-Capacity cDNA Reverse Transcription Kit. Quantitative real-time RT-PCR was performed on a Lightcycler 480 system (Roche) using a iQ™ SYBR® Green SuperMix (Bio-Rad) with cDNA and primers (0.5 μM). The sequence primers used for analysis were as follows: IL-6 forward, 5′-TAGTCCTTCCTACCCCAATTTCC-3′. IL-6 reverse, 5′-TTGGTCAGCCACTCCTTC-3′. IL-1β forward, 5′-GCAACTGTTCCTGAACTCAAC-3′. IL-1β reverse, 5′-ATCTTTTGGGGTCCGTCAACT-3′. IL-1α-forward, 5′-GCACCTTACACCTACCAGAGT-3′. IL-1α reverse, 5′-TGCAGGTCATTTAACCAAGTGG-3′. TNFα forward, 5′-CAGGCGGTGCCTATGTCTC-3′. TNFα reverse, 5′-CGATCACCCCGAAGTCAGTAG-3′. 36B4 forward, 5′-TCCAGGCTTTGGGCATCA-3′. 36B4 reverse, 5′-CTTTATCAGCTGCACATCACTCAGA-3′. Changes in gene expression were evaluated using the $-\Delta\Delta$Ct method.

Global DNA Methylation Analysis

Genomic DNA (50 ng/μl) was obtained as described before and quantified using the SYBR Green I protocol (Gragene, DNA Genotek Inc., Canada). For the global methylation analysis (Shiratori et al., 2016), 800 ng of DNA was digested with *Hpa*II (H) and with *Msp*I (M) restriction enzymes and incubated at 37°C for 2 h. Afterward, samples were incubated with the final extension reaction (1.7 × PCR buffer, 0.75 U Taq DNA polymerase) (Thermo Fisher Scientific) and 17 nM of TAMRA-dCTP (Jena Bioscience) for 1 h at 58°C in complete darkness. Aliquots of each final extension reaction were placed in 384-well black plates (Greiner Bio-One). The incorporation of TAMRA-dCTP fluorescence was directly measured using the

Infinite M1000-Tecan microplate reader (excitation/emission 535/590 nm). Fluorescence polarization values (FP) were computed by the i-control^{TM} software (Tecan). The average of the FP values was calculated for each condition: FPSD, FPH, and FPM. The FPH and FPM values were normalized by subtraction of the FPSD value. Once the FP values of each sample were normalized, the 5 mC content of the genomic DNA was obtained with the following formula:% 5 mC ADN = (1-(FPH/FPM)) × 100.

Statistical Analyses

All statistical tests were performed using the GraphPad Prism Version 7. For the *in vivo* data including the real-time RT-PCR analysis, we used one-way ANOVA, followed by a Bonferroni's *post hoc* test. The differences between the groups of operant training test were tested by two-way repeated measures ANOVA. For the *in vitro* data including the real time RT-PCR and phagocytosis analysis, we used one-way ANOVA, followed by a Tukey's *post hoc* test from one independent experiment of a total of four. Data are presented as mean ± SEM. The significance levels displayed on figures are as follows: $^{*}p < 0.05$, $^{**}p < 0.01$, $^{***}p < 0.001$.

RESULTS

Maternal Programming by Cafeteria Diet Favors Addiction-Like Behavior in Offspring

We initially evaluated the effect of cafeteria nutritional programming on addiction-like behavior in the offspring using the operant training response to get a cafeteria-like precision pellet. We identified responders to operant training based on number of lever presses during the FR1 and FR5 protocols. Analysis of self-administration during the FR5 schedule did not show effect on the total population of the first filial generation of offspring (F1) subjects from the cafeteria diet exposure during programming when compared with F1 control diet subjects (two-way repeated measures ANOVA, $p < 0.001$) (**Supplementary Figure S1A**). Data generated from the PR schedule also confirms that cafeteria programming does not affect lever presses responses in the F1 subjects (**Supplementary Figure S1B**). We previously reported that nutritional programming with CAF diet sets a low and high response to operant training for natural rewards during FR5 and PR schedules (Camacho, 2017). To diagnose addiction-like and non-addiction-like behavior phenotypes in the offspring subjects, we calculated the intake and motivation scores by integrating lever presses during the FR5 and PR schedules, respectively, as reported (Bock et al., 2013; Le et al., 2017). We use the $\times = \frac{X_i - \overline{X}}{s.d}$, where X_i is the behavior value for each rat, $\overline{X}$ is the mean behavior value for all the rats, and *s.d.* is the standard deviation of the population behavior value. We identified addiction-like and non-addiction-like behavior in the offspring by the FR5/PR ratio by setting a +0.5 or −0.5 score at "*x*" and "*y*" axis to characterize the addiction or non-addiction-like behavior subjects, respectively. Initially, we found that maternal programming by cafeteria diet exposure increases the number of F1 subjects diagnosed as addiction-like behavior when compared with control chow diet (chow = 11 vs. CAF = 14) (**Figures 1B,C**). Characterizing the F1 offspring showing major addiction-like behavior phenotype, we found that subjects of mothers exposed to CAF diet ($n = 10$) showed significant response to operant training schedule displaying high lever responses when compared to high responders ($n = 10$) of chow-exposed mothers (**Figure 1D**). No changes in lever responses were found in the non-addiction-like behavior subjects programmed by CAF or chow diets. This evidence confirms that caloric nutritional intake during pregnancy seems to modulate susceptibility to maximize operant responses to palatable food in offspring.

Methyl-Donor Diet Reverts Addiction-Like Behavior in Offspring

Maternal programming by external stimuli actively modulates epigenetic landscape, including the DNA methylome. We tested the effect of CAF diet exposure during programming on global DNA methylation and its modulation by methyl-donor supplementation [betaine (5 g/kg of diet), choline (5.37 g/kg of diet), folic acid (5.5 mg/kg of diet), and vitamin B12 (0.5 mg/kg of diet)] on addiction-like behavior. We found that programming by CAF diet actively increases global 5-methylcytosine DNA levels in the NAc shell and no changes were found in the PFC of offspring (**Figures 2A,B**). Unexpectedly, methyl-donor supplementation decreases 5-methylcytosine DNA levels similar to control values in the offspring (**Figure 2A**); however, it efficiently decreases the number of subjects displaying lever presses response on the FR5 and PR schedule (**Supplementary Figures S2A,B**). As before, we diagnosed the number of subjects showing addiction-like behavior diagnosed by the FR5/PR ratio by setting a +0.5 or −0.5 score at "*x*" and "*y*" axis to characterize the addiction- or non-addiction-like behavior. We identified that methyl donors decrease the addiction-like behavior displaying 14 offspring of CAF vs. 4 subjects included into the CAF-methyl donors (**Figure 2C**). Also, methyl donors efficiently decrease the number of events during the PR protocol (**Figure 2D**). These data propose that exposure to methyl groups during CAF programming decreases the 5-methylcytosine DNA levels in NAc shell and efficiently revert addiction-like behavior in the offspring.

Methyl Supplementation to CAF Diet Increases Feed, Fasting, and Ghrelin-Sensitive Food Intake in Offspring

Next, we identified the effect of maternal CAF and/or methyl-donor supplementation on physiological fast-feeding and ghrelin-sensitive food intake. We have recently reported that maternal programming by CAF diet primes ghrelin response to food intake in the offspring (Maldonado-Ruiz et al., 2019). Ghrelin has also been reported to modulate addiction-like behavior by its positive effects on the reward circuit. Our data initially showed that offspring from CAF diet-fed mothers showed increase in food intake of chow diet during feed and fasting scenarios, which is exacerbated when exposed to CAF

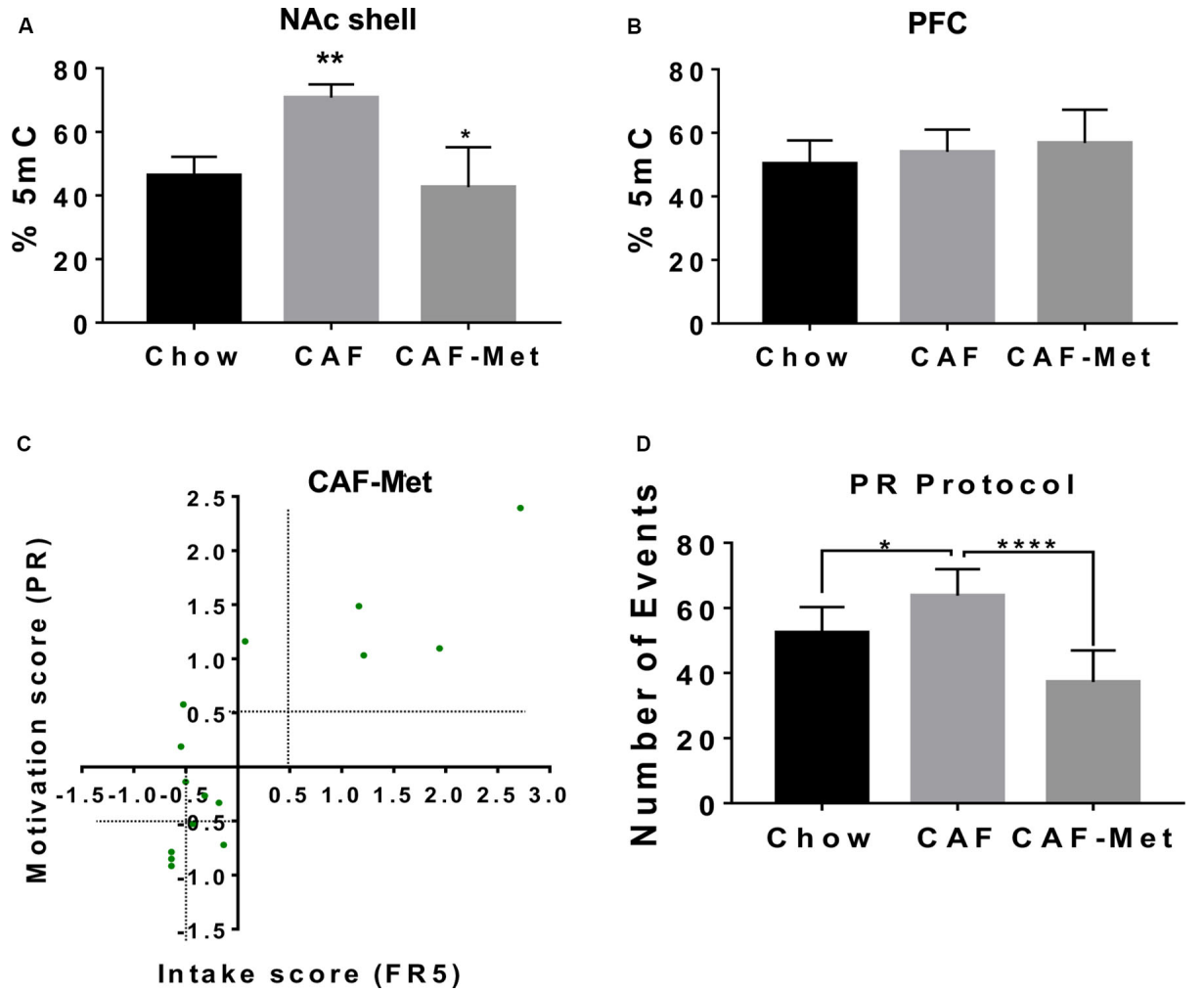

FIGURE 2 | Methyl donors revert addiction-like behavior in the offspring. We fed female Wistar rats for 9 weeks as described with CAF + methyl donors (CAF + Met, $n = 5$). Offspring was fed with control diet and was trained in the operant training test protocol. **(A,B)** Global DNA methylome in NAc shell and PFC were identified using fluorescence polarization. Molecular characterization of pro-inflammatory expression and global DNA methylome in the NAc shell were performed in non-addiction and addiction-like behavior subjects. Graphs show mean ± SEM. Statistical significance after using one-way ANOVA, followed by a Bonferroni's *post hoc* test. The differences between the groups of operant training test were tested by two-way repeated measures ANOVA. $^{*}p < 0.05$ for CAF vs. CAF-Met; $^{**}p < 0.01$ for CAF vs. chow. **(C)** Intake/motivation score for individual offspring subjects from mothers exposed to chow or CAF + Met diet followed the $\times = (\times i - \times^{--})/(s.d)$ analysis (chow, $n = 10$; CAF, $n = 14$; CAF-Met, $n = 4$). **(D)** Number of events during PR protocol of subjects exposed to chow or CAF or CAF + Met diet during programming. Graphs show mean ± SEM. Statistical significance after using one-way ANOVA, followed by a Bonferroni's *post hoc* test. The differences between the groups of operant training test were tested by two-way repeated measures ANOVA. $^{*}p < 0.05$ for CAF vs. chow; $^{****}p < 0.0001$ for CAF vs. CAF-Met.

diet (**Figure 3A**). Notably, programming by methyl donors leads to a substantial increase in CAF diet intake during the feed state, and a significant chow and CAF diet intake after fasting (**Figure 3A**). Also, methyl donors increase chow and CAF diet intake, up to twice and three times higher after intraperitoneal saline administration (**Figure 3B**). Remarkably, methyl donors promote a substantial increase up to three to five times of chow and CAF diet intake in the offspring following ghrelin systemic administration (**Figure 3B**). These results suggest that maternal programming by CAF diet actively promotes food intake by potentially priming ghrelin sensitivity in offspring, which is substantially exacerbated when exposed to methyl donors.

Maternal Programming by CAF Diet Promotes Pro-inflammatory Expression in the NAc Shell of Addiction-Like Behavior Subjects

We compared mRNA expression of proinflammatory cytokines involved in metabolic inflammation in subjects exposed to chow or CAF diets during programming. We found an increase in the IL-6 cytokine mRNA expression in the NAc shell of addiction-like behavior subjects programmed by CAF exposure when compared with non-addiction-like subjects or with chow-programmed F1 subjects (**Figure 4A**). Also, we found a decrease in the expression of IL-1β and no changes in TNF-α mRNA expression in the

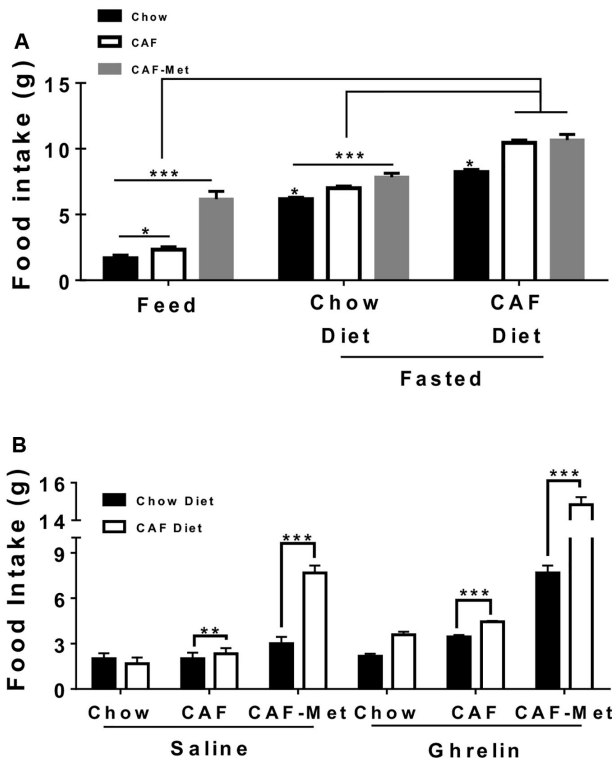

FIGURE 3 | Effect of maternal nutritional programming on fed-fasting and ghrelin-sensitive food intake in offspring. **(A)** Maternal programming was performed by exposing chow or CAF or CAF + Met diet and daily food intake was quantified for each group (Feed state). Chow and CAF diet consumption during 4 h in offspring was registered after fasting for 16 h and refeeding. **(B)** Chow and/or CAF diet intake for 2 h after subcutaneous 0.2 μg/kg ghrelin administration (n = 10–12 per group). Graphs show normalized data of the mean ± SEM. Two-way ANOVA followed by Bonferroni multiple comparison test; $^{*}p < 0.05$, $^{**}p < 0.01$, $^{***}p < 0.001$.

same addiction-like behavior of subjects programmed by CAF exposure when compared with non-addiction-like subjects or with chow-programmed F1 subjects (**Figures 4B,C**).

Methylation Modulates Pro-inflammatory Cytokines Expression in Microglia Cells

Maternal programming by CAF exposure activates global DNA methylation, which correlates with an IL-6 increase and an IL-1β decrease in the NAc shell of addiction-like behavior subjects, we tested whether methylation/demethylation pharmacologic modulation promotes/reverts to a pro-inflammatory profile expression in the SIM-A9 microglia cells. Initially, we found a dose-dependent effect of 5-AZA or SAM on the MTT reduction showing no changes in cell survival at 75 nM 5-AZA and 250 μM SAM (**Figure 5A**). We did not find changes in IL-6, IL-1β, and TNF-1α gene expression followed by 5-AZA or SAM stimulation (data not shown). Real-time PCR analysis identified that favoring global DNA methylation by SAM incubation increases up to 292% and 200% IL-6 and IL-1β gene expression, respectively,

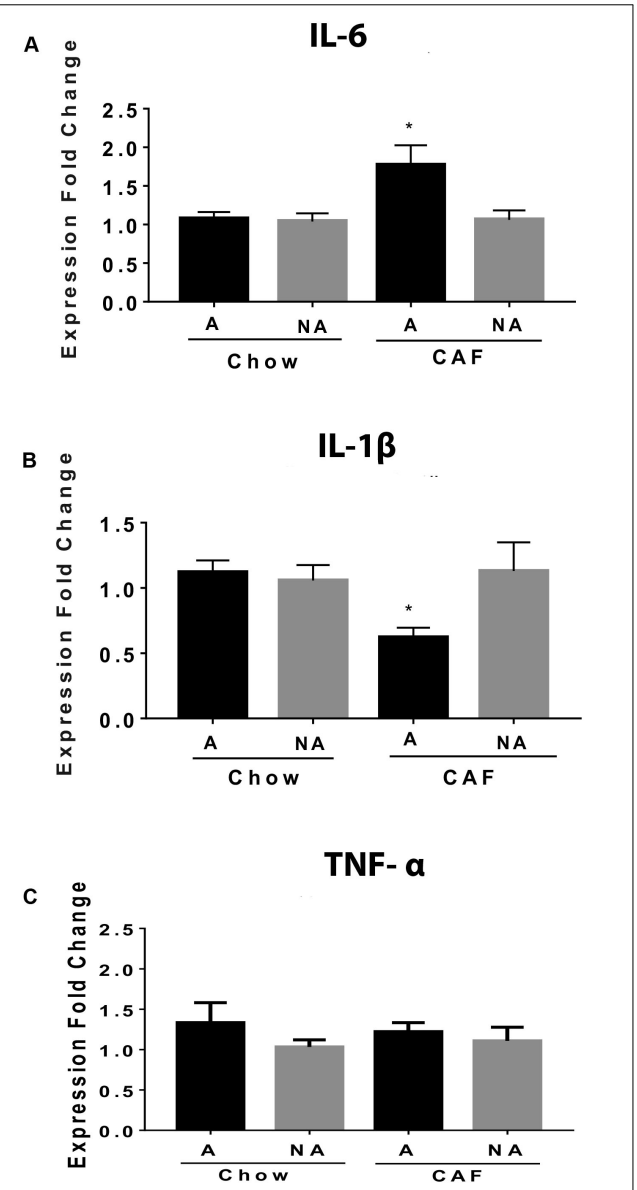

FIGURE 4 | Maternal programming by CAF diet promotes IL-6 expression in the NAc shell of addiction-like behavior subjects. Maternal programming by chow or CAF diet exposure and addiction-like and non-addiction-like behavior diagnosis was performed as described. NAc shell was isolated following stereotaxic coordinates, total DNA/RNA was isolated by purification kit (QIAGEN), and RT-PCR analysis was performed by standardized methods. IL-6 **(A)** and IL-1β **(B)**, and TNF-α **(C)** mRNA expression was performed by selective primers and standardized methods. Graphs show normalized data of the mean ± SEM (n = 10–12 per group). Statistical significance after using one-way ANOVA, followed by a Bonferroni's *post hoc* test. For IL-6, $^{*}p < 0.05$ for A chow vs. A CAF; for IL-1β, $^{*}p < 0.05$ for A CAF vs. A chow and NA CAF. A, Addiction-like; NA, Non-addiction-like.

following 6 h LPS incubation compared to LPS or LPS + 5-AZA treatments (**Figures 5B,C**). Conversely, active TNF-1α gene expression during LPS stimulation does not seem to depend on methylation/demethylation, given that SAM or 5-AZA incubation substantially downregulate TNF-1α gene activation

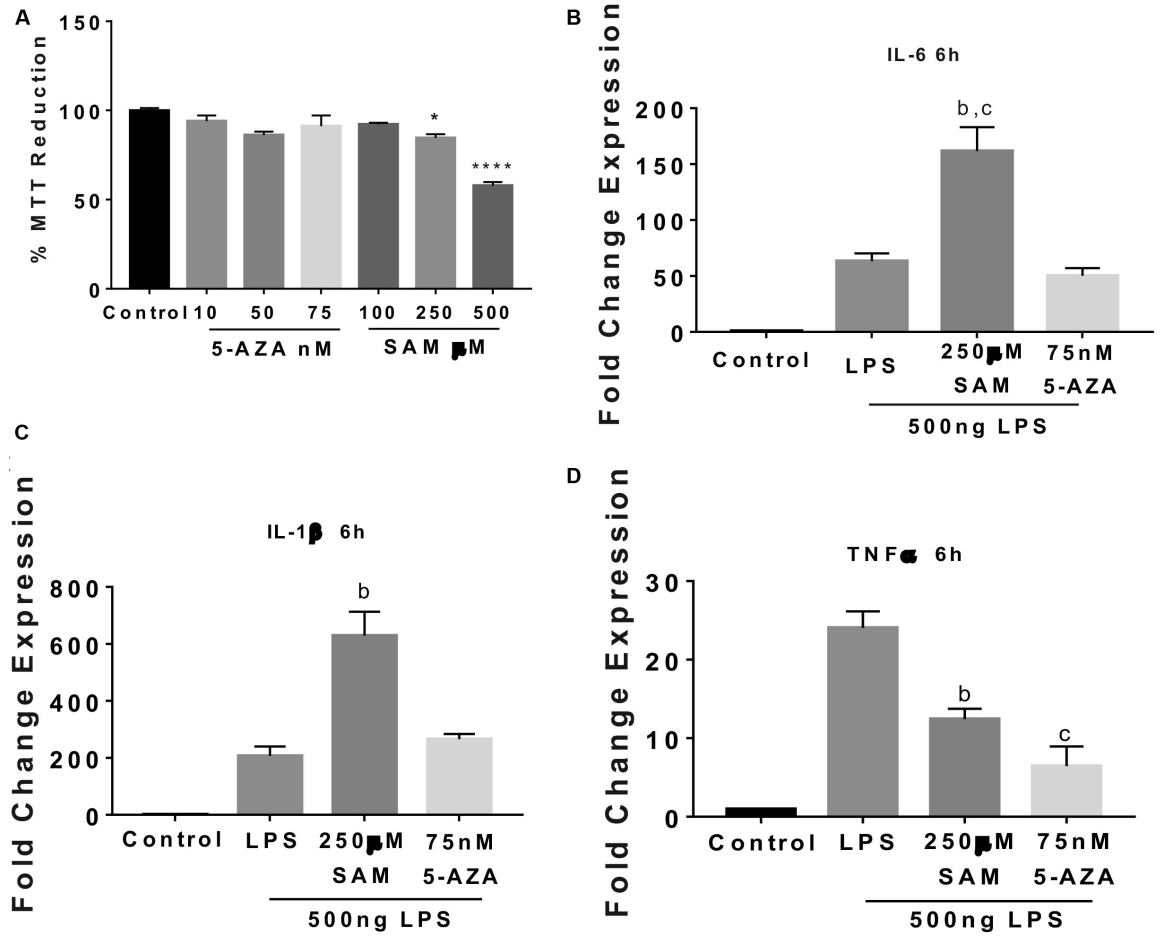

FIGURE 5 | Methylation activates IL-6 and IL-1β gene expression followed by LPS stimulation in microglia cells. **(A)** Dose-dependent microglia cell viability during 24 h 5-AZA or SAM incubation was registered using standardized MTT protocols. Graphs show normalized data of the mean ± SEM for $n = 4$ and statistical significance after using one-way ANOVA with *post hoc* Tukey's test. $^{*}p < 0.05$, $^{****}p < 0.0001$. IL-6 **(B)**, IL-1β **(C)**, and TNF-1α **(D)** RT-PCR gene expression after 24 h 75 nM 5-AZA or 250 μM SAM pre-incubation followed by 6 h 500 ng of LPS (stock 1 μg/ml). Graphs show normalized data of the mean ± SEM relative quantification using 36B4 as a normalizing gene from one independent experiment of a total of four. Statistical significance after using one-way ANOVA with Tukey's multiple comparisons test. For IL-6, $^{b}p < 0.001$ vs. LPS or vs. $^{c}p < 0.0001$ vs. 5-AZA; for IL-1β, $^{b}p < 0.001$ vs. 5-AZA, and for TNF-1α, $^{b}p < 0.001$ vs. LPS or vs. $^{c}p < 0.0001$ vs. LPS. 5-AZA, 5-Aza-2′-deoxycytidine; SAM, S-(5′-adenosyl)-L-methionine; PAL, palmitic acid.

up to 48% and 28%, respectively, when compared with LPS effect (**Figure 5D**).

We also evaluated the effect of methylation/demethylation on IL-6, IL-1β, and TNF-1α gene expression following PAL stimulation. We have reported that intraventricular PAL injection in rats or incubation in microglia cells promotes IL-6, IL-1β, and TNF-1α cytokine release in microglia cells (Maldonado-Ruiz et al., 2019). Also, we have found that maternal programming by CAF diet sets a hypothalamic microglia activation in the offspring (Maldonado-Ruiz et al., 2019). We found that 5-AZA-induced demethylation actively promotes IL-6 and IL-1β gene expression following 6 h of 100 μM PAL stimulation and no changes by 24 h when compared with PAL itself (**Figures 6A–D**). Of note, replicating the results found during LPS stimulation, IL-1 alpha and TNF-1α gene expression during 5-AZA or SAM and 100 μM PAL incubation do not seem to be mediated by methyl donors given that 5-AZA or SAM actively promotes a downregulation of gene activation by 6 h (**Figures 6E,G**). Again, these effects are reverted to 48% and 28% of the control values after 5-AZA or SAM pre-incubation, respectively, followed by 24 h of PAL stimulation (**Figures 6F,H**). These results confirm that demethylation primes IL-6 and IL-1β gene activation following PAL or LPS stimulation.

Methylation Modulates Microglia Phagocytosis in Culture

Finally, we tested if methylation/demethylation potentially coordinates microglia phagocytosis following LPS or PAL incubation. Initially, we characterized a significant reduction of basal microglia phagocytosis followed by 5-AZA incubation when compared with basal microglia phagocytosis, LPS, or following SAM-induced methylation (**Figures 7A,B**).

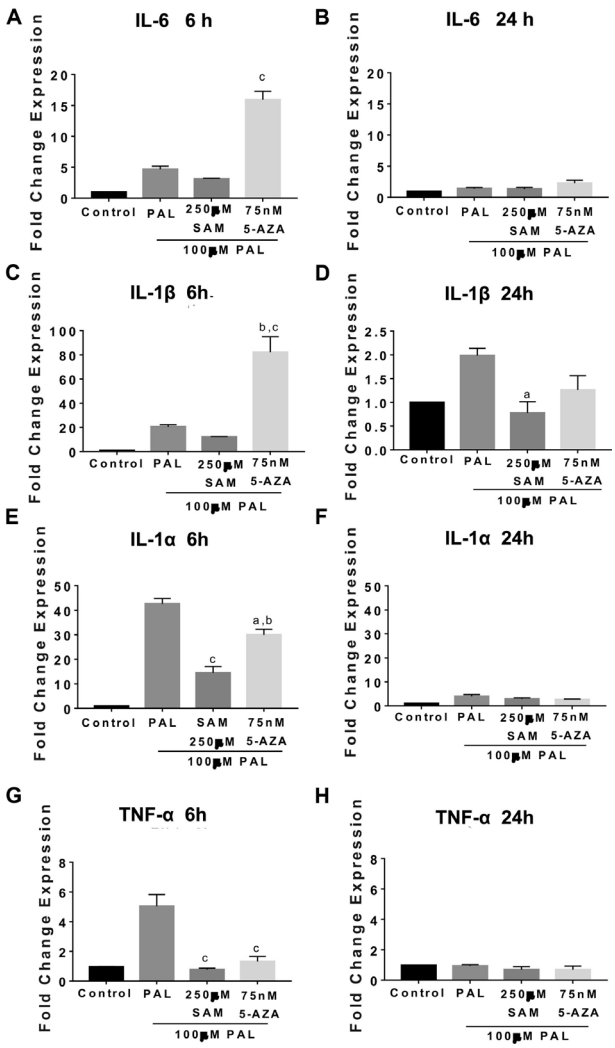

FIGURE 6 | Demethylation activates IL-6 and IL-1β gene expression followed palmitic acid stimulation in microglia cells. Microglia cells were pre-incubated with 75 nM 5-AZA or 250 μM SAM for 24 h followed by 6 or 24 h stimulation of 100 μM PAL. IL-6 **(A,B)**, IL-1β **(C,D)**, IL-1α **(E,F)**, and TNF-1α **(G,H)** RT-PCR gene expression. Graphs show normalized data of the mean ± SEM relative quantification using 36B4 as a normalizing gene from one independent experiment of a total of four. Statistical significance after using one-way ANOVA with Tukey's multiple comparisons test. For IL-6, $^{c}p < 0.0001$ vs. PAL and SAM; TNF-1α, $^{c}p < 0.0001$ vs. PAL; IL-1α $^{a}p < 0.05$ vs. PAL, $^{b}p < 0.001$ vs. SAM, and $^{c}p < 0.0001$ vs. PAL. 5-AZA. 5-AZA: 5-Aza-2′-deoxycytidine, SAM: S-(5′-adenosyl)-L-methionine, PAL, palmitic acid. IL-1β, $^{a}p < 0.05$ vs. PAL, $^{b}p < 0.001$ vs. PAL, and $^{c}p < 0.0001$ vs. SAM.

As expected, LPS stimulation efficiently activates microglia phagocytosis, which is blocked by 5-AZA demethylation induced at 6 and 24 h (**Figures 7C,D**). Also, methyl donors by SAM incubation are capable of preventing LPS-induced phagocytosis at least by 6 h and no effect at 24 h (**Figures 7C,D**). On the other hand, PAL shows a significant phagocytosis activation at 24 h, which is also reverted by 5-AZA pre incubation (**Figures 7E,F**). No changes in microglia phagocytosis were identified by SAM incubation followed by PAL stimulation (**Figures 7E,F**).

DISCUSSION

We report that maternal programming by exposure to hypercaloric diet elicits significant motivation to work for food evidenced by positive lever press responses to caloric pellets in the offspring. Notably, we found that hypercaloric diet intake promotes global DNA methylation in the NAc shell of subjects with addiction-like behavior, which correlates with an upregulation of IL-6 gene expression. We confirm that methyl donor's exposure during programming efficiently decreases addiction-like behavior for caloric pellets in offspring, but instead, they showed a substantial ghrelin-sensitive response for food intake. These results suggest that maternal programming by hypercaloric diet selectively modulates the NAc shell methylome, favoring IL-6 gene expression, which is associated with incentive motivation for natural rewards and ghrelin-sensitive food intake response in the offspring.

In this study, we contribute to characterize the detrimental effect of maternal programming by caloric diets on incentive motivation behavior for food in the offspring. We identified that caloric overnutrition during pregnancy and lactation increases the number of offspring subjects that show addiction-like behavior for caloric pellets when compared with the offspring from mothers exposed to chow diet. Our results agree with previous reports confirming a hedonic phenotype to natural and non-natural rewards in the programmed offspring (Ong and Muhlhausler, 2011; Peleg-Raibstein et al., 2016; Sarker et al., 2018). Of interest, under FR1, FR5, and PR schedules, we identified two responder groups of subjects that displayed low and high motivation for lever presses, which are also identified under cocaine response (Verheij and Cools, 2011; Yamamoto et al., 2013), suggesting that susceptibility among individuals to addiction or external choices depends on genetic, epigenetic, and environmental factors (Pierce et al., 2018). Of note, motivation to work for hypercaloric food during the PR schedule showed a higher scale-up response in the offspring programmed by CAF diet, such as that reported for cocaine, alcohol, nicotine, heroin, and methamphetamine in rats (Peleg-Raibstein et al., 2016). It is important to mention that chronic food restriction in rats actively increases dopamine levels in NAc, leading to augmentation of hedonic behavior (D'Cunha et al., 2017). We used a food restriction protocol in order to enhance the lever presses response during the FR1 schedule; however, we evaluated the hedonic phenotype for natural rewards in the FR5 and PR schedules (4 and 7 days after the *ad libitum* feeding schedules). This protocol allows us to selectively characterize the effect of maternal programming on hedonic rather than metabolic parameters. In line with this evidence, humans have shown increased caloric food liking and/or increased hunger ratings in subjects classified as food addicts (Loxton and Tipman, 2017; Ruddock et al., 2017). Mechanistically, it has been proposed that excessive high-energy food consumption seems to negatively modulate a hedonic phenotype in animal models (Kenny, 2011; Barry et al., 2018; Ducrocq et al., 2019), in part, by downregulating the D2 dopamine receptors (Johnson and Kenny, 2010; Winterdahl et al., 2019), and/or reduced dopamine release (Avena and Bocarsly, 2012). In our context, it seems

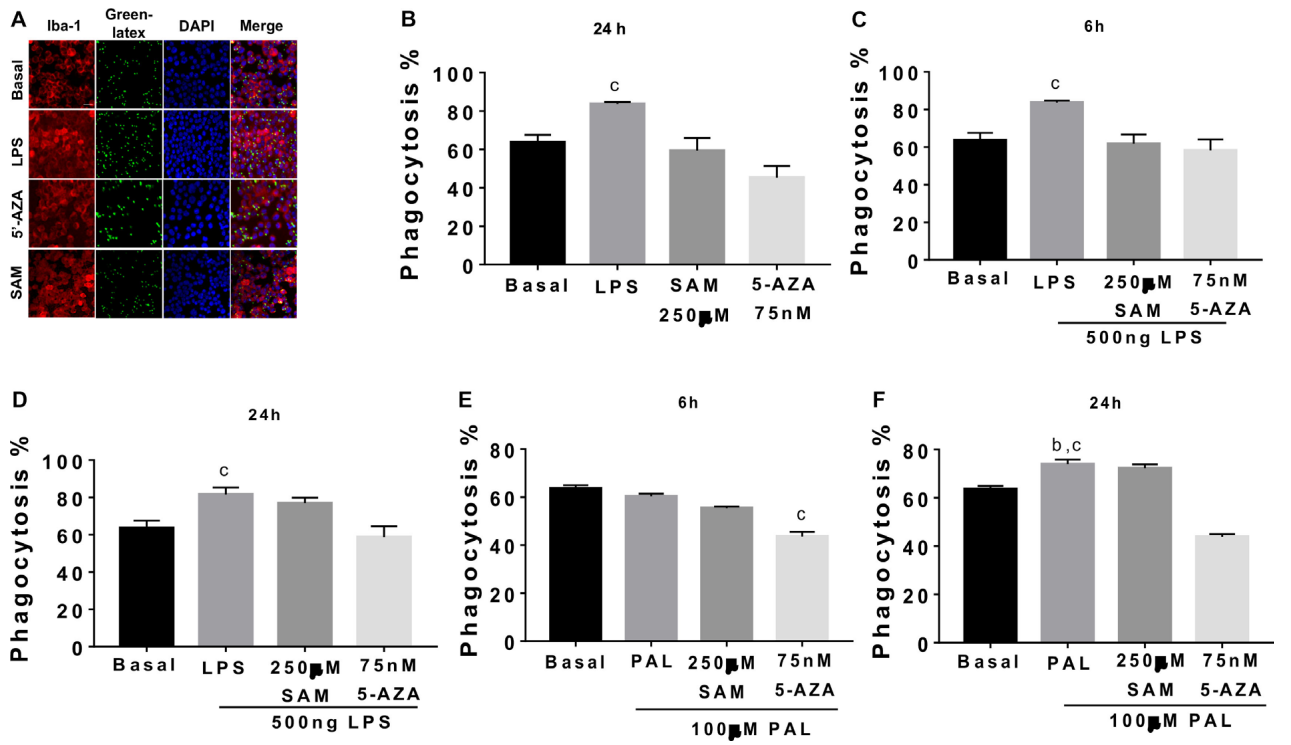

FIGURE 7 | Demethylation inhibits microglia phagocytosis in microglia cells. **(A,B)** Microglia cells were pre-incubated with 75 nM 5-AZA or 250 μM SAM for 24 h, or LPS followed by pre-opsonized green fluorescent latex beads incubation for 1 h at 37°C. Qualitative phagocytosis was evaluated using immunofluorescence against anti Iba-1 (1: 200) followed by goat anti-rabbit IgG coupled to Alexa Fluor 546 (1:1000) and VECTASHIELD mounting medium with DAPI. Fluorescent signals were detected by confocal-laser microscopy using an Olympus BX61W1 microscope with an FV1000 module with diode laser and ImageJ software. $^{c}p < 0.0001$ for LPS vs. Basal, SAM and 5-AZA. **(C,D)** After 5-AZA or SAM incubation, microglia cells were treated with 500 ng of LPS for 6 or 24 h, respectively, and pre-opsonized green fluorescent latex beads were incubated as before.$^{c}p < 0.0001$ for LPS vs. Basal, SAM + LPS and 5-AZA + LPS and $^{c}p < 0.0001$ for LPS vs. Basal and 5-AZA + LPS, respectively. **(E,F)** After 5-AZA or SAM incubation, microglia cells were treated with 100 μM PAL for 6 or 24 h, respectively, and pre-opsonized green fluorescent latex beads were incubated as before. Graphs show normalized data of the mean ± SEM relative to % phagocytosis of microglia cells from one independent experiment of a total of four. Statistical significance after using one-way ANOVA with Tukey's multiple comparisons test. $^{c}p < 0.0001$ for PAL vs. 5-AZA + PAL; $^{b}p < 0.001$ for PAL vs. Basal and $^{c}p < 0.0001$ for PAL vs. 5-AZA + PAL.

that maternal programming by caloric exposure and/or food restriction primes a new state of reward deficiency integrating lower availability dopamine receptors and dopamine release, which might favor impulsiveness for unhealthy eating in order to cope against deficient dopaminergic neurotransmission (Dietrich et al., 2014; Bongers et al., 2015). Taken together, our work reaffirms the proposal that fetal programming by hypercaloric diet in mothers favors motivating behavior toward natural high caloric value rewards in the offspring (Claycombe et al., 2015; Edlow, 2017), which might replicate major hedonic value for food in subjects classified as food addicts (Loxton and Tipman, 2017; Ruddock et al., 2017).

Here, we reported for the first time that CAF diet exposure during pregnancy and lactation leads to selective global DNA methylation in the NAc shell and no changes in the PFC of addict offspring subjects. DNA methylation is a deep coordinator of fetal programming by assisting selective developmental states capable of modulating long-lasting changes in brain plasticity related to motivation addiction (Honegger and de Bivort, 2018). In our maternal programming model, pregnant females are expected to have uneven litter load during gestation and might be exposed to differential fetal programming, which denotes a potential limitation of the murine model. However, litters were adjusted to the same number in the chow and CAF experimental groups. Molecular epigenetic signatures for setting food addiction in the offspring are not totally understood because food is a natural and necessary reward for animals and humans when compared with drugs or alcohol. For example, changes in DNA methylation could be responsible for neuroplasticity changes induced by addictive drugs, such as repeated cocaine administration reduced global levels of H3K9 dimethylation in the NAc, which correlates with changes in dendritic spines (Maze et al., 2010). Also, changes of the histone dimethyltransferase G9a in the NAc shell actively affect cocaine self-administration in rats (Anderson et al., 2018, 2019). Of importance, DNA methylation in NAc during drug addiction seems to respond to a time-dependent regulation, enhancing DNA methylation in the NAc after 30 days of cocaine withdrawal (Massart et al., 2015), suggesting that an increase in DNA methylation is responsible for cocaine craving. In agreement with these data, we found that programming by CAF diet substantially increases global DNA methylation in the NAc shell of addict offspring that are

no longer exposed to CAF diet. Recent evidence have identified that CAF programming promotes D2 dopamine receptor DNA methylation in NAc of the offspring (Rossetti et al., 2020), which potentially might explain the impulsiveness for unhealthy eating. Notably, methyl donors revert the percentage of global DNA methylation and block addiction-like behavior in the offspring. Our data agree with the fact that chronic treatment with the methyl-donor methionine inhibits cocaine-induced conditioned place preference in rats (Tian et al., 2012), which seems to depend on cocaine-induced c-Fos expression in the NAc (Wright et al., 2015). Also, it has been reported that fetal programming by high-fat diet promotes global DNA hypomethylation in the offspring reward circuit (Skinner et al., 2011; Carlin et al., 2013), and in fact, it is also detected in response to fetal programming by environmental exposure to toxins (Baccarelli and Bollati, 2009), during restriction of nutrients *in utero* or prenatal exposure to cocaine (Novikova et al., 2008). In addition, global hypomethylation correlates with an increased expression of opioid receptors and the dopamine transporter in the NAc of the high-fat diet-programmed offspring (Carlin et al., 2013). Conversely, maternal diet supplementation with methyl donors seems to be beneficial by restoring weight gain and food intake in animals exposed to caloric diet (Carlin et al., 2013). Alternatively, methyl-donor supplementation during programming might also contribute to additional metabolic or systemic molecular pathways away to the effects in DNA methylation during neonatal development. For instance, methyl-donor infusion in piglets increases creatine, whereas it decreases phosphatidylcholine levels in liver (Robinson et al., 2016). Creatine synthesis itself requires glycine and an amidino group (provided by arginine) and a methyl group (provided by SAM) (Brosnan et al., 2009), supporting the notion that methyl donors modulates amino acids metabolism in energy-demand tissues including brain. Finally, in a remarkable report, Rizzardi et al. (2019) identified 12 Mb of differentially methylated CG regions in flash-frozen postmortem human tissues including dorsolateral PFC, hippocampus, NAc, and anterior cingulate gyrus implicated in neuropsychiatric disorders, including addiction (Rizzardi et al., 2019). Our data suggest a differential and opposite effect of drugs and food on DNA methylation in NAc; however, in both scenarios, NAc methylation favors addiction-like behavior.

One of the major results from our study proposes that maternal programming by methyl donors decreases the incentive to work for natural rewards; however, it does prime a metabolic aberrant phenotype promoting overfeeding during fasting and ghrelin-sensitive schedules. We have previously reported that CAF diet primes a fasting and ghrelin-sensitive food intake response in the offspring when compared with the offspring of mothers exposed to chow diet (Maldonado-Ruiz et al., 2019). Overfeeding in the programmed offspring might be explained by two scenarios, firstly, postnatal high caloric diet exposure has been identified to induce hypermethylation of the Pomc promoter, blocking leptin signaling and favoring food consumption and weight gain (Marco et al., 2013; Zhang et al., 2014). In fact, higher methylation levels at the proopiomelanocortin (POMC) CpG sites +136 bp, and +138 bp and lower methylation of the neuropeptide Y promoter in human leukocytes have been associated to weight gain (Crujeiras et al., 2013). A potential second scenario might be related with hypomethylation in the neuropeptide Y promoter (Lazzarino et al., 2017) favoring overfeeding after fasting or ghrelin administration in the offspring. We have reported that fetal programming by CAF diet exposure exacerbates hypothalamic c-fos neuronal response to ghrelin in the offspring (Maldonado-Ruiz et al., 2019), suggesting that DNA methylation during maternal CAF exposure might disrupt the expression of food intake neuropeptides favoring ghrelin-sensitive orexigenic signaling.

Next, we characterized the molecular immune signatures of fetal programming in the offspring that favor or correlate with addiction-like behavior. We have reported that maternal programming by CAF exposure leads to hypothalamic microglia activation in the offspring (Maldonado-Ruiz et al., 2019). Our *in vivo* data show a higher expression of IL-6 in the NAc shell of subjects that exhibited addiction-like behavior. Our *in vitro* experiments indicate that LPS or PAL incubation efficiently activates TNF-α, IL-6, and IL-1α gene expression. Also, methyl-donor incubation activates or decreases IL-6 and IL-1α gene expression following LPS or PAL stimulation, respectively. Our results agree with recent reports demonstrating that 5-AZA-induced demethylation significantly increases IL-6 and IL-8 gene expression in human dental pulp cells (Mo et al., 2019) and in polymorphonuclear cells (Shen et al., 2016) followed by LPS stimulation. Potentially, we propose that DNA methylation might coordinate a pro- and anti-inflammatory profile in macrophages toward both M1 and M2 phenotypes. For example, LPS efficiently leads to SOCS1 gene promoter methylation in macrophages favoring secretion of TNF-α and IL-6 cytokines (Cheng et al., 2014). Global DNA hypermethylation has also been reported in inflamed tissues of obesogenic-diabetic mellitus mice models, showing an M1 phenotype in macrophages (Babu et al., 2015; Kapellos and Iqbal, 2016). In our context, positive energy balance such as the obesogenic-diabetic mellitus mice models are closely related to the metabolic failure found in our maternal programming model (Cardenas-Perez et al., 2018), suggesting that global DNA methylation in NAc might potentially be associated to positive energy balance. Finally, our *in vitro* experiments identified that demethylation selectively blocks phagocytosis in microglia during LPS or PAL stimulation. There are no available studies regarding the effect of DNA methylation/demethylation on phagocytosis in microglia, which allow us to integrate this mechanism on addiction behavior. A previous study reported 5-AZA-induced demethylation and significantly increased efferocytosis in alveolar macrophages from COPD patients (Barnawi et al., 2017), which potentially reflects a pathological scenario linked to immunity.

We propose that maternal programming increases susceptibility to addiction-like behavior in the offspring integrating global DNA methylation in the NAc shell, which correlates with IL-6 gene expression. CAF diet made of lipids such as PAL might imitate foreign compounds and initiate a proinflammatory immune signaling in the brain to create its rewarding and/or overfeeding effects.

DATA AVAILABILITY STATEMENT

All relevant data are contained within the manuscript.

ETHICS STATEMENT

The animal study was reviewed and approved by the Local Animal Care Committee (BI0002) at the Universidad Autónoma de Nuevo León, Mexico.

AUTHOR CONTRIBUTIONS

GC-C, LM-M, RM-R, MC-T, SB-V, and AC-M: conceptualization. GC-C, LM-M, MC-T, SB-V, RM-R, DR-P, DR-R, GL, LG-O, and AC-M: investigation. GC-C, LM-M, RM-R, MC-T, SB-V, DR-R, GL, and AC-M: methodology. DR-P, GL, LG-O, and AC-M: supervision and visualization. GC-C, LM-M, RM-R, MC-T, DR-P, DR-R, GL, LG-O, and AC-M: writing – review and editing.

FUNDING

This work was funded by the National Council of Science and Technology in Mexico (CONACYT) (CB-2015-255317 to AC-M), 855559 CONACYT for GC-C, 582196 CONACYT for LM-M, 573686 CONACYT for RM-R, and 650620 CONACYT for MC-T.

ACKNOWLEDGMENTS

The authors thank M. S. Alejandra Arreola-Triana for her support on editing this manuscript.

SUPPLEMENTARY MATERIAL

The Supplementary Material for this article can be found online at: https://www.frontiersin.org/articles/10.3389/fnins.2020.00452/full#supplementary-material

REFERENCES

Alfonso-Loeches, S., Pascual-Lucas, M., Blanco, A. M., Sanchez-Vera, I., and Guerri, C. (2010). Pivotal role of TLR4 receptors in alcohol-induced neuroinflammation and brain damage. *J. Neurosci.* 30, 8285–8295. doi: 10.1523/JNEUROSCI.0976-10.2010

Anderson, E. M., Larson, E. B., Guzman, D., Wissman, A. M., Neve, R. L., Nestler, E. J., et al. (2018). Overexpression of the histone dimethyltransferase G9a in nucleus accumbens shell increases cocaine self-administration, stress-induced reinstatement, and anxiety. *J. Neurosci.* 38, 803–813. doi: 10.1523/JNEUROSCI.1657-17.2017

Anderson, E. M., Sun, H., Guzman, D., Taniguchi, M., Cowan, C. W., Maze, I., et al. (2019). Knockdown of the histone di-methyltransferase G9a in nucleus accumbens shell decreases cocaine self-administration, stress-induced reinstatement, and anxiety. *Neuropsychopharmacology* 44, 1370–1376. doi: 10.1038/s41386-018-0305-4

Attarzadeh-Yazdi, G., Arezoomandan, R., and Haghparast, A. (2014). Minocycline, an antibiotic with inhibitory effect on microglial activation, attenuates the maintenance and reinstatement of methamphetamine-seeking behavior in rat. *Prog. Neuropsychopharmacol. Biol. Psychiatry* 53, 142–148. doi: 10.1016/j.pnpbp.2014.04.008

Avena, N. M., and Bocarsly, M. E. (2012). Dysregulation of brain reward systems in eating disorders: neurochemical information from animal models of binge eating, bulimia nervosa, and anorexia nervosa. *Neuropharmacology* 63, 87–96. doi: 10.1016/j.neuropharm.2011.11.010

Babu, M., Devi, T. D., Mäkinen, P., Kaikkonen, M., Lesch, H. P., Junttila, S., et al. (2015). Differential promoter methylation of macrophage genes is associated with impaired vascular growth in ischemic muscles of hyperlipidemic and type 2 diabetic mice: genome-wide promoter methylation study. *Circ. Res.* 117, 289–299. doi: 10.1161/CIRCRESAHA.115.306424

Baccarelli, A., and Bollati, V. (2009). Epigenetics and environmental chemicals. *Curr. Opin. Pediatr.* 21, 243–251.

Barnawi, J., Jersmann, H., Haberberger, R., Hodge, S., and Meech, R. (2017). Reduced DNA methylation of sphingosine-1 phosphate receptor 5 in alveolar macrophages in COPD: a potential link to failed efferocytosis. *Respirology* 22, 315–321. doi: 10.1111/resp.12949

Barry, R. L., Byun, N. E., Williams, J. M., Siuta, M. A., Tantawy, M. N., Speed, N. K., et al. (2018). Brief exposure to obesogenic diet disrupts brain dopamine networks. *PLoS One* 13:e0191299. doi: 10.1371/journal.pone.0191299

Bock, R., Hoon Shin, J., Kaplan, A. R., Dobi, A., Markey, E., Kramer, P. F., et al. (2013). Strengthening the accumbal indirect pathway promotes resilience to compulsive cocaine use. *Nat. Neurosci.* 16, 632–638. doi: 10.1038/nn.3369

Bongers, P., Van de Giessen, E., Roefs, A., Nederkoorn, C., Booij, J., Van den Brink, W., et al. (2015). Being impulsive and obese increases susceptibility to speeded detection of high-calorie foods. *Health Psychol.* 34, 677–685. doi: 10.1037/hea0000167

Brosnan, J. T., Wijekoon, E. P., Warford-Woolgar, L., Trottier, N. L., Brosnan, M. E., Brunton, J. A., et al. (2009). Creatine synthesis is a major metabolic process in neonatal piglets and has important implications for amino acid metabolism and methyl balance. *J. Nutr.* 139, 1292–1297. doi: 10.3945/jn.109.105411

Brown, K. T., Levis, S. C., O'Neill, C. E., Northcutt, A. L., Fabisiak, T. J., Watkins, L. R., et al. (2018). Innate immune signaling in the ventral tegmental area contributes to drug-primed reinstatement of cocaine seeking. *Brain Behav. Immun.* 67, 130–138. doi: 10.1016/j.bbi.2017.08.012

Camacho, A. (2017). Obesogenic diet intake during pregnancy programs aberrant synaptic plasticity and addiction-like behavior to a palatable food in offspring. *Behav. Brain Res.* 330, 46–55. doi: 10.1016/j.bbr.2017.05.014

Caputi, F. F., Palmisano, M., Carboni, L., Candeletti, S., and Romualdi, P. (2016). Opioid gene expression changes and post-translational histone modifications at promoter regions in the rat nucleus accumbens after acute and repeated 3,4-methylenedioxy-methamphetamine (MDMA) exposure. *Pharmacol. Res.* 114, 209–218. doi: 10.1016/j.phrs.2016.10.023

Cardenas-Perez, R. E., Fuentes-Mera, L., De La Garza, A. L., Torre-Villalvazo, I., Reyes-Castro, L. A., Rodriguez-Rocha, H., et al. (2018). Maternal overnutrition by hypercaloric diets programs hypothalamic mitochondrial fusion and metabolic dysfunction in rat male offspring. *Nutr. Metab.* 15, 1–16. doi: 10.1186/s12986-018-0279-6

Carlin, J. L., George, R., and Reyes, T. M. (2013). Methyl donor supplementation blocks the adverse effects of maternal high fat diet on offspring physiology. *PLoS One* 8:e63549. doi: 10.1371/journal.pone.0063549

Chen, J. X., Huang, K. M., Liu, M., Jiang, J. X., Liu, J. P., Zhang, Y. X., et al. (2017). Activation of TLR4/STAT3 signaling in VTA contributes to the acquisition and maintenance of morphine-induced conditioned place preference. *Behav. Brain Res.* 335, 151–157. doi: 10.1016/j.bbr.2017.08.022

Cheng, C., Huang, C., Ma, T. T., Bian, E. B., He, Y., Zhang, L., et al. (2014). SOCS1 hypermethylation mediated by DNMT1 is associated with lipopolysaccharide-induced inflammatory cytokines in macrophages. *Toxicol. Lett.* 225, 488–497. doi: 10.1016/j.toxlet.2013.12.023

Christ, A., Günther, P., Lauterbach, M. A. R., Duewell, P., Biswas, D., Pelka, K., et al. (2018). Western diet triggers NLRP3-dependent innate immune reprogramming. *Cell* 172, 162–175.e14. doi: 10.1016/j.cell.2017.12.013

Claycombe, K. J., Brissette, C. A., and Ghribi, O. (2015). Epigenetics of inflammation, maternal infection, and nutrition. *J. Nutr.* 145, 1109S–1115S. doi: 10.3945/jn.114.194639

Courtney, A. L., PeConga, E. K., Wagner, D. D., and Rapuano, K. M. (2018). Calorie information and dieting status modulate reward and control activation during the evaluation of food images. *PLoS One* 13:e0204744. doi: 10.1371/journal.pone.0204744

Crujeiras, A. B., Campion, J., Díaz-Lagares, A., Milagro, F. I., Goyenechea, E., Abete, I., et al. (2013). Association of weight regain with specific methylation levels in the NPY and POMC promoters in leukocytes of obese men: a translational study. *Regul. Pept.* 186, 1–6. doi: 10.1016/j.regpep.2013.06.012

D'Cunha, T. M., Daoud, E., Rizzo, D., Bishop, A. B., Russo, M., Mourra, G., et al. (2017). Augmentation of heroin seeking following chronic food restriction in the rat: differential role for dopamine transmission in the nucleus accumbens shell and core. *Neuropsychopharmacology* 42, 1136–1145. doi: 10.1038/npp.2016.250

de la Garza, A. L., Garza-Cuellar, M. A., Silva-Hernandez, I. A., Cardenas-Perez, R. E., Reyes-Castro, L. A., Zambrano, E., et al. (2019). Maternal flavonoids intake reverts depression-like behaviour in rat female offspring. *Nutrients* 11:572. doi: 10.3390/nu11030572

Dietrich, A., Federbusch, M., Grellmann, C., Villringer, A., and Horstmann, A. (2014). Body weight status, eating behavior, sensitivity to reward/ punishment, and gender: relationships and interdependencies. *Front. Psychol.* 5:1073. doi: 10.3389/fpsyg.2014.01073

DiFeliceantonio, A. G., and Small, D. M. (2019). Dopamine and diet-induced obesity. *Nat. Neurosci.* 22, 1–2. doi: 10.1038/s41593-018-0304-0

Ducrocq, F., Hyde, A., Fanet, H., Oummadi, A., Walle, R., De Smedt-Peyrusse, V., et al. (2019). Decrease in operant responding under obesogenic diet exposure is not related to deficits in incentive or hedonic processes. *Obesity* 27, 255–263. doi: 10.1002/oby.22358

Edlow, A. G. (2017). Maternal obesity and neurodevelopmental and psychiatric disorders in offspring. *Prenat. Diagn.* 37, 95–110. doi: 10.1002/pd.4932

Gold, M. S., Blum, K., Febo, M., Baron, D., Modestino, E. J., Elman, I., et al. (2018). Molecular role of dopamine in anhedonia linked to reward deficiency syndrome (RDS) and anti-reward systems. *Front. Biosci.* 10, 309–325. doi: 10.2741/s518

Hofford, R. S., Russo, S. J., and Kiraly, D. D. (2018). Neuroimmune mechanisms of psychostimulant and opioid use disorders. *Eur. J. Neurosci.* 50, 2562–2573. doi: 10.1111/ejn.14143

Honegger, K., and de Bivort, B. (2018). Stochasticity, individuality and behavior. *Curr. Biol.* 28, R8–R12. doi: 10.1016/j.cub.2017.11.058

Johnson, P. M., and Kenny, P. J. (2010). Dopamine D2 receptors in addiction-like reward dysfunction and compulsive eating in obese rats. *Nat. Neurosci.* 13, 635–641. doi: 10.1038/nn.2519

Kapellos, T. S., and Iqbal, A. J. (2016). Epigenetic control of macrophage polarisation and soluble mediator gene expression during inflammation. *Mediators Inflamm.* 2016:6591703. doi: 10.1155/2016/6591703

Kashima, D. T., and Grueter, B. A. (2017). Toll-like receptor 4 deficiency alters nucleus accumbens synaptic physiology and drug reward behavior. *Proc. Natl. Acad. Sci. U.S.A.* 114, 8865–8870. doi: 10.1073/pnas.1705974114

Kenny, P. J. (2011). Reward mechanisms in obesity: new insights and future directions. *Neuron* 69, 664–679. doi: 10.1016/j.neuron.2011.02.016

Koob, G. F., and Volkow, N. D. (2016). Neurobiology of addiction: a neurocircuitry analysis. *Lancet Psychiatry* 3, 760–773. doi: 10.1016/S2215-0366(16)00104-8

Land, B. B., and DiLeone, R. J. (2012). Losing the lust for life: a new role for an old feeding peptide? *Neuron* 75, 360–362. doi: 10.1016/j.neuron.2012.07.018

Lazzarino, G. P., Andreoli, M. F., Rossetti, M. F., Stoker, C., Tschopp, M. V., Luque, E. H., et al. (2017). Cafeteria diet differentially alters the expression of feeding-related genes through DNA methylation mechanisms in individual hypothalamic nuclei. *Mol. Cell. Endocrinol.* 450, 113–125. doi: 10.1016/j.mce.2017.05.005

Le, Q., Yan, B., Yu, X., Li, Y., Song, H., Zhu, H., et al. (2017). Drug-seeking motivation level in male rats determines offspring susceptibility or resistance to cocaine-seeking behaviour. *Nat. Commun.* 8:15527. doi: 10.1038/ncomms15527

Levenson, J. M., Roth, T. L., Lubin, F. D., Miller, C. A., Huang, I. C., Desai, P., et al. (2006). Evidence that DNA (cytosine-5) methyltransferase regulates synaptic plasticity in the hippocampus. *J. Biol. Chem.* 281, 15763–15773. doi: 10.1074/jbc.M511767200

Lewitus, G. M., Konefal, S. C., Greenhalgh, A. D., Pribiag, H., Augereau, K., and Stellwagen, D. (2016). Microglial TNF-α suppresses cocaine-induced plasticity and behavioral sensitization. *Neuron* 90, 483–491. doi: 10.1016/j.neuron.2016.03.030

Lian, H., Roy, E., and Zheng, H. (2016). Microglial phagocytosis assay. *Bio Protoc.* 6:e1988. doi: 10.21769/bioprotoc.1988

Loxton, N. J., and Tipman, R. J. (2017). Reward sensitivity and food addiction in women. *Appetite* 115, 28–35. doi: 10.1016/j.appet.2016.10.022

Maag, J. L. V., Kaczorowski, D. C., Panja, D., Peters, T. J., Bramham, C. R., Wibrand, K., et al. (2017). Widespread promoter methylation of synaptic plasticity genes in long-term potentiation in the adult brain in vivo. *BMC Genomics* 18:250. doi: 10.1186/s12864-017-3621-x

Maldonado-Ruiz, R., Cárdenas-Tueme, M., Montalvo-Martínez, L., Vidaltamayo, R., Garza-Ocañas, L., Reséndez-Perez, D., et al. (2019). Priming of hypothalamic ghrelin signaling and microglia activation exacerbate feeding in rats' offspring following maternal overnutrition. *Nutrients* 11:1241. doi: 10.3390/nu11061241

Marco, A., Kisliouk, T., Weller, A., and Meiri, N. (2013). High fat diet induces hypermethylation of the hypothalamic Pomc promoter and obesity in post-weaning rats. *Psychoneuroendocrinology* 38, 2844–2853. doi: 10.1016/j.psyneuen.2013.07.011

Massart, R., Barnea, R., Dikshtein, Y., Suderman, M., Meir, O., Hallett, M., et al. (2015). Role of DNA methylation in the nucleus accumbens in incubation of cocaine craving. *J. Neurosci.* 35, 8042–8058. doi: 10.1523/jneurosci.3053-14.2015

Maze, I., Covingtoni, H. E., Dietz, D. M., Laplant, Q., Renthal, W., Russo, S. J., et al. (2010). Essential role of the histone methyltransferase G9a in cocaine-induced plasticity. *Science* 327, 213–216. doi: 10.1126/science.1179438

Mo, Z., Li, Q., Cai, L., Zhan, M., and Xu, Q. (2019). The effect of DNA methylation on the miRNA expression pattern in lipopolysaccharide-induced inflammatory responses in human dental pulp cells. *Mol. Immunol.* 111, 11–18. doi: 10.1016/j.molimm.2019.03.012

Mohn, F., Weber, M., Rebhan, M., Roloff, T. C., Richter, J., Stadler, M. B., et al. (2008). Lineage-specific polycomb targets and de novo DNA methylation define restriction and potential of neuronal progenitors. *Mol. Cell* 30, 755–766. doi: 10.1016/j.molcel.2008.05.007

Mychasiuk, R., Muhammad, A., Ilnytskyy, S., and Kolb, B. (2013). Persistent gene expression changes in NAc, mPFC, and OFC associated with previous nicotine or amphetamine exposure. *Behav. Brain Res.* 256, 655–661. doi: 10.1016/j.bbr.2013.09.006

Netea, M. G. (2013). Training innate immunity: the changing concept of immunological memory in innate host defence. *Eur. J. Clin. Investig.* 43, 881–884. doi: 10.1111/eci.12132

Northcutt, A. L., Hutchinson, M. R., Wang, X., Baratta, M. V., Hiranita, T., Cochran, T. A., et al. (2015). DAT isn't all that: cocaine reward and reinforcement require Toll-like receptor 4 signaling. *Mol. Psychiatry* 20, 1525–1537. doi: 10.1038/mp.2014.177

Novikova, S. I., He, F., Bai, J., Cutrufello, N. J., Lidow, M. S., and Undieh, A. S. (2008). Maternal cocaine administration in mice alters DNA methylation and gene expression in hippocampal neurons of neonatal and prepubertal offspring. *PLoS One* 3:e1919. doi: 10.1371/journal.pone.0001919

Ong, Z. Y., and Muhlhausler, B. S. (2011). Maternal "junk-food" feeding of rat dams alters food choices and development of the mesolimbic reward pathway in the offspring. *FASEB J.* 25, 2167–2179. doi: 10.1096/fj.10-178392

Pascual, M., Baliño, P., Alfonso-Loeches, S., Aragón, C. M. G., and Guerri, C. (2011). Impact of TLR4 on behavioral and cognitive dysfunctions associated with alcohol-induced neuroinflammatory damage. *Brain Behav. Immun.* 25(Suppl. 1), S80–S91. doi: 10.1016/j.bbi.2011.02.012

Paxinos, G., and Watson, C. (2007). *The Rat Brain in Stereotaxic Coordinates*, 6th Edn. Cambridge, MA: Academic Press.

Peleg-Raibstein, D., Sarker, G., Litwan, K., Krämer, S. D., Ametamey, S. M., Schibli, R., et al. (2016). Enhanced sensitivity to drugs of abuse and palatable foods following maternal overnutrition. *Transl. Psychiatry* 6:e911. doi: 10.1038/tp.2016.176

Pierce, R. C., Fant, B., Swinford-Jackson, S. E., Heller, E. A., Berrettini, W. H., and Wimmer, M. E. (2018). Environmental, genetic and epigenetic contributions to cocaine addiction. *Neuropsychopharmacology* 43, 1471–1480. doi: 10.1038/s41386-018-0008-x

Richardson, N. R., and Roberts, D. C. S. (1996). Progressive ratio schedules in drug self-administration studies in rats: a method to evaluate reinforcing efficacy. *J. Neurosci. Methods* 66, 1–11. doi: 10.1016/0165-0270(95)00153-0

Rizzardi, L. F., Hickey, P. F., Rodriguez DiBlasi, V., Tryggvadóttir, R., Callahan, C. M., Idrizi, A., et al. (2019). Neuronal brain-region-specific DNA methylation and chromatin accessibility are associated with neuropsychiatric trait heritability. *Nat. Neurosci.* 22, 307–316. doi: 10.1038/s41593-018-0297-8

Robinson, J. L., McBreairty, L. E., Randell, E. W., Brunton, J. A., and Bertolo, R. F. (2016). Restriction of dietary methyl donors limits methionine availability and affects the partitioning of dietary methionine for creatine and phosphatidylcholine synthesis in the neonatal piglet. *J. Nutr. Biochem.* 35, 81–86. doi: 10.1016/j.jnutbio.2016.07.001

Rossetti, M. F., Schumacher, R., Gastiazoro, M. P., Lazzarino, G. P., Andreoli, M. F., Stoker, C., et al. (2020). Epigenetic dysregulation of dopaminergic system by maternal cafeteria diet during early postnatal development. *Neuroscience* 424, 12–23. doi: 10.1016/j.neuroscience.2019.09.016

Ruddock, H. K., Field, M., and Hardman, C. A. (2017). Exploring food reward and calorie intake in self-perceived food addicts. *Appetite* 115, 36–44. doi: 10.1016/j.appet.2016.12.003

Sarker, G., Berrens, R., von Arx, J., Pelczar, P., Reik, W., Wolfrum, C., et al. (2018). Transgenerational transmission of hedonic behaviors and metabolic phenotypes induced by maternal overnutrition. *Transl. Psychiatry* 8:195. doi: 10.1038/s41398-018-0243-2

Schwarz, J. M., and Bilbo, S. D. (2013). Adolescent morphine exposure affects long-term microglial function and later-life relapse liability in a model of addiction. *J. Neurosci.* 33, 961–971. doi: 10.1523/JNEUROSCI.2516-12.2013

Schwarz, J. M., Hutchinson, M. R., and Bilbo, S. D. (2011). Early-life experience decreases drug-induced reinstatement of morphine CPP in adulthood via microglial-specific epigenetic programming of anti-inflammatory IL-10 expression. *J. Neurosci.* 31, 17835–17847. doi: 10.1523/JNEUROSCI.3297-11.2011

Shen, J., Liu, Y., Ren, X., Gao, K., Li, Y., Li, S., et al. (2016). Changes in DNA methylation and chromatin structure of pro-inflammatory cytokines stimulated by LPS in broiler peripheral blood mononuclear cells. *Poult. Sci.* 95, 1636–1645. doi: 10.3382/ps/pew086

Shi, H., Kokoeva, M. V., Inouye, K., Tzameli, I., Yin, H., and Flier, J. S. (2006). TLR4 links innate immunity and fatty acid-induced insulin resistance. *J. Clin. Investig.* 116, 3015–3025. doi: 10.1172/JCI28898

Shiratori, H., Feinweber, C., Knothe, C., Lötsch, J., Thomas, D., Geisslinger, G., et al. (2016). High-throughput analysis of global DNA methylation using methyl-sensitive digestion. *PLoS One* 11:e0163184. doi: 10.1371/journal.pone.0163184

Skinner, M. K., Manikkam, M., and Guerrero-Bosagna, C. (2011). Epigenetic transgenerational actions of endocrine disruptors. *Reprod. Toxicol.* 308, 1466–1469. doi: 10.1016/j.reprotox.2010.10.012

Snider, S. E., Hendrick, E. S., and Beardsley, P. M. (2013). Glial cell modulators attenuate methamphetamine self-administration in the rat. *Eur. J. Pharmacol.* 701, 124–130. doi: 10.1016/j.ejphar.2013.01.016

Tanda, G., Mereu, M., Hiranita, T., Quarterman, J. C., Coggiano, M., and Katz, J. L. (2016). Lack of specific involvement of (+)-Naloxone and (+)-Naltrexone on the reinforcing and neurochemical effects of cocaine and opioids. *Neuropsychopharmacology* 41, 2772–2781. doi: 10.1038/npp.2016.91

Tian, W., Zhao, M., Li, M., Song, T., Zhang, M., Quan, L., et al. (2012). Reversal of cocaine-conditioned place preference through methyl supplementation in mice: altering global DNA methylation in the prefrontal cortex. *PLoS One* 7:e33435. doi: 10.1371/journal.pone.0033435

van Galen, K. A., ter Horst, K. W., Booij, J., la Fleur, S. E., and Serlie, M. J. (2018). The role of central dopamine and serotonin in human obesity: lessons learned from molecular neuroimaging studies. *Metabolism* 85, 325–339. doi: 10.1016/j.metabol.2017.09.007

Verheij, M. M. M., and Cools, A. R. (2011). Reserpine differentially affects cocaine-induced behavior in low and high responders to novelty. *Pharmacol. Biochem. Behav.* 98, 43–53. doi: 10.1016/j.pbb.2010.11.021

Volkow, N. D., Wang, G. J., and Baler, R. D. (2011). Reward, dopamine and the control of food intake: implications for obesity. *Trends Cogn. Sci.* 15, 37–46. doi: 10.1016/j.tics.2010.11.001

Volkow, N. D., Wang, G. J., Tomasi, D., and Baler, R. D. (2013). Obesity and addiction: neurobiological overlaps. *Obes. Rev.* 14, 2–18. doi: 10.1111/j.1467-789X.2012.01031.x

Volkow, N. D., and Wise, R. A. (2005). How can drug addiction help us understand obesity? *Nat. Neurosci.* 8, 555–560. doi: 10.1038/nn1452

Winterdahl, M., Noer, O., Orlowski, D., Schacht, A. C., Jakobsen, S., Alstrup, A. K. O., et al. (2019). Sucrose intake lowers μ-opioid and dopamine D2/3 receptor availability in porcine brain. *Sci. Rep.* 9:16918. doi: 10.1038/s41598-019-53430-9

Wohleb, E. S., Franklin, T., Iwata, M., and Duman, R. S. (2016). Integrating neuroimmune systems in the neurobiology of depression. *Nat. Rev. Neurosci.* 17, 497–511. doi: 10.1038/nrn.2016.69

Wright, K. N., Hollis, F., Duclot, F., Dossat, A. M., Strong, C. E., Francis, T. C., et al. (2015). Methyl supplementation attenuates cocaine-seeking behaviors and cocaine-induced c-Fos activation in a DNA methylation-dependent manner. *J. Neurosci.* 35, 8948–8958. doi: 10.1523/JNEUROSCI.5227-14.2015

Yamamoto, D. J., Nelson, A. M., Mandt, B. H., Larson, G. A., Rorabaugh, J. M., Ng, C. M. C., et al. (2013). Rats classified as low or high cocaine locomotor responders: a unique model involving striatal dopamine transporters that predicts cocaine addiction-like behaviors. *Neurosci. Biobehav. Rev.* 37, 1738–1753. doi: 10.1016/j.neubiorev.2013.07.002

Yuan, N., Chen, Y., Xia, Y., Dai, J., and Liu, C. (2019). Inflammation-related biomarkers in major psychiatric disorders: a cross-disorder assessment of reproducibility and specificity in 43 meta-analyses. *Transl. Psychiatry* 9:233. doi: 10.1038/s41398-019-0570-y

Zhang, X., Yang, R., Jia, Y., Cai, D., Zhou, B., Qu, X., et al. (2014). Hypermethylation of Sp1 binding site suppresses hypothalamic POMC in neonates and may contribute to metabolic disorders in adults: impact of maternal dietary CLAs. *Diabetes* 63, 1475–1487. doi: 10.2337/db13-1221

Conflict of Interest: The authors declare that the research was conducted in the absence of any commercial or financial relationships that could be construed as a potential conflict of interest.

nutrients

MDPI

Article

Priming of Hypothalamic Ghrelin Signaling and Microglia Activation Exacerbate Feeding in Rats' Offspring Following Maternal Overnutrition

Roger Maldonado-Ruiz [1,2], Marcela Cárdenas-Tueme [3], Larisa Montalvo-Martínez [1,2], Roman Vidaltamayo [4], Lourdes Garza-Ocañas [5], Diana Reséndez-Perez [3] and Alberto Camacho [1,2,*]

1 Department of Biochemistry, College of Medicine, Universidad Autónoma de Nuevo León, Monterrey, C.P. 64460, México; rogalmalruiz@gmail.com (R.M.-R.); lj_montalvo.mtz@hotmail.com (L.M.-M.)
2 Neurometabolism Unit. Center for Research and Development in Health Sciences, Universidad Autónoma de Nuevo León, Monterrey, C.P. 64460, México
3 Department of Cell Biology and Genetics, College of Biological Sciences, Universidad Autónoma de Nuevo León, Monterrey, C.P. 64460, México; marcela.cdns@gmail.com (M.C.-T.); diaresendez@gmail.com (D.R.-P.)
4 Department of Basic Science, School of Health Sciences, Universidad de Monterrey, San Pedro Garza, N.L. 66238, México; roman.vidaltamayo@udem.edu
5 Departamento de Farmacologia y Toxicología, College of Medicine, Universidad Autonoma de Nuevo Leon, Monterrey, C.P. 64460, México; logarza@live.com.mx
* Correspondence: acm590@hotmail.com; Tel.: +01-52(81)8329-4050

Received: 30 March 2019; Accepted: 29 May 2019; Published: 31 May 2019

Abstract: Maternal overnutrition during pregnancy leads to metabolic alterations, including obesity, hyperphagia, and inflammation in the offspring. Nutritional priming of central inflammation and its role in ghrelin sensitivity during fed and fasted states have not been analyzed. The current study aims to identify the effect of maternal programming on microglia activation and ghrelin-induced activation of hypothalamic neurons leading to food intake response. We employed a nutritional programming model exposing female Wistar rats to a cafeteria diet (CAF) from pre-pregnancy to weaning. Food intake in male offspring was determined daily after fasting and subcutaneous injection of ghrelin. Hypothalamic ghrelin sensitivity and microglia activation was evaluated using immunodetection for Iba-1 and c-Fos markers, and Western blot for TBK1 signaling. Release of TNF-alpha, IL-6, and IL-1β after stimulation with palmitic, oleic, linoleic acid, or C6 ceramide in primary microglia culture were quantified using ELISA. We found that programmed offspring by CAF diet exhibits overfeeding after fasting and peripheral ghrelin administration, which correlates with an increase in the hypothalamic Iba-1 microglia marker and c-Fos cell activation. Additionally, in contrast to oleic, linoleic, or C6 ceramide stimulation in primary microglia culture, stimulation with palmitic acid for 24 h promotes TNF-alpha, IL-6, and IL-1β release and TBK1 activation. Notably, intracerebroventricular (i.c.v.) palmitic acid or LPS inoculation for five days promotes daily increase in food intake and food consumption after ghrelin administration. Finally, we found that i.c.v. palmitic acid substantially activates hypothalamic Iba-1 microglia marker and c-Fos. Together, our results suggest that maternal nutritional programing primes ghrelin sensitivity and microglia activation, which potentially might mirror hypothalamic administration of the saturated palmitic acid.

Keywords: ghrelin; hypothalamic inflammation; microglia; nutritional programing

1. Introduction

Maternal obesity or maternal overnutrition during pregnancy and lactation programs an adverse uterine milieu leading to defects in organ function and metabolism in offspring [1,2]. Programing involves a new setting of peripheral and central pathways including energy expenditure and appetite regulation, which potentially increase the susceptibility for obesity and metabolic-related pathologies in adult offspring [2]. Maternal nutritional programming by cafeteria diet (CAF) in murine models sets metabolic alterations including impaired insulin sensitivity, hypertension, endothelial dysfunction, increased adiposity [3–5], and altered appetite regulation (hyperphagia) [2,6].

Food intake is actively regulated by ghrelin, which is the only known appetite-inducing peptide produced by endocrine cells of the gastric mucosa [7,8]. Ghrelin induces a powerful orexigenic signal by activating the secretagogue receptors of growth hormone (GHSR) expressed in the hypothalamic POMC of the arcuate nucleus (ARC) and the NPY/AgRP neurons of the paraventricular nucleus (PVH) [7,8]. Maternal programming by overnutrition increases plasma ghrelin levels in both dams and their offspring [9]; Additionally, neonatal overfeeding disrupts ghrelin signaling [10] and induces overweight into adulthood in both males and females [11,12]. Maternal nutritional programming by overnutrition also stimulates proliferation of neuroepithelial and neuronal precursor cells in the hypothalamus during the embryonic period, leading to differentiation and proliferation of orexigenic peptide-producing neurons [13]. Furthermore, a recent clinical study demonstrated that the maternal prenatal lipid profile was associated with the offspring's eating behavior and energy intake [14]. This evidence proposes that maternal nutritional programming might set an orexigenic phenotype in the offspring by increasing plasma ghrelin levels and orexigenic neuronal expression in the hypothalamic nucleus.

Maternal obesity or maternal overnutrition is also associated with a positive inflammatory profile, known as metabolic inflammation. For instance, free fatty acids accumulation in plasma during maternal programming promote a central and peripheral inflammatory response through toll-like receptor 4 (TLR-4) activation [15–17]. In addition, clinical evidence showed substantial increased expression of TLR-4, IL-6, and IL-8 in the placenta of obese women [18], and TLR-4 ablation in the ARC nucleus of murine models prevents obesity [19].

In the brain, hypothalamic microglia actively responds to accumulation of saturated fatty acids following caloric exposure in murine models [11,12]. We have reported that the saturated lipid palmitic acid leads to the activation of the TLR-4-TBK1 pathway in the hypothalamus of obese murine models, which correlates with insulin resistance [20]. Of note, initial reports identified that chronic microglia activation following caloric exposure correlates with ghrelin resistance in the hypothalamus [21]. Conversely, genetic ablation of microglia leads to anorexia and weight loss [22]. Of importance, seminal studies have identified that plasma lipid profile selectively regulates ghrelin sensitivity. For instance, lipid infusions in humans suppresses the GHSR effects of ghrelin [23]. Additionally, in vitro studies identified that prolonged exposure to unsaturated fatty acids activates ghrelin sensitivity, potentially due to an increase in the GHSR in lipid rafts [24]. This evidence suggests that unsaturated or saturated plasma lipid profiles promote microglia activation, leading to positive or negative ghrelin sensitivity, respectively. It is unknown whether overnutrition during maternal programming primes hypothalamic ghrelin signaling in offspring, promoting increased food intake in adulthood. The current study was designed to identify the effect of maternal nutritional programming by caloric exposure on ghrelin-induced activation of hypothalamic neurons and food intake regulation in the offspring.

2. Materials and Methods

2.1. Reagents and Antibodies

Reagents and antibodies used in our experimental design are showed in Tables 1 and 2, respectively.

Table 1. List of reagents

Reagent	Catalog	Application (conc.)	Manufacturer
Ghrelin		i.c.v	Sigma-Aldrich, St. Louis, MO, USA
Dulbecco's Modified Eagle's Medium high glucose	G8903 D5648	PC	Sigma-Aldrich, St. Louis, MO, USA
L-15 Medium (Leibovitz)	L4386	PC	Sigma-Aldrich, St. Louis, MO, USA
Palmitic acid	P0500	i.c.v. and PC	Sigma-Aldrich, St. Louis, MO, USA
Palmitoleic acid	P9417	PC	Sigma-Aldrich, St. Louis, MO, USA
Linoleic acid	L1376	PC	Sigma-Aldrich, St. Louis, MO, USA
Stearic acid	S47S1	PC	Sigma-Aldrich, St. Louis, MO, USA
N-hexanoyl-D-esfingosin	H6524	PC	Sigma-Aldrich, St. Louis, MO, USA
lipopolysaccharide (LPS) *Escherichia coli* 0111: B4	L2630	i.c.v. and PC	Sigma-Aldrich, St. Louis, MO, USA
Rat TNF-α ELISA Ready-SET-Go!	88-7340	ELISA	eBioscience, San Diego, CA, USA
Rat IL-6 ELISA kit	RAB0311	ELISA	Sigma-Aldrich, St. Louis, MO, USA
Rat IL-1β ELISA kit	RAB0277	ELISA	Sigma-Aldrich, St. Louis, MO, USA

PC: primary microglia cell culture; i.c.v: intracerebroventricular injection.

Table 2. List of antibodies

Antibody	Catalog	Application (conc.)	Host	Manufacturer
Anti-NAK	ab40676	WB (1:1000)	Rabbit	abcam, Cambridge, MA, USA
Anti-p-NAK S172	ab109272	WB (1:1000)	Rabbit	abcam, Cambridge, MA, USA
Anti-p-NF-κB p65 S536	3033S	WB (1:1000)	Rabbit	Cell Signaling, Beverly, MA, USA
Anti-p- NF-κB p65	8242S	WB (1:1000)	Rabbit	Cell Signaling, Beverly, MA, USA
Anti- β-Actin	8457P	WB (1:5000)	Rabbit	Cell Signaling, Beverly, MA, USA
Anti-rabbit IgG-HRP	sc-2370	WB (1:1000)	Cow	Santa Cruz Biotech., Dallas, TX, USA
Alexa fluor 488 anti-rabbit	A-11034	IF (1:1000)	Goat	Thermo Fisher Scientific, Waltham, MA, USA
Alexa fluor 546 anti-rabbit	A-11035	IF (1:1000)	Goat	Thermo Fisher Scientific, Waltham, MA, USA
Anti-c-fos	ab190289	IF (1:1000)	Rabbit	abcam, Cambridge, MA, USA
Anti-Iba-1	ab178847	IF (1:200)	Rabbit	abcam, Cambridge, MA, USA

WB: western blot; IF: Immunofluorescence.

2.2. Animals and Housing

All the experiments were performed using two-month-old wild-type female Wistar rats (initial body weight 200–250 g). Animals were handled according to the NIH guide for the care and use of laboratory animals (NIH Publications No. 80–23, revised in 1996). We followed the Basel Declaration to implement the ethical principles of Replacement, Reduction and Refinement of experimental animal models. Our study was approved by the local Animal Care Committee (BI0002). Rats were housed individually in Plexiglas-style cages, maintained at 20–23 °C in a temperature-controlled room with a 12-h light/dark cycle. Water was available ad libitum in the home cage. Food availability is described below.

2.3. Diets

The standard chow diet formula contained 57% carbohydrates, 13% lipids, and 30% proteins, caloric density = 3.35 kcal/g (LabDiet, St. Louis, MO 63144, 5001, Cat. D12450B). Cafeteria (CAF) diet was made of liquid chocolate, biscuits, bacon, fries potatoes, standard diet, and pork paté based on a 1:1:1:1:1:1:2 ratio, respectively; total calories 3.72 kcal/g in 39% carbohydrates, 49% lipids, 12% proteins, and 513.53 mg of sodium, caloric density = 3.72 kcal/g, as we reported before [5]. It is important to note that the CAF diet simulates the feeding habits of human populations in North America [25].

2.4. Maternal Nutritional Programming Model

Programing and mating experiments were performed using 12-week-old male and 10-weel-old virgin female Wistar rats. Animals were acclimated to the animal facility seven days prior to the nutritional programming protocol in standard conditions with ad libitum access to food and water. Female rats (n = 6) were randomized into two batches of three animals each, one for the control chow diet and the second for the CAF diet, as we reported [5]. After randomization, female rats were exposed ad libitum to specific formula diets three weeks before mating. Rats were mated with age-matched Wistar males for two days and males were removed from the home cage. Pregnancy diagnosis was performed in females after mating by vaginal plug. Female rats lacking copulation plugs were returned to the home cage for a second mating. Pregnant rats were kept on the same diet until birth and lactation. Male offspring from mothers exposed to Chow or CAF diets were weaned at post-natal day 21, grouped into 10–12 subjects per group and exposed to control Chow diet (Control Chow and CAF programmed groups) for nine weeks. During the experiment, body weight and food intake were measured weekly (Figure 1a).

2.5. Analysis of Ghrelin Signaling for Chow and CAF Exposure in Offspring

The offspring from mothers exposed to Chow (n = 10–12) or CAF (n = 10–12) diet were fasted for 16 h by removing their food at 18:00 PM. To measure total food intake, Chow and CAF diets were weighed and placed inside the cages, where they were left for 4 h, after which food was removed and weighed. Additionally, after removing the food, Chow or CAF programmed offspring were injected intradermically with 0.2 micrograms/kg of ghrelin (n = 10–12) or saline (n = 10–12), and food was placed in their cages for 2 h (see Table 1 for reagents). Rats were allowed to eat ad libitum, and then food was removed and weighed.

This procedure allowed each subject to be its own control for the ghrelin effect. Next, rats were intracardially perfused and processed for immunohistochemistry against c-Fos for neuronal and Iba-1 for microglia activation (see Table 2 for antibodies), as described below.

2.6. Intracardiac Perfusion

After 2 h of ghrelin administration, the offspring was anesthetized by 1 mL pentobarbital (PiSA Agropecuaria) i.p. overdose. A dermal dissection was performed from the abdominal region to the upper part of the thoracic cage, exposing the heart. Then, the left ventricle of the heart was perforated following its apex and a cut was made in the right atrium in order to open the circulatory system. Rats were intracardially perfused with 250 mL 0.1 M phosphate-buffered saline (PBS) + 10 U/mL heparin followed by 250 mL paraformaldehyde 4% in PBS 0.1M (PFA) using an infusion pump (Fisher Scientific GP1000) at a flow rate of 15 mL/min. The brains were collected, and samples were stored in 4% PFA + PBS 0.1 M at 4 °C for 24 hours and changed to 10%, 20%, and 30% sucrose before cutting. We obtained 40-µm coronal sections in the rostral-caudal direction between bregma −1.58 and −1.94 mm for the ARC, and between bregma −0.70 and −0.94 mm for the PVN using a cryostat; the sections were processed for immunohistochemistry as described below. Anatomical limits of each brain region were identified using the Paxinos and Watson Atlas [26].

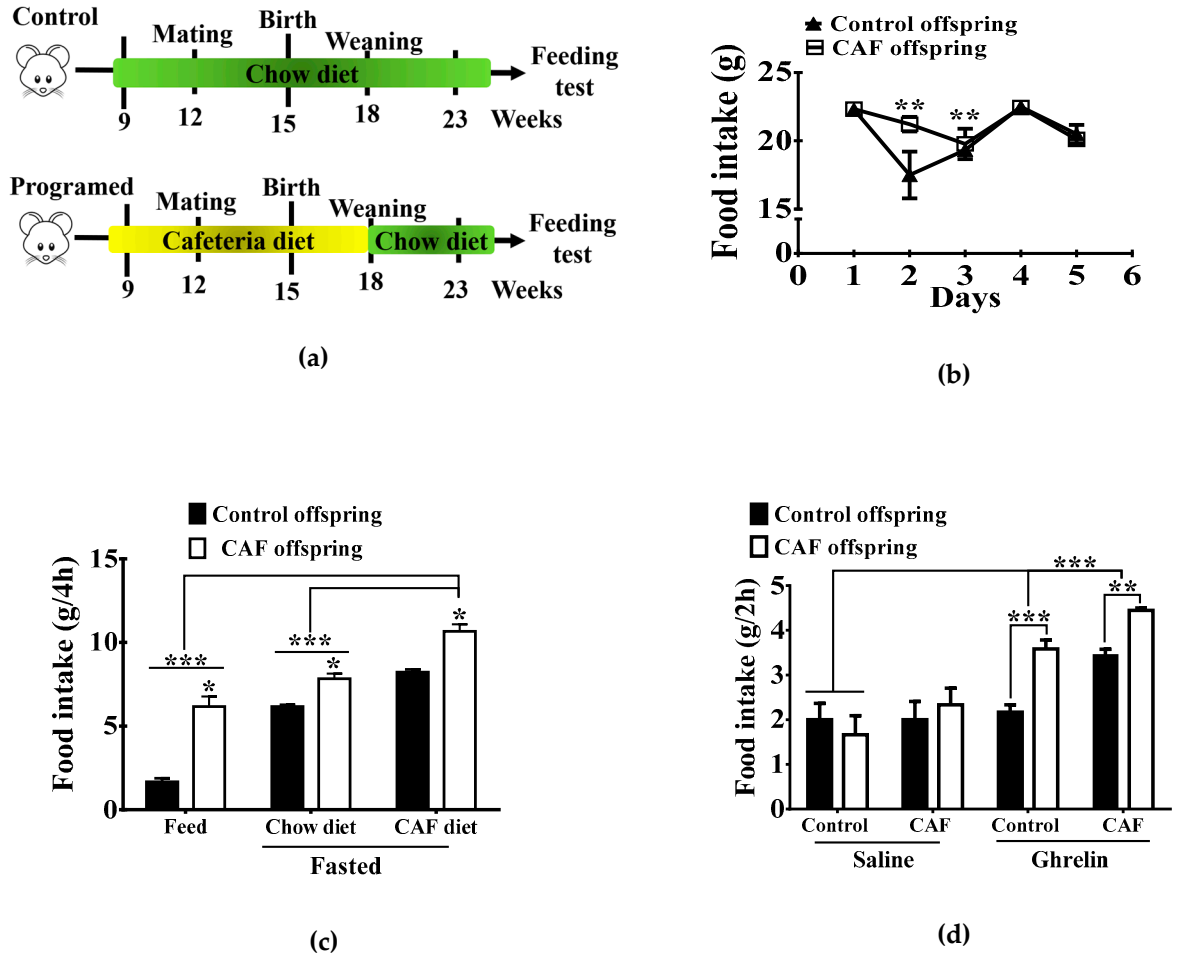

Figure 1. Effect of maternal nutritional programming on food intake in male offspring. (**a**) Maternal programing was performed by exposing Chow or CAF diet for nine weeks including pre-pregnancy, pregnancy and lactation. After weaning the offspring of both (CAF and Chow diets) was exposed to Chow diet for 5 weeks, by two months of age (week 23) we performed the feeding test. (**b**) Daily food intake by both Chow offspring and CAF diet offspring. (**c**) Chow and CAF diet consumption during 4 h in offspring after fasting for 16 h and refeeding. (**d**) Food intake for 2 h after administration with ghrelin 0.2 µg/Kg SC. (control diet group n = 10–12; cafeteria diet (CAF) group n = 10–12; the graphs show normalized data of the mean ± S.E.M. Two-way ANOVA followed by Tukey multiple comparation test; * p <0.05, ** p <0.01, *** p <0.001).

2.7. Tissue Sample Collection

The second batch of offspring (n = 10–12 each) were sacrificed by decapitation at nine weeks of age. Blood samples were collected in 500-µL tubes (Beckton Dickinson) and plasma fraction was isolated by centrifugation at 4 °C and frozen at −80 °C. ARC and PVN-DMN of hypothalamus were dissected and frozen immediately at 80 °C for Western blot analysis.

2.8. Stereotaxic Surgery and I.C.V. Ghrelin Administration

A third batch of rats was selected for stereotaxic brain surgeries to selectively stimulate the hypothalamic region. In brief, all surgeries were carried out using aseptic techniques and animals were injected with ketamine (100 mg/kg, i.p.) + xylazine (10 mg/kg, i.p.) to induce anesthesia and analgesia, respectively. By eight weeks of age, male rats (n = 36) were implanted with a cannula in the third ventricle following the stereotaxic coordinates, AP: −2.56, mL: 0, DV: −9.4 according to the rat brain atlas [26]. The animals were allowed to recover for seven days and placed into three experimental groups (n = 8/group) for five days i.c.v administration of: 1) artificial cerebrospinal fluid (ACSF)

(Control), 2) 40 µg/µL palmitic acid (PAL), and 3) 2 µg/µL lipopolysaccharide (LPS) (*Escherichia coli* 0111: B4). We performed a single i.c.v administration of ACSF, PAL or LPS using an infusion pump at 2 µL flux rate. We quantified total food intake per day as well as glucose and insulin following the i.c.v administration of 1µg/µL ghrelin.

2.9. Glucose and Insulin Tolerance Test (GTT, ITT) and Ghrelin Sensitivity Assessments

Following i.c.v administration, males were fasted for 8 or 12 h and were intraperitoneally injected with 1 U of insulin/100 g or 40% glucose/kg body weight, respectively. Blood glucose levels were quantified at 0, 15, 30, 45, 60, 90, and 120 min, as described previously [5]. A week after GTT and ITT assessments, rats were i.c.v. injected with ghrelin (1 µg/µL) and we quantified total food intake for two hours. Subjects were transcardially perfused as described and processed for immunohistochemistry analysis as described below.

2.10. Microglia Primary Culture and Treatments

Cerebral cortices from the postnatal day 2 (P2) Wistar rat pups were surgically dissected, harvested, the meninges and blood vessels were removed, and the parenchyma minced and triturated in Leibovitz's L-15 Medium (Thermo Fisher Scientific, Waltham, Massachusetts) + 0.1% bovine serum albumin (BSA) with 4.5 g/L glucose, 100 U/mL penicillin, and 0.1 mg/mL streptomycin. Suspended cells were filtered (70 mm) and plated on T-75 Flasks containing 10 mL of Dulbecco's Modified Eagle's medium (DMEM) (SIGMA, San Luis, MO, USA); media were replenished every two days, resulting in mixed glial monolayers. Two weeks later, the flasks were shaken (200 rpm) for two hours (37 °C) to specifically release microglia.

Microglia culture were 70–80% confluent and stimulated for 24h with one of each fatty acids as follow: 100 µM palmitic acid, 100 µM palmitoleic acid, 100 µM stearic acid and 100 µM linoleic acid (Sigma-Aldrich, San Luis, MO, USA), 25 µM N-hexanoyl-D-sphingosine (C6) or 0.1 µg/mL LPS. Culture medium was recovered to perform the IL-6, IL-1β, and TNF-alpha ELISA tests. All fatty acids were first solubilized in DMEM media containing 10% of free fatty acid BSA, then administered in each well. Microglia were harvested and total protein was extracted using lysis buffer for Western blot analysis as described below.

2.11. Cytokine Measurements

Levels of IL-6, IL-1β, and TNF- alpha in culture medium of microglia following fatty acids or LPS stimulation were measured by ELISA (Sigma-Aldrich, St. Louis, MO, USA), following the manufacturer's instructions.

2.12. Immunohistochemistry Analysis by Confocal Imaging

Frozen brain sections were air dried at room temperature (RT) for one hour to prevent sections from falling off the slides during antibody incubations. Afterwards, the slices were washed three times for 5 min with 1X PBS + 0.1% TritonX-100 (PBST) and the slices were blocked in PBST + 10% goat serum for an hour. Subsequently, brain sections were incubated with PBST + 5% goat serum with the primary antibody anti-Iba-1 (1:200) or anti-c-Fos (1:1000) at 4 °C overnight. Subsequently, the slices were washed in PBST three times and then incubated for three hours with the secondary antibodies Alexa Fluor 488 Rabbit Goat Anti-Rabbit (IgG) for C-Fos or Alexa Fluor 546 Goat Anti-Rabbit (IgG) for Iba-1, each diluted in PBST + 5% goat serum (1:1000). Afterwards, brain sections were washed three times with PBST and air-dried at RT. Finally, brain sections were mounted using Vectashield with DAPI (Vector Laboratories, Burlingame, CA, USA) on coverslips.

2.13. Western Blot Analysis

Microglia culture samples and ARC and PVN-DMN hypothalamic biopsies were incubated in lysis buffer solution (150 mM NaCl, 25 mM Tris–HCl pH 7.5, containing 50 mM NaF, 10 mM NaP2O7, 1 mM Sodium orthovanadate, complete protease inhibitor cocktail (Roche, Mannheim, Germany) 0.5% Triton X-100) followed by sonication (for 5 s at 1500 Hz on ice). Samples were centrifuged for 10 min at 1500× *g* and protein concentration were determined by the bicinchoninic acid (BCA) assay at a concentration of 40 µg/µL. Samples were mixed with Laemmli buffer and then heated t 90 °C for 5 min and subjected to SDS–PAGE. Proteins were electrophoretically transferred to nitrocellulose membranes. The membrane was then blocked for 2 h at RT in TBS-T buffer (10mM Tris, 0.9% NaCl, 0.1% Tween 20, pH 7.5) containing 5% BSA. Membranes were incubated overnight with primary antibodies at 4 °C: TBK1 (1:1000), TBK1-pSer172, anti-NF-κB (1:1000), NF-κB-pSer536 (1:1000), anti-actin (1:2000). Membranes were washed (4 times/5 min) in TBS-T and incubated for 1 h with horseradish peroxidase (HRP)-conjugated secondary antibody. Proteins were detected by ECL, which were read employing the ChemiDoc™ XRS+ System (BIO-RAD) and quantified densitometrically with the 1.31V ImageJ software (Wayne Rasband, National Institutes of Health, Bethesda, MD, USA).

2.14. Statistical Analysis

Statistical analyses were conducted using the Prism 7 GraphPad software. Western blot data were analyzed using the unpaired Student's *t*-test. We used two-way ANOVA followed by Tukey for multiple comparations. Data are presented as mean ± SD. The significance levels displayed on figures are as follows: * $p < 0.05$, ** $p < 0.01$, *** $p < 0.001$.

3. Results

3.1. Maternal Nutritional Programming Exacerbates Ghrelin Sensitivity in Offspring, Leading to an Increase in Food Intake

First, we aimed to identify the effect of maternal nutritional programming by caloric exposure on basal and ghrelin-induced food intake regulation in the offspring. We found that offspring showed a significant transient increase of food intake by day two during the five days schedule, with no changes on total basal food intake (Figure 1b). Additionally, offspring programmed by the CAF diet exhibited an increase in Chow and CAF food intake after 14 h fasting when compared with offspring exposed to Chow diet during programming (Figure 1c). Of note, incentive food intake behavior in the programmed offspring was sensitive to ghrelin administration. We found that subcutaneous ghrelin injection significantly increased Chow and CAF diet intake in offspring programmed by maternal CAF compared with Chow programmed offspring (Figure 1d). These results suggest that maternal programming by CAF diet actively promotes food intake by potentially priming ghrelin sensitivity in offspring.

3.2. Maternal Programming by CAF Exposure Sets Activation of Hypothalamic Ghrelin-Sensitive C-Fos Neurons in Offspring

Next, we sought to identify if ghrelin sensitivity correlated with neuronal response and microglia activation in the hypothalamic ARC nucleus. We used a 120-min time-frame schedule following systemic ghrelin administration to identify central neuronal c-fos activation in the ARC nucleus leading to food intake response, as reported [27]. We found that offspring programmed by a maternal CAF diet exposure showed substantial microglia activation evidenced by an increase in the Iba-1 marker (Figure 2a). Additionally, CAF diet exposure promoted a higher neuronal c-fos expression in ARC when compared with matched controls (Figure 2b). Together, these results confirm that maternal programming is able to sensitize central neuronal activation in the hypothalamus of offspring following systemic ghrelin administration, which correlates with central microglia activation.

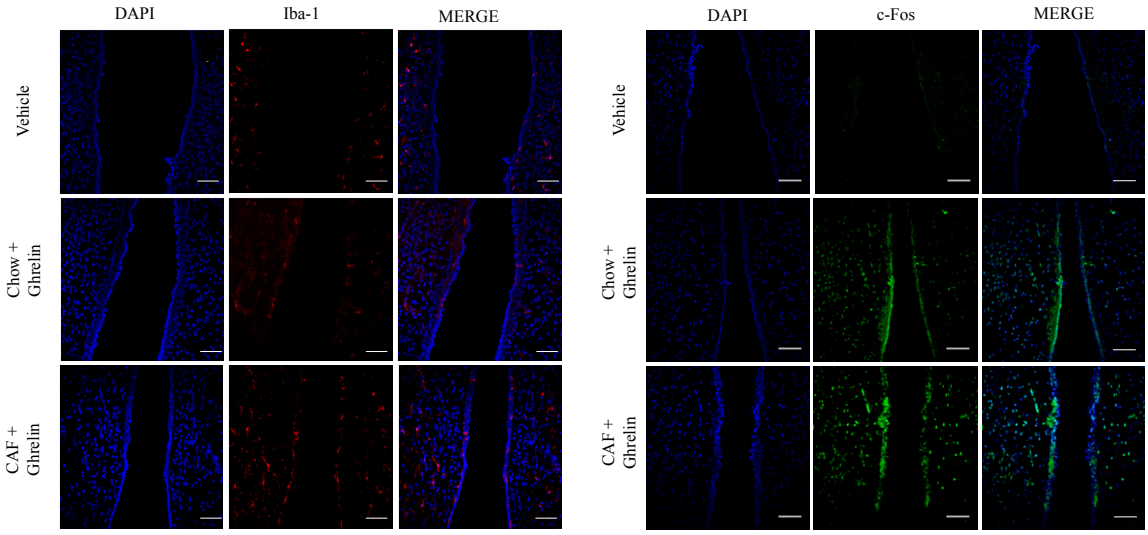

(**a**) (**b**)

Figure 2. Maternal programming leads to microglia activation and c-Fos response in hypothalamus. Offspring was programmed by CAF diet exposure as previously described, and 0.2 micrograms/kg ghrelin was intradermically administered, and subjects were intracardially perfused with 0.1M PBS + heparin followed by PBS + 4% PFA. Hypothalamic sections were obtained using a cryostat, according to the Paxinos and Watson Atlas. Immunofluorescence to identify microglia activation was performed using the Iba-1 antibody (1:200) following by the secondary antibody Alexa Fluor 546 Goat Anti-Rabbit (IgG) (1:1000) (**a**). c-Fos activation was identified by anti c-Fos (1:1000) and Alexa Fluor 488 Rabbit Goat Anti-Rabbit (1:1000) (**b**). Brain sections were mounted using Vectashield with DAPI (Vector Laboratories) on coverslips. (n = 3). PBS, phosphate-buffered saline, PFA, paraformaldehyde.

3.3. Saturated Lipids Activate a Pro-Inflammatory Stage in Microglia

To identify whether positive energy balance in offspring after programming selectively displayed microglia activation and ghrelin sensitivity, we initially characterized potential lipid species showing a pro-inflammatory profile using a microglia in vitro system. We performed saturated or unsaturated fatty acids stimulation for 24 h and quantified TNF-alpha, IL-6, and IL-1β release, as described. We found that the C16:0-saturated palmitic acid incubation efficiently promotes TNF-alpha, IL-6 and IL-1β release when compared with control, whereas the C18:0 long-chain stearic acid promotes TNF-alpha release with no changes in IL-6 and IL-1β (Figure 3a–c). Additionally, palmitoleic acid (C16:1), the monounsaturated form of palmitic acid promoted the production of IL-6, whereas the C6 ceramide (C18:1/6:0) decreased it (Figure 3b). Finally, the polyunsaturated linoleic acid (C18:2) incubation did not show changes in the pro-inflammatory profile of microglia (Figure 3a–c).

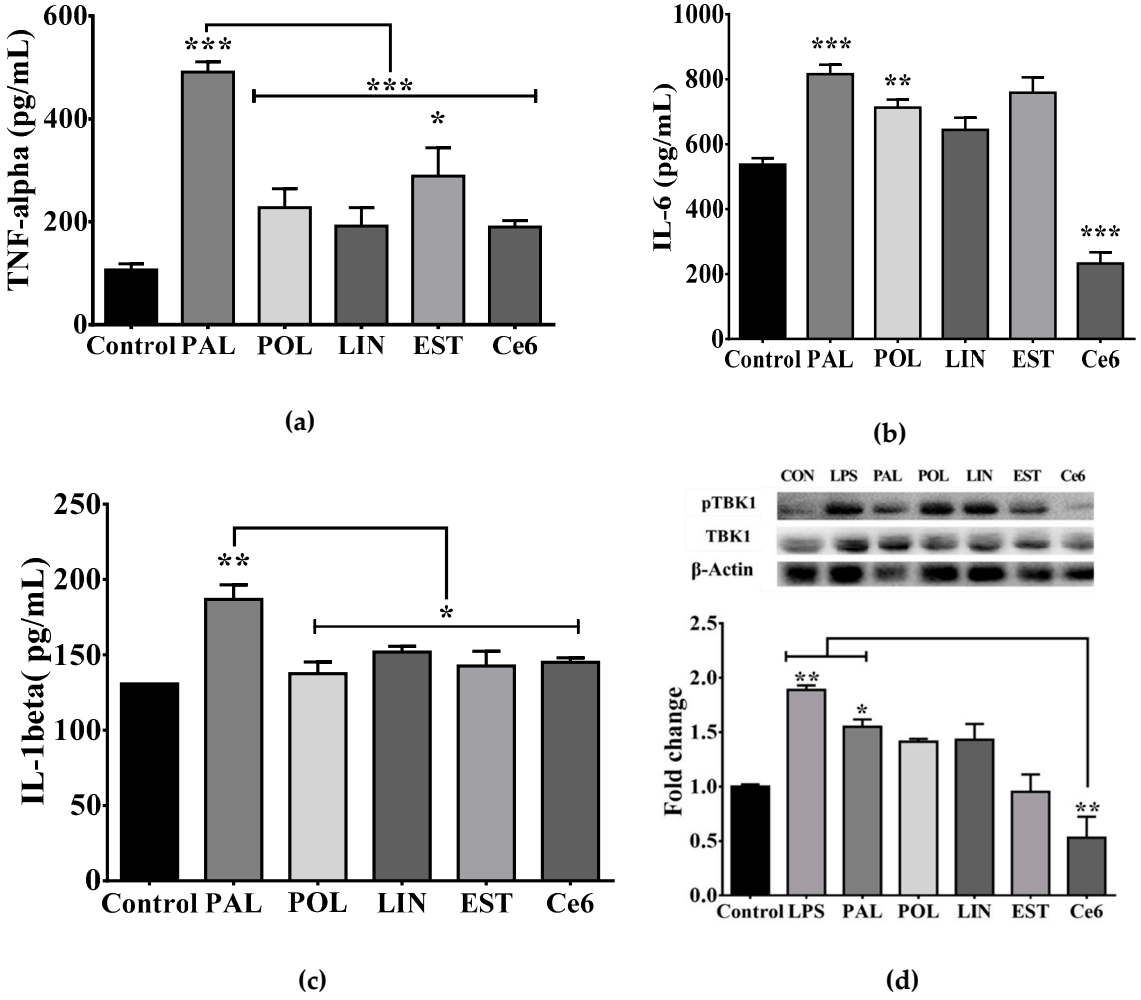

Figure 3. Palmitic acid incubation leads to cytokine production and TBK1 pathway activation in primary microglia. (**a**) TNF-alpha secretion, (**b**) IL-6 secretion or (**c**) IL-1β secretion by primary microglia culture following 1% BSA-FFA (Control); 100 μM palmitic acid, palmitoleic acid, linoleic acid or stearic acid or 25 μM C6 ceramide incubation for 24h. TNF-alpha, IL-6 and IL-1β secretion were quantified by ELISA following the manufacturer's instructions ($n = 4$). (**d**) TBK1 phosphorylation following saturated and unsaturated fatty acids stimulation was identified using western blot analysis. The graphs show normalized data of the mean ± S.E.M. Two-way ANOVA followed by Tukey multiple comparation test; * $p < 0.05$, ** $p < 0.01$, *** $p < 0.001$). TBK1, TANK-binding kinase 1, BSA-FFA, Bovine serum albumin-free fatty acids (FFA).

We previously reported that palmitic acid leads to the TLR4-TBK1 pathway activation in the hypothalamus of obese murine models, which correlates with systemic insulin resistance [20]. We identified whether stimulation with saturated and unsaturated fatty acids lead to TBK1 activation in microglia cultures. Our results show that both the positive inflammatory reagent, LPS, and palmitic acid elicit a significant activation of the TBK1 pathway in microglia cells (Figure 3d). Of importance, the C6 ceramide blocks the TBK1 pathway activation (Figure 3d), which correlates with no changes in TNF-alpha and IL-1β release (Figure 3a,b) with a decrease in the IL-6 release (Figure 3c). Our results confirmed the saturated palmitic acid as a reliable lipid species leading to pro-inflammatory state in microglia cells.

3.4. Hypothalamic Palmitic Acid Inoculation Promotes Increase in Total Food Intake

We determined whether central administration of the pro-inflammatory modulator palmitic acid disrupted plasma glucose homeostasis and/or food intake response. We found that i.c.v administration

of palmitic acid for 5 days partially increased plasma glucose levels following insulin administration, however, it did not change total glucose homeostasis evidenced by area under the curve (AUC) quantification (Figure 4a,b). Additionally, we found no changes in glucose homeostasis addressing by the GTT (Figure 4c,d).

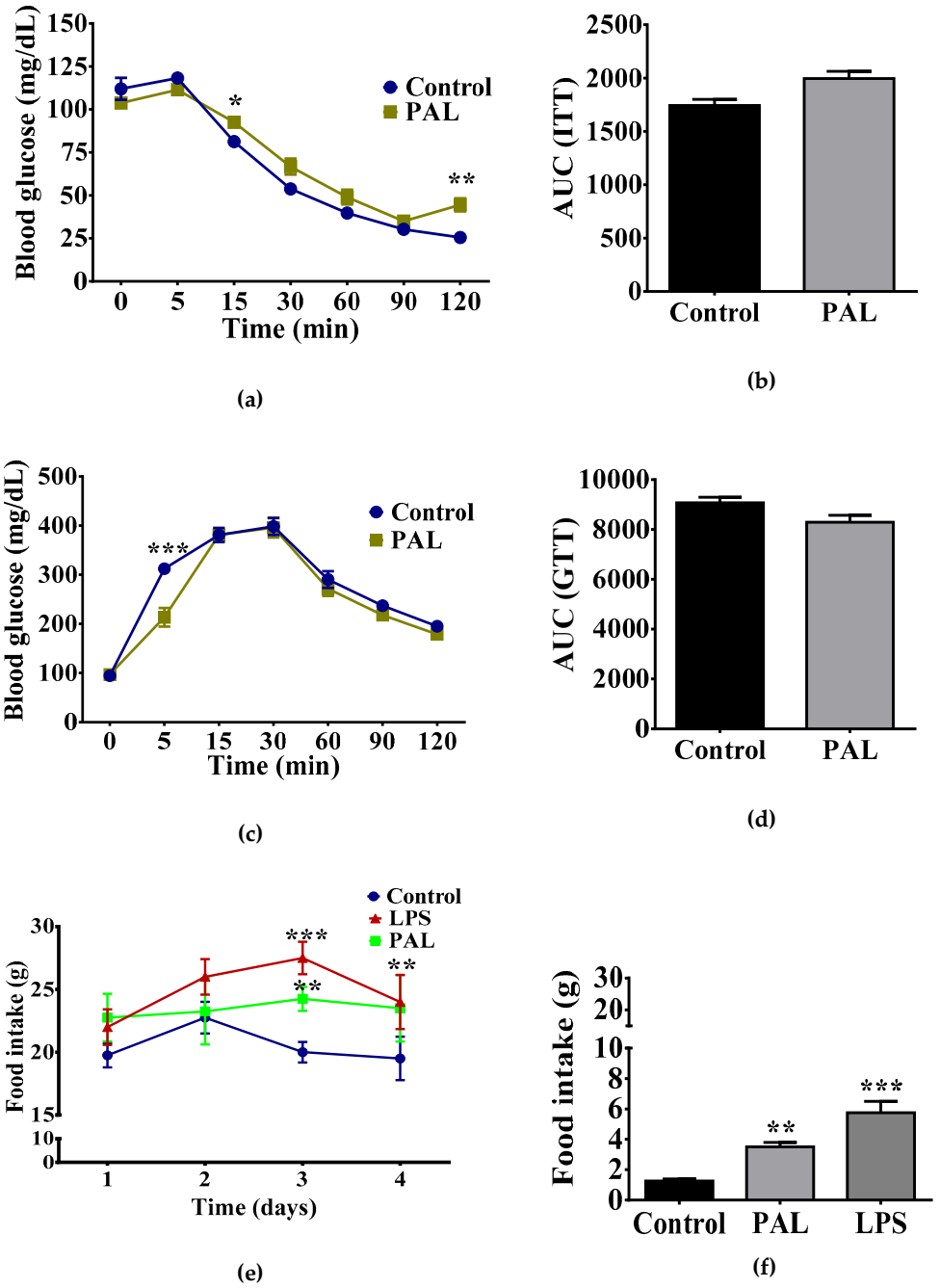

Figure 4. Chronic i.c.v. palmitic acid administration sensitizes ghrelin signaling leading to food intake increase. ITT and area under the curve (AUC) (**a**–**b**) and GTT and AUC (**c**–**d**) were analyzed following i.c.v of 2 µg/mL LPS or 40 µg/µL palmitic acid administration for five days. Daily food intake quantification following palmitic acid, LPS or ACSF administration (**e**). Ghrelin-sensitive food intake was analyzed by day 5 after 2 h, 1 µg/µL ghrelin i.c.v. administration (**f**). The graphs show normalized data of the mean ± S.E.M., Student's *t*-test, * $p < 0.05$). ($n = 4$, the results are shown as the mean ± S.E.M. Two-way ANOVA followed by Tukey multiple comparation test; * $p < 0.05$, ** $p < 0.01$, *** $p < 0.001$). LPS, Lipopolysaccharides, ACSF, artificial cerebrospinal fluid.

Next, we hypothesized that the pro-inflammatory modulator palmitic acid might reproduce the increase in food intake found in the offspring of mothers exposed to CAF diet. We administered LPS, palmitic acid or vehicle via i.c.v for five days and we quantified basal food intake and food intake following i.c.v administration of ghrelin (1 μg/μL). We found a time-dependent increase of daily total food intake during LPS or palmitic acid schedule when compared with ACSF administration (Figure 4e). Additionally, we identified that five days of palmitic acid administration results in a 3.5-fold increase of food intake following i.c.v. administration of ghrelin when compared with the control group (Figure 4f). Of note, i.c.v. administration of the pro-inflammatory reagent LPS reproduces the total food intake induced by ghrelin administration (Figure 4f). These results support the hypothesis that saturated lipids sensitize hypothalamic ghrelin signaling, leading to exacerbation of food intake.

3.5. Hypothalamic Saturated Lipids Stimulation Activates Microglia and Ghrelin-Sensitive Neurons

At this final stage, we integrated the in vivo and in vitro results identified in Figures 1–4, supporting the effect of saturated palmitic acid on microglia activation and increased food intake in programmed offspring. We determined that palmitic acid promoted hypothalamic microglia activation and that it correlated with ghrelin-sensitive neuronal activation. We found that i.c.v. palmitic acid administration for five days following by ghrelin stimulation promoted a significant increase of microglia activation in the ARC of the hypothalamus, evidenced by immunofluorescence stain of the IBA1 marker when compared with the vehicle (Figure 5a). We also confirmed that palmitic acid promoted an increase in the c-fos immunosignal, confirming neuronal activation in the ARC nucleus (Figure 5b).

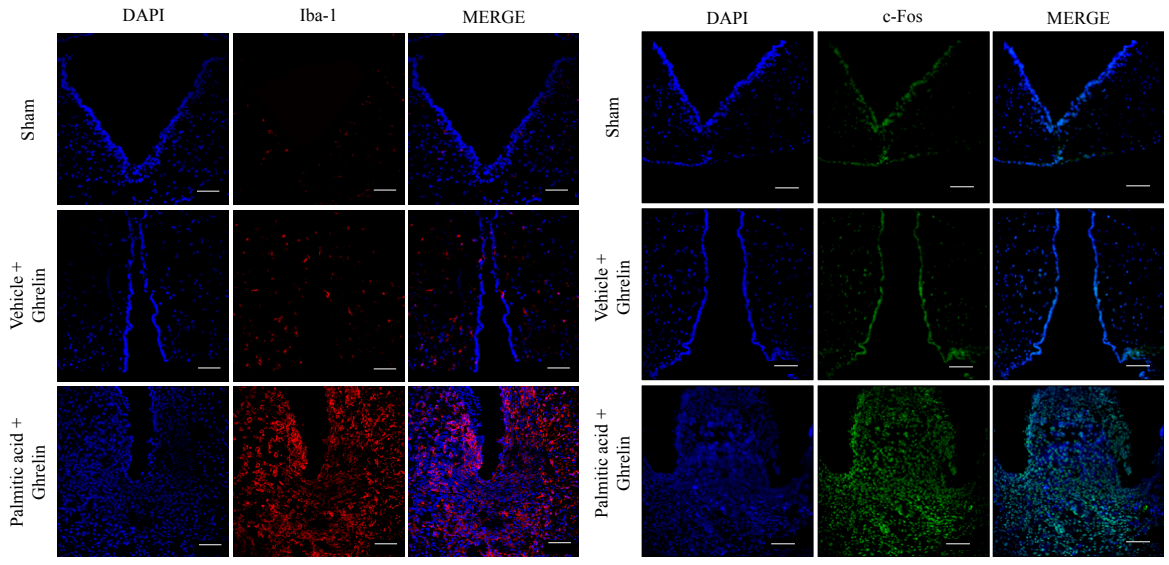

Figure 5. *Cont.*

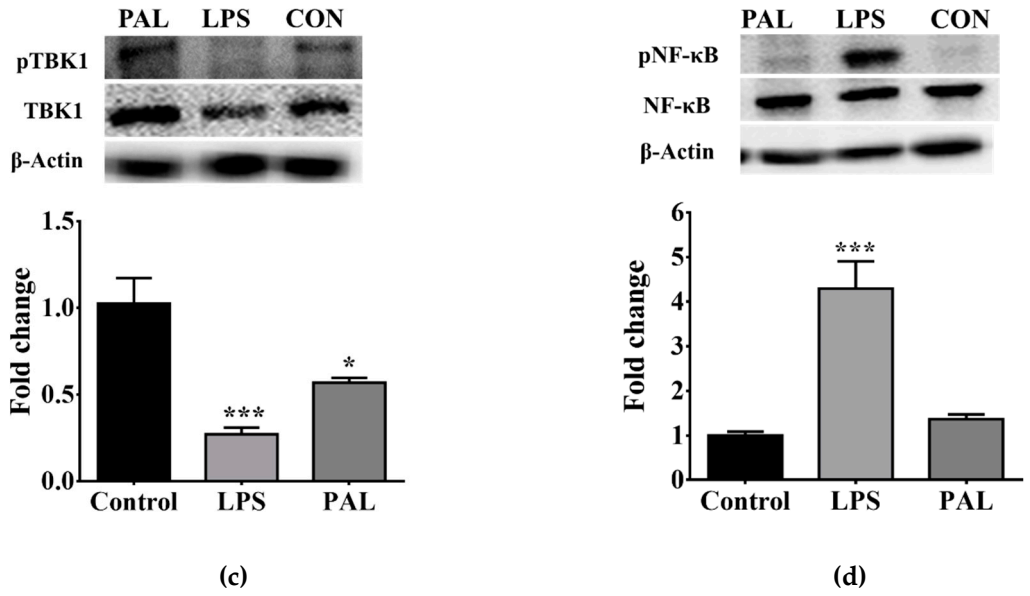

Figure 5. Palmitic acid promotes microglia activation and c-fos response in hypothalamus. Rats were i.c.v. administered with, ACSF, 2 μg/μL LPS or 40μg/μL palmitic acid for 5 days and vehicle or ghrelin was injected into the third ventricle by day 5. Immunofluorescence against Iba-1 marker (microglia activation) (**a**) or c-fos activation were performed as described in Figure 4 (**b**). (**c** and **d**) Changes in TBK1 and NF-κB phosphorylation in the ARC of hypothalamus were identified using western blot analysis following i.c.v. ACSF, LPS or palmitic acid administration for five days (n = 4 per group). The graphs show normalized data of the mean ± S.E.M. Two-way ANOVA followed by Tukey multiple comparation test; * $p < 0.05$, *** $p < 0.001$). TBK1, TANK-binding kinase 1, BSA-FFA, Bovine serum albumin-free fatty acids, ACSF, cerebrospinal fluid, PAL, palmitic acid, LPS, lipopolysaccharide.

Finally, microglia activation in the ARC nucleus of the hypothalamus after palmitic acid administration was also evaluated by analyzing the TLR4-TBK1 pathway. Western blot analysis showed a decrease of the nuclear factor kappa B (NF-κB) phosphorylation following palmitic acid stimulation, which is also promoted by LPS (Figure 5c). As expected, LPS administration promoted a four-fold increase of NF-κB phosphorylation in the ARC of the hypothalamus and no changes were found after stimulation with palmitic acid (Figure 5d).

4. Discussion

Extensive evidence has confirmed that maternal obesity or maternal overnutrition during pregnancy and lactation negatively modulate peripheral and central pathways disturbing basal energy homeostasis and appetite regulation in the offspring [1,2]. We, and others, have identified that maternal nutritional programming by CAF diet exposure in murine models sets metabolic alterations [3–5] and defective behaviors, including addiction-like behavior [6,28], which potentially contributes to hyperphagia [2]. Here, by using in vitro and in vivo experimental approaches we suitably identified the lipotoxic effect of the saturated lipid species palmitic acid as a potential trigger to promote hypothalamic microglia activation and actively sensitize the central effects of ghrelin on food intake. Notably, we also discovered that maternal programming by CAF diet exposure also reproduces the effect of palmitic acid in the hypothalamus by priming the central ghrelin response for feeding in the offspring. Based on our results, we propose that palmitic acid might be considered a lipid species capable of dynamically priming hypothalamic ghrelin sensitivity to food intake in the offspring of mothers programmed by caloric diets.

A key contribution of our study is that nutritional programming by CAF exposure increases basal feeding response and ghrelin-sensitivity in the offspring. Initially, daily food intake was not increased on CAF diet –programmed groups, however, we did observe hyperphagia following plasma increase

of ghrelin levels by fasting or SC ghrelin injection. As already proposed, maternal programming by caloric exposure increases ghrelin levels in the offspring [9], which may contribute to the hyperphagic phenotype during fasting in our model. On this context, in a parallel scenario we identified that maternal programming primes hypothalamic neuronal activation in the offspring, evidenced by an increase in c-fos expression in the ARC nucleus, which is also exacerbated by i.c.v. or subcutaneous ghrelin administration. This suggests that priming of central ghrelin signaling exacerbates feeding in the context of fasting or pharmacologic plasma ghrelin increase. Our data agree with the effects of maternal nutritional programming by caloric diets in murine models, which stimulates the proliferation of orexigenic peptide–producing neurons [13] and leads to hyperphagia in the offspring [2]. Notably, the effect of plasma lipidomic profile leading to food intake in humans suggests that the higher prenatal triglycerides plasma concentrations in humans were associated with higher food responsiveness in offspring at 5 years old [14]. These results are also in line with murine models showing that increased perinatal triglyceride concentrations correlate with hyperphagia in the offspring [29]. Together, these results propose that nutritional programing by CAF diet primes the ghrelin response for Chow and CAF feeding in the offspring.

Maternal obesity or maternal overnutrition promotes free fatty acid accumulation in plasma, which is associated with central and peripheral inflammatory response, potentially throughout the TLR-4 pathway [13–15]. In fact, TLR-4, IL-6, and IL-8 expression have been identified in the placenta of obese women when compared with lean women [16]. In murine models, plasma accumulation of saturated fatty acids in diet-induced obesity activates hypothalamic microglia [18,19]. In fact, there is an interactive crosstalk integrating central and peripheral immunity regulating hypothalamic nodes for metabolic and feeding homeostasis [16]. For instance, we have reported that the saturated lipid palmitic acid leads to the TLR-4-TBK1 pathway activation in the hypothalamus of obese murine models, which correlates with insulin resistance [19]. Here we hypothesized that maternal programming by CAF exposure sets a plasma lipotoxic profile in the offspring, leading to central microglia activation. Our experimental in vitro data allowed us to propose that, in contrast to the unsaturated lipid species such as the palmitoleic acid, linoleic acid or even, the C6 ceramide, the saturated lipid species palmitic acid, is an effective pro-inflammatory mediator in microglia activating the IL-6, IL-1β and TNF-alpha cytokines release. Additionally, LPS stimulation in microglia cells closely reproduces the pro-inflammatory profile found during palmitic acid stimulation, supporting the negative effect of palmitic acid.

One of the most outstanding results in our study is the major effect of hypothalamic palmitic acid inoculation on sensitizing ghrelin response for food intake. Ghrelin has been reported as a molecule that prevents the lipotoxic effects of palmitic acid stimulation in diverse cell types, including hepatocytes, pancreatic β-cells, and myoblasts [30–32]. In fact, ghrelin also exerts immunomodulatory effects on macrophages, T lymphocytes and microglia, guiding these cells towards an anti-inflammatory phenotype during obesity-induced inflammation [16,33]. In addition, ghrelin regulates by antagonizing TNF-α/NF-κB and TLR-4 signaling pathways [16,34] associated whit metabolic inflammation on the brain [35]. In any case, does hypothalamic microglia activation by palmitic acid explains the priming ghrelin response in the offspring programmed by CAF diet exposure? Programming the offspring with CAF diet exposure closely replicates microglia activation in the ARC nucleus of the hypothalamus, evidenced by an increase in the Iba-1 marker staining. Our results agree with previous data showing that systemic LPS inoculation activates central microglia [11,12,36]. In the beginning, clinical evidence, reported that the microglial inhibitor minocycline induced weight loss as a major side-effect [37]. Experimental basic evidence confirms that transient pharmacologic microglia depletion in murine models leaded to food intake decrease and weight loss [22]. Supporting our findings, neonatal overfed rats show hypothalamic microglia activation positive for Iba-1 and IL-6 and NF-κB expression, which correlates with accelerated weight gain [38]. However, additional experimental evidence does not support this scenario by showing that LPS, certain cytokines (e.g., IL-1β and TNF-α) and dietary lipids sets, in fact, a pathological state known as sickness-associated anorexia [16,39], which actively induces

IL-1β and TNF-α mRNA expression in the ARC nucleus of the hypothalamus [40]. Additionally, weight loss and anorexia in mice do not show a peripheral or central pro-inflammatory phenotype [22], and pharmacologic microglia ablation does not promote changes in mice body weight [41].

We suggest that an explanation to this discrepancy might be associated with a time-dependent pro-inflammatory profile including LPS, palmitic acid and dietary lipids in our model, and potential hormone and metabolic profiles modulating central and peripheral immune activation. For instance, inflammation and gliosis are detected in rat and mouse ARC nucleus within the first few days following high-fat diet exposure, before obesity develops [42], suggesting that a positive inflammatory profile promotes central leptin and insulin resistance [16], which potentially leads to an increase in plasma leptin levels favoring weight gain [43]. Additionally, hypothalamic microglia activation by lipid over supply might prime ghrelin sensitivity, potentially due to an increase in the GHSR into lipid rafts [24]. In any case, based on these data we propose that during the maternal CAF diet programming, palmitic acid might be one lipid species capable of promoting central microglia activation in the offspring.

Our study still lacks evidence if maternal programming by a CAF diet leads to plasma and brain increases of palmitic acid to support its effect on microglia activation and ghrelin sensitivity. Reports have shown that mice exposed to a western-style high fat diet for 16 weeks experienced a C16:0 saturated lipid increase in plasma and brain [44], including hippocampus [45]. In fact, an increase in plasma palmitic acid has been identified in healthy overweight subjects showing upper tertiles (T3) according to L4 visceral fat area [46]. Importantly, the direct effect of palmitic acid intake on brain function and its correlation with positive inflammatory immune profile in humans, was recently identified, showing that three-week high palmitic acid diet intake promotes an increase in the basal ganglia activation which correlates with IL-6, IL-18, and IL-1β plasma accumulation [47]. Finally, experimental evidence has also confirmed that the integrity of the blood brain barrier is compromised following western diet exposure in mice [48], which tentatively suggests that selective fatty acids incorporation into the brain might be favored during blood-brain barrier disruption and contribute to palmitic acid flux to the hypothalamus, a region lacking a blood-brain barrier.

5. Conclusions

Our results support the hypothesis that maternal programming by CAF diet exposure primes a hypothalamic ghrelin response leading to food intake exacerbation in male offspring. Of note, caloric programing also replicates the central microglia activation and ghrelin sensitivity found during intraventricular palmitic acid administration. We propose that palmitic acid might be considered a lipid species involved in priming of hypothalamic ghrelin sensitivity to food intake in the offspring during CAF diet exposure.

Author Contributions: Conceptualization: R.M.-R., M.C.-T., and A.C.; investigation: R.M.-R., M.C.-T., L.M.-M., R.V., D.R.-P., and A.C.; methodology: R.M.-R., M.C.-T., L.M.-M., R.V., and A.C.; supervision: R.V., D.R.-P., L.G.-O and A.C.; visualization: R.V., D.R.-P., L.G.-O and A.C.; writing—review and editing: R.M.-R., M.C.-T., L.G.-O and A.C.

Funding: This work was funded by National Council of Science and Technology in Mexico (CONACYT) (CB-2015-255317 to Alberto Camacho and CB-2013-220342 to Roman Vidaltamayo), 582196 CONACYT for Larisa Montalvo-Martínez, 573686 CONACYT for Roger Maldonado-Ruiz, 650620 CONACYT for Marcela Cárdenas-Tueme and División de Extensión, Consultoría e Investigación, Universidad de Monterrey grants (Plan de Investigación 2018 and 2019) to R. Vidaltamayo.

Acknowledgments: The authors thank M.S. Alejandra Arreola-Triana for her support on editing this manuscript.

Conflicts of Interest: The authors declare no conflict of interest.

References

1. Alfaradhi, M.Z.; Kusinski, L.C.; Fernandez-Twinn, D.S.; Pantaleão, L.C.; Carr, S.K.; Ferland-McCollough, D.; Yeo, G.S.H.; Bushell, M.; Ozanne, E.S. Maternal Obesity in Pregnancy Developmentally Programs Adipose Tissue Inflammation in Young, Lean Male Mice Offspring. *Endocrinology* **2016**, *157*, 4246–4256. [CrossRef] [PubMed]
2. Reynolds, C.M.; Segovia, S.A.; Vickers, M.H. Experimental models of maternal obesity and neuroendocrine programming of metabolic disorders in offspring. *Front. Endocrinol. (Lausanne)* **2017**, *8*, 1–11. [CrossRef]
3. Frihauf, J.B.; Fekete, É.M.; Nagy, T.R.; Levin, B.E.; Zorrilla, E.P. Maternal Western diet increases adiposity even in male offspring of obesity-resistant rat dams: Early endocrine risk markers. *Am. J. Physiol. Integr. Comp. Physiol.* **2016**, *311*, R1045–R1059. [CrossRef] [PubMed]
4. Taylor, P.D.; Samuelsson, A.-M.; Poston, L. Maternal obesity and the developmental programming of hypertension: A role for leptin. *Acta Physiol.* **2014**, *210*, 508–523. [CrossRef] [PubMed]
5. Cardenas-Perez, R.E.; Fuentes-Mera, L.; de la Garza, A.L.; Torre-Villalvazo, I.; Reyes-Castro, L.A.; Rodriguez-Rocha, H.; Garcia-Garcia, A.; Corona-Castillo, J.C.; Tovar, A.R.; Zambrano, E.; et al. Maternal overnutrition by hypercaloric diets programs hypothalamic mitochondrial fusion and metabolic dysfunction in rat male offspring. *Nutr. Metab. (London)* **2018**, *15*, 38. [CrossRef] [PubMed]
6. Camacho, A.; Montalvo-Martinez, L.; Cardenas-Perez, R.E.; Fuentes-Mera, L.; Garza-Ocañas, L. Obesogenic diet intake during pregnancy programs aberrant synaptic plasticity and addiction-like behavior to a palatable food in offspring. *Behav. Brain Res.* **2017**, *330*, 46–55. [CrossRef]
7. Nakazato, M.; Murakami, N.; Date, Y.; Kojima, M.; Matsuo, H.; Kangawa, K.; Matsukura, S. A role for ghrelin in the central regulation of feeding. *Nature* **2001**, *409*, 194–198. [CrossRef]
8. Perelló, M.; Zigman, J.M. The Role of Ghrelin in Reward-Based Eating. *Biol. Psychiatry* **2012**, *72*, 347–353. [CrossRef] [PubMed]
9. Słupecka, M.; Romanowicz, K.; Woliński, J. Maternal high-fat diet during pregnancy and lactation influences obestatin and ghrelin concentrations in milk and plasma of Wistar rat dams and their offspring. *Int. J. Endocrinol.* **2016**, *2016*, 1–9. [CrossRef] [PubMed]
10. Sominsky, L.; Ziko, I.; Spencer, S.J. Neonatal overfeeding disrupts pituitary ghrelin signalling in female rats long-term; Implications for the stress response. *PLoS ONE* **2017**, *12*, e0173498. [CrossRef] [PubMed]
11. Valdearcos, M.; Douglass, J.D.; Robblee, M.M.; Dorfman, M.D.; Stifler, D.R.; Bennett, M.L.; Gerritse, I.; Fasnacht, R.; Barres, B.A.; Thaler, J.P.; et al. microglial inflammatory signaling orchestrates the hypothalamic immune response to dietary excess and mediates obesity susceptibility. *Cell Metab.* **2017**, *26*, 185–197. [CrossRef] [PubMed]
12. Valdearcos, M.; Robblee, M.M.; Benjamin, D.I.; Nomura, D.K.; Xu, A.W.; Koliwad, S.K. microglia dictate the impact of saturated fat consumption on hypothalamic inflammation and neuronal function. *Cell Rep.* **2014**, *9*, 2124–2139. [CrossRef]
13. Chang, G.-Q.; Gaysinskaya, V.; Karatayev, O.; Leibowitz, S.F. Maternal high-fat diet and fetal programming: Increased proliferation of hypothalamic peptide-producing neurons that increase risk for overeating and obesity. *J. Neurosci.* **2008**, *28*, 12107–12119. [CrossRef] [PubMed]
14. Dieberger, A.; de Rooij, S.; Korosi, A.; Vrijkotte, T. Maternal lipid concentrations during early pregnancy and eating behaviour and energy intake in the offspring. *Nutrients* **2018**, *10*, 1026. [CrossRef] [PubMed]
15. Rogero, M.; Calder, P. Obesity, inflammation, toll-like receptor 4 and fatty acids. *Nutrients* **2018**, *10*, 432. [CrossRef]
16. Maldonado-Ruiz, R.; Fuentes-Mera, L.; Camacho, A. Central modulation of neuroinflammation by neuropeptides and energy-sensing hormones during obesity. *Biomed Res. Int.* **2017**, *2017*, 1–12. [CrossRef] [PubMed]
17. Milanski, M.; Degasperi, G.; Coope, A.; Morari, J.; Denis, R.; Cintra, D.E.; Tsukumo, D.M.L.; Anhe, G.; Amaral, M.E.; Takahashi, H.K.; et al. Saturated fatty acids produce an inflammatory response predominantly through the activation of TLR4 signaling in hypothalamus: Implications for the pathogenesis of obesity. *J. Neurosci.* **2009**, *29*, 359–370. [CrossRef] [PubMed]
18. Yang, X.; Li, M.; Haghiac, M.; Catalano, P.M.; O'Tierney-Ginn, P.; Mouzon, S.H. Causal relationship between obesity-related traits and TLR4-driven responses at the maternal–fetal interface. *Diabetologia* **2016**, *59*, 2459–2466. [CrossRef]

19. Zhao, Y.; Li, G.; Li, Y.; Wang, Y.; Liu, Z. Knockdown of Tlr4 in the arcuate nucleus improves obesity related metabolic disorders. *Sci. Rep.* **2017**, *7*, 7441. [CrossRef]
20. Delint-Ramirez, I.; Ruiz, R.M.; Torre-Villalvazo, I.; Fuentes-Mera, L.; Ocañas, L.G.; Tovar, A.; Camacho, A. Genetic obesity alters recruitment of TANK-binding kinase 1 and AKT into hypothalamic lipid rafts domains. *Neurochem. Int.* **2015**, *80*, 23–32. [CrossRef]
21. Naznin, F.; Toshinai, K.; Waise, T.M.Z.; NamKoong, C.; Moin, A.S.M.; Sakoda, H.; Nakazato, M. Diet-induced obesity causes peripheral and central ghrelin resistance by promoting inflammation. *J. Endocrinol.* **2015**, *226*, 81–92. [CrossRef]
22. De Luca, S.N.; Sominsky, L.; Soch, A.; Wang, H.; Ziko, I.; Rank, M.M.; Spencer, S.J. Conditional microglial depletion in rats leads to reversible anorexia and weight loss by disrupting gustatory circuitry. *Brain Behav. Immun.* **2019**, *77*, 77–91. [CrossRef] [PubMed]
23. Broglio, F.; Gottero, C.; Benso, A.; Prodam, F.; Destefanis, S.; Gauna, C.; Maccario, M.; Deghenghi, R.; van der Lely, A.J.; Ghigo, E. Effects of ghrelin on the insulin and glycemic responses to glucose, arginine, or free fatty acids load in humans. *J. Clin. Endocrinol. Metab.* **2003**, *88*, 4268–4272. [CrossRef] [PubMed]
24. Delhanty, P.J.D.; van Kerkwijk, A.; Huisman, M.; van de Zande, B.; Verhoef-Post, M.; Gauna, C.; Hofland, L.; Themmen, A.P.N.; van der Lely, A.J. Unsaturated fatty acids prevent desensitization of the human growth hormone secretagogue receptor by blocking its internalization. *AJP Endocrinol. Metab.* **2010**, *299*, E497–E505. [CrossRef] [PubMed]
25. Sampey, B.P.; Vanhoose, A.M.; Winfield, H.M.; Freemerman, A.J.; Muehlbauer, M.J.; Fueger, P.T.; Newgard, C.B.; Makowski, L. Cafeteria diet is a robust model of human metabolic syndrome with liver and adipose inflammation: comparison to high-fat diet. *Obesity* **2011**, *19*, 1109–1117. [CrossRef]
26. Paxinos, G.; Watson, C. *The Rat Brain in Stereotaxic Coordinates*, 6th ed.; Academic Press: San Diego, CA, USA, 2007; 456p.
27. Cabral, A.; Valdivia, S.; Fernandez, G.; Reynaldo, M.; Perello, M. divergent neuronal circuitries underlying acute orexigenic effects of peripheral or central ghrelin: Critical role of brain accessibility. *J. Neuroendocrinol.* **2014**, *26*, 542–554. [CrossRef]
28. De la Garza, A.; Garza-Cuellar, M.; Silva-Hernandez, I.; Cardenas-Perez, R.; Reyes-Castro, L.; Zambrano, E.; Gonzalez-Hernandez, B.; Garza-Ocañas, L.; Fuentes-Mera, L.; Camacho, A. Maternal flavonoids intake reverts depression-like behaviour in rat female offspring. *Nutrients* **2019**, *11*, 572. [CrossRef]
29. Sullivan, E.L.; Smith, M.S.; Grove, K.L. perinatal exposure to high-fat diet programs energy balance, metabolism and behavior in adulthood. *Neuroendocrinology* **2011**, *93*, 1–8. [CrossRef]
30. Wang, W.; Zhang, D.; Zhao, H.; Chen, Y.; Liu, Y.; Cao, C.; Han, L.; Liu, G. Ghrelin inhibits cell apoptosis induced by lipotoxicity in pancreatic β-cell line. *Regul. Pept.* **2010**, *161*, 43–50. [CrossRef]
31. Zhang, S.; Mao, Y.; Fan, X. Inhibition of ghrelin o-acyltransferase attenuated lipotoxicity by inducing autophagy via AMPK–mTOR pathway. *Drug Des. Devel. Ther.* **2018**, *12*, 873–885. [CrossRef]
32. Mosa, R.M.H.; Zhang, Z.; Shao, R.; Deng, C.; Chen, J.; Chen, C. Implications of ghrelin and hexarelin in diabetes and diabetes-associated heart diseases. *Endocrine* **2015**, *49*, 307–323. [CrossRef] [PubMed]
33. Harvey, R.E.; Howard, V.G.; Lemus, M.B.; Jois, T.; Andrews, Z.B.; Sleeman, M.W. The Ghrelin/GOAT system regulates obesity-induced inflammation in male mice. *Endocrinology* **2017**, *158*, 2179–2189. [CrossRef] [PubMed]
34. Qu, R.; Chen, X.; Hu, J.; Fu, Y.; Peng, J.; Li, Y.; Chen, J.; Li, P.; Liu, L.; Cao, J.; et al. Ghrelin protects against contact dermatitis and psoriasiform skin inflammation by antagonizing TNF-α/NF-κB signaling pathways. *Sci. Rep.* **2019**, *9*, 1348. [CrossRef]
35. Maldonado-Ruiz, R.; Montalvo-Martínez, L.; Fuentes-Mera, L.; Camacho, A. Microglia activation due to obesity programs metabolic failure leading to type two diabetes. *Nutr. Diabetes* **2017**, *7*, e254. [CrossRef]
36. Muhammad, T.; Ikram, M.; Ullah, R.; Rehman, S.; Kim, M. Hesperetin, a Citrus flavonoid, attenuates lps-induced neuroinflammation, apoptosis and memory impairments by modulating TLR4/NF-κB signaling. *Nutrients* **2019**, *11*, 648. [CrossRef] [PubMed]
37. Levkovitz, Y.; Mendlovich, S.; Riwkes, S.; Braw, Y.; Levkovitch-Verbin, H.; Gal, G.; Fennig, S.; Treves, I.; Kron, S. A Double-blind, randomized study of minocycline for the treatment of negative and cognitive symptoms in early-phase schizophrenia. *J. Clin. Psychiatry* **2010**, *71*, 138–149. [CrossRef]

38. Ziko, I.; de Luca, S.; Dinan, T.; Barwood, J.M.; Sominsky, L.; Cai, G.; Kenny, R.; Stokes, L.; Jenkins, T.A.; Spencer, S.J. Neonatal overfeeding alters hypothalamic microglial profiles and central responses to immune challenge long-term. *Brain. Behav. Immun.* **2014**, *41*, 32–43. [CrossRef]
39. Van Niekerk, G.; Isaacs, A.W.; Nell, T.; Engelbrecht, A.-M. Sickness-Associated Anorexia: Mother Nature's Idea of Immunonutrition? *Mediators Inflamm.* **2016**, *2016*, 1–12. [CrossRef] [PubMed]
40. Wisse, B.E.; Ogimoto, K.; Tang, J.; Harris, M.K.; Raines, E.W.; Schwartz, M.W. Evidence that lipopolysaccharide-induced anorexia depends upon central, rather than peripheral, inflammatory signals. *Endocrinology* **2007**, *148*, 5230–5237. [CrossRef]
41. Djogo, T.; Robins, S.C.; Schneider, S.; Kryzskaya, D.; Liu, X.; Mingay, A.; Gillon, C.J.; Kim, J.H.; Storch, K.-F.; Boehm, U.; et al. Adult NG2-glia are required for median eminence-mediated leptin sensing and body weight control. *Cell Metab.* **2016**, *23*, 797–810. [CrossRef]
42. Thaler, J.; Yi, C.; Schur, E.; Guyenet, S.; Hwang, B.; Dietrich, M.; Zhao, X.; Sarruf, D.; Izgur, V.; Maravilla, K.; et al. Obesity is associated with hipothalamic injury in rodents and humans. *J. Clin. Investig.* **2011**, *122*, 153. [CrossRef]
43. Morton, G.J.; Meek, T.H.; Schwartz, M.W. Neurobiology of food intake in health and disease. *Nat. Rev. Neurosci.* **2014**, *15*, 367–378. [CrossRef] [PubMed]
44. Rodriguez-Navas, C.; Morselli, E.; Clegg, D.J. Sexually dimorphic brain fatty acid composition in low and high fat diet-fed mice. *Mol. Metab.* **2016**, *5*, 680–689. [CrossRef] [PubMed]
45. Spinelli, M.; Fusco, S.; Mainardi, M.; Scala, F.; Natale, F.; Lapenta, R.; Mattera, A.; Rinaudo, M.; Puma, D.D.L.; Ripoli, C.; et al. Brain insulin resistance impairs hippocampal synaptic plasticity and memory by increasing GluA1 palmitoylation through FoxO3a. *Nat. Commun.* **2017**, *8*, 2009. [CrossRef]
46. Kang, M.; Lee, A.; Yoo, H.J.; Kim, M.; Kim, M.; Shin, D.Y.; Lee, J.H. Association between increased visceral fat area and alterations in plasma fatty acid profile in overweight subjects: a cross-sectional study. *Lipids Health Dis.* **2017**, *16*, 248. [CrossRef]
47. Dumas, J.A.; Bunn, J.Y.; Nickerson, J.; Crain, K.I.; Ebenstein, D.B.; Tarleton, E.K.; Makarewicz, J.; Poynter, M.E.; Kien, C.L. Dietary saturated fat and monounsaturated fat have reversible effects on brain function and the secretion of pro-inflammatory cytokines in young women. *Metabolism* **2016**, *65*, 1582–1588. [CrossRef]
48. Hsu, T.M.; Kanoski, S.E. Blood-brain barrier disruption: Mechanistic links between Western diet consumption and dementia. *Front. Aging Neurosci.* **2014**, *6*, 6. [CrossRef]

Hindawi
BioMed Research International
Volume 2018, Article ID 8061389, 11 pages
https://doi.org/10.1155/2018/8061389

Review Article

Maternal Overnutrition Programs Central Inflammation and Addiction-Like Behavior in Offspring

Larisa Montalvo-Martínez,[1] Roger Maldonado-Ruiz,[1] Marcela Cárdenas-Tueme,[2] Diana Reséndez-Pérez,[2] and Alberto Camacho [1,3]

[1]*Department of Biochemistry, College of Medicine, Universidad Autónoma de Nuevo Leon, San Nicolás de los Garza, NL, Mexico*
[2]*Department of Cell Biology and Genetics, College of Biological Sciences, Universidad Autónoma de Nuevo Leon, San Nicolás de los Garza, NL, Mexico*
[3]*Neurometabolism Unit, Center for Research and Development in Health Sciences, Universidad Autónoma de Nuevo Leon, San Nicolás de los Garza, NL, Mexico*

Correspondence should be addressed to Alberto Camacho; acm590@hotmail.com

Academic Editor: Gang Liu

Obesity or maternal overnutrition during pregnancy and lactation might have long-term consequences in offspring health. Fetal programming is characterized by adaptive responses to specific environmental conditions during early life stages. Programming alters gene expression through epigenetic modifications leading to a transgenerational effect of behavioral phenotypes in the offspring. Maternal intake of hypercaloric diets during fetal development programs aberrant behaviors resembling addiction in offspring. Programming by hypercaloric surplus sets a gene expression pattern modulating axonal pruning, synaptic signaling, and synaptic plasticity in selective regions of the reward system. Likewise, fetal programming can promote an inflammatory phenotype in peripheral and central sites through different cell types such as microglia and T and B cells, which contribute to disrupted energy sensing and behavioral pathways. The molecular mechanism that regulates the central and peripheral immune cross-talk during fetal programming and its relevance on offspring's addictive behavior susceptibility is still unclear. Here, we review the most relevant scientific reports about the impact of hypercaloric nutritional fetal programming on central and peripheral inflammation and its effects on addictive behavior of the offspring.

1. Introduction

According to the World Health Organization, nearly 39% of adults aged 18 years and over were overweight in 2016, and 13% were obese. Maternal obesity adversely impacts both maternal and offspring health, increasing the susceptibility to show metabolic abnormalities later in life such as obesity, dyslipidemia, type 2 diabetes mellitus, and hypertension as well as behavioral disorders related to schizophrenia, autism, and compulsive eating disorders [1, 2]. Maternal obesity or maternal overnutrition programs metabolic and hormonal nodes that modulate neuronal development during embryogenesis. For instance, neuronal maturation, including axonal pruning, synaptic plasticity, and stable tract formation between structures, is selectively programmed during pregnancy and lactation by consumption of high-sugar, high-fat, or high-sugar-high-fat diet formulas. Under this scenario, nutritional programming defines after-weaning selective behavioral phenotypes in offspring that might be exacerbated during adulthood, such as incentive-motivation behaviors leading to compulsive eating disorders.

Maternal obesity or overnutrition during fetal programming activates molecular and cellular mechanisms that command a new physiological state that might compromise basic metabolic and neuronal homeostasis. Metabolic imbalance during obesity can lead to overactivation of the immune system, triggering a process of chronic inflammation evidenced in animal models and humans. In fact, nutritional programming by hypercaloric diets promotes an inflammatory phenotype that contributes to disrupted energy sensing

pathways in metabolic-relevant systems including adipose tissue, liver, pancreas, muscle, and the brain. Inflammation in the brain is associated with a cross-talk between peripheral and central cell types that potentially activates microglia in the brain. However, it is still unclear which immune cells infiltrate into the fetal brain leading to microglia activation and neuroinflammation during maternal nutritional programming. Moreover, it is unknown if maternal overnutrition during fetal programming originates central inflammation by microglial activation in the absence of peripheral immune cells infiltration. Finally, the role of neuroinflammation during maternal nutritional programming and its effects on defective behavior related to compulsive eating disorders in the offspring have only started to be dissected. In this review, we will discuss the role of maternal programming on peripheral and central immune cross-talk and its relevance in the development of incentive-motivation behavior such as addiction in the offspring.

Obesity is a metabolic condition showing positive energy balance driven by several factors including human genetics, life style, environment, body activity, and diet [6]. At first, obesity was conceived as a metabolic disorder showing an increase in white adipose tissue mass-modulated exclusively by the peripheral nervous system. However, recent evidence shows that the central nervous system (CNS) plays a major role in the modulation of adipose tissue mass and function. Also, the CNS is a major regulator of food intake and metabolism and seeks for rewards such as food; in a pathological state, CNS activation might lead to addiction-like behavior [7].

2. Obesity Is a Potential Deregulator of Energy-Satiety Integration in the CNS, Leading to Overfeeding

In nature, all living organisms require energy to sustain life and perform activities. Energy is mainly provided by food assigned into three main formulas such as proteins, carbohydrates, and fats. However, energy surplus such as overnutrition disrupts metabolic and hormonal homeostasis and has harmful consequences in health. On this matter, metabolic and hormonal signals from the periphery arrive to the CNS to give a message about the energy balance of the body. The CNS integrates these signals through evolutionary-conserved neuronal tracts connecting peripheral organs to selective brain structures. For instance, the brainstem receives information from the gut, while the hypothalamus integrates circulating/humoral signals. The brainstem and hypothalamus control satiety and integrate these signals by saying when and how much to eat [7]. However, under a pathological scenario satiety might be overestimated, leading to activation of the reward system, which modulates the incentive motivation to work and search for food despite an "apparent" satiety signal. The reward system integrates dopaminergic neurons located in the ventral tegmental area (VTA) that project to the nucleus accumbens (NAc) and also innervate several regions of the prefrontal cortex (PFC), central amygdala, basolateral amygdala (BLA), and hippocampus and dopamine neurons in the substantia nigra (SN) that project to the dorsal striatum, which has traditionally been associated with appetitive learning, performance, and motivation [8]. It has been hypothesized that incentive motivation for palatable food contributes to overfeeding during obesity [9, 10]. For instance, an evasion of satiety has been identified in obesity leading to positive energy balance and an increase of body mass index [11, 12]. Several researchers propose that, like drug-addiction, obesity sets an altered motivational behavior for seeking foods rich in fat and sugars (hypercaloric) that have high reward value (pleasant), which is potentially dependent on dopamine neurotransmission [10].

The proposal that overeating during obesity might be considered as food addiction in the Diagnostic and Statistical Manual of Mental Disorders (DSM) was initially based on phenotypic similarities between patterns of overeating in obese individuals and drug abuse in addicted persons. It has been shown in both animal models and humans that repeated exposure to high-fat or high-sugar diets disrupts the integration of energy-satiety peripheral signals into the CNS, leading to overfeeding which indeed shares behavioral similarities to addiction [10, 13]. For instance, obese humans might experience the following: (1) enhanced motivation over hypercaloric food intake including recurrent and excessive consumption, (2) an increased time spent seeking palatable food in contrast to habitual activities, and (3) frequent or permanent relapse to hypercaloric foods after dieting. Of note, obesity or palatable food overconsumption might be subject-specific and it is potentially modulated by environment-subject interaction. Based on this proposal, researchers have applied a selective Yale Food Addiction Scale (YFAS) to provide a standardized measure for the assessment and diagnosis of food addiction based mainly on substance dependence criteria [14, 15]. These evidences suggest that overfeeding during obesity might be related to incentive motivation for palatable food in human and animals. However, are humans born addicted or do they become addicted to food?

3. Potential Role of Fetal Programming by Hypercaloric Food in the Development of Addictive Behaviors in the Offspring

Exposure to hypercaloric foods impacts the individual metabolic-hormonal settings of mothers and fathers and might also affect their offspring. Substantial scientific evidence has demonstrated the detrimental role of hypercaloric food intake during pregnancy and lactation leading to a failure in metabolic homeostasis, favoring the development of incentive-motivation behavior for food in the offspring. In this context, epidemiological data from human catastrophes such as the Dutch famine (1944), the siege of Leningrad (1942–1944), the great Chinese famine (1958–1961), and also the Överkalix study (1890-present) have shown that changes in diet intake regarding overfeeding or fasting are associated with disorders in the offspring such as diabetes mellitus type 2 and cardiovascular diseases [16–19]. In addition, there is evidence of behavioral alterations, including schizophrenia [20–22], affective disorders [23], and addiction [24, 25]. Based

on this data, Barker (1998) proposed the "Barker hypothesis" suggesting that the transgenerational effect of diet exposure during pregnancy modulates metabolic and behavioral phenotypes in the offspring, a mechanism known as "fetal programming" [26]. In specific, this hypothesis claims that oversupply or absence of energy intake during embryonic-fetal development provides the fetus with physiological adaptations to a new milieu of metabolic-hormonal threshold to face a potential adverse postnatal environment similar to those whose parents were exposed to fetal programming. In fact, any stimulus or insult throughout embryonic-fetal development, including stress, infections, substance abuse, overnutrition, and behavioral alterations, might result in molecular adaptations that produce permanent structural, physiological, and metabolic changes in the fetus. Also, fetal programming might increase the risk of serious physiological problems in perinatal stages including miscarriage, fetal-congenital anomalies, thromboembolism, and gestational diabetes.

Initial reports demonstrated that energy-dense food disrupts the appetite-energy sensing and satiety systems, exacerbating the reward for food. Also, excessive consumption of palatable food can lead to a profound hyposensitivity to reward, leading to compulsive eating behavior similarly observed during drug seeking [27]. Nutritional programming in murine models induces alterations in behavior and synaptic plasticity, favoring higher consumption and sensitization to alcohol, methamphetamines, and cocaine [28, 29]. Maternal exposure to hypercaloric diets during pregnancy or lactation has shown to increase the long-term preference for junk food in the offspring [30], potentially associated with repeated, intermittent increases in extracellular dopamine (DA) in the NAc and the VTA [31–35]. Molecularly, these synaptic plasticity changes show greater expression of the ΔFosB gene [28] and both dopamine (e.g., DR2, DAT) and opioid pathway genes expression (e.g., the μ-opioid receptor) at early stages of development [35–39]. In fact, the opioid pathway regulates the rewarding effects of palatable food; an injection of μ-opioid agonists in the NAc increases preference for high-fat or sugar-rich foods [40, 41], and its antagonists decrease palatable food predilection, even at doses that show no effect on standard food intake [42, 43]. In addition, fetal programming by drugs such as nicotine exposure during pregnancy might also disrupt brain gene expression involved in neuronal glutamatergic (e.g., GluA1, GluA2, and CaMKIIα) and dopaminergic (e.g., DR2, DAT, and DR1) signaling plasticity in the hippocampus [44, 45], the laterodorsal tegmental nucleus [46], and the NAc [47–49]. In murine maternal overnutrition models, a transcription modulation of glutamatergic and dopaminergic systems in the NAc and prefrontal cortex that increases fat/sugar food preferences in the offspring has been identified [50–53] (Figure 1).

In humans, it is still under investigation if obesity or maternal overnutrition during pregnancy leads to the development of food addiction in the offspring. Initial reports found that children from obese mothers or mothers with eating disorders presented more binge eating and night eating [54, 55] and consumed more carbohydrates compared to their normal weight counterparts [56]. Also, a positive correlation between addicted parents and food addiction in their offspring has been proven [57], although epidemiological studies are needed to support these findings.

4. Obesity and Maternal Overfeeding Promote Peripheral and Central Inflammatory Response

An organism's first line of defense is the innate immune system and it includes physical barriers such as the skin, specific cell types such as macrophages, and complement proteins. The second line of defense is the inflammatory response which consists of an innate cellular system and humoral response that happens during injury to restore physiological homeostasis. The function of the immune system is not limited to fighting infections and repairing tissue damage, it also plays a key role in shaping neuronal tracts during CNS development. For instance, cells from the innate immune system, such as microglia, regulate neurogenesis, synaptic plasticity, and synaptic striping, and are the major antigen-presenting cells (APC) in the CNS [58]. Cross-talk between peripheral immune system and brain-resident immune cells is in part regulated by B and T lymphocytes, macrophages, and antibodies which migrate and penetrate the blood-brain barrier (BBB) [58, 59] and have also been reported in the cerebrospinal fluid [60]. Under an altered physiological scenario, peripheral immune cells located in the brain become proinflammatory entities and secrete cytokines promoting an exacerbated immune response by microglia. By doing this, peripheral immune cells integrate positive feedback with microglia that modulates neural growth and development [61]. Microglial cells are the brain-resident macrophages of the CNS; these oversee surveillance of the CNS integrity and respond to pathogens and injuries and also to very subtle alterations in their microenvironment [62]. In healthy brains, microglia remain in a ramified stated, and when activated, they enlarge their cell body, change to a phagocytic state, and execute similar functions to those of other tissue-resident macrophages such as proinflammatory cytokines secretion, antigen presentation, and ROS production and phagocytosis, leading to neuroinflammation [63]. Under this scenario, neuroinflammation is beneficial because it removes debris or dysfunctional neurons; under a pathological state, however, microglia activation is upregulated and can be damaging to neurons because of the excessive release of ROS and proinflammatory cytokines, leading to neuroinflammation [64], and might contribute to tissue damage and disease pathology. Although microglial activation could be harmful, microglia are necessary to provide essential trophic factors for the survival of neurons, like brain-derived neurotrophic factor (BDNF) and glial-derived neurotrophic factor (GDNF) [63].

An atypical form of inflammation, primarily induced by fatty acids accumulation in selective energy-dependent tissues including liver, adipose tissue, muscle, and brain occurs when there is a positive energy balance, as found in obesity or maternal overnutrition, [65]. Fatty acids promote

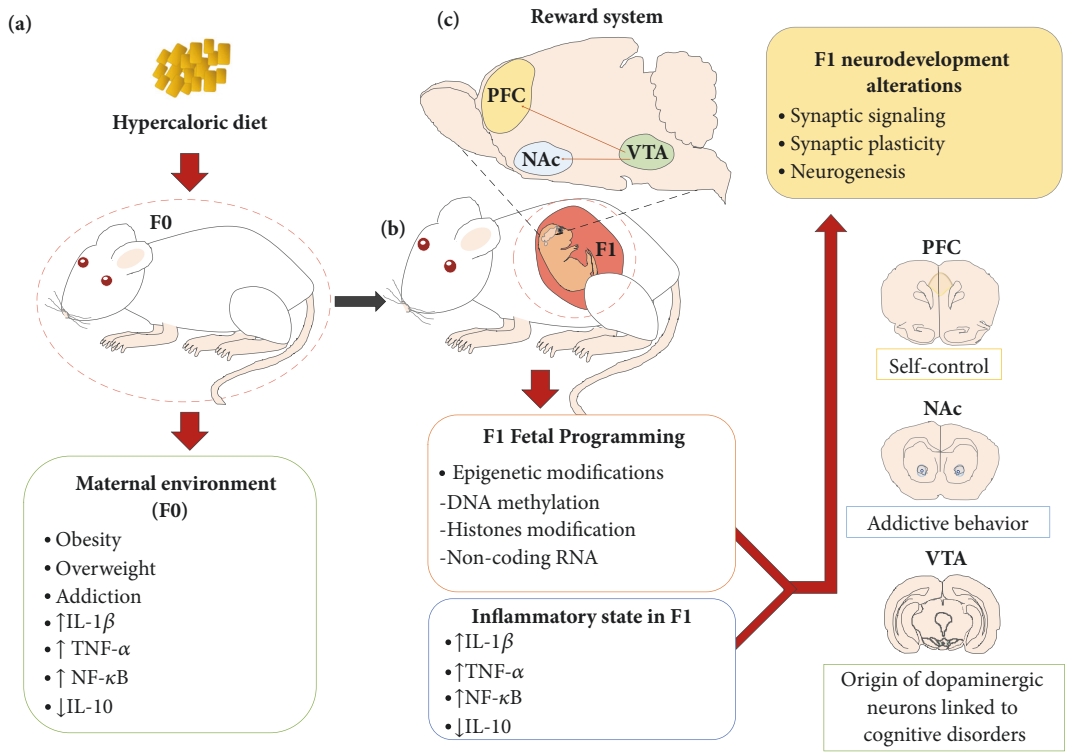

Figure 1: Maternal programming by hypercaloric diets increases the development of addictive behavior in offspring. (a) Hypercaloric diet intake or obesity during pregnancy leads to activation of an inflammatory state of mothers (F0), favoring aversive intrauterine environment and selective increase in proinflammatory markers. (b) Positive inflammatory state in mothers correlates with the one in the offspring (F1) and also with activation of fetal epigenetic program including DNA methylation, histone modification (ip acetylation, methylation, sumoylation, and ubiquitination), and noncoding RNAs (ip miRNA, piRNA, and lncRNA), which are capable of altering gene expression profile in selective regions belonging to the reward system: prefrontal cortex (PFC), nucleus accumbens (NAc), and ventral tegmental area (VTA). (c) Epigenetic programming associates with neurodevelopment alterations in F1 including synaptic signaling, synaptic plasticity, and neurogenesis which contributes to addictive-like behavior.

a type of body inflammation termed "metainflammation" or "metabolic inflammation," which involves several immune cells (T, B lymphocytes and microglia) and proinflammatory mediators (cytokines and chemokines) leading to metabolic and neurodegenerative disorders [66, 67]. Obesity or overnutrition during pregnancy leads to maternal immune activation (MIA), which favors changes in plasma and placental tissue-specific lipidomic profile, recruiting lipid species to membrane Toll-Like Receptor 4 (TLR4) and activating the nuclear factor-kappa B (NF-κB) pathway, through an increase of TLR2, TLR4, IL-6, IL-18, and TNF-α mRNA levels and macrophage markers cluster of differentiation including (CD)11b, CD14, and CD68 [68–70]. Maternal overnutrition in a sheep model of obesity demonstrated that inflammatory markers such as CD-68, TGF-β1, and TNF-α found in the mother are also identified in the offspring after birth [71]. These evidences show that imbalances in the peripheral and immune system cross-talk might compromise early stages of CNS development and differentiation potentially contributes to epilepsy, schizophrenia, cerebral palsy, Parkinson disease (PD), Alzheimer disease (AD), and ASD [72].

5. Central-Peripheral Immune System Cross-Talk Regulates Synaptic Plasticity, Neurogenesis, and Neurodegeneration

As mentioned before, neuroinflammation is how the innate immune system protects the CNS and controls initial stimulus, and although it is intended to be protective and beneficial, out-of-control inflammation can be fatal and contribute to tissue damage and disease pathology, including neurodegeneration [73]. Substantial scientific evidence has shown that neuroinflammation commands changes in cerebral plasticity and influences synaptic function and memory [72]. However, there are no conclusive data showing a cause-effect relationship in terms of the role of cytokines on synaptic plasticity modulation in the NAc, as a trigger to addictive behavior. Some data from neuroimmune interactions in humans in the behavioral response to drugs have shown small clues about their clinical relevance; however, these studies do not identify the molecular mechanisms of such interactions [74, 75]. Cause-effect relationship is even harder to identify because the CNS shows a selective cytokine profile when compared to peripheral cytokines during drug exposure. For instance,

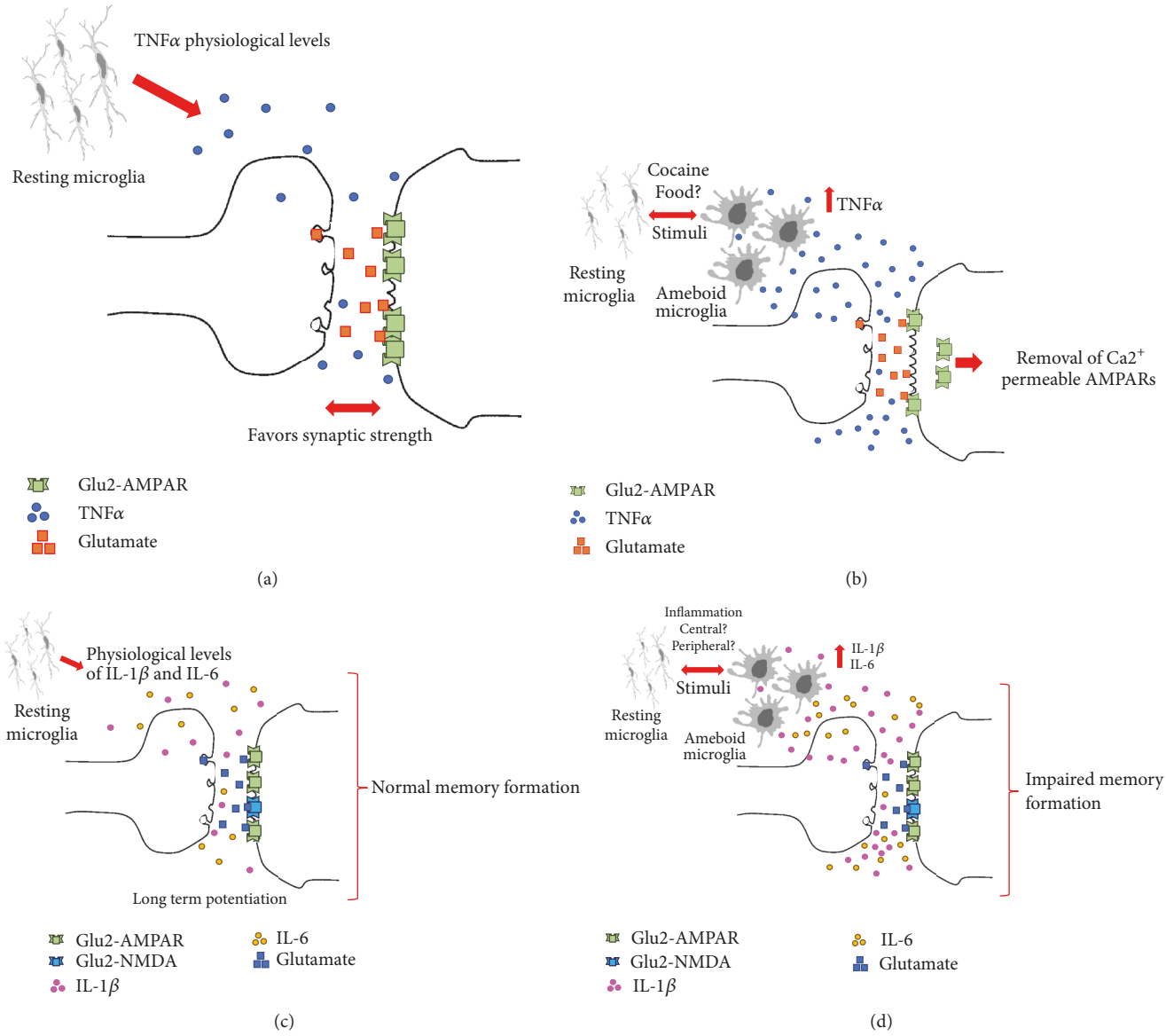

Figure 2: Synaptic modulation by cytokine levels. (a) According to Bettie and cols. in 2002 and Stellwagen and cols. in 2006 results TNF-α was demonstrated to promote normal expression of AMPARs favoring synaptic strength at excitatory synapses. (b) In contrast, high levels of TNF-α can affect synaptic plasticity by removing of Ca2+-permeable AMPARs from plasma membrane according to Lewitus et al., 2014 (b). (c) Physiological levels of IL-1β and IL-6 are detrimental to maintain and modulate hippocampus activity [3, 4]. (d) Excess of IL-1β and IL-6 affect LTP and impair memory formation [3, 5].

Calipari and colleagues did not find differences between the TNF-α expression in serum when mice were exposed to cocaine [76]. However, Lewitus et al. identified TNF-α release from microglia after cocaine consumption as a potential regulation of neuronal and behavioral plasticity during both the induction and expression of drug-induced behaviors [77]. Molecularly, initial reports have shown that glia releases TNF-α to fit surface expression of AMPARs, favoring the synaptic strength at excitatory synapses [78, 79]. In fact, TNF-α stimulation in brain slices reduced corticostriatal synaptic strength by removing of Ca2+ permeable AMPARs from the plasma membrane [80], suggesting that high levels of TNF-α affect synaptic plasticity, but physiological levels favor brain development and synaptic strength [79] (Figure 2). These evidences reinforce the previous hypothesis that TNF-α profile in the CNS modulates synaptic plasticity during addiction; however, it is still unknown whether central TNF-α accumulation might be a node of inflammatory activation during addiction or there is a cause-effect relationship involving a cross-talk between peripheral and central mechanism.

Synaptic plasticity during addiction might also be modulated by chemokines. For instance, the CCL4 and CCL17 chemokines and their ligand CCL25 are upregulated in microglia following morphine treatment and might also

induce local chemotaxis of axon terminals or dendritic spines. Blocking the synthesis of certain chemokines prevents the relapse of drug-seeking behavior following drug reexposure months later [81]. In addition, the modulation of the G-CSF chemokine concentration in the NAc and the prefrontal cortex is crucial to alter the motivation of cocaine consumption but not of food [76]. Together, chemokines have a very profound neuromodulatory effect on the regulation of neural circuits involved in addiction, but the molecular mechanisms on this scenario still need to be described in detail.

Central and peripheral immune cross-talk response might also modulate hippocampal neurogenesis. It has been reported that when $CD4^+$ T lymphocytes are systemically depleted in mice, there are reduced hippocampal neurogenesis, learning impairment, and a decrease in BDNF secretion in the brain, whereas inoculation of $CD4^+$ T lymphocytes promotes hippocampal neurogenesis and restores the deficits observed before [82, 83]. In models of autoimmune encephalitis in which inflammatory responses are upregulated, synaptic plasticity in the hippocampus and long-term potentiation (LTP) are affected because of the high levels of IL-1β. While peripheral inflammatory responses related to TNF-α and IL-6 have been identified to modulate hippocampus activity [84, 85], it has not been fully described whether central IL-1β comes from infiltrating lymphocytes or activated microglia within the CNS [86]. In any case, central physiological levels of IL-1β are detrimental, because excessive cytokines level or blockage of IL- 1 signaling through IL-1ra has been reported to cause memory impairment [87], potentially due to Ca^{2+} influx throughout NMDA receptors, Src kinases activation, and NR2A/B subunits phosphorylation [88].

As mentioned before for TNF-α and IL-1β, initial reports characterized that the IL-6 cytokine is required in normal physiological levels for the formation of LTP, but levels above normal affect memory formation and learning [89, 90]. Supporting those findings, IL-6 KO mice display memory impairment [84] and show reduced proliferating neuronal stem cells (NSCs) in the hippocampus [91]. Under physiological conditions, IL-6 is related to neural plasticity and NSCs proliferation through the JAK/STAT, MAPK/cAMP, Ras-MAPK, and PI3K pathways [92]. Lastly, the immune system is involved in regulation of hippocampal neurogenesis, through the kynurenine pathway [93], affecting directly the hippocampal neurogenesis and memory and learning processes [82] (Figure 2).

A positive inflammatory profile including the IL-1, IL-6, IL-1β, TNF-α, and IFN-γ has been evidenced in a wide range of neurodegenerative diseases. In particular, TNF-α production by active microglia is highly related to IFN-γ secreted by T cells into the CNS parenchyma [3]. Secreted IFN-γ and other inflammation mediators activate the MEK/ERK signaling pathway leading to TNF-α production and neuronal death [4]. Also, TNF-α and IFN-γ lead to microglial nitric oxide (NO) production, favoring oxidative stress, inhibiting neuronal respiration, and favoring neuronal apoptosis [94]. Of note, these responses seem to be independent, although there might be a node at different time-frame. For instance, the TNF-α targets its own receptor to activate the NF-κB-dependent proinflammatory pathway and the expression of inducible NO synthase (iNOS) that mediates NO production, which is regulated by NF-κB and STAT transcription factors [95].

In addition, IL-6 also might potentially favor neuronal death. By promoting the formation of the IL-6/IL-6R/gp130 complex, the proinflammatory IL-6 activates the JAK1, JAK2, and TYK2 pathway and promotes the phosphorylation of STAT1 and STAT3. In specific, IL-6 favors neuronal death by the STAT1 nuclear transcription factor, which associates with transcription of IFNs, including type I (IFN-α, IFN-β, and IFN-ω) and type II (IFN-γ), all of them involved in detrimental innate immune responses. However, IL-6 might also be anti-inflammatory and promote cell survival through STAT3-PI3K/Akt signaling activation by regulating cell cycle proteins (CDK2), antiapoptotic proteins (Bcl-2), and proapoptotic proteins (Bax, Bad, and caspase-9) [5, 96]. Thus, IL-6 secretion by activated microglia regulates inflammatory mediators and shows a dual role that prevents or promotes neuronal death.

In summary, because of their dual roles associated with threshold levels, cytokines in the brain may help to maintain cerebral homeostasis having a beneficial effect in normal physiological conditions; uncontrolled or chronic neuroinflammation, however, leads to neurodegeneration, disruption of cerebral plasticity, cognitive changes, and the appearance of aberrant behavior, also defined as "sickness behavior" by Cibelli and colleagues [74].

6. Epigenetic Mechanisms during Fetal Programming and Transgenerational Inheritance of Addictive Phenotype

By now, we have shown evidences that metabolic inflammation during pregnancy leads to chronic inflammation in offspring that might disrupt synaptic plasticity and set a self-perpetuating cycle of addictive excessive consumption of natural and synthetic rewards [28, 97]. Despite the lack of epidemiological studies addressing the impact of human obesity or maternal overnutrition as a node to promote addiction-like phenotypes in offspring, recent evidence suggests that addiction in humans might have a common root from transgenerational inheritance, given that biomarkers that share identity in drug programming and addictive behavior have been previously described [98–101]. A transgenerational inheritance of addiction, eating disorders, or pathological phenotypes in offspring is modulated directly by epigenetics, which programs and adapts organisms in the early stages of development to face sudden changes in the environment, compared with evolutionary and natural selection processes, which tend to be slow [102]. Epigenetics refer to the mechanisms of long-term or stable regulation of gene expression that do not involve a change in gene sequences including DNA methylation and histone modification such as acetylation, sumoylation, ubiquitination, and methylation, as well as gene expression regulated by

noncoding RNAs, miRNAs, piRNAs, and lncRNA [103]. The role of maternal programing by overnutrition during pregnancy and its effects on epigenetics linked to a proinflammatory profile in offspring have not been deeply analyzed yet. Initial work has shown that epigenetics modulate the immune system and potentially affects the CNS during pregnancy [103]. A recent paper identified that fat diet primes an epigenomic reprogramming of myeloid progenitor cells that led to an increased proliferation and enhanced innate immune responses [104], which the authors named as "innate immune memory" or "trained immunity," able to mediate metabolic reprogramming for prolonged periods of time [105]. On this context, using a fetal-programing murine model with hypercaloric diet, Edlow et al. (2016) identified a significant number of deregulated miRNAs implicated in immune and proinflammatory processes, death cellular, adipogenesis and cellular stress in the males of offspring [106] (Figure 1). In humans, a positive correlation between body mass index (BMI) during prepregnancy with adiposity and inflammatory markers in offspring at birth has been demonstrated [107]. Also, Alexander and col. (2018) reported alterations in the methylation profile of genes involved in mitochondrial function, DNA repair, oxidative stress and inflammation in the placenta of children who were born from mothers with type 2 diabetes mellitus [108]. Of importance, a study in humans revealed that an adherence to Mediterranean diet for 5 years ended up in a significant increase in DNA methylation which positively correlated with a reduction in the concentrations of TNF-α, sICAM-1, and CRP [109].

These evidences suggest that gestational exposure to high-fat and high-sugar diets in murine models results in a disruption of the central reward system, which correlates with epigenetic biomarkers found in addicted-programed subjects. Programming sets the brain to potentiate changes in neuroplasticity [97, 110], neuronal death, neurotoxicity [111], etc., in postnatal life, which leads to the development of cognitive disorders such as addiction [112–115]. It is still under investigation if humans share the aberrant reward plasticity that has been described in murine models.

7. Conclusions

Maternal overnutrition leads to fetal adaptive responses which sets a neuronal gene expression program in offspring. Selective intake of diets rich in fats and sugars at critical stages recruit central and peripheral inflammatory cell type markers, such as microglia and T and B cells, which disrupt energy sensing and behavioral pathways increasing the susceptibility to show aberrant behaviors similar to addiction. In fact, an addictive phenotype might be transgenerational when inherited by selective epigenetic activation during fetal programming. These evidences propose the immune system activation by nutritional programming during gestation as a node to modulate changes in neuroplasticity related to incentive behavior phenotypes which must be addressed deeply for a better understanding.

Disclosure

Alberto Camacho's present/permanent address is as follows: Department of Biochemistry, Faculty of Medicine, Universidad Autónoma de Nuevo León, San Nicolás de los Garza, NL, México, and Center for Research and Development in Health Sciences, Universidad Autónoma de Nuevo León, San Nicolás de los Garza, NL, México.

Conflicts of Interest

The authors report no conflicts of interest.

Acknowledgments

The authors thank M.S. Alejandra Arreola-Triana for her support on editing this manuscript. This work was funded by National Council of Science and Technology in Mexico (CONACYT) (255317), 582196 CONACYT for Larisa Montalvo-Martínez and 573686 CONACYT for Roger Maldonado-Ruiz.

References

[1] P. Chavatte-Palmer, A. Tarrade, and D. Rousseau-Ralliard, "Diet before and during pregnancy and offspring health: The importance of animal models and what can be learned from them," *International Journal of Environmental Research and Public Health*, vol. 13, no. 6, article no. 586, 2016.

[2] A. G. Edlow, "Maternal obesity and neurodevelopmental and psychiatric disorders in offspring," *Prenatal Diagnosis*, vol. 37, no. 1, pp. 95–110, 2017.

[3] E. Martin, T. Ganz, and R. I. Lehrer, "Defensins and other endogenous peptide antibiotics of vertebrates," *Journal of Leukocyte Biology*, vol. 58, no. 2, pp. 128–136, 1995.

[4] R. M. Ransohoff and B. Engelhardt, "The anatomical and cellular basis of immune surveillance in the central nervous system," *Nature Reviews Immunology*, vol. 12, no. 9, pp. 623–635, 2012.

[5] W. Lin and Y. Lin, "Interferon-γ inhibits central nervous system myelination through both STAT1-dependent and STAT1-independent pathways," *Journal of Neuroscience Research*, vol. 88, no. 12, pp. 2569–2577, 2010.

[6] A. van der Klaauw and I. Farooqi, "The hunger genes: pathways to obesity," *Cell*, vol. 161, no. 1, pp. 119–132, 2015.

[7] K. Kim, R. J. Seeley, and D. A. Sandoval, "Signalling from the periphery to the brain that regulates energy homeostasis," *Nature Reviews Neuroscience*, vol. 19, no. 4, pp. 185–196, 2018.

[8] S. J. Russo and E. J. Nestler, "The brain reward circuitry in mood disorders," 2013.

[9] Y.-H. Yu, J. R. Vasselli, Y. Zhang, J. I. Mechanick, J. Korner, and R. Peterli, "Metabolic vs. hedonic obesity: A conceptual distinction and its clinical implications," *Obesity Reviews*, vol. 16, no. 3, pp. 234–247, 2015.

[10] N. D. Volkow, R. A. Wise, and R. Baler, "The dopamine motive system: Implications for drug and food addiction," *Nature Reviews Neuroscience*, vol. 18, no. 12, pp. 741–752, 2017.

[11] D. S. Ludwig, K. E. Peterson, and S. L. Gortmaker, "Relation between consumption of sugar-sweetened drinks and childhood obesity: a prospective, observational analysis," *The Lancet*, vol. 357, no. 9255, pp. 505–508, 2001.

[12] National Institutes of Health and N.H.L. Institute and Blood Institute, "Maintaining a Healthy Weight On the Go: A Pocket Guide," *NIH Public Access*, pp. 1–24, 2010.

[13] P. J. Kenny, "Common cellular and molecular mechanisms in obesity and drug addiction," *Nature Reviews Neuroscience*, vol. 12, no. 11, pp. 638–651, 2011.

[14] A. N. Gearhardt, W. R. Corbin, and K. D. Brownell, "Preliminary validation of the Yale Food Addiction Scale," *Appetite*, vol. 52, no. 2, pp. 430–436, 2009.

[15] E. M. Schulte and A. N. Gearhardt, "Development of the Modified Yale Food Addiction Scale Version 2.0," *European Eating Disorders Review*, vol. 25, no. 4, pp. 302–308, 2017.

[16] C. E. Aiken and S. E. Ozanne, "Transgenerational developmental programming," *Human Reproduction Update*, vol. 20, no. 1, Article ID dmt043, pp. 63–75, 2014.

[17] M. Lalande, "Parental imprinting and human disease," *Annual Review of Genetics*, vol. 30, pp. 173–195, 1996.

[18] A. Vaiserman, "Early-life origin of adult disease: Evidence from natural experiments," *Experimental Gerontology*, vol. 46, no. 2-3, pp. 189–192, 2011.

[19] Y. Li, Y. He, L. Qi et al., "Exposure to the Chinese famine in early life and the risk of hyperglycemia and type 2 diabetes in adulthood," *Diabetes*, vol. 59, no. 10, pp. 2400–2406, 2010.

[20] E. Susser, R. Neugebauer, H. W. Hoek et al., "Schizophrenia after prenatal famine further evidence," *Archives of General Psychiatry*, vol. 53, no. 1, pp. 25–31, 1996.

[21] D. St Clair, M. Xu, P. Wang et al., "Rates of adult schizophrenia following prenatal exposure to the Chinese famine of 1959-1961," *Journal of the American Medical Association*, vol. 294, no. 5, pp. 557–562, 2005.

[22] M.-Q. Xu, W.-S. Sun, B.-X. Liu et al., "Prenatal malnutrition and adult Schizophrenia: Further evidence from the 1959-1961 chinese famine," *Schizophrenia Bulletin*, vol. 35, no. 3, pp. 568–576, 2009.

[23] A. S. Brown, J. Van Os, C. Driessens, H. W. Hoek, and E. S. Susser, "Further evidence of relation between prenatal famine and major affective disorder," *The American Journal of Psychiatry*, vol. 157, no. 2, pp. 190–195, 2000.

[24] E. J. Franzek, N. Sprangers, A. C. J. W. Janssens, C. M. Van Duijn, and B. J. M. Van De Wetering, "Prenatal exposure to the 1944-45 Dutch 'hunger winter' and addiction later in life," *Addiction*, vol. 103, no. 3, pp. 433–438, 2008.

[25] R. C. Painter, T. J. Roseboom, and O. P. Bleker, "Prenatal exposure to the Dutch famine and disease in later life: An overview," *Reproductive Toxicology*, vol. 20, no. 3, pp. 345–352, 2005.

[26] D. J. P. Barker, "In utero programming of chronic disease," *Clinical Science*, vol. 95, no. 2, pp. 115–128, 1998.

[27] M. Lenoir, F. Serre, L. Cantin, and S. H. Ahmed, "Intense sweetness surpasses cocaine reward," *PLoS ONE*, vol. 2, no. 8, article no. e698, 2007.

[28] D. Peleg-Raibstein, G. Sarker, K. Litwan et al., "Enhanced sensitivity to drugs of abuse and palatable foods following maternal overnutrition," *Translational Psychiatry*, vol. 6, no. 10, article no. e911, 2016.

[29] M. E. Bocarsly, J. R. Barson, J. M. Hauca, B. G. Hoebel, S. F. Leibowitz, and N. M. Avena, "Effects of perinatal exposure to palatable diets on body weight and sensitivity to drugs of abuse in rats," *Physiology & Behavior*, vol. 107, no. 4, pp. 568–575, 2012.

[30] S. A. Bayol, S. J. Farrington, and N. C. Stickland, "A maternal "junk food" diet in pregnancy and lactation promotes an exacerbated taste for "junk food" and a greater propensity for obesity in rat offspring," *British Journal of Nutrition*, vol. 98, no. 4, pp. 843–851, 2018.

[31] V. Bassareo and G. Di Chiara, "Differential influence of associative and nonassociative learning mechanisms on the responsiveness of prefrontal and accumbal dopamine transmission to food stimuli in rats fed ad libitum," *The Journal of Neuroscience*, vol. 17, no. 2, pp. 851–861, 1997.

[32] A. Hajnal, G. P. Smith, and R. Norgren, "Oral sucrose stimulation increases accumbens dopamine in the rat," *American Journal of Physiology-Regulatory, Integrative and Comparative Physiology*, vol. 286, no. 1, pp. R31–R37, 2004.

[33] N.-C. Liang, A. Hajnal, and R. Norgren, "Sham feeding corn oil increases accumbens dopamine in the rat," *American Journal of Physiology-Regulatory, Integrative and Comparative Physiology*, vol. 291, no. 5, pp. R1236–R1239, 2006.

[34] P. Rada, N. M. Avena, and B. G. Hoebel, "Daily bingeing on sugar repeatedly releases dopamine in the accumbens shell," *Neuroscience*, vol. 134, no. 3, pp. 737–744, 2005.

[35] L. Naef, L. Moquin, G. Dal Bo, B. Giros, A. Gratton, and C.-D. Walker, "Maternal high-fat intake alters presynaptic regulation of dopamine in the nucleus accumbens and increases motivation for fat rewards in the offspring," *Neuroscience*, vol. 176, pp. 225–236, 2011.

[36] Z. Y. Ong and B. S. Muhlhausler, "Maternal "junk-food" feeding of rat dams alters food choices and development of the mesolimbic reward pathway in the offspring," *The FASEB Journal*, vol. 25, no. 7, pp. 2167–2179, 2011.

[37] Z. Y. Ong, A. F. Wanasuria, M. Z. P. Lin, J. Hiscock, and B. S. Muhlhausler, "Chronic intake of a cafeteria diet and subsequent abstinence. Sex-specific effects on gene expression in the mesolimbic reward system," *Appetite*, vol. 65, pp. 189–199, 2013.

[38] J. R. Gugusheff, S. E. Bae, A. Rao et al., "Sex and age-dependent effects of a maternal junk food diet on the mu-opioid receptor in rat offspring," *Behavioural Brain Research*, vol. 301, pp. 124–131, 2016.

[39] B. M. Fritz, B. Muñoz, F. Yin, C. Bauchle, and B. K. Atwood, "A High-fat, High-sugar 'Western' Diet Alters Dorsal Striatal Glutamate, Opioid, and Dopamine Transmission in Mice," *Neuroscience*, vol. 372, pp. 1–15, 2018.

[40] M. Zhang, B. A. Gosnell, and A. E. Kelley, "Intake of high-fat food is selectively enhanced by Mu opioid receptor stimulation within the nucleus accumbens," *The Journal of Pharmacology and Experimental Therapeutics*, vol. 285, no. 2, pp. 908–914, 1998.

[41] M. Zhang and A. E. Kelley, "Enhanced intake of high-fat food following striatal mu-opioid stimulation: Microinjection mapping and Fos expression," *Neuroscience*, vol. 99, no. 2, pp. 267–277, 2000.

[42] A. E. Kelley, E. P. Bless, and C. J. Swanson, "Investigation of the effects of opiate antagonists infused into the nucleus accumbens on feeding and sucrose drinking in rats," *The Journal of Pharmacology and Experimental Therapeutics*, vol. 278, no. 3, pp. 1499–1507, 1996.

[43] M. J. Glass, C. J. Billington, and A. S. Levine, "Opioids and food intake: Distributed functional neural pathways?" *Neuropeptides*, vol. 33, no. 5, pp. 360–368, 1999.

[44] H. Wang, M. I. Dávila-García, W. Yarl, and M. C. Gondré-Lewis, "Gestational nicotine exposure regulates expression of AMPA and NMDA receptors and their signaling apparatus in

developing and adult rat hippocampus," *Neuroscience*, vol. 188, pp. 168–181, 2011.

[45] K. Parameshwaran, M. A. Buabeid, S. S. Karuppagounder et al., "Developmental nicotine exposure induced alterations in behavior and glutamate receptor function in hippocampus," *Cellular and Molecular Life Sciences*, vol. 69, no. 5, pp. 829–841, 2012.

[46] L. F. McNair and K. A. Kohlmeier, "Prenatal nicotine is associated with reduced AMPA and NMDA receptor-mediated rises in calcium within the laterodorsal tegmentum: A pontine nucleus involved in addiction processes," *Journal of Developmental Origins of Health and Disease*, vol. 6, no. 3, pp. 225–241, 2014.

[47] K. D. Carr, L. S. Chau, S. Cabeza de Vaca et al., "AMPA receptor subunit GluR1 downstream of D-1 dopamine receptor stimulation in nucleus accumbens shell mediates increased drug reward magnitude in food-restricted rats," *Neuroscience*, vol. 165, no. 4, pp. 1074–1086, 2010.

[48] J. L. Cornish and P. W. Kalivas, "Glutamate transmission in the nucleus accumbens mediates relapse in cocaine addiction.," *The Journal of Neuroscience*, vol. 20, no. 15, p. RC89, 2000.

[49] T. M. Tzschentke and W. J. Schmidt, "Glutamatergic mechanisms in addiction," *Molecular Psychiatry*, vol. 8, no. 4, pp. 373–382, 2003.

[50] C. R. Pinheiro, E. G. Moura, A. C. Manhães et al., "Concurrent maternal and pup postnatal tobacco smoke exposure in Wistar rats changes food preference and dopaminergic reward system parameters in the adult male offspring," *Neuroscience*, vol. 301, pp. 178–192, 2015.

[51] C. R. Pinheiro, E. G. Moura, A. C. Manhães et al., "Maternal nicotine exposure during lactation alters food preference, anxiety-like behavior and the brain dopaminergic reward system in the adult rat offspring," *Physiology & Behavior*, vol. 149, pp. 131–141, 2015.

[52] M. F. Oginsky, P. B. Goforth, C. W. Nobile, L. F. Lopez-Santiago, and C. R. Ferrario, "Eating 'Junk-Food' Produces Rapid and Long-Lasting Increases in NAc CP-AMPA Receptors: Implications for Enhanced Cue-Induced Motivation and Food Addiction," *Neuropsychopharmacology*, vol. 41, no. 13, pp. 2977–2986, 2016.

[53] A. Camacho, L. Montalvo-Martinez, R. E. Cardenas-Perez, L. Fuentes-Mera, and L. Garza-Ocañas, "Obesogenic diet intake during pregnancy programs aberrant synaptic plasticity and addiction-like behavior to a palatable food in offspring," *Behavioural Brain Research*, vol. 330, pp. 46–55, 2017.

[54] A. Lamerz, J. Kuepper-Nybelen, N. Bruning et al., "Prevalence of obesity, binge eating, and night eating in a cross-sectional field survey of 6-year-old children and their parents in a German urban population," *Journal of Child Psychology and Psychiatry and Allied Disciplines*, vol. 46, no. 4, pp. 385–393, 2005.

[55] J. A. Lydecker and C. M. Grilo, "Fathers and mothers with eating-disorder psychopathology: Associations with child eating-disorder behaviors," *Journal of Psychosomatic Research*, vol. 86, pp. 63–69, 2016.

[56] R. Rising and F. Lifshitz, "Relationship between maternal obesity and infant feeding-interactions," *Nutrition Journal* , vol. 4, article no. 17, 2005.

[57] T. Burrows, J. Skinner, M. A. Joyner, J. Palmieri, K. Vaughan, and A. N. Gearhardt, "Food addiction in children: Associations with obesity, parental food addiction and feeding practices," *Eating Behaviors*, vol. 26, pp. 114–120, 2017.

[58] R. Maldonado-Ruiz, L. Montalvo-Martínez, L. Fuentes-Mera, and A. Camacho, "Microglia activation due to obesity programs metabolic failure leading to type two diabetes," *Nutrition & Diabetes*, vol. 7, no. 3, p. e254, 2017.

[59] L. B. Buckman, A. H. Hasty, D. K. Flaherty et al., "Obesity induced by a high-fat diet is associated with increased immune cell entry into the central nervous system," *Brain, Behavior, and Immunity*, vol. 35, pp. 33–42, 2014.

[60] N. Strazielle, R. Creidy, C. Malcus, J. Boucraut, and J. F. Ghersi-Egea, "T-Lymphocytes traffic into the brain across the blood-csf barrier: Evidence using a reconstituted choroid plexus epithelium," *PLoS ONE*, vol. 11, no. 3, Article ID e0150945, 2016.

[61] M. R. Buehler, "A proposed mechanism for autism: An aberrant neuroimmune response manifested as a psychiatric disorder," *Medical Hypotheses*, vol. 76, no. 6, pp. 863–870, 2011.

[62] D. Soulet and S. Rivest, "Microglia," *Current Biology*, vol. 18, no. 12, pp. R506–R508, 2008.

[63] M. W. Salter and B. Stevens, "Microglia emerge as central players in brain disease," *Nature Medicine*, vol. 23, no. 9, pp. 1018–1027, 2017.

[64] R. von Bernhardi, L. Eugenín-von Bernhardi, and J. Eugenín, "Microglial cell dysregulation in brain aging and neurodegeneration," *Frontiers in Aging Neuroscience*, vol. 7, article 124, 2015.

[65] S. Carobbio, V. Pellegrinelli, and A. Vidal-Puig, "Adipose tissue function and expandability as determinants of lipotoxicity and the metabolic syndrome," *Advances in Experimental Medicine and Biology*, vol. 960, pp. 161–196, 2017.

[66] C. Han, M. Rice, and D. Cai, "Neuroinflammatory and autonomic mechanisms in diabetes and hypertension," *American Journal of Physiology-Endocrinology and Metabolism*, vol. 311, no. 1, pp. E32–E41, 2016.

[67] R. Maldonado-Ruiz, L. Fuentes-Mera, and A. Camacho, "Central Modulation of Neuroinflammation by Neuropeptides and Energy-Sensing Hormones during Obesity," *BioMed Research International*, vol. 2017, 2017.

[68] P. C. Calder, "N-3 Fatty acids, inflammation and immunity: new mechanisms to explain old actions," *Proceedings of the Nutrition Society*, vol. 72, no. 3, pp. 326–336, 2013.

[69] L. A. J. O'Neill and D. Grahame Hardie, "Metabolism of inflammation limited by AMPK and pseudo-starvation," *Nature*, vol. 493, no. 7432, pp. 346–355, 2013.

[70] K. D. Getz, M. T. Anderka, M. M. Werler, and S. S. Jick, "Maternal Pre-pregnancy Body Mass Index and Autism Spectrum Disorder among Offspring: A Population-Based Case–Control Study," *Paediatric and Perinatal Epidemiology*, vol. 30, no. 5, pp. 479–487, 2016.

[71] A. B. Ghnenis, J. F. Odhiambo, R. J. McCormick, P. W. Nathanielsz, and S. P. Ford, "Maternal obesity in the ewe increases cardiac ventricular expression of glucocorticoid receptors, proinflammatory cytokines and fibrosis in adult male offspring," *PLoS ONE*, vol. 12, no. 12, 2017.

[72] M. L. Estes and A. K. McAllister, "Maternal immune activation: Implications for neuropsychiatric disorders," *Science*, vol. 353, no. 6301, pp. 772–777, 2016.

[73] R. M. Ransohoff, "How neuroinflammation contributes to neurodegeneration," *Science*, vol. 353, no. 6301, pp. 777–783, 2016.

[74] M. Cibelli, A. R. Fidalgo, N. Terrando et al., "Role of interleukin-1β in postoperative cognitive dysfunction," *Annals of Neurology*, vol. 68, no. 3, pp. 360–368, 2010.

[75] M. J. Lacagnina, P. D. Rivera, and S. D. Bilbo, "Glial and Neuroimmune Mechanisms as Critical Modulators of Drug Use and Abuse," *Neuropsychopharmacology*, vol. 42, no. 1, pp. 156–177, 2017.

[76] E. S. Calipari, A. Godino, E. G. Peck et al., "Granulocyte-colony stimulating factor controls neural and behavioral plasticity in response to cocaine," *Nature Communications*, vol. 9, no. 1, 2018.

[77] G. M. Lewitus, S. C. Konefal, A. D. Greenhalgh, H. Pribiag, K. Augereau, and D. Stellwagen, "Microglial TNF-α Suppresses Cocaine-Induced Plasticity and Behavioral Sensitization," *Neuron*, vol. 90, no. 3, pp. 483–491, 2016.

[78] E. C. Beattie, D. Stellwagen, W. Morishita et al., "Control of synaptic strength by glial TNFα," *Science*, vol. 295, no. 5563, pp. 2282–2285, 2002.

[79] D. Stellwagen and R. C. Malenka, "Synaptic scaling mediated by glial TNF-α," *Nature*, vol. 440, no. 7087, pp. 1054–1059, 2006.

[80] G. M. Lewitus, H. Pribiag, R. Duseja, M. St-Hilaire, and D. Stellwagen, "An adaptive role of TNFα in the regulation of striatal synapses," *The Journal of Neuroscience*, vol. 34, no. 18, pp. 6146–6155, 2014.

[81] J. M. Schwarz, S. H. Smith, and S. D. Bilbo, "FACS analysis of neuronal-glial interactions in the nucleus accumbens following morphine administration," *Psychopharmacology*, vol. 230, no. 4, pp. 525–535, 2013.

[82] S. A. Wolf, B. Steiner, A. Akpinarli et al., "CD4-positive T lymphocytes provide a neuroimmunological link in the control of adult hippocampal neurogenesis," *The Journal of Immunology*, vol. 182, no. 7, pp. 3979–3984, 2009.

[83] O. Leiter, G. Kempermann, and T. L. Walker, "A Common Language: How neuroimmunological cross talk regulates adult hippocampal neurogenesis," *Stem Cells International*, vol. 2016, 2016.

[84] P. C. Baier, U. May, J. Scheller, S. Rose-John, and T. Schiffelholz, "Impaired hippocampus-dependent and -independent learning in IL-6 deficient mice," *Behavioural Brain Research*, vol. 200, no. 1, pp. 192–196, 2009.

[85] H. Tan, J. Cao, J. Zhang, and Z. Zuo, "Critical role of inflammatory cytokines in impairing biochemical processes for learning and memory after surgery in rats," *Journal of Neuroinflammation*, vol. 11, article no. 93, 2014.

[86] R. Nisticò, F. Mori, M. Feligioni, F. Nicoletti, and D. Centonze, "Synaptic plasticity in multiple sclerosis and in experimental autoimmune encephalomyelitis," *Philosophical Transactions of the Royal Society B: Biological Sciences*, vol. 369, no. 1633, Article ID 20130162, 2014.

[87] I. Goshen, T. Kreisel, H. Ounallah-Saad et al., "A dual role for interleukin-1 in hippocampal-dependent memory processes," *Psychoneuroendocrinology*, vol. 32, no. 8-10, pp. 1106–1115, 2007.

[88] B. Viviani, S. Bartesaghi, F. Gardoni et al., "Interleukin-1β enhances NMDA receptor-mediated intracellular calcium increase through activation of the Src family of kinases," *The Journal of Neuroscience*, vol. 23, no. 25, pp. 8692–8700, 2003.

[89] H. Wei, K. K. Chadman, D. P. McCloskey et al., "Brain IL-6 elevation causes neuronal circuitry imbalances and mediates autism-like behaviors," *Biochimica et Biophysica Acta (BBA) - Molecular Basis of Disease*, vol. 1822, no. 6, pp. 831–842, 2012.

[90] D. Balschun, W. Wetzel, A. Del Rey et al., "Interleukin-6: a cytokine to forget," *The FASEB Journal*, vol. 18, no. 14, pp. 1788–1790, 2004.

[91] K. K. Bowen, R. J. Dempsey, and R. Vemuganti, "Adult interleukin-6 knockout mice show compromisedneurogenesis," *NeuroReport*, vol. 22, no. 3, pp. 126–130, 2011.

[92] M. K. Kang and S. K. Kang, "Interleukin-6 induces proliferation in adult spinal cord-derived neural progenitors via the JAK2/STAT3 pathway with EGF-induced MAPK phosphorylation," *Cell Proliferation*, vol. 41, no. 3, pp. 377–392, 2008.

[93] P. A. Zunszain, C. Anacker, A. Cattaneo et al., "Interleukin-1β: a new regulator of the kynurenine pathway affecting human hippocampal neurogenesis," *Neuropsychopharmacology*, vol. 37, no. 4, pp. 939–949, 2012.

[94] T. B. Bassani, M. A. B. F. Vital, and L. K. Rauh, "Neuroinflammation in the pathophysiology of Parkinson's disease and therapeutic evidence of anti-inflammatory drugs," *Arquivos de Neuro-Psiquiatria*, vol. 73, no. 7, pp. 616–623, 2015.

[95] E. Mass, I. Ballesteros, M. Farlik et al., "Specification of tissue-resident macrophages during organogenesis," *The New York Academy of Sciences*, vol. 353, no. 6304, 2016.

[96] V. Arulampalam, I. Kolosenko, L. Hjortsberg, A.-C. Björklund, D. Grandér, and K. P. Tamm, "Activation of STAT1 is required for interferon-alpha-mediated cell death," *Experimental Cell Research*, vol. 317, no. 1, pp. 9–19, 2011.

[97] M. Gutiérrez-Martos, B. Girard, S. Mendonça-Netto et al., "Cafeteria diet induces neuroplastic modifications in the nucleus accumbens mediated by microglia activation," *Addiction Biology*, 2017.

[98] I. Donkin, S. Versteyhe, L. R. Ingerslev et al., "Obesity and bariatric surgery drive epigenetic variation of spermatozoa in humans," *Cell Metabolism*, vol. 23, no. 2, pp. 369–378, 2016.

[99] K. L. H. Wu, C.-W. Wu, Y.-L. Tain et al., "Environmental stimulation rescues maternal high fructose intake-impaired learning and memory in female offspring: Its correlation with redistribution of histone deacetylase 4," *Neurobiology of Learning and Memory*, vol. 130, pp. 105–117, 2016.

[100] M. L. Holland, R. Lowe, P. W. Caton et al., "Early-life nutrition modulates the epigenetic state of specific rDNA genetic variants in mice," *Science*, vol. 353, no. 6298, pp. 495–498, 2016.

[101] J. Rijlaarsdam, C. A. M. Cecil, E. Walton et al., "Prenatal unhealthy diet, insulin-like growth factor 2 gene (IGF2) methylation, and attention deficit hyperactivity disorder symptoms in youth with early-onset conduct problems," *Journal of Child Psychology and Psychiatry and Allied Disciplines*, vol. 58, no. 1, pp. 19–27, 2017.

[102] J. Bohacek and I. M. Mansuy, "Molecular insights into transgenerational non-genetic inheritance of acquired behaviours," *Nature Reviews Genetics*, vol. 16, no. 11, pp. 641–652, 2015.

[103] D. Álvarez-Errico, R. Vento-Tormo, M. Sieweke, and E. Ballestar, "Epigenetic control of myeloid cell differentiation, identity and function," *Nature Reviews Immunology*, vol. 15, no. 1, pp. 7–17, 2015.

[104] A. Christ, P. Günther, M. A. Lauterbach et al., "Western Diet Triggers NLRP3-Dependent Innate Immune Reprogramming," *Cell*, vol. 172, no. 1-2, pp. 162–175.e14, 2018.

[105] M. G. Netea, J. Quintin, and J. W. M. van der Meer, "Trained immunity: a memory for innate host defense," *Cell Host & Microbe*, vol. 9, no. 5, pp. 355–361, 2011.

[106] A. G. Edlow, F. Guedj, J. L. A. Pennings, D. Sverdlov, C. Neri, and D. W. Bianchi, "Males are from Mars, and females are from Venus: Sex-specific fetal brain gene expression signatures in a mouse model of maternal diet-induced obesity," *American Journal of Obstetrics & Gynecology*, vol. 214, no. 5, pp. 623–623e10, 2016.

[107] K. McCloskey, A.-L. Ponsonby, F. Collier et al., "The association between higher maternal pre-pregnancy body mass index and

increased birth weight, adiposity and inflammation in the newborn," *Pediatric Obesity*, vol. 13, no. 1, pp. 46–53, 2018.

[108] J. Alexander, A. M. Teague, J. Chen et al., "Offspring sex impacts DNA methylation and gene expression in placentae from women with diabetes during pregnancy," *PLoS ONE*, vol. 13, no. 2, p. e0190698, 2018.

[109] A. Arpón, J. I. Riezu-Boj, F. I. Milagro et al., "Adherence to Mediterranean diet is associated with methylation changes in inflammation-related genes in peripheral blood cells," *Journal of Physiology and Biochemistry*, vol. 73, no. 3, pp. 445–455, 2016.

[110] S. Hao, A. Dey, X. Yu, and A. M. Stranahan, "Dietary obesity reversibly induces synaptic stripping by microglia and impairs hippocampal plasticity," *Brain, Behavior, and Immunity*, vol. 51, pp. 230–239, 2016.

[111] C. F. Kessing and W. R. Tyor, "Interferon-α induces neurotoxicity through activation of the type i receptor and the GluN2A subunit of the NMDA receptor," *Journal of Interferon & Cytokine Research*, vol. 35, no. 4, pp. 317–324, 2015.

[112] F. Crews, J. Zou, and L. Qin, "NIH public access," *Brain, Behavior, and Immunity*, vol. 25, pp. 1–20, 2013.

[113] F. T. Crews, T. J. Walter, L. G. Coleman, and R. P. Vetreno, "Toll-like receptor signaling and stages of addiction," *Psychopharmacology*, vol. 234, no. 9-10, pp. 1483–1498, 2017.

[114] R. Harricharan, O. Abboussi, and W. M. U. Daniels, "Addiction: A dysregulation of satiety and inflammatory processes," *Progress in Brain Research*, vol. 235, pp. 65–91, 2017.

[115] N. Wakida, N. Kiguchi, F. Saika, H. Nishiue, Y. Kobayashi, and S. Kishioka, "CC-chemokine ligand 2 facilitates conditioned place preference to methamphetamine through the activation of dopamine systems," *Journal of Pharmacological Sciences*, vol. 125, no. 1, pp. 68–73, 2014.